AEROSPACE REPORT NO.
ATR-74(7333)-1, VOL. II

System Cost/Performance Analysis (Study 2.3) Final Report

Volume II
Study Results

Prepared by T. KAZANGEY
Guidance and Control Division
Engineering Science Operations

28 SEPT 1973

Prepared for OFFICE OF MANNED SPACE FLIGHT
NATIONAL AERONAUTICS AND SPACE ADMINISTRATION
Washington, D. C.

Contract No. NASW-2472

Systems Engineering Operations
THE AEROSPACE CORPORATION

(NASA-CR-135902) SYSTEM COST/PERFORMANCE ANALYSIS (STUDY 2.3). VOLUME 2: STUDY RESULTS Final Report, 1 Sep. 1972 - 31 Aug. 1973 (Aerospace Corp., El Segundo, Calif.) ~~376~~ p HC $21.00 CSCL 14A G3/34

372

N73-33920
Unclas
15820

Aerospace Report No.
ATR-74(7333)-1, Vol. II

SYSTEM COST/PERFORMANCE ANALYSIS
(STUDY 2.3) FINAL REPORT
Volume II. Study Results

Prepared by

T. Kazangey
Guidance and Control Division
Engineering Science Operations

28 SEPT 1973

Systems Engineering Operations
THE AEROSPACE CORPORATION
El Segundo, California

Prepared for

OFFICE OF MANNED SPACE FLIGHT
NATIONAL AERONAUTICS AND SPACE ADMINISTRATION
Washington, D. C.

Contract No. NASW-2472

Aerospace Report No.
ATR-74(7333)-1, Vol. II

SYSTEM COST/PERFORMANCE ANALYSIS
(STUDY 2.3) FINAL REPORT

Volume II: Study Results

Prepared by

T. Kazangey
T. Kazangey
Control and Electromechanical
Subdivision
Guidance and Control Division

Approved by

D. J. Griep
D. J. Griep, Director
Control and Electromechanical
Subdivision
Guidance and Control Division
Engineering Science Operations

L. R. Sitney
L. R. Sitney, Associate Group
Director
Advanced Vehicle Systems Directorate
Systems Planning Division

FOREWORD

This report covers those activities conducted under Study 2.3, System Cost/Performance Analysis, under NASA Contract No. NASW-2472 from 1 September 1972 through 31 August 1973. The Aerospace Corporation Task Manager was T. Kazangey. The NASA Technical Director was R. R. Carley. The NASA review team consisted of the following persons: C. M. Akridge, W. S. Rutledge, G. E. Mosakowski, D. B. Clemens, H. Mandell, R. W. Abel, T. Campbell, and W. Little.

The author acknowledges with graditude the many individuals at The Aerospace Corporation who contributed to this effort.

ABSTRACT

The principal objective of this task was to identify and quantify the relationships between performance, safety, cost, and schedule parameters in support of an overall effort to generate program models and methodology that provide insight into the effect of changes in specific system functional requirements on a total space vehicle program.

A first step in the development of such a methodology was to use a specific space vehicle system, the attitude control system (ACS). A modeling methodology was selected that develops a consistent set of quantitative relationships among performance, safety, cost, and schedule, based on the characteristics of the components utilized in candidate mechanisms. These descriptive equations were developed for a three-axis, earth-pointing, mass expulsion ACS. A data base describing typical candidate ACS components was implemented, along with a computer program to perform sample calculations.

This approach implemented on a computer is capable of determining the effect of a change in functional requirements to the ACS mechanization and the resulting cost and schedule. By a simple extension of this modeling methodology to the other systems in a space vehicle, a complete space vehicle model can be developed.

The methodology development began with a review of performance models, cost models, and data bases in order to determine their utility for this task. The results of the review revealed many costing methodologies, with the extremes being the "dollar per kilogram" and "cannot be done without designing the system first" approaches. The modeling approaches reviewed did not provide quantitative relationships between the performance, safety, cost, and schedule parameters of the particular system studied. In

particular, none of the costing methodologies was capable of predicting the effect of a change in payload or mission functional requirements on the cost and schedule of the particular system studied. In addition to a lack of suitable costing methodologies, the review revealed a need for the detailed ACS component data.

The quantitative relationships termed "aggregate equations" were written to describe the performance, safety, cost, and schedule of a specific ACS in terms of the components used in the specific ACS configuration. The equations were termed "aggregate equations," because the independent variables that describe the ACS were "aggregated" into fundamental relationships to the parameters of performance, safety, cost, and schedule. For example, the aggregate equation for the pointing accuracy of a three-axis, mass expulsion, earth-pointing control system considers performance parameters such as attitude sensor noise and misalignment, gyroscope drift and misalignment, signal processor noise, and control system deadband. Each of these performance parameters is multiplied by a computed sensitivity coefficient and combined appropriately in a worst case and/or root-sum-square manner to form the aggregate equation for the pointing accuracy of a three-axis, mass expulsion control system. Aggregate equations were developed for each of the parameters of performance, safety, cost, and schedule to form the set of quantitative descriptive equations for a single type of control system (three-axis, mass expulsion, earth-pointing). Other control system configurations, e.g., dual spin, require a different set of aggregate equations to define the performance, safety, cost, and schedule relationships.

The modeling methodology developed begins with the description of the mission and payload functional requirements and, via a filtering technique, selects the most applicable control method (such as gravity gradient, mass expulsion control, momentum storage, or spin stabilization) that will satisfy all the mission and payload functional requirements. For each control method, a functional block diagram is drawn, depicting generically the type of components that will be used to mechanize the particular ACS. Using the selected functional block diagram, the aggregate equations for performance, safety, cost, and schedule are written and incorporated into the computer program implementing the model. The specific components needed to mechanize the ACS are selected by the program, using the performance aggregate equations and the appropriate data base. The model proceeds by first accessing a data base consisting of all ACS components and choosing the cheapest ACS components, assuming a low-cost ACS is our objective. The characteristics of these components are used in the pointing aggregate equations to compute the pointing accuracy. If the computed system pointing accuracy does not meet or exceed the desired pointing accuracy, the program then selects the next least expensive component, assuming that more money buys better components. This process is iterated until the desired pointing accuracy requirement is met. The use of the aggregate equations and the data base accession were facilitated by programming the aggregate equations on a digital computer in this study. This computer program is capable of examining many combinations of components and storing those hardware configurations that have met or exceeded the desired pointing accuracy requirement.

The next step is to use the safety aggregate equations to evaluate those hardware configurations that have met or exceeded the desired pointing accuracy requirement. The safety considerations consist of failure rate, failure detection probability, and false alarm probability and hazard assessment (TNT equivalent and single-point failures[1]). The failure rate aggregate equation determines the level (and configuration) of redundancy (and component quality) necessary to satisfy the payload and mission reliability requirements. The failure detection and false alarm probability aggregate equations quantify the level of system monitoring (onboard or ground-based) needed to meet system success criteria. Those ACS hardware configurations that meet or exceed all the safety requirements are recorded by the computer program. The power, weight, volume, thermal specification, vibration specification, and ambient pressure specification for the selected hardware configurations are then computed using the appropriate aggregate equations. Thus, for a

[1] The model only considers these parameters conceptually.

given configuration, a set of applicable components is chosen (based, for example, on minimum cost or on schedule requirements) from the data base. This configuration satisfies all the performance and safety requirements. After the set of applicable components has been selected, the centralization of major components is considered. For example, should the space vehicle use a centralized power supply or separate power supplies for each subsystem? Also, the trade between centralized signal processing versus separate signal processing must be considered. Finally, the total ACS cost and schedule are predicted using the cost and schedule aggregate equations. This process may be iterated to meet cost or schedule requirements. One of the features of this aggregate equation approach is the ability to establish sensitivities to changes in functional requirements. One need only change the performance requirement (for example, pointing accuracy) and let the process iterate again to get new results.

The aggregate equations are computerized so that many combinations of ACS components can be examined to determine the best ACS mechanization for a variety of tradeoff criteria in a short period of time. This allows the user to determine the sensitivity of cost and schedules to functional requirements in a rapid manner, which is necessary in a proposal or preliminary design phase. A computerized model is adaptable to the changing needs of a program, since specific aggregate equations may be upgraded as a project progresses from its conceptual phase through the critical design phase. As increasingly definitive ACS configurations and data base material become available during the design phase, specific aggregate equations and data may be easily changed via computer algorithms to reflect the normal progression of the design process.

In addition to the ACS, attention was directed to the power conditioning subsystem, the thermal control subsystem, and the ground support systems. A "first-cut" set of aggregate equations was developed for the power conditioning subsystem. The thermal control subsystem and the ground support systems were examined to identify the pertinent factors needed to develop a "first-cut" set of aggregate equations.

CONCLUSIONS

The principal objective of this task was to identify and quantify the interrelationships between and within the performance, safety, cost, and schedule parameters in support of an overall effort to generate program models and methodology that provide insight into the effect of changes in specific system functional requirements on the total vehicle program. So that this objective could be accomplished, a viable Cost/Performance Model methodology that identified and quantified these relationships via "aggregate equations" was developed for a specific space vehicle system, the attitude control system (ACS). This methodology is designed to be applicable to all phases of a project. As the design progresses, the model and the supporting data base may be updated with more definitive information. A sample case of the model was implemented on a CDC 7600 computer for a three-axis stabilized, earth-pointing, mass expulsion ACS. In its computerized form, the model provides the designer with an interactive capability. It allows the designer to input specific data on selected components and system requirements and, by root-sum-square and/or worst case analyses, to select hardware configurations.

The computer model aids the designer in evaluating trade studies and simplifies the achievement of a balanced system design, since the impact of changes in functional requirements (performance and safety) on the total vehicle program (cost and schedule) can be easily determined. This model will also be useful for evaluating the effect of new technology or standardized components by making suitable entries in the data base representing proposed component characteristics. If this modeling methodology is extended to other systems in a space vehicle, a complete space vehicle model can be developed.

Sample calculations were run for several performance and safety requirements, using a sample data base. For these restrictive cases, the model results are consistent with conventional cost-versus-weight cost estimating relationships (CERs). At the same time, the model is capable of providing insight into the effect of other variables (e.g., reliability and power) on system cost; this capability is not available using conventional CERs. This model also emphasizes the fact that system-cost-versus-system-weight relationships are discrete cost/weight points with significant gaps, rather than the continuous relationship implied by the data averaging approach of a conventional CER.

The model presently provides a means of determining a unified estimate of performance, safety, cost, and schedule on a single type of ACS for the use of both performance and cost analysts. With refinement of some aggregate equations and extension to other ACS types, this model will be applicable to trade studies concerning most ACS requirements. Similarly, it can be applied to other space vehicle systems as the required aggregate equations become available. If fully developed, the model will provide a single tool to determine a unified estimate of performance, safety, cost, and schedule for a vehicle that supports both cost and performance analyses.

RECOMMENDATIONS

This task developed a Cost/Performance Model methodology through a consistent set of aggregate equations relating performance, safety, cost, and schedule parameters. A sample case was developed for a three-axis, earth-pointing, mass expulsion attitude control system (ACS) in an on-orbit operational mode. This approach, implemented on a computer, is capable of determining the effect of a change in functional requirements to the ACS mechanization and the resulting cost and schedule. If this modeling methodology is extended to other systems in a space vehicle, a complete space vehicle model can be developed. Specific aggregate equations, such as the performance and safety aggregate equations, were developed to a greater level of detail than other aggregate equations. It is recommended that the aggregate equations developed during this study be "refined," especially for parameters such as power, weight, volume, specifications, cost, and schedules. For example, there is no relationship between the cost and schedule aggregate equations. Further development should be undertaken to include this interrelationship. The present safety equations compute hardware reliability and failure detection probability; however, further development and review of the approach is required to quantify failure modes and detection probability, based on component characteristics in the data base, as well as to combine these to an overall value for probability of successful operation of the ACS during the entire mission duration.

Additional development is required to generalize the Cost/Performance Model sample equations for the ACS. Specifically, aggregate equations should be developed for other control methods (i.e., gravity gradient, momentum storage, and spin-stabilized) and for other operational modes (i.e., acquisition and powered flight). Quantitative relationships must still be developed for component centralizations and propellant hazards.

This task has considered only one type of space vehicle system in detail. If a total vehicle program is to be generated, aggregate equations for remaining space vehicle systems and for support systems (e.g., ground support equipment, flight operations) must be written. The modeling methodology has the capability of developing performance aggregate equations as either worst case and/or root-sum-square combinations. In the sample calculations, however, only root-sum-square combinations were implemented. The equations should be generalized to also compute worst case performance. The validity of aggregate equations depends on the quantity and quality of component and system data. It is recommended that the development of the component data base to support a total vehicle model be continued. The possibility of providing this data by having data collected for Resource Data Storage and Retrieval (REDSTAR) system at the component level should be investigated. It will be necessary, however, to have additional component data items such as accuracies, reliabilities, and failure detection capabilities added to the REDSTAR format. The data collected should be reviewed by both cost and performance analysts to ensure that the model outputs are satisfactory for evaluation of both performance and cost of a system.

After the additional development recommended above, sample cases should be computed that can be compared with results from the vehicle synthesis model and the Space Transportation System cost-estimating relationships (CERs). Following validation, this model should be usable in conjunction with these models to provide better cost and schedule estimates.

It is recommended that the fiscal year 1974 effort include extension of the model to other space vehicle systems; improvement of the data base to be acceptable for both performance and cost analyses; testing of the capability of the model to predict space vehicle interrelationships; and a user review to evaluate the potential of the model to assist in programmatic change control such as configuration management.

CONTENTS

CONTENTS (Continued)

CONTENTS (Continued)

CONTENTS (Continued)

CONTENTS (Continued)

CONTENTS (Continued)

CONTENTS (Continued)

PRECEDING PAGE BLANK NOT FILMED

FIGURES

FIGURES (Continued)

FIGURES (Continued)

TABLES

TABLES (Continued)

TABLES (Continued)

TABLES (Continued)

TABLES (Continued)

1. INTRODUCTION

A. TASK OBJECTIVE

As the space program matures into an applications industry, greater emphasis will be placed on improving the ability to predict the effect of program requirements on cost and schedules. Current advanced studies are estimating benefits for standardized subsystems and components, on-orbit servicing, and ground refurbishment of spacecraft, etc. Cost-estimating techniques that give greater insight earlier in the program cycle are required. As a step in this direction, this study was initiated to identify and quantify the interrelationships between and within the performance, safety, cost, and schedule parameters as delineated in Table 1-1. These data would then be used to support an overall NASA effort to generate program models and methodology that would provide the needed insight into the effect of changes in specific system functional requirements (performance and safety) on a total vehicle program (cost and schedule).

B. STUDY APPROACH

The initial planning of the task divided the effort into six subtasks. The effort began with two subtasks. The first, development of flow charts of the design process, included a literature search and the initial development of modeling methodology. The second subtask developed background information on other modeling methodologies and on data bases. The remaining tasks included data development to collect properly formatted component data for sample calculations, refinement of the modeling methodology, the calculation of a sample case, and the preliminary modeling of other related subsystems.

The attitude control system (ACS) was selected as the first space vehicle system to be used in the development of a modeling methodology described by such quantitative relationships. So that an early assessment of

Table 1-1. Model Parameters

1.0.0	PERFORMANCE		
	1.1.0	Technical Characteristics	
		1.1.1 1.1.2 1.1.3 1.1.4	System peculiar; (i.e., no fewer than four items, no more than ten items)
	1.2.0	Power	
		1.2.1	Average
		1.2.2	Peak
	1.3.0	Weight	
	1.4.0	Volume	
	1.5.0	Vibration Specification	
		1.5.1	Random (g rms)
		1.5.2	Non-random
	1.6.0	Temperature Specification	
		1.6.1	Radiation
		1.6.2	Conduction
	1.7.0	Ambient Pressure Specification	
2.0.0	SAFETY AND HAZARDS		
	2.1.0	Failure Assessment	
		2.1.1	Failure rate
		2.1.2	Number of single point failure locations
		2.1.3	Number of dual point failure locations
	2.2.0	Failure Detection Probability	
	2.3.0	False Alarm Probability	
	2.4.0	Hazard Potential	
		2.4.1	Latent energy
		2.4.2	Radiation energy

Table 1-1. Model Parameters (Continued)

3.0.0	COST		
	3.1.0	Design and Development	
		3.1.1	Engineering
		3.1.2	Development
	3.2.0	Build and Checkout	
		3.2.1	Tooling
		3.2.2	Manufacturing
		3.2.3	Quality control
		3.2.4	Clerical
	3.3.0	Test Hardware	
	3.4.0	Training and Simulation	
	3.5.0	Support for 10 to 15 Years in Service Life	
	3.6.0	Management	
4.0.0	SCHEDULE (Time for Completion)		
	4.1.0	Proposal	
	4.2.0	Preliminary Design and System Analysis	
	4.3.0	Subsystem Analysis, Design, and Breadboard Testing	
	4.4.0	Prototype Design, Fabrication, and Test	
	4.5.0	Subsystem Production Engineering, Fabrication, and Testing	
	4.6.0	System Integration and Test	
	4.7.0	Flight Test Phase (Flights 1 to 5)	
	4.8.0	Initial Operational Phase (Flights 6 to 20)	
	4.9.0	Operational Phase (Remaining Flights)	

the modeling methodology could be obtained, the sample case was restricted to a single type of ACS to demonstrate the feasibility of the approach prior to a wider application. The actual modeling methodology selected for this study develops a consistent set of quantitative relationships among performance, safety, cost, and schedule, based on the characteristics of the components utilized in candidate mechanisms. These descriptive equations were developed for a three-axis, earth-pointing, mass expulsion ACS. A data base describing typical candidate ACS components was developed, and sample calculations were performed on a digital computer. This approach, implemented on a computer, is capable of determining the effect of a change in functional requirements to the ACS mechanization and the resulting cost and schedule. If this modeling methodology is extended to other systems in a space vehicle, a complete space vehicle model can be developed.

Section 1. C reviews the development of background information and the modeling techniques considered that ultimately led to the cost/performance methodology developed under Task 2. 3.

C. BACKGROUND INFORMATION STUDY

At the start of the study, a review of potentially applicable cost modeling techniques was conducted. Included in this model review were the SAMSO/Aerospace cost-schedule models, the General Electric Co. design guide for ACS, the Honeywell cost analysis, the Resource Data Storage and Retrieval (REDSTAR) data base, and the Optimized Design Integration System (ODIN) and Integrated Programs for Aerospace Vehicles Design (IPAD) Programs. The following paragraphs present a brief description of the material reviewed.

Several distinct SAMSO/Aerospace cost-schedule models were reviewed during the early stages of Task 2. 3. These models are discussed in some detail in Section 2. In general, the models all use a cost-estimating relationship (CER) approach to cost-out a specific type of system. Separate CERs are often used for each program phase, such as the design, development, test, and evaluation phase; first article production; and ongoing operations. In each CER, cost is related to some distinct physical parameter such as weight or volume. Often a CER is developed using statistical least-squares regression on data obtained from previous programs; these "static" costs are distributed over time by a learning or improvement curve that takes into account reduced per-unit costs as production increases. In addition, inflation factors are usually included to account for reduction in purchasing power per dollar with increasing time. Finally, scheduling models are defined as a function of time and may run from simple, straight-line spreads to skewed variations of the normal distribution curve. Various input and output formats are employed, with input requirements primarily set by the type of CERs used and with output formats determined by the level of output detail in the work breakdown structure (WBS) and by schedule resolution.

In addition to the SAMSO/Aerospace models, other models and data bases were reviewed. These include a General Electric design guide for developing a satellite ACS, given mission requirements; the USAF 375 Series Manuals, which are structured along cost-accounting lines; and a Honeywell, Inc. cost analysis study. A portion of the Honeywell study consisted of a historical review of stabilization and control systems for Apollo, Gemini, and the F-104. An important conclusion of the Honeywell study was that an uncertain relationship exists between the weight of ACS space hardware and its cost. As mentioned previously, this relationship forms the basis of many CERs used by the space industry.

Included in the development of background information were reviews of several approaches to data base formulation and management. The REDSTAR system was one of those considered. It was the result of a 1972 fiscal year study, entitled Application of Engineering Cost Analysis, by Planning Research Corporation.

The WBS used in REDSTAR is divided inconveniently for an ACS designer; it tends to scatter ACS elements through a number of categories. This lack of correspondence between the WBS and the attitude control function does not mean that REDSTAR is not applicable to cost/performance modeling.

However, a translation matrix, as developed in this study, would have to be used to interpret the WBS in a manner useful to a model that includes system performance as an integral part of its methodology.

Several in-house data base systems used by The Aerospace Corporation were also reviewed. Unfortunately, very little component data of the nature required for a cost/performance-oriented model of the type developed in this study were found.

As the final task in development of background information, the ODIN and IPAD Programs were investigated. The ODIN integrates computer-implemented models used for various aspects of system design and provides an optimum systems engineering approach to overall vehicle design. The IPAD supports the engineering design team by implementing, as much as possible, the computation and data management aspects of the design process. Conceptually, the Cost/Performance Model could be one module of the ODIN or IPAD system.

D. MODELING APPROACHES

In the conceptual stage of Task 2.3, effort was devoted to the initial formulation of an approach to cost/performance modeling. During this stage, a number of methodologies were conceived and required evaluation. The following criteria were formulated to judge each concept in a complete and objective manner and were used to evaluate the utility of each approach:

1. A prime objective is to determine sensitivity of cost to changes in requirements.
2. The modeling methodology must not impose a cumbersome reporting structure on the contractor.
3. The modeling methodology must reflect costs from all phases of development through operations.
4. The approach taken should reflect current design practice and tradeoff procedures.
5. The model should achieve a balanced total vehicle design, considering total life-cycle costs in terms of performance, safety, and schedule requirements.

In general, all modeling approaches considered can be subdivided into two basic categories. Bottom-up approaches, the first category, depend on development of a system design. Estimates of tasks, material costs, manpower requirements, and schedules are made at each identifiable level of system integration; total estimates are obtained by summing individual costs and schedules.

Top-down models, the second category, are essentially the CER approach described previously. As CERs have been unsuccessful in meeting the prime criterion of determining cost sensitivity to program requirement changes, top-down approaches were judged unacceptable for a Cost/Performance Model. Further, it was thought that a model oriented from the bottom up could lead to fulfillment of the previously stated criteria.

A model, called the "minimum" model, was hypothesized as a basis for development of a cost/performance methodology. The minimum model considered, but did not adequately quantify, the performance, safety, cost, and schedule of an ACS. The "minimum" model was later expanded and became the Cost/Performance Model. Starting with functional payload requirements, a filter algorithm would be developed to determine an attitude control method to satisfy these requirements. Once the basic type of ACS, such as momentum storage, mass expulsion, or other applicable method, was determined, various design configurations would be considered.

Several models were examined in attempts to implement the minimum model. Details of two of these approaches and their applicability to a cost/performance modeling viewpoint are given in Section 3.

E. COST/PERFORMANCE MODELING METHODOLOGY

The modeling approaches reviewed did not provide quantitative relationships among the performance, safety, cost, and schedule parameters for an ACS. When both the top-down and bottom-up approaches were reconsidered, it was decided that a Cost/Performance Model oriented from the bottom up could lead to a model employing quantitative expressions that would output performance and cost sensitivities. A set of basic equations, termed "aggregate equations," was written to describe the performance, safety, cost, and schedule of the ACS in terms of the equipment used in a selected configuration. The equations were termed "aggregate equations," because the independent variables describing the ACS were "aggregated" into fundamental relationships to the elements of performance, safety, cost, and schedule. For example, the aggregate equation for the pointing accuracy of a three-axis ACS considers variables such as attitude sensor noise and misalignment, gyroscope drift and misalignment, signal processor noise, and control system deadband. Each of these variables is multiplied by a computed sensitivity coefficient and combined in a worst case and/or root-sum-square manner to form the aggregate equation for the ACS pointing accuracy.

The Cost/Performance Model was developed using aggregate equations in conjunction with minimum model elements. The flow diagram from this model is shown in Figure 1-1. Starting with payload functional requirements, a filtering technique (search/sort/filter) is used to determine an attitude control method (such as a gravity gradient, mass expulsion control, momentum storage, or spin stabilization) that will satisfy the functional requirements. The selection of an attitude control method is made because each different ACS configuration has its own set of performance aggregate equations. Other relationships, such as the aggregate equations for safety, cost, weight, etc., remain unchanged or require only minor modifications, such as changing coefficients. Once a basic control method is determined, the type of equipment needed to mechanize the ACS can be selected by iteration. Accessing a data base consisting of all ACS components suitable for this control method, the model first inserts the cheapest component into the pointing-accuracy aggregate equation, assuming low-cost ACS is our objective, and computes the pointing accuracy. If the pointing accuracy is poorer than desired, the model then selects the next least expensive set of components, iterating until the desired pointing accuracy is met.

The next step is to use the safety aggregate equations to evaluate those hardware configurations that have met or exceeded the desired pointing

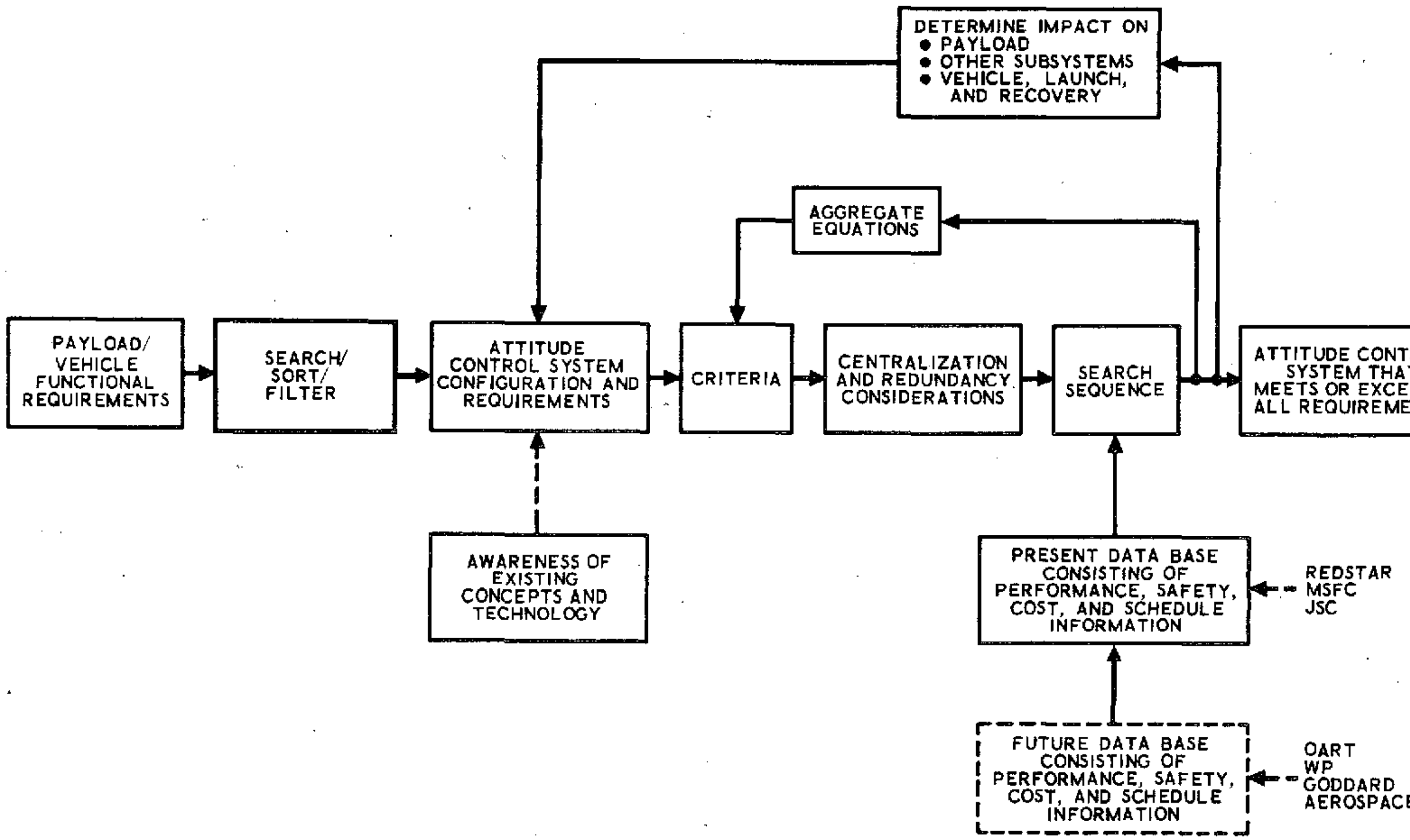

Figure 1-1. Cost/Performance Model

accuracy requirement. The safety considerations consist of failure rate, failure detection probability, and the false alarm probability and hazard assessment (single point failures and TNT equivalent[1]). The failure rate aggregate equation determines the necessary level (and configuration) of redundancy (and component quality) to satisfy the payload and mission reliability requirements. The failure detection and false alarm probability aggregate equations quantify the level of system monitoring (onboard or ground-based) needed to meet system success criteria. Those ACS hardware configurations that meet or exceed all safety requirements are recorded by the computer program. The power, weight, volume, thermal specification, vibration specification, and ambient pressure specification for the selected hardware configurations are then computed using the appropriate aggregate equations. Thus, for a given configuration, a set of applicable components is chosen (based for example, on minimum cost or on schedule requirements) from the data base. This configuration satisfies all the performance and safety requirements. After the set of applicable components has been selected, the centralization of major components is considered. For example, should the ACS use a centralized power supply or separate power supplies? Also, the trade between centralized signal processing versus separate signal processing must be considered. Finally, the total ACS cost and schedule are predicted using the cost and schedule aggregate equations. This process may be iterated to meet cost or schedule requirements. One feature of this aggregate equation approach is the ability to establish sensitivities to changes in functional requirements. One need only change the performance requirement (for example, pointing accuracy) and let the process iterate again to produce new results.

The following sections describe the major elements of the Cost/Performance Model, starting with the search/sort/filter technique that selects an attitude control method based on a set of performance requirements. Following the filter description, the aggregate equations and their relationship in forming the Cost/Performance Model are discussed.

[1] The model only considers these parameters conceptually.

1. SEARCH/SORT/FILTER TECHNIQUE

In the development of the search/sort/filter technique, the usual problem of attempting to find a system that meets certain requirements was inverted. The approach is based on the existence of only a finite number of attitude control methods. The problem is then worked in a manner to determine what requirements are met or exceeded by each individual method. Once this information has been tabulated for all attitude control methods, sorting the possible attitude control techniques by searching through the search/sort/filter matrix to find systems meeting the requirements is a straightforward problem.

The input to the filter is based on ACS requirements originating from the character of the mission and thenature of the payload. The requirements delineate orbital characteristics, spacecraft orientation, spacecraft performance, and general vehicle characteristics. For example, the mission and payload requirements determine the orbit of the spacecraft, the duration or lifetime of the vehicle, the nominal orientation, the attitude and attitude accuracy of the ACS, and the stationkeeping and reorientation requirements.

ACS requirements derived from the basic mission and payload requirements are categorized, and, in general, multiple control methods may seem appropriate for a given set of ACS requirements. Therefore, a rationale is required to choose among the possible candidates. This rationale is provided by functional requirements, with performance, safety, cost, and schedule providing quantitative criteria for tradeoff studies in the detailed engineering analysis of the ACS.

The output of the filter is the one or more control methods appropriate for the mission under consideration. For the Task 2.3 study, various attitude control methods are classified as active, semi-active, or inactive.

An active control method uses one or more feedback loops to maintain the vehicle attitude within specified limits. Such a closed-loop system is completely self-contained by the spacecraft.

An inactive attitude control technique directs the vehicle orientation by a passive feedback system. No sensors, control logic, or actuators are required by an inactive attitude control technique.

The semi-active category covers all schemes that employ some of the elements of an active control technique. This may take the form of attitude sensors so that the spacecraft orientation may be estimated by ground-based data processing.

In all, nine distinct types of attitude control were considered, in which inactive and semi-active configurations are possible for five of the attitude control techniques. Three methods employ active or at least semi-active control methods to provide stabilization. Finally, a method was included to cover those cases where multiple sources of control torque can be used successfully in concert (for example, combined gravity gradient and magnetic stabilization).

2. AGGREGATE EQUATIONS AND FUNCTIONAL BLOCK DIAGRAMS

Aggregate equations are the primary elements of the Cost/Performance Model; however, these equations depend on the particular ACS mechanization selected. Thus, as a starting point in the determination of aggregate equations, functional requirements are translated into function block diagrams to determine general ACS mechanizations and associated aggregate equations. Next, centralization and redundancy would be considered, leading to specific block diagrams from which more detailed aggregate equations are ultimately derived.

Functional requirements are considered for the following four classes of vehicles:

Class	Type of Vehicle
1	Unmanned, expendable, autonomous
2	Unmanned, reusable, autonomous
3	Manned, reusable, autonomous
4	Manned, reusable, using ground support

Requirements for these vehicles are tabulated, and their functional ACS block diagrams are discussed for both coast and powered-flight phases. The aggregate equations for each ACS type that can be selected by the filter must be formulated and available to the Cost/Performance Model. Thus, following selection of a particular ACS mechanization by the search/sort/filter, a specific set of aggregate equations would be selected. These equations quantitatively relate performance, safety, cost, and schedule of the mechanization. As a demonstration of how this is accomplished, aggregate equations are discussed in the context of their implementation as a digital computer simulation. This discussion is presented to aid illustration of the flow of information through the Cost/Performance Model and to provide a natural transition to the description of the Cost/Performance Simulation following the discussion of aggregate equations.

a. Performance Aggregate Equations

Aggregate equations were developed for a Tug-type vehicle with a three-axis mass expulsion ACS, using horizon scanners for pitch and roll reference and gyrocompassing for yaw reference. This particular type of mechanization is typified by the Agena vehicle.

Vehicle attitude is sensed by a three-axis, body-mounted inertial reference unit containing integrating gyros referenced to earth coordinates by horizon scanning and gyrocompassing. Fixed attitude with respect to the earth is maintained by a pitch program giving the required orbital pitch-over rate.

An illustration of a typical performance aggregate equation is the pitch attitude error equation. This equation is derived in this report and quantifies pitch attitude error in coast flight in terms of the control system deadband and errors associated with components such as the pitch gyro, horizon sensor, and electronics. If the instrument or component errors are known and stored in a computer-implemented data base, the pitch attitude error may be calculated and compared to an allowable error entered as an input to the computer-implemented Cost/Performance Model. Furthermore, the same sort of calculation and comparison could be performed for each ACS channel and for each complete combination of sensors stored in the data base. Thus, if the data base contains information characterizing three distinct inertial measurement units (IMUs) and five horizon sensors, a total of 15 IMU/horizon sensor combinations would be available to implement the ACS, and each would have a distinct pitch channel attitude error as calculated by the pitch aggregate equation.

The above described method of forming and evaluating ACSs is basic to the Cost/Performance Model. Only systems (combinations of data base components) meeting performance requirements are stored and subjected to further processing as defined by additional performance, safety, cost, and schedule aggregate equations. Additional performance-oriented processing includes calculation of propellant consumption, power, weight, or vibration.

Not all performance aggregate equation results are subject to an evaluation or comparison procedure. While ACS accuracy in a given channel is compared to an allowable error, system weight, power, or propellant consumption typically is merely calculated and stored as a characteristic descriptive of a specific ACS. These items often represent impacts on subsystems other than the ACS, and would provide information to other modules of an expanded Cost/Performance Simulation. Subsequent iterations would be performed to ensure a balance between the impact on various subsystems to ensure a balanced vehicle design.

b. Safety Aggregate Equations

As a result of satisfying certain performance aggregate equations, a finite number of ACS configurations are formed by the Cost/Performance Model. As the next step in processing these configurations, the safety aggregate equations are introduced. These equations are categorized as failure rate, failure detection probability, and false alarm probability aggregate equations.

The failure rate equation is used to calculate the reliability of each ACS configuration. This calculation is performed at a module level, with the ACS viewed as consisting of four separate modules. The modules considered are the sensor, processor, actuator, and energy source modules. Each identifiable ACS component is considered as an element of one of these modules. Thus, horizon sensors and IMUs would be categorized in the sensor module; computers or control logic, in the processor module; pumps, in the actuator module; and propellant tanks, in the energy source module. Failure rate information stored in the data base for each component is extracted as needed by the Cost/Performance Model. These are combined by safety aggregate equations to form failure rates for each module of the first ACS configuration stored as a result of previous processing by performance aggregate equations. Module failure rates are combined by still other safety aggregate equations to calculate total ACS reliability for a given mission duration.

Again, as in the previous performance aggregate equation processing scheme, the calculated reliability of each particular ACS configuration is evaluated against a specified or acceptable level provided as a model input. However, the ACS configuration is not discarded, as it was during performance evaluation, if it does not meet the specified reliability level. Instead, a search for the lowest reliability module is initiated. Upon identification, this module is paralleled by an identical unit, and suitable aggregate equations are used to recalculate the system reliability. The evaluation and paralleling process continues until the lowest reliability module is triply redundant. If the system still does not meet the specified reliability, it is deleted from consideration as a viable single-string ACS. However, should it, at any time, meet or surpass the required input reliability level, aggregate equations are used to calculate system failure detection and false alarm probabilities. In addition, system characteristics such as weight, volume, and total component cost are updated and stored. These items must be updated in case the paralleling process has changed ACS total system characteristics. This process continues until each ACS stored as a result of meeting performance requirements has been processed.

The safety aggregate equation procedure described above essentially constitutes one-third of the total safety aggregate equation process. Following completion of the basic scheme, the whole procedure is repeated with each ACS configuration mechanized, first as an active/standby (dual string) ACS, and then as a triply redundant ACS using voting. The terms "active/standby" and "triply redundant" here refer to complete ACSs in addition to modular levels of redundancy. For this reason, a separate set of aggregate equations is used for processing single-string, active/standby, and triply redundant systems.

The possible number of acceptable ACS mechanizations following safety aggregate equation processing is triple the number of systems that successfully passed the performance aggregate equation process. This fact is accounted for in the computer-implemented Cost/Performance Model, by keeping track of three complete sets of system characteristics for each ACS configuration originally meeting or surpassing performance requirements.

Details of safety aggregate equations and flow charts depicting the processing schemes discussed above are presented in the main body and appendixes of this volume.

c. Cost Aggregate Equations

Two costing techniques are presented in the main body of this report. The first develops cost aggregate equations, using a data base structured in a manner similar (but not identical) to the REDSTAR data base mentioned previously. This technique results in six cost categories, each described by an aggregate equation that is a function of various labor rates, task man-hours, material costs, and the number of specific items required, such as engineering drawings. Summation of costs for each category determines the total cost of the ACS. These cost aggregate equations, to be a useful tool, require data in a very detailed WBS format. Unfortunately, such data generally are not available until a design has progressed into its intermediate phase. An alternate component costing technique was therefore developed to calculate costs in the very early design phase. This alternate technique, described below, is the one used in the cost/performance computer simulation.

The component cost approach, which is the second costing approach, develops cost aggregate equations based on the cost of ACS components selected via the performance and safety aggregate equations and requirements. This costing technique requires each ACS component to have non-recurring and recurring cost information as part of its data base. This cost information is available from the REDSTAR data base. Aggregate equations then sum non-recurring material costs for each component used in a specific ACS mechanization to determine total non-recurring material costs for each program phase, such as the design and development or the build and check-out phase. The form of the non-recurring material cost aggregate equation is a sum of the non-recurring costs of the ACS components multiplied by an inflation factor. Phase costs are then summed to determine total non-recurring material costs.

ACS non-recurring systems engineering costs are defined as a function of total non-recurring material costs, and the material and systems engineering costs are finally summed to give total ACS non-recurring costs.

Total recurring cost aggregate equations are structured in much the same manner as the non-recurring cost equations. Finally, ACS total costs are obtained by adding recurring, non-recurring, and management costs, where management cost is a percentage of total ACS cost. If more than one ACS is produced, a learning curve is used to account for reduced unit cost as additional units are built.

d. Schedule Aggregate Equations

Schedule aggregate equations determine the amount of series time required to develop an operational ACS. This determination is accomplished by dividing the life cycle of the system into nine phases, beginning with the proposal phase and ending with the operational phase. Aggregate equations then describe each phase time in terms of the manpower available to complete a specific phase.

So that required manpower can be estimated, manpower aggregate equations are formulated, based on activities associated with each phase. Schedule analysis matrices and flow charts are used as a master list from which to select pertinent activities. The charts and matrices take into account various schedule parameters, such as sequence constraints, man-loading limitations, production quantity, production rate, and delivery span.

F. COST/PERFORMANCE SIMULATION

This section presents a brief summary of the Cost/Performance Simulation to show the manner in which aggregate equations interact with the cost performance data base and among themselves.

Figure 1-2 presents an overview of the ACS Cost/Performance Simulation. The flow is the same for batch process operations as for on-line terminal operation.

As depicted in Figure 1-2, entry of model variables and matrices initializes the program. A complex data base results from the many inputs required to define various ACS components. Therefore, the program is structured to allow entry of a stored data base, followed by easy program data base modifications or additions.

The data base actually implemented is the Table 1-1 data base presented in detail in Section 6 of this report. It is essentially a list of all components available to configure various types of ACSs, with each component described in terms of parameters required as inputs to performance, safety, cost, and schedule aggregate equations.

Following the first initialization phase, consisting of data base entry and modification, data are provided for the various performance, safety, cost, and schedule criteria to be used in the program during execution. For example, performance criteria (such as the required coast flight attitude control accuracy in roll, pitch, and yaw axes) are the inputs during this

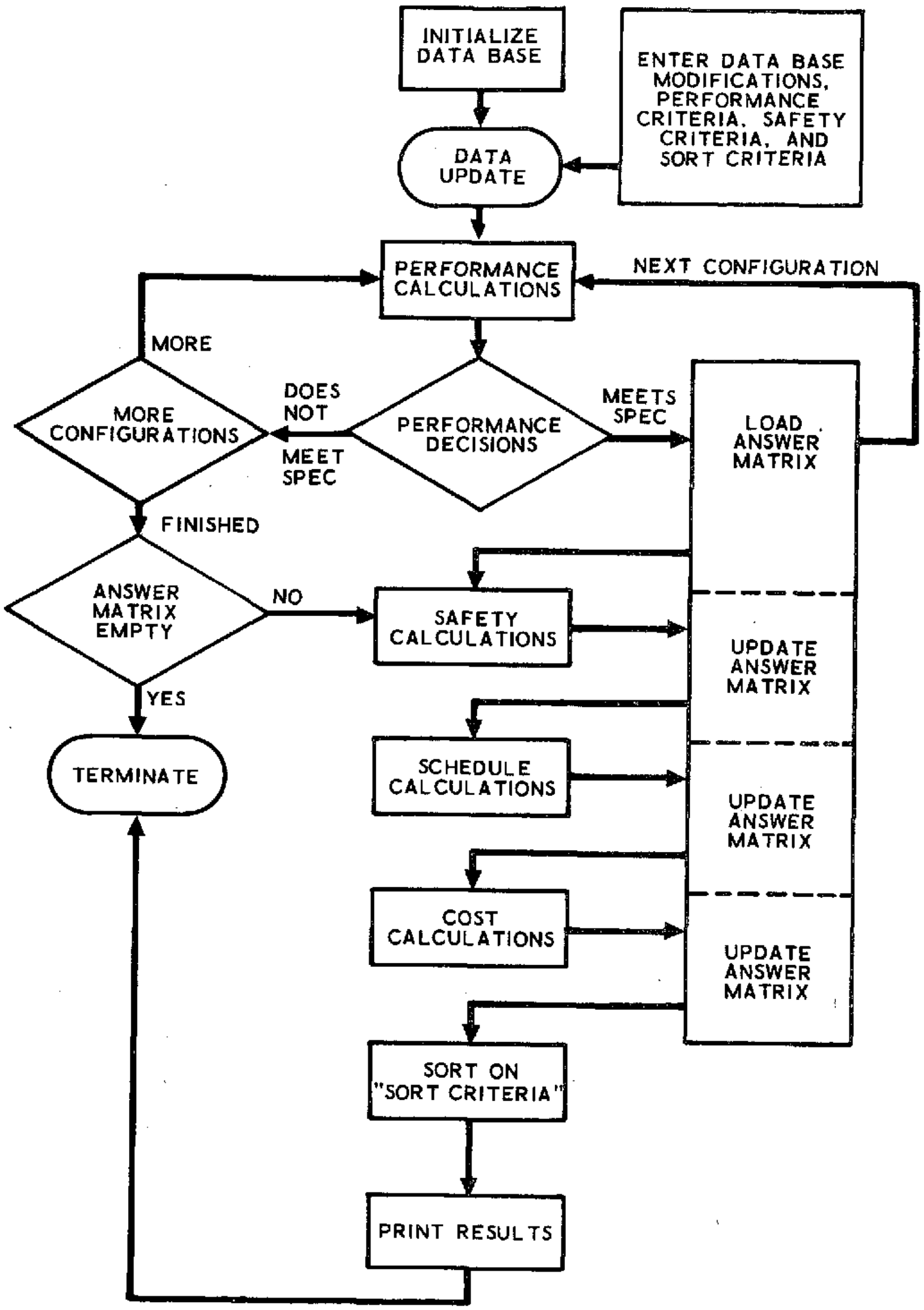

Figure 1-2. Cost/Performance Simulation Overview

second phase of the program initialization procedure. These inputs are used to evaluate acceptability of specific ACS configurations as described in the discussion of aggregate equations. A similar input would specify a required ACS mission success probability, and set a criterion for acceptance of each candidate ACS configuration during program execution of safety aggregate equations. Final inputs prior to program execution provide sort criteria that will format program outputs by ranking acceptable ACS configurations according to cost, reliability, accuracy, or any other criterion calculable, using aggregate equations implemented in the simulation.

As described previously, the safety aggregate equation module immediately follows implementation of the performance module in the sequence of operations performed during execution of the Cost/Performance Simulation. All ACS configurations that have successfully passed performance criteria and are stored in the answer matrix are screened by the safety module, as indicated in Figure 1-2. Those single-string systems not meeting reliability criteria are upgraded by paralleling the lowest reliability module in the ACS sensor, processor, actuator, energy source module string. The total reliability of the improved system is then recalculated and checked for compliance with reliability specifications. If the system is still unacceptable, paralleling of the weakest module continues. (The weakest module may or may not be the same module paralleled previously.) This process is continued until the system is acceptable, or until a module exceeds triple redundancy, at which point the program rejects the configuration as unacceptable in a single-string mechanization and proceeds to evaluation of the next configuration. Should the system meet reliability criteria, failure detection probability and false alarm probability are calculated for the configuration, and the system is stored in the answer matrix as an acceptable single-string mechanization.

After all configurations stored in the answer matrix have been evaluated for compliance with reliability criteria when mechanized as a single-string ACS, the program proceeds to evaluate each configuration in an active/standby ACS mechanization. As before, paralleling of modules is allowed to upgrade reliability of the active/standby mechanizations, and individual modules are held to maximums of triple redundancy. Systems meeting reliability criteria have failure detection and false alarm probabilities calculated, and are then stored in the answer matrix as an acceptable active/standby mechanization.

Following evaluation of all answer matrix entries as active/standby mechanizations, the program evaluates each entry in the answer matrix mechanized as triply redundant ACS with voting. In this sample mechanization, upgrading of individual modules by paralleling is not allowed, as the total ACS is already triply redundant. Other calculcations proceed much as described for previous mechanizations, and detailed flow charts of the procedures described above are provided in Section 5 of this report.

Configurations not meeting reliability criteria after safety module processing are deleted from the answer matrix, and the program proceeds to processing of schedule and cost aggregate equations.

Upon completion of the ACS requirements phase of initialization, the program begins execution of performance aggregate equations and decisions.

In the performance module of the Cost/Performance Simulation, the acceptability of each candidate ACS is evaluated by comparing calculated ACS performance, as determined by performance aggregate equations, to required ACS performance parameters entered during program initialization. The flow of calculations in this module may be relatively simple, such as those shown in Figure 1-2, or they may be more complex and essentially represent a basic error analysis of a particular ACS configuration. In general, use of the simulation during early conceptual phases of a program would rest on several baseline ACSs, with each specific baseline defined by a separate set of aggregate equations. Later applications could be based on a single ACS configuration requiring a single set of performance aggregate equations. The program is structured to accept these intermodule changes without disrupting the basic intramodule interactions that form the basis of the Cost/Performance Simulation.

Regardless of the level of sophistication of the performance aggregate equations, all ACS configurations passing the performance criteria are stored in the answer matrix. This matrix maintains a dynamic record of the characteristics of ACS configurations that have met or surpassed criteria entered during program initialization, such as total ACS weight or an identifier of a particular data base component that is a part of a specific ACS configuration.

Schedule and cost calculations are a straightforward implementation of the schedule/cost aggregate equations; however, the present sample program does not implement schedule equations. Present plans call for presenting schedule results as charts showing major program milestones for each configuration stored in the answer matrix. Each chart would be keyed to the printout of other information for the particular configuration that it represents; the total package represents complete assessment results of all ACS configurations meeting performance and safety criteria. For ease in evaluating various ACS configurations, printouts are ordered according to the particular criteria entered by the operator.

G. INTERACTION WITH OTHER SUBSYSTEMS

The interaction of the ACS with some of the other subsystems was briefly considered. A generalized guideline for the development of a power conditioning system for the ACS is given in Section 7. The major thermal drivers that influence the design and operation of typical ACS components are identified in Section 8. The nature of the requirements placed on the ground support equipment (GSE) by the ACS is discussed in Section 9.

H. COST/PERFORMANCE MODEL SAMPLE CALCULATION-CER COMPARISON

Figure 1-3 compares sample calculations of the Cost/Performance Simulation with a cost-versus-weight CER developed at SAMSO. The Cost/Performance Simulation output of cost versus weight for a three-axis ACS is

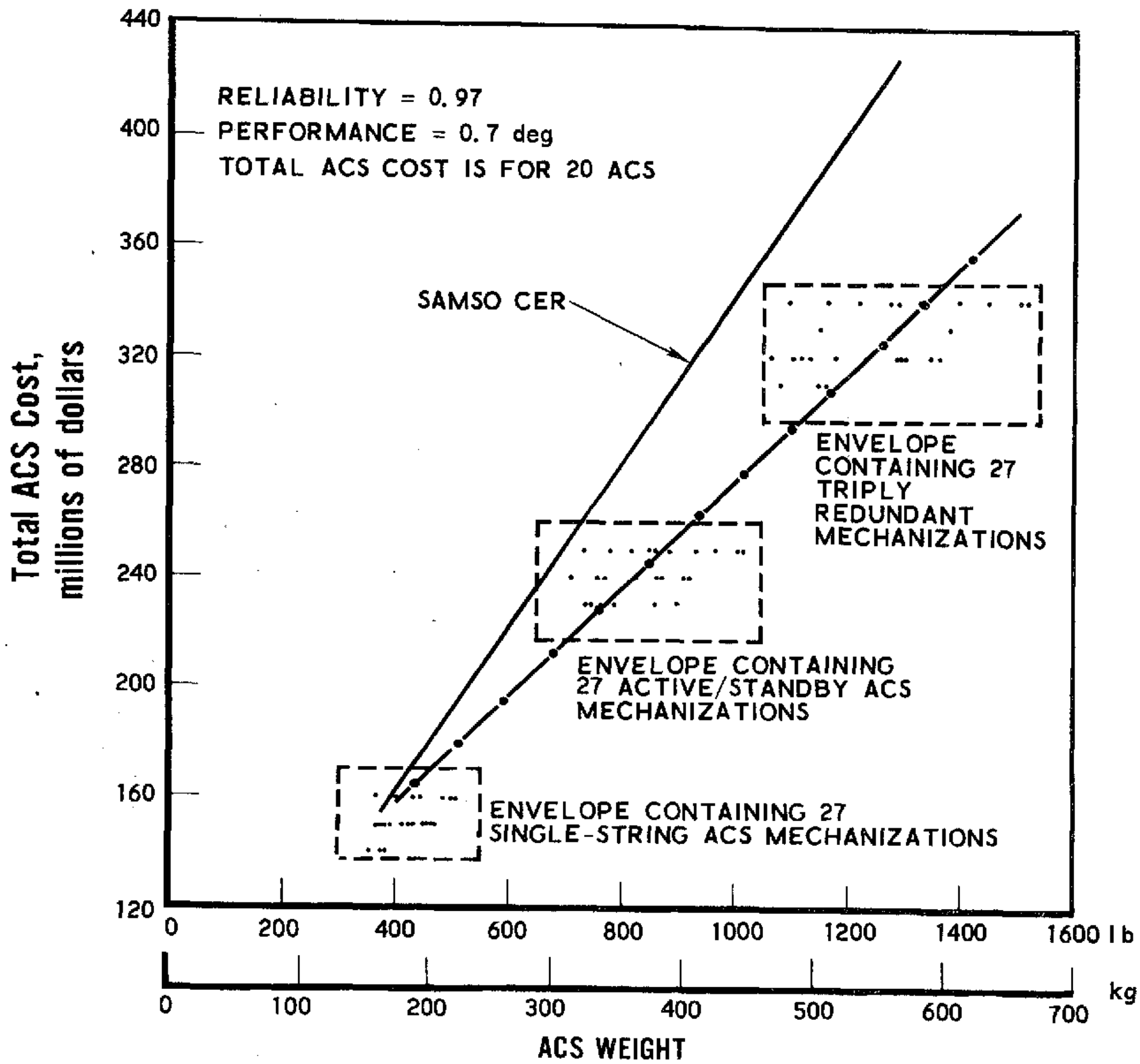

Figure 1-3. Total ACS Cost vs ACS Weight

consistent with the cost-versus-weight CER developed at SAMSO. CER results were obtained by summing DDTE costs, with first article cost adjusted by a learning curve to obtain the cost of 20 systems. These results were obtained using a data base consisting of three distinct horizon sensors, three star references, and three IMUs. This gives a total of 27 unique ACS component combinations or 81 ACSs, counting single-string, active/standby, and triply redundant mechanizations.

Figure 1-4 shows the cost-versus-reliability relationship for the same 20 systems. Details of this and other simulation results are given in Appendix C.

It is concluded, based on the curves of Figure 1-3, that Cost/Performance Model results are in substantial agreement with results obtained using conventional approaches. However, the Cost/Performance Model provides a more detailed insight and a potential for accomplishing sensitivity studies, using up-to-date data bases, and for performing trade studies between various subsystems unobtainable using converntional approaches; it also indicates regions where components are not available.

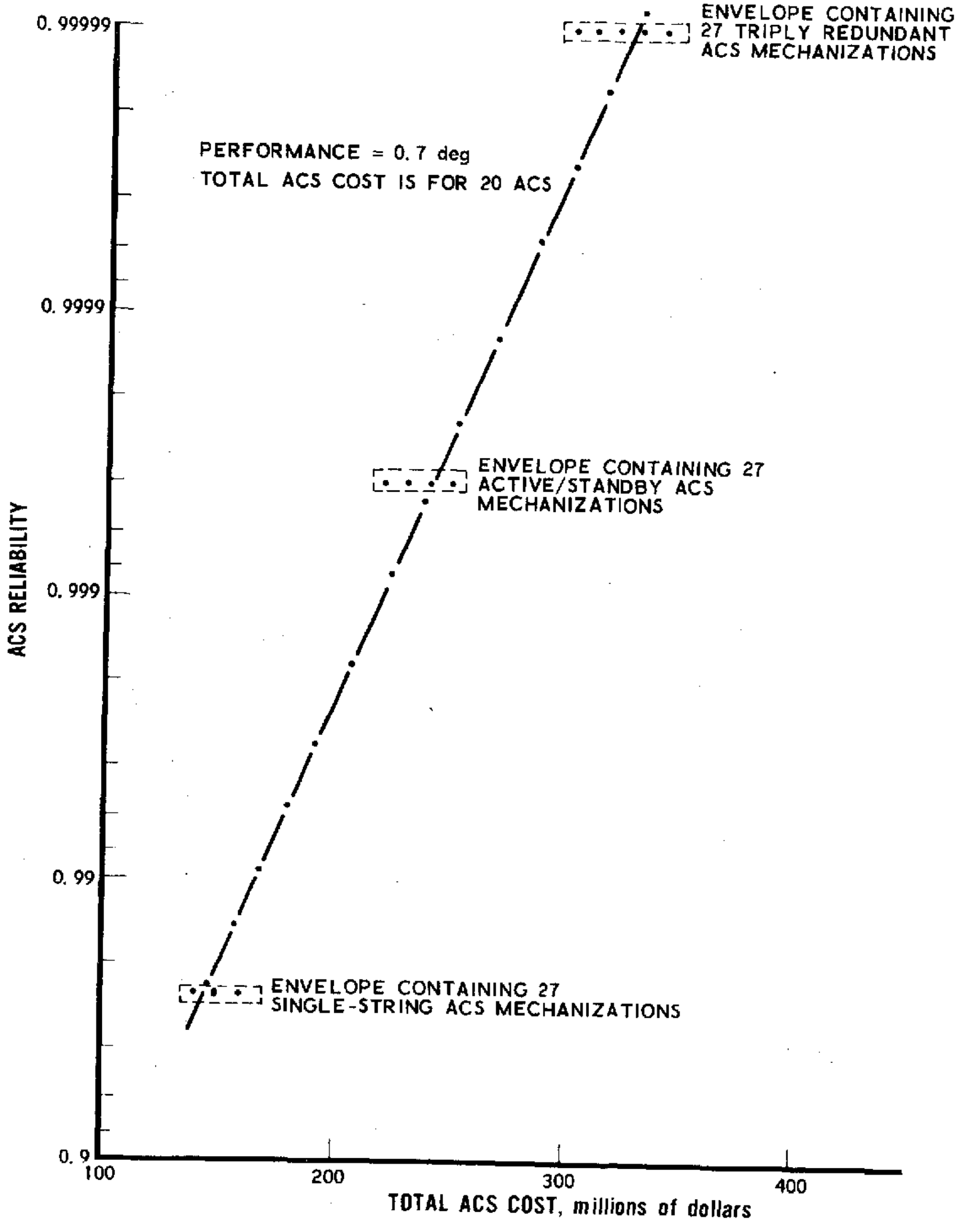

Figure 1-4. ACS Reliability vs Total ACS Cost

2. BACKGROUND INFORMATION DEVELOPMENT

A review of existing cost and performance estimating techniques and data bases was conducted to provide a basis for the development of a new methodology for relating performance, safety, cost, and schedule for an attitude control system (ACS). A literature search was conducted to ascertain related work already performed and to determine the strengths and limitations of existing techniques, and their applicability to any new methodology. As a part of the background information, a baseline ACS configuration was defined, and its requirements were developed.

A. REVIEW OF MODELS/PROGRAMS

This section summarizes and critiques the major aspects of existing cost and performance models as applied to the ACS. The review covered three Aerospace and SAMSO models (SAMSO/RAMMSS Model, Solid Rocket Motor Cost Model, Large Solid Rocket Motor Sizing Program); two joint NASA/Aerospace models (Space Transportation Model, Vehicle Synthesis Program); and other related models and material [General Electric Attitude Control Design Model, USAF System Command 375 Series Manuals, Honeywell Cost Analysis Study, Optimal Design Integration System (ODIN), and Integrated Programs for Aerospace Vehicles Design (IPAD) Programs].

A model is a set of equations and related mathematical expressions describing the essence of a problem. A cost model provides estimates of the cost of performing tasks and producing hardware and software. The reliability of these estimates is dependent on the quantity and quality of applicable data, and the use of analytical tools, logic, and reasonable intuition. The quality of the output is a direct function of the time and analysis devoted to the development of the model.

Data are input to a model in several ways. Data may be used to develop cost estimating relationships (CERs), which are then utilized in the model. Data used as standard values among different systems for which estimates are being prepared are written in the program. System dependent data are entered by the analyst for each system design being evaluated.

The output of a model is determined by the customer's needs. One model may be developed for several different users, in which case the output must satisfy the combined needs of the users. The output requirements vary from detail to summary data, tabular and graphic displays, static (non-time-phased) or dynamic (time-phased) printouts, with or without derivation methodology and backup data. The analyst must know the customer's needs and satisfy those needs with appropriate output.

A dynamic or time-phased model can become complex, large, and unwieldy because of the interaction of the time-influenced routines and the amount of data required to define parameters as functions of time. Among the commonly used relationships is the learning curve that takes into account the reduction of the cost per unit with increased production. Escalation and discounting functions are also time-oriented and reflect the change in value of dollars with time. Scheduling routines are time-defined and may range in complexity from simple statistical models to sophisticated routines taking into account such factors as series and parallel operations, critical paths, long-lead-time items, and the impact of unforeseen changes.

Two approaches, commonly referred to as "top-down" and "bottom-up," were apparent in the models reviewed. A top-down approach utilizes relations derived by curve-fitting or regression analysis on historical data. A common example of this approach consists of CERs, which are used in many of the models reviewed. The CERs have two major shortcomings relative to the desired goals of the new cost/performance methodology: first, existing CERs (i.e., dollars per kilogram) do not reflect cost sensitivity to changes in functional requirements; second, in most cases, not enough data on similar systems is available to derive statistically valid relations.

In a bottom-up approach, a system or subsystem configuration is defined, and such parameters as cost are derived by combining the costs of the individual modules or components. The disadvantage of this approach is that a detailed system configuration is usually not available during the preliminary stages of the design process, when a cost/performance model would be most useful. The advantage of such an approach is that its outputs are sensitive to changes in functional requirements.

A common element in many of the reviewed models is a work breakdown structure (WBS). A WBS is a master structure that categorizes the elements or components of systems and subsystems to provide a consistent framework for collecting and reporting data on costs, schedules, and procurement. Each element of a WBS represents the summation of all tasks, products, and costs specifically identified to a particular system or subsystem. A specific example of a WBS and several of its elements is given in the description of the Resource Data Storage and Retrieval (REDSTAR) data base in Section 2. B. 1.

1. REVIEW OF AEROSPACE AND SAMSO MODELS/PROGRAMS

a. SAMSO/RAMMSS Cost Model

The Resources Analysis Model for Military Space Systems (RAMMSS) utilizes the basic subsystem CERs defined in the SAMSO Unmanned Spacecraft Cost Model (Ref. 1), and time-phases the program activities. The purpose of the model is to determine the time-phased, life-cycle costs of unmanned spacecraft systems.

The initial model (November 1969) contains the data from which the major subsystem CER coefficients were developed. The CERs and the associated statistical analyses are also presented. This model utilizes a brief and relatively simple WBS. The Phase I update (August 1971) upgrades and expands the original data set. The basic model utilizes cartesian linear CERs of the form $Y = A+B\cdot X$; the updated model also utilizes log linear equations of the form $Y = C+A\cdot X^B$ if a greater degree of correlation is obtained.

The costs are presented in seven activity phases:

(1) Appropriation 3600 - research, development, test, and evaluation (RDTE)

(2) Appropriation 3020 - initial investment

(3) Appropriation 3020 - replacement investment

(4) Appropriation 3080 - other investment
(5) Appropriation 3300 - military construction
(6) Appropriation 3400 - operations and maintenance
(7) Appropriation 3500 - pay and allowances.

The major subsystems evaluated in the model are

(1) Structure
(2) Thermal control
(3) Propulsion
(4) Telemetry, tracking, and command
(5) Mission equipment
(6) Electrical power supply
(7) Attitude control
(8) Dispenser.

Input data to the computer program are of two types, non-repetitive and repetitive. The non-repetitive data are input once and are applicable to all systems being evaluated. Some data are stored and become part of the computer program. The primary input describes the methodology and ground rules, and the characteristics of the subsystems, program schedule, and other equipment.

The output data constitute a complete package in a form deliverable to the customer. The costs are presented at several levels of detail; date, title, recipient, and preparing analysts are printed, and supporting information is included to provide the customer with sufficient information to evaluate the costs. The output from the model includes static (non-time-phased) costs by phase by detail cost element; time-phased cost by phase by major cost element (both inflated and uninflated); and cost summary by appropriation numbers. In addition, a time-phased graphic display of the program activities is included.

The RAMMSS model is capable of producing total life-cycle costs for unmanned spacecraft systems, based on historically derived CERS.

b. <u>Solid Rocket Motor Cost Model</u>

The Solid Rocket Motor (SRM) Cost Model (Ref. 2) provides a systematic and standardized procedure for estimating life-cycle costs of SRM booster configurations, based on the Space Transportation System cost methodology. In this model, an SRM Cost Model has been developed for booster configurations of the type used on the Space Shuttle. Most of the cost data were obtained from the study of SRMs for a Space Shuttle performed by the SRM manufacturer's representative of the 3.05-m (120-in.) and 3.96-m (156-in.) parallel or series burn booster configurations.

Most CER coefficients were developed from four or fewer data points, which represented the existing data base for large SRMs.

The life cycle is divided into three phases: RDTE, investment, and operations. The functions and equipment unique to the recoverable booster program are

(1) RDTE
  (a) Recovery system
  (b) Training of recovery personnel
  (c) Test operations, recovery of flight test vehicles
  (d) Recovery facilities and ground support equipment (GSE)

(2) Investment
  (a) Additional recovery facilities and GSE
  (b) Refurbishment of research and development hardware

(3) Operations
  (a) Recovery operations
  (b) Maintenance of recovery fleet
  (c) Replacement training of recovery personnel
  (d) Maintenance of recovery facilities and GSE
  (e) Refurbishment support.

The design and performance parameters examined for developing CERs were thrust, total impulse, motor weight, mass fraction, and propellant specific impulse. A combination of quantity and either total impulse or weight provides a good estimate of solid motor production costs.

The data is input under the following headings:

(1) Refurbishment factor

(2) Rail freight cost per 454 kg (1000 lb)

(3) Water shipment cost per booster

(4) Number of new fleet boosters

(5) Number of new fleet motors

(6) Number of flight tests

(7) Number of flight test motors

(8) Number of equivalent ground test motors

(9) Number of equivalent initial spares motors

(10) Average number of launches per year

(11) Maximum number of launches per year

(12) Number of motors per booster

(13) Number of equivalent spares support motors

(14) Number of uses per motor

(15) Number of years flight test operations

(16) Number of years operations phase

(17) Number of years test operations

(18) Total number of operations phase launches

(19) Stage weight

- (a) Stage structure weight
- (b) Recovery system weight
  1. Parachute system weight
  2. Retro rockets weight

(20) Propulsion weight

- (a) Primary (SRM) weight
  1. Case and insulation weight
  2. Nozzle weight
  3. TVC weight
  4. Other weight
  5. Propellant weight
- (b) Secondary weight

(21) Total motor gross weight.

The output from the model is presented as seven different cost groups:

(1) Program cost estimate summary
(2) First unit cost
(3) RDTE cost
(4) New fleet hardware cost
(5) Investment cost
(6) Operations cost
(7) Direct operating cost.

The model is designed to determine the life-cycle cost of an SRM booster as utilized in the Space Transportation System (STS) cost model. It is compatible with the Earth-to-Orbit Shuttle (EOS) methodology.

As with most statistical models, the weaknesses are the limited number of data points consisting of real and hypothetical values. An expansion of the data base could benefit this model and many other cost-predicting models.

c. Large Solid Rocket Motor Sizing Program

The Large Solid Rocket Motor Sizing Program (Ref. 3) configures an SRM launch vehicle that satisfies specific missions, and utilizes inputs of the structure, weight, propulsion, aerodynamics, cost, and mission. The program output defines the internal ballistics of each stage, and lists weight and cost data for the total vehicle and component parts.

The program determines and stores the characteristics of each stage of an n-stage vehicle, starting with the upper stage and concluding with the first stage. These stored data are used to calculate the vehicle characteristics. Two subprograms are utilized to determine the characteristics based on and compatible with the given set of input data defining each stage. The first subprogram determines realistic internal ballistics based on and compatible with the given set of input data defining each stage. The second subprogram determines the component weight for each stage, sums the component weights into a stage weight, and finally, from the stage weights, determines a vehicle weight statement. This subprogram is dependent on input data and information generated by the internal ballistics subprogram. The parameters required for a trajectory simulation are transferred from the stored vehicle characteristics to the trajectory program. The trajectory program alters the sizing input parameters until the trajectory constraint is satisfied. Then the program lists the vehicle configuration, the stage-by-stage configuration, and the pertinent design parameters before terminating.

The program contains a number of options; one is a cost option. The basic cost model utilizes equations of the form

$$Y = \sum_{i=1}^{M} A_i + \sum_{i=1}^{N} X_i$$

where the X_i are complicated equations of the form $X = \Pi B z^a$. These equations are not unlike CERs, although they are more directly based on the performance aspects of SRM design. The coefficients in the models are based on historical data. Guidance system costs are input as separate costs.

Although not directly applicable to the ACS Cost/Performance Model undertaken in this study, the program is an interesting application of the performance and design aspects of a subsystem to cost estimating.

2. REVIEW OF JOINT AEROSPACE AND NASA MODELS/PROGRAMS

a. Space Transportation System Model

The STS Model consists of the EOS Methodology, the Orbit-to-Orbit Shuttle (OOS) Methodology, the STS Computer Program, and several supporting data reports (Refs. 4 through 7). The model determines the time-phased, life-cycle costs of a reusable STS for injecting payloads into earth orbit and maneuvering payloads between orbits.

There are two separate and complete methodologies, one for the EOS and one for the OOS. The same WBS is used in both models. The RDTE phase is comprised of four major elements: conceptual and definition, engineering development, technology support, and Government program management. The investment phase is comprised of four major elements: facilities and equipment, reusable vehicle fleet, expendable hardware, and Government program management. The operations phase is comprised of three major elements: operations, spares and propellant support, and range/base support.

The costs of the primary elements are based on CERs. The CERs are derived from basic data contained in Ref. 4, Volume III. The CER coefficients are based on statistical least-squares regressions. The costs of the other elements are based on factors, fixed throughputs, and summations.

Input data to the computer program are of two types, Level I and Level II. Level I data are independent variables (such as weight, thrust, and man-years) and describe a particular system design. The Level II data are constants and exponents of the CERs.

The output of the computer program consists of two principal categories: the basic output report and the time-phased output report. The basic report provides a static (non-time-phased) display of all costs in the STS life cycle. The time-phased report, an optional feature, provides a summary of major cost elements in the life cycle on an annual basis. These time-phased costs can be displayed in base year (current) dollars, in actual year (adjusted for inflation) dollars, or in present value dollars. The life-cycle costs are separated into RDTE, investment, and operational phases. In addition to these three phases, a fourth block, identified as "vehicle first-unit costs," is utilized in the model.

The STS Cost Model is a joint NASA/USAF tool. The model was designed specifically to develop total system costs for alternative STS concepts. The WBS is tailored to provide cost estimates of the most significant elements in the three major program phases. The CERs and factors used in the model to estimate the costs were obtained from programs similar to projected STS programs.

Many of the CERs and factors are based on a limited number of data points. The methodology has been developed, to a large degree, from the Gemini and Apollo Programs. Because the STS Program may extend the state of the art significantly, the applicability of some earlier program data must be reevaluated as the program progresses. The statistical analyses that can be performed are severely limited by the small data set for many of the cost elements.

b. Vehicle Synthesis Program

Programs similar to the present (September 1972) Vehicle Synthesis Program (VSP) have been used at The Aerospcae Corporation for several years (Ref. 8). The VSP document was written in response to a request from the Manned Spacecraft Center Operations Analysis Branch. These personnel were interested in the program because of its adaptability to cost sensitivity studies being conducted by the Operations Analysis Branch. The computer program optimizes the Shuttle configuration with respect to weight, and permits the assessment of variations in design parameters such as payload weight, velocity increments, and propellant specific impulse.

The VSP computer program, which is described in this section, was adapted for a single Space Shuttle configuration. This configuration, one of two Space Shuttles then being considered by NASA, consists of a drop-tank orbiter using LO_2/LH_2 propellants, which is boosted by twin solid-propellant rocket motors. The orbiter and booster rockets thrust simultaneously until the SRMs are depleted. The orbiter continues thrusting after booster staging until the desired orbit is achieved.

The VSP determines changes in vehicle size and weight that occur when certain vehicle parameters are varied. The most commonly varied parameters are

(1) Payload weight
(2) Payload bay volume
(3) Drop tank weight ratio
(4) Propellant specific impulse
(5) Contingency factor for weight growth.

Since many of the subsystem weight relationships contain the total vehicle weight as a parameter, iterative methods are used to obtain convergence.

The first iteration calculates the orbiter weight. The second iteration determines the booster size necessary to achieve the desired total ΔV. The third iteration manipulates the weights of the booster and orbiter until the desired ΔV split between the two is attained.

All the weight-estimating equations are based on the application of correlation methods employing contractor's historical data. The total vehicle weight is determined as the sum of the weights of 20 subsystems. This VSP was not incorporated in this study, since the weight-estimating relationships are based on the correlation of historical data, and not on functional requirements. The VSP could be used in a total vehicle program, since the VSP Program deals with the weight of an entire vehicle, rather than merely ACS weight.

3. REVIEW OF OTHER MODELS/PROGRAMS AND RELATED MATERIAL

a. General Electric Attitude Control Design Model

In June 1965, General Electric Co. completed Research and Investigation on Satellite Attitude Control (Ref. 9). This work developed a design guide based on the design flow pictured in Figure 2-1. This model is based on the mission parameters given to the design engineer. The required vehicle control torques and control system power are derived from the specified mission parameters. The design guide establishes tradeoff data such that when a specific vehicle mission is defined, the optimum ACS can be designed and constructed. Therefore, the study is divided into four main parts:

(1) Preparation of a design data guide

(2) Application of the ACS model to validate the design guide

(3) Investigation of means to produce control moments

(4) Investigation of space power systems to provide energy to the ACS.

The design guide indicates the tie-in between the vehicle attitude control, energy source, and mission requirements. This guide provides the design engineer with data that facilitates the determination of the optimum control and power source for a given vehicle and mission. The optimum

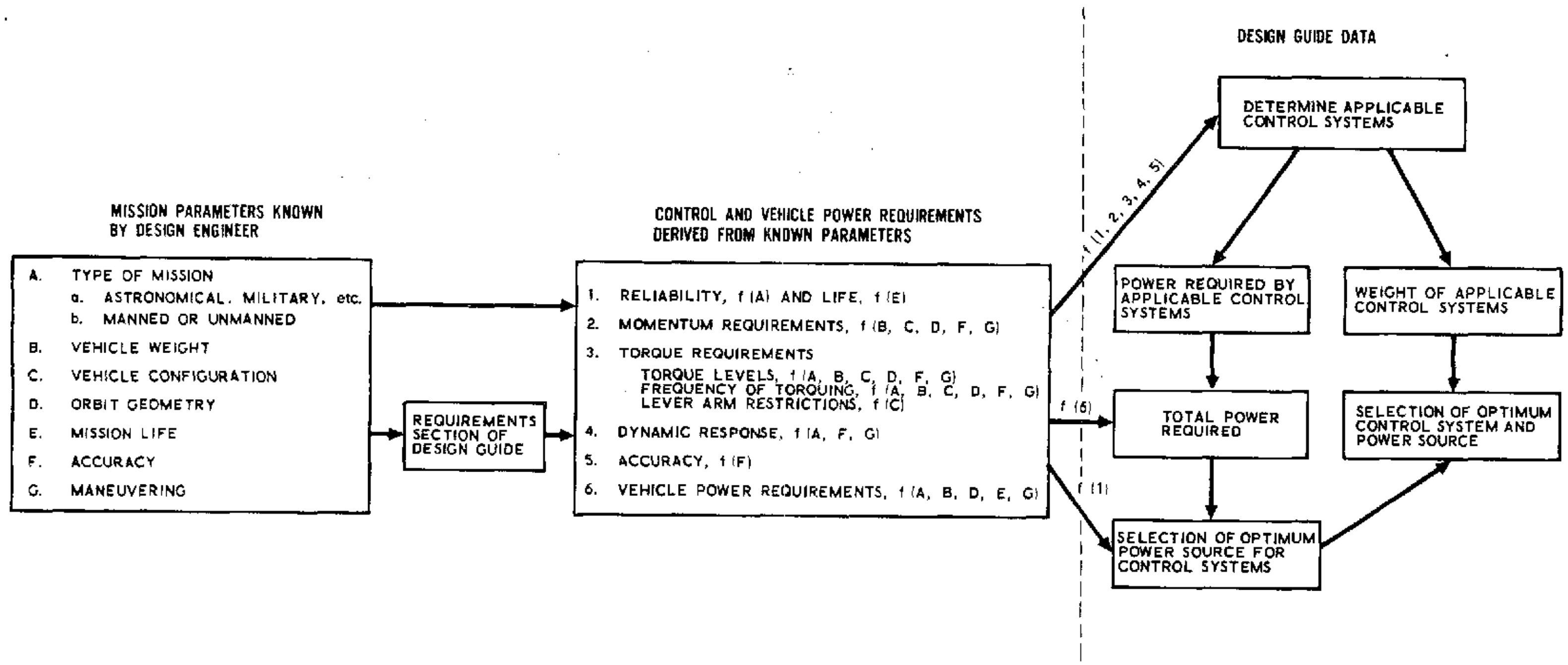

Figure 2-1. Flow Chart Exhibiting Selection of Optimum Control System and Power Sources

system is achieved when performance and reliability requirements are satisfied and weight and power are minimized. The secondary factors of producibility, maintainability, and cost must also be favorable. Representative categories of vehicles and missions are considered to present the tradeoff data.

In all, six distinct missions are considered: military, astronomical, meteorological, communications, space environment, and space station. The implications of these different missions are reflected in the required pointing accuracy, mission duration, and reliability.

Four categories of space vehicles are considered to further define the scope of the design guide:

(1) Class A: a vehicle with few or no control requirements, such as the Tiros satellite

(2) Class B: a vehicle with a three-axis ACS requirement and a weight between 181.4 kg (400 lb) and 907.2 kg (2000 lb), as, for example, the Nimbus weather satellite

(3) Class C: a vehicle with the same control requirements as Class B, but a weight of 907.2 kg (2000 lb) to 4536 kg (10,000 lb), with Orbiting Astrological Observatory (OAO) as an example

(4) Class D: a large vehicle such as a space station, with a weight between 4536 kg (10,000 lb) and 90,720 kg (200,000 lb).

The requirements for a Class A vehicle indicate that sufficient control torque can be obtained from magnetic torquing, spin stabilization, or passive stabilization. The requirements for three-axis active stabilization for Class B, C, and D vehicles can be met with control moment gyros, conventional mass expulsion, or electric propulsion.

The second portion of this study validates the design guide by the construction of an ACS model and the investigation of two case studies. The first study models the fluid flywheel for a hypothetical mission. The second case models the Nimbus satellite as a state-of-the-art system; the ACS determined in this study is nearly identical to the actual ACS used on the vehicle.

The data on control systems in the design guide are developed in the third study, which investigated space vehicle attitude control techniques. Major emphasis was placed on four actuation methods: inertia wheels, fluid flywheel, control moment gyro, and conventional mass expulsion. For each of these control techniques, descriptions of all the different components of the system are carried out. A method of selecting the optimum components for various methods is treated. Steady-state and dynamic analyses of each system are performed to determine its ability to meet mission requirements.

A reliability analysis of these four control techniques is conducted using a statistical method to estimate system failure rates. The reliability of the four techniques is predicted for mission durations of 1 month, 1 year, and 5 years.

The fourth and final portion of this study considers power subsystems for the space vehicle. The three energy sources considered are solar, chemical, and nuclear. Conversion devices are used to generate electrical power from these sources. The power conversion devices are considered with respect to state of the art, reliability, weight, problem areas, and environmental effects. This information is used to synthesize power subsystems for the three primary energy sources.

While the General Electric method embodies some of the concepts (performance and safety) of the model under development in this study, it cannot be used as the basis of the Cost/Performance Model because

(1) The General Electric method is an open-loop process. It is essential that feedback be included in the design method so that cost and schedule results of the selected design be reviewed with respect to the importance of the requirements.

(2) The other major requirement factors — cost, schedule, maintainability, and producibility — are not clearly identified. Their importance is treated only in a qualitative manner. It is necessary to quantify these factors if they are to contribute to a balanced design technique.

(3) There is no consideration of the contribution of the attitude sensor characteristics to the overall ACS performance, weight, power, reliability, cost, and schedule. The role of the sensor in the design process must be identified and quantified.

b. USAF Systems Command 375 Series Manuals

The 375 Series Manuals (Refs. 10 to 16) were published in the mid-1960s and constituted an AFSC attempt to provide a procedural baseline for management of programs involving relatively complex hardware, software, and management interfaces. Thus, review of the manuals was predicated on the belief that the 375 Series Manuals might provide insight into the modeling of the design process.

The Systems Engineering Management Manual (AFSC 375-5) serves two purposes: first, it defines a common system analysis process that leads to system definition in terms of performance requirements on a total system basis; second, it provides a detailed sequential road map of engineering actions during a system's life cycle. The focus of the manual was to ensure that the elements of a system design were directly derivable from the program requirements. However, the cost estimating performed within the framework of the manual was generally directed toward estimating the tasks to be performed to meet the program requirements, rather than deriving costs directly from the program requirements. The cost management was structured using traditional accounting procedures without relating costs to specific requirements. Thus, the structure of the manual appears to be of limited utility in attacking the objectives of this task.

The manuals do contain a comprehensive description of the entire process of system acquisition and deployment, and serve as a useful checklist for determining the completeness of models structured within this task.

c. Honeywell Cost Analysis Study

In December 1969, Honeywell, Inc. completed an Advanced Spacecraft Subsystem Cost Analysis Study (Ref. 17). The study consisted of a historical review of the Stabilization and Control Systems provided by Honeywell for the Apollo Block I and Block II, Gemini, and F-104. The general objective of the study was to systematically collect and document existing information pertaining to the three programs into a thorough and consistent data bank. The data bank was to be used to develop techniques for estimating subsystem requirements.

The primary objective of the study was to develop a data book documenting all significant events and activities in the actual hardware development programs. The data book isolated those items that had a significant and correlatable influence on cost, weights, or development lead times. It also presented quantifiable design elements of the actual subsystems and examined the difficulty of each from a state-of-the-art standpoint.

Secondary objectives were

(1) To develop and test a subsystem cost-estimating technique that fully utilizes Apollo, Gemini, and F-104 experience

(2) To develop time-phased estimates of the development costs and other resource requirements for prospective spacecraft subsystems.

In accomplishing the primary objective of the study, Honeywell compiled and extensively cataloged the cost elements of the three programs. For this reason, the data handbook may be useful in Task 2.3 when model testing is contemplated.

Honeywell attempted to create a cost-estimating tool, using the cost data from the three programs, estimated relative complexity factors for the planned function, program management, inflation factors, and a division between recurring and non-recurring cost elements. Difficulties with the model result from the subjective nature of the relative complexity estimation, and, more importantly, from ambiguity or lack of definition of the equipment and tasks related to the planned functions.

By conducting an internal survey of 48 supervisors and managers, Honeywell also attempted to identify the "cost driving" elements of a program. The survey concluded that the following four elements were the primary cost drivers:

(1) System performance requirements
(2) Program duration
(3) Changes
(4) Extent of system responsibility.

The Honeywell study activity resulted in two major conclusions. First, the study showed no usable correlation between weight and cost for Stabilization and Control Systems (SCSs). Previous cost analysts have demonstrated consistent cost/weight ratios; cost estimators, in turn, have used these ratios to estimate costs. Second, the study showed that two SCSs may differ markedly in weight, volume, cost, and task performed.

d. ODIN and IPAD Programs

As the final task in the background information development, the ODIN and IPAD Programs were investigated. ODIN (Ref. 18), a system developed at Langley Research Center, consists of a data base, the DIALOG executive, and a collection of modules describing various aspects of the technology used in spacecraft design. (See Figure 2-2.) ODIN integrates computer models for various aspects of system design to facilitate an optimum system engineering approach to vehicle design that does not require a newly written program for each task. In addition, it provides the simultaneous availability of many different design evaluations and also provides a common data base for these design evaluations. The common data base can be particularly important, because the evaluation of competing systems using separate programs with different data bases produces results that may not be directly comparable.

Conceptually, the Cost/Performance Model would be one of the modules of the ODIN system and would provide cost/performance tradeoff capability.

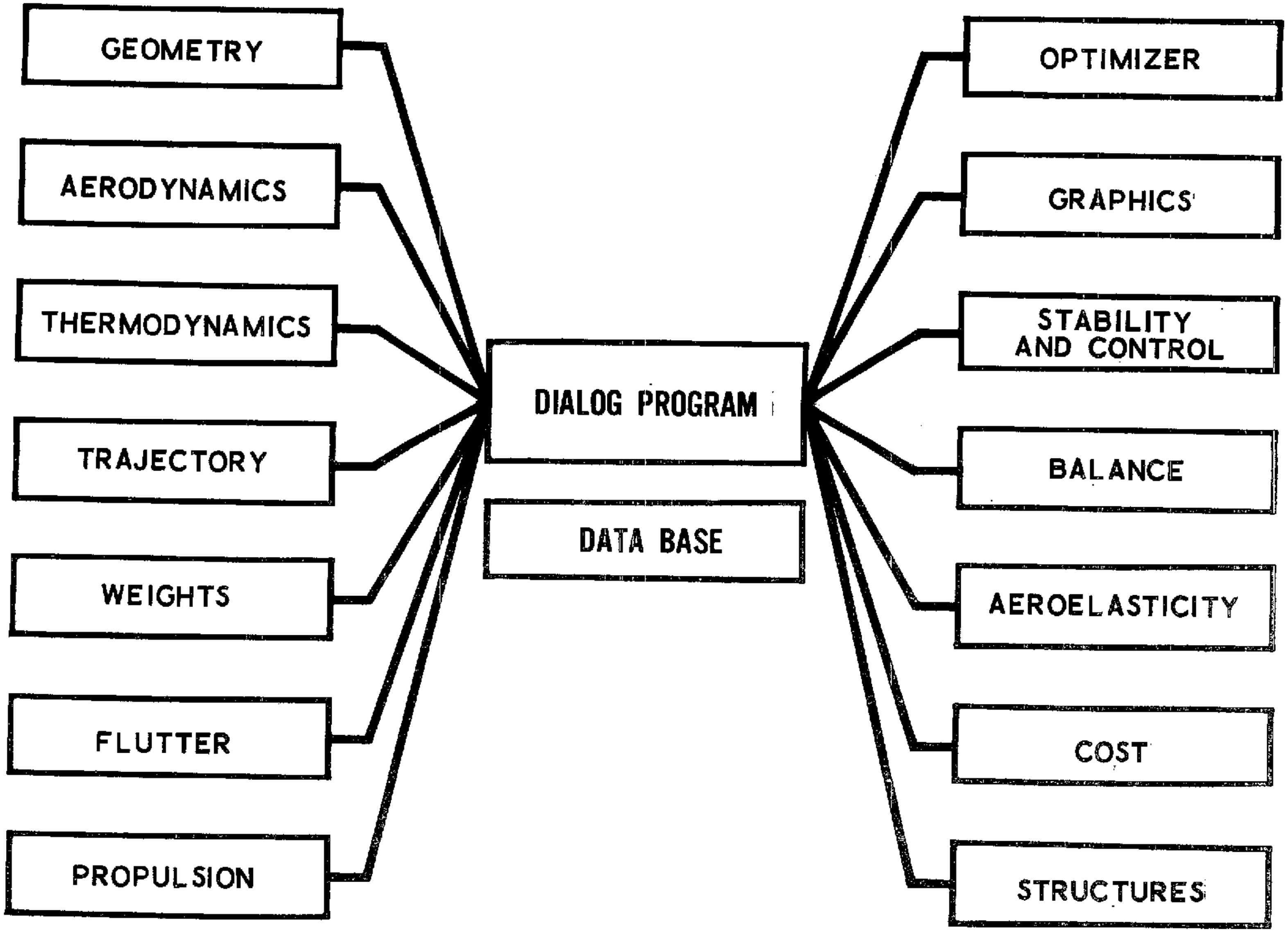

Figure 2-2. Optimal Design Integration System

IPAD (Ref. 19), also developed at Langley Research Center, supports the engineering design team by implementing, as much as possible, the computational and data management aspects of the aircraft design process. One objective of the IPAD concept is the capability of evolving with change, without rebuilding the computer model to accommodate changes in the design process. IPAD is organized in a modular fashion, with self-contained component programs that correspond to major disciplines (i. e., structures, aerodynamics, or propulsion), subdisciplines, or computational tasks involved in the aircraft design process. The modules are linked through an executive program and utilize a common data base. Figure 2-3, from Ref. 19, shows the program organization.

B. DATA BASES

As integral part of the background information development, it was necessary to investigate the existing data bases.

The key to making meaningful estimates on the relationship among performance, safety, cost, and schedules is the access to a properly-structured set of data involving the prior experience of space programs. It is not intended that the modeling methodology be strictly constrained to work on any particular data base. In fact, it is fully expected that data not currently available will be necessary to perform the costing analyses. It is expected that the methodology developed here make as much use as possible of existing data bases.

Two collections of existing data bases are described: REDSTAR is of primary interest, since it was developed for NASA by Planning Research Corporation as part of the Application of Engineering Cost Analysis; the other is an Aerospace collection of data on various programs.

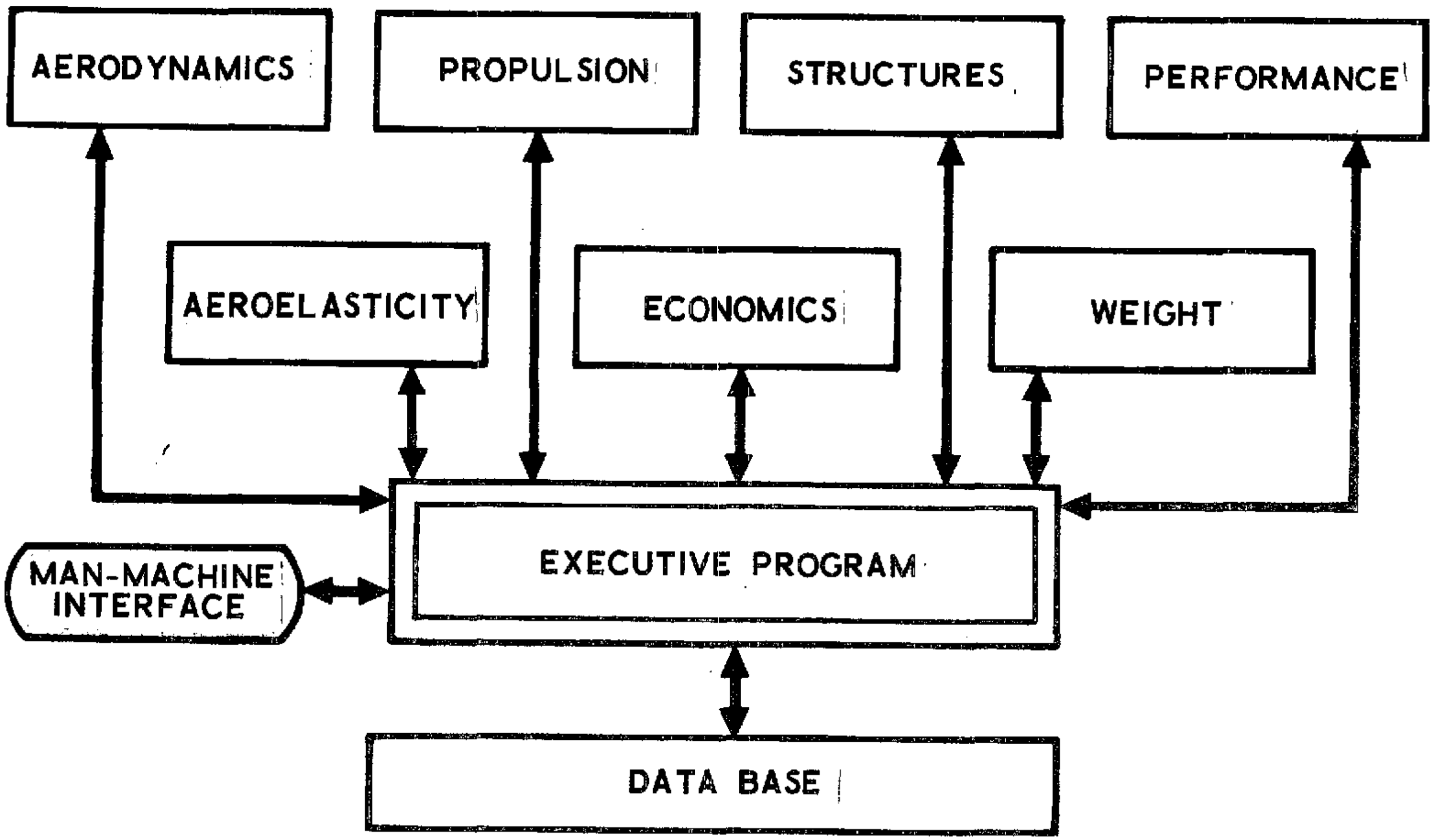

Figure 2-3. Conceptual Organization of Integrated Programs for Aerospace Vehicles Design (IPAD)

1. REDSTAR DATA BASE SYSTEM

In fiscal year 1972, Planning Research Corporation prepared a study entitled Application of Engineering Cost Analysis (Ref. 20). The REDSTAR data base system was developed as a part of that fiscal year 1972 study.

The REDSTAR data base was developed as a general purpose data system intended to file and retrieve all possible elements describing a program. The data are to include technical and other characteristics, as well as cost. The key to the entire data system is the WBS. Other elements of the data system are the Subdivision of Work Structure (SOWS) and the Elements of Cost (EOC). As shown in Figures 2-4 and 2-5, the data base is a three-dimensional matrix of elements. The WBS is common to all the categories. Planning Research Corporation has defined the WBS to six levels:

a. Program
b. Project
c. System
d. Group
e. Subsystem
f. Component.

For example, one might look up characteristics of the star tracker (Level f) of the Guidance and Navigation Subsystem (Level e) of the Avionics Group (Level d) of the Spacecraft System (Level c) of the Spacecraft Systems Projects (Level b) of the Program XYZ (Level a). A complete breakdown of the WBS is given in Ref. 20 to Level e with some examples to Level f. It was intended that the structure be developed to lower levels as required for specific programs. WBS elements were selected according to the following criteria:

a. WBS elements shall be entirely end-item hardware.
b. WBS elements of a general nature have been selected for Aerospace system application. Specific identification of all entries shall be required for each program.
c. The WBS shall not be aligned to any specific corporation or NASA Center organization.

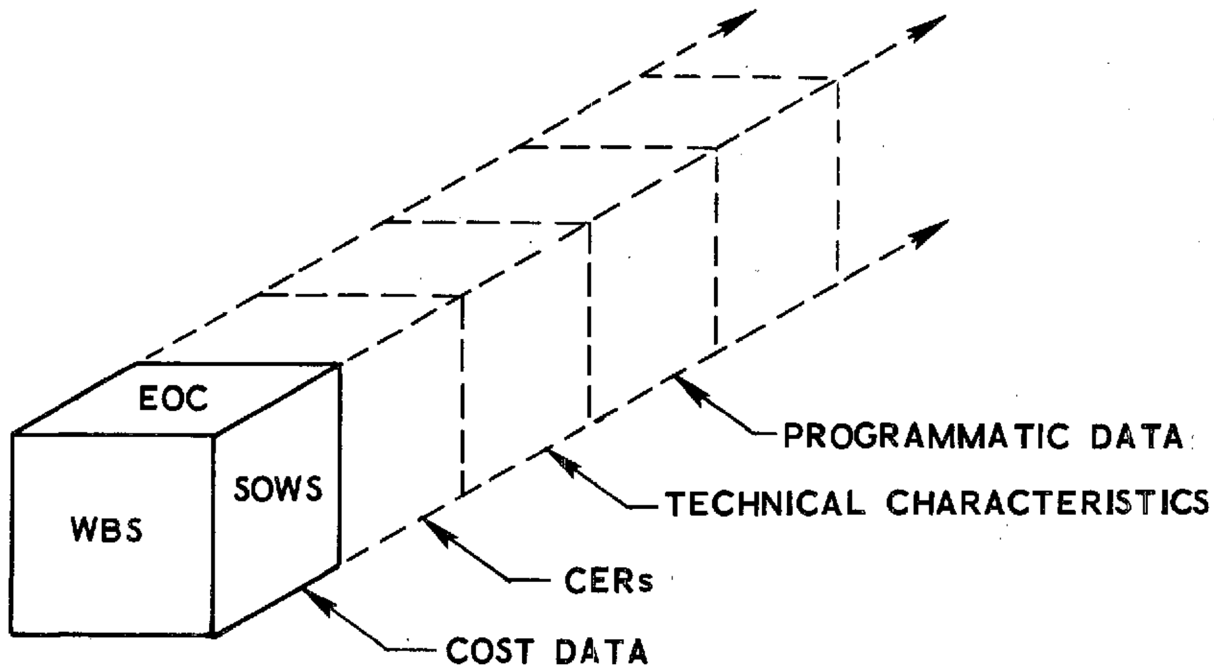

Figure 2-4. WBS/SOWS/EOC Matrix Contents

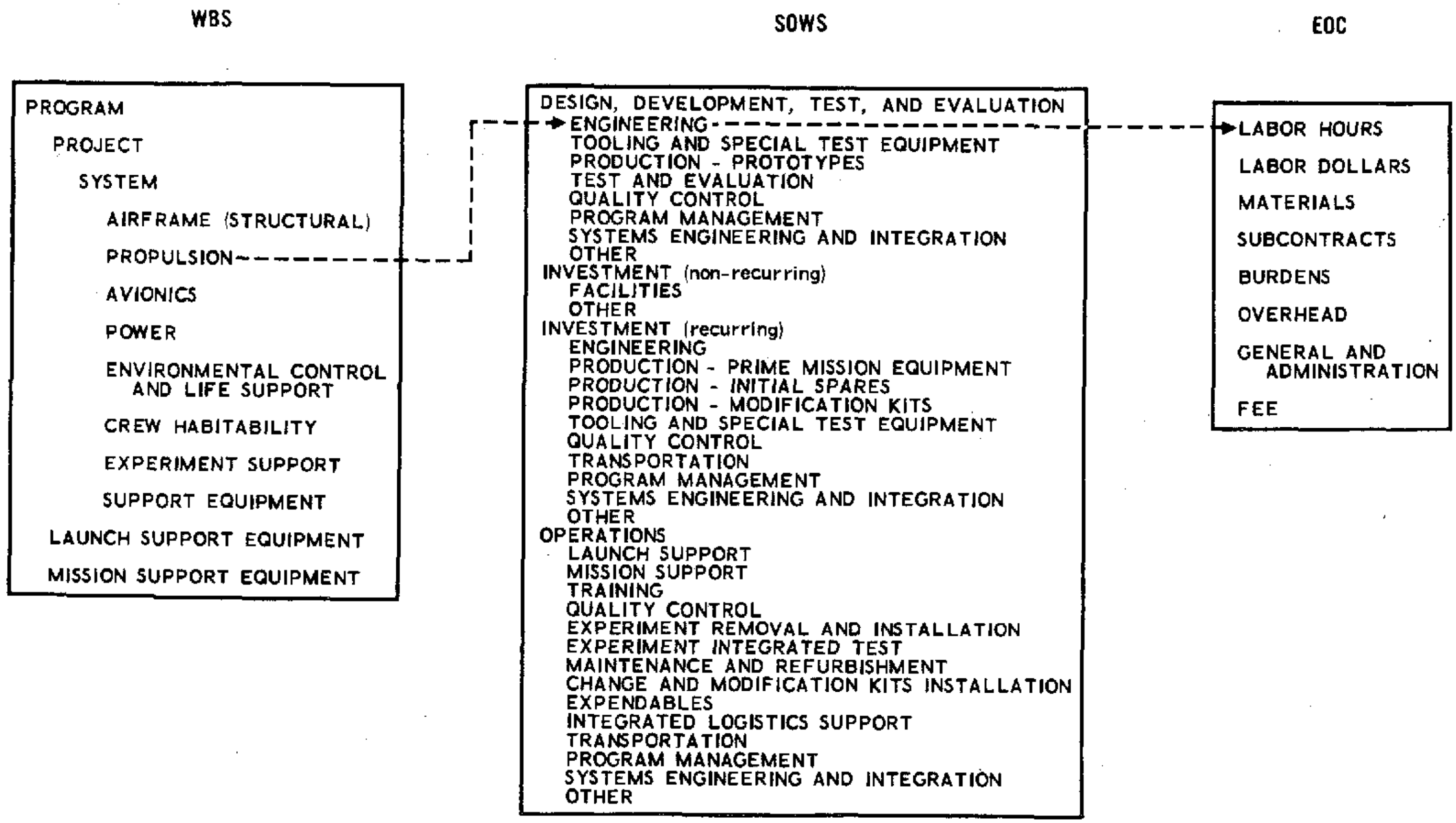

Figure 2-5. WBS/SOWS/EOC Breakdown

d. Terminology shall be consistent with past and current efforts on WBS as applied by MSFC, other NASA centers, and DoD.

e. Under each level (program, project, system, group, and subsystem), a WBS element identified as "other" shall be included. This element shall be included to permit items peculiar to the next lower level (stage integration hardware; interprogram, project, or system hardware integration). This element shall be required to permit total task and cost traceability.

The major effort to date has been on the cost descriptions. For each WBS element, the costs are further divided into the SOWS and EOC. The SOWS subdivides the cost among the various categories shown in Table 2-1, while the EOC allows distinction between labor, material, etc., as shown in Table 2-2. Data for some programs have been entered into REDSTAR by NASA. While it is still preliminary and not fully checked out, some use could be made of it. Great care will be required to ensure that costs are properly allocated to the various categories.

Each element represents the summation of all tasks, products, and costs specifically identified to an element or its subelements, including all directly related support efforts. The life-cycle phasing of each element into design, development, test and evaluation; investment/recurring; investment/non-recurring; and operations can be obtained from a matrix of the WBS and SOWS elements. The functional components of each phase can also be included in the WBS/SOWS if this additional information is desired.

When one embarks on the assessment of the cost/performance tradeoffs of an ACS, one problem with the WBS is encountered immediately. The structure is not divided in the way an ACS designer views his system, and the category autopilot is by no means the whole ACS. In fact, a preliminary search through the WBS reveals many categories that must be present for the ACS to function. (See Table 2-3.) Some of these, such as power, are really peripheral to the controls, while others, such as thruster and horizon sensors, are generally considered an integral part of the controls.

This lack of correspondence between the WBS and functional breakdown does not necessarily mean that the WBS cannot be used. However,

Table 2-1. SOWS Elements

Design, Development, Test and Evaluation
Engineering
Tooling and special test equipment
Production-prototypes
Test and evaluation
Quality control
Program management
Systems engineering and integration
Other
Investment (Non-Recurring)
Facilities
Other
Investment (Recurring)
Engineering
Production - prime mission equipment
Production - initial spares
Production - modification kits
Tooling and special test equipment
Quality control
Transportation
Program management
Systems engineering and integration
Other
Operations
Launch support
Mission support
Training
Quality control
Experiment removal and installation
Experiment integrated test
Maintenance and refurbishment
Change and modification kits installation
Expendables
Integrated logistics support
Transportation
Program management
Systems engineering and integration
Other

Table 2-2. EOC Breakdown

Labor Hours
Labor Dollars
Material
Other Direct Costs
Burdens and Overhead
General and Administration
Fee

Table 2-3. WBS Elements That Are Part of an ACS

01	Structure
01-02	Aerosurfaces (all subdivisions)
02	Propulsion
02-01	Main propulsion
02-01-07	Thrust vector control
02-01-16	Thrust vector control
02-02	Orbit maneuvering
02-02-07	Thrust vector control
02-04	Attitude control propulsion (all subdivisions)
03	Avionics
03-01	Guidance and navigation
03-01-01	Inertial measurement unit
03-01-02	Star tracker
03-01-03	Solar tracker
03-01-04	Horizon tracker
03-02	Stability control
03-03-01	Autopilot
03-03-02	Control moment gyros
03-03-03	Gravity gradients
03-03-04	Magnetic moment
03-05	Display and control
03-05-01	Flight displays
03-05-04	Manual control entry
03-05-06	Electronics
03-06	Data management
03-06-01	Computer
03-06-02	Storage devices
03-06-03	Data interface unit
03-06-04	Software
03-07	Signal distribution (all)
06	Power
02-02	Fluid
06-02-01	Hydraulic
06-02-02	Pneumatic

a translation matrix will be necessary to convert the functional breakdown to WBS. Care will have to be exercised to ensure that no elements are left out or repeated.

2. AEROSPACE DATA BASES

a. Satellite Cost Data

Some data is available in-house from a variety of satellite cost programs. A number of data collections exist independently, and are used for various purposes. A typical data system divides the satellite into a variety of subsystems similar to those for REDSTAR, although not identical in its breakdown. One data format describes characteristics such as number of units, technical characteristics, and weight. A second format describes cost data divided into major categories: engineering; development; tooling; manufacturing; quality control; clerical; and other. Unfortunately, little if any component data is available. Cost data exist in this data system for the following programs:

(1) VELA
(2) VASP
(3) Program 191
(4) Program 777
(5) Defense Support Program (DSP)
(6) Nimbus
(7) Applications Technology Satellite (ATS)
(8) Pioneer
(9) Orbiting Geophysical Observatory (OGO)
(10) Lunar Orbiter.

b. Attitude Reference System Data

As forerunner of the present task, a small effort (Ref. 21) was conducted in fiscal year 1972 at The Aerospace Corporation to gather data on attitude reference systems that could later be employed to determine relationships between the following parameters:

(1) Technical characteristics
(2) Safety/reliability
(3) Cost
(4) Schedules.

Data were tabulated on 15 different stabilization units for which Aerospace had information available. This material was examined for possible relationships between certain parameters.

Ultimately, development is desired of a model for a complete attitude reference system expressing relationships between the following items:

(1) Technical Characteristics
  (a) Accuracy
  (b) Power consumption
  (c) Volume
  (d) Weight
  (e) Vibration levels
  (f) Temperature range
  (g) Ambient pressure range
  (h) Functional requirements
(2) Safety/Reliability
  (a) Failure
  (b) Failure detection
(3) Cost
  (a) Design and development
  (b) Build and checkout
  (c) Test rigs and vehicles
  (d) Training and simulation
  (e) 10-year support
  (f) Management interface

(4) Schedules

   (a) Sequence restraints

   (b) Man-loading limitations

   (c) Other.

In view of the small magnitude of the initial effort (approximately 1.5 man-months), gathering data on all the above factors was, of course, not possible, and priorities had to be assigned for this first-level effort. Accordingly, the tabulation was confined to the parameters listed below. These were judged to be the most important and the most likely to show interrelationships. Also, the study was limited to the stabilization package portion of the ACSs, since information was available on more of these units than on other parts of the system, such as horizon sensors or star trackers. The parameters selected were

(1) Gyro bias drift rate uncertainty

(2) Weight

(3) Power consumption

(4) Reliability

(5) Recurring cost.

While the emergence of some definite correlations between cost and performance was expected, when accuracy and reliability were plotted against cost, no definite trends were generally apparent. Two problems were encountered that may contribute to this: first, accurate cost information was difficult to obtain, and separation of development costs from recurring costs was even more difficult; second, when data were compared, it was found that no two units differ in only one characteristic. Thus, in comparing two units of different accuracies, there was also a variation of other parameters. This study had attempted to use statistical methods to define the relationships between performance and cost. As with many statistical approaches, there are almost never enough data to satisfy all the theorems necessary to achieve sufficient confidence in the results. It was concluded that a very thorough breakdown of all cost data will be necessary to achieve the objectives of cost/performance modeling with this approach, and that this information will have to be carefully weighed for such factors as maturity of design, number of units manufactured, possible future overruns, and influence of concurrent programs. In addition, many more parameters will require evaluation if a complete model is to be developed.

C. SPACE VEHICLES DESCRIPTION

Because this task is concerned with the cost/performance methodology for a three-axis mass expulsion ACS, two vehicles typical of this type, the standard Agena and the NASA Space Tug, were reviewed with an emphasis on the ACS design. A brief description of the Agena ACS is given, as it is typical of a Tug-type vehicle. Also, a review of the Tug control requirements was conducted to ensure that the modeling methodology was closely tied to current industry versions of such systems. Both North American Rockwell (Ref. 22) and Lockheed (Ref. 23) reports were reviewed to establish these requirements.

1. STANDARD AGENA

The standard Agena was developed for use in a multistage space vehicle as one of the upper stages. It is adaptable to various combinations of program booster, payload, and support hardware. Its mission capabilities include functional programming; a single-, dual-, or triple-start propulsion system; attitude sensing and control; ground command response; data recording and telemetry; and payload support.

The standard Agena Guidance and Flight Control System performs the attitude control functions necessary to accomplish the vehicle mission. During coasting flight following separation of the Agena from the booster, the ACS controls the vehicle to a local vertical orientation. Vehicle attitude is sensed by a three-axis inertial reference package (IRP), which is referenced to the earth by an infrared horizon sensor and by gyrocompassing techniques. Attitude errors are electronically converted to error signals that control corrective forces applied to the vehicle by pulsed cold-gas thrust valves.

The major components and their functions in this system are described in the following sections.

a. <u>Guidance Module</u>

The guidance module is located in the forward section of the Agena. The module structure assembly is precision-fitted and aligned to each individual vehicle. The assembly contains mounting surfaces for the IRP, the horizon sensor, and several other components. Each component is optically aligned to the module structure assembly, permitting precise alignment of the guidance module with the body axes of the vehicle.

b. <u>Inertial Reference Package</u>

The IRP is the primary attitude-sensing component of the guidance system. It contains three single-degree-of-freedom gyros. The gyro input axes are orthogonal and oriented along the body axes of the vehicle (roll, pitch, and yaw as defined in Figure D-1, Appendix D). The gyros sense angular rotations of the vehicle about the body axes and generate attitude error signals. The pitch gyro receives an open-loop pitchover command of orbital rate to maintain the vehicle in a constant attitude with respect to the earth. For most standard Agena missions, the desired vehicle orientation is that in which the nose is forward and the vertical axis of the vehicle passes through the earth's center.

c. <u>Horizon Sensor</u>

The horizon sensor, consisting of two infrared-sensitive sensing heads and an electronic signal mixer box, provides the IRP with an earth reference. The two sensor heads scan the space below the vehicle in conical patterns, and detect the discontinuity in the infrared radiation between earth and space. The horizon sensor generates pitch and roll output signals whenever the vehicle is misoriented with respect to the local vertical. When the vehicle has a roll attitude error, one sensor head obtains a signal for a longer period of time than the other. Roll attitude errors are, therefore, detected by comparing the output of one sensor head with the other. Each sensor head provides pitch information independently by comparing the earth scan with an internally-generated reference pulse. The sensor outputs are used to correct the gyros, which, in turn, correct the vehicle. The horizon sensor provides the gyros with a long-term earth reference that eliminates the accumulation of attitude error due to gyro drifts.

d. Gyrocompassing

Gyrocompassing is the technique of coupling the horizon sensor roll signal into the yaw gyro. Consider a vehicle that has very slowly yawed to the right as a result of yaw gyro drift, causing a portion of the orbital angular velocity vector to be projected along the vehicle's roll axis. As a result, a roll attitude error develops. This roll attitude error is the key to the gyrocompassing technique, for the continuing existence of a horizon sensor roll signal, assuming negligible roll gyro drift, is an indication of a yaw attitude error in the vehicle. Large yaw errors are reduced by coupling the roll horizon scanner error signal to the yaw gyro. Since the roll loop responds much faster than the yaw loop, any persistent roll error drives the yaw attitude error slowly toward null.

e. Flight Control System

During coasting periods, the flight control system provides control of the vehicle attitude in response to error signals generated by the gyros in the IRP. These error signals are processed by the appropriate electronics channel in the flight control electronics package, and the corresponding pneumatic valves are energized. Compressed gas from the thrust control valves provides the energy to correct the vehicle attitude error. Basic components of each channel are an input amplifier, demodulator, lead network, integrating amplifier, a pair of Schmitt triggers, and a pair of power stages that actuate the pneumatic thrusters.

2. NASA SPACE TUG

The Tug is the third stage of the STS; the first and second stages are the booster and the orbiter, respectively. The purpose of the STS

Program is to reduce the cost of space missions through the reuse of the Shuttle and Tug. The main cost reduction is obtained through the return and reuse of payloads. The capability of retrieving payloads is the most important new operational capability of the STS. If one is to appreciate the Tug's attitude control requirements, it is necessary to consider the requirements on the Tug itself.

a. Tug Requirements

According to the latest issue of the Baseline Tug Definition Document (Ref. 24), the Tug must have the capability of delivering a payload to its destination, maneuvering to the vicinity of another payload to be returned, docking with and capturing the payload, preparing the payload for return, and then returning to the Shuttle.

The Tug is to be designed as an unmanned autonomous vehicle, although remote man-in-the-loop TV for final payload docking operations may be used as required in conjunction with rendezvous and docking laser radar. Although the Tug will be carried by the manned Shuttle, the Tug is to be designed for ground-based operation only, with all payload/Tug assembly, propellant loading, maintenance repair, and refurbishment to be performed on the ground. The design mission life of the Tug is tentatively set for 20 missions (ground refurbishment of subsystems after each mission is acceptable). The Tug is tentatively to be designed for a mission completion probability of 0.97. The design on-orbit stay time is 6 days for each mission. (It must also stay 1 additional day in the Shuttle cargo bay.) Since the major concept of the STS is reusability, the Tug itself must be designed so that it can be retrieved.

Since the Tug is a payload relative to the Shuttle, the Tug must satisfy all the constraints imposed by the Shuttle, including weight and volume (the Tug and payload must fit inside the Shuttle cargo bay), and must also satisfy Shuttle environmental characteristics, including loads, thermal, acoustic, vibration, and vacuum. The basic Tug requirements are summarized in Table 2-4.

Table 2-4. Tug Requirements

Mission:	Payload delivery Payload retrieval Return to Shuttle
Guidelines:	Unmanned operation Ground-based support only 97% mission completion probability On-orbit staytime of 6 days Retrieval of the Tug
Shuttle Interface:	Satisfaction of constraints imposed by Shuttle

b. Tug Control Requirements

The control system must provide attitude control of the Tug during separation from the Shuttle. An auxiliary propulsion system (mass expulsion) is used for three-axis control during all Tug mission phases, except during powered flight (main engine burns). During powered flight, the main engine is gimbaled by electromechanical servoactuators for pitch and yaw control, while roll control is provided by the auxiliary propulsion system (as during non-powered flight). Attitude control includes attitude maneuvering (reorientation). The control system must also provide relative position and velocity control during rendezvous and docking maneuvers (with a payload and with the Shuttle). The basic Tug guidance, navigation, and control requirements are summarized in Table 2-5.

c. Baseline Tug Control Subsystem Configuration

Reference 24 specifies a baseline Tug control subsystem configuration consisting of the equipment listed in Table 2-6 to perform the above control requirements. This configuration was selected after several preliminary design studies by North American Rockwell Space Division and by McDonnell Douglas Astronautics Company. Table 2-7 describes the control avionics components of the baseline configuration as selected by North American Rockwell (from Ref. 22). NASA's Baseline Tug Definition Document (Ref. 24) does not include any avionics performance data.

Actuator sizing data depends on the mass properties of the Tug (with and without a payload). Table 2-8 presents the baseline mass properties. Based on these mass properties, Tables 2-9 and 2-10 present the thruster and thrust vector control requirements. Table 2-11 presents the docking accuracy for docking with a three-axis controlled payload (and with the Shuttle). The docking requirements for docking with a spinning payload have not yet been established.

Table 2-5. Tug Guidance, Navigation, and Control Requirements

Determine linear and rotational position and velocity of tug
Provide attitude control (including three-axis maneuvering)
Provide position and velocity control during rendezvous and docking

Table 2-6. Baseline Tug Control System Components

Sensors:	Inertial measurement unit Star tracker Horizon sensor Autocollimator Laser radar TV camera
Actuators:	Main engine thrust vector control actuators (pitch and yaw) Thrusters (three-axis rotational and translational)
Computer:	(For processing sensors, computing actuation signals, and monitoring performance)
Electronics:	(For interfacing among sensors, actuators, and computer)

Table 2-7. Control Avionics Component Characteristics Summary

Component	Performance Requirements (3σ)	Function	No. per Vehicle	Redundancy Level[a]	Weight	Power (W)
1. Strapdown, 6-axis Inertial Measurement Unit (including preprocessor)		Provides short-term inertial attitude and state vector information	1	FO/FO/FS	29.5 kg (65 lb)	144
Random drift	±0.1°/hr	Provides angular rate information for vehicle stabilization and control				
G-sensitive drift	±0.3°/hr/g					
Acceleration bias drift	$\pm 0.00061\ m/sec^2$ ($\pm 0.002\ ft/sec^2$)	Preprocessor provides coordinate transformation and failure detection and isolation				
G-sensitive bias	$\pm 0.00183\ m/sec^2/g$ ($\pm 0.006\ ft/sec^2/g$)					
2. Gimbaled Star Tracker		Provides attitude update to the inertial measurement unit	2	FO/FS	11.3 kg (25 lb)	18
Azimuth and elevation error		Provides star angle information for star/horizon navigation (state vector update)				
3. Earth Horizon Tracker		Provides earth local vertical information for star/horizon navigation (state vector update)	1	FO/FS	20.4 kg (45 lb)	38
System accuracy						
Altitude range	185-46,300 km (100-25,000 nmi)	Provides a source of derived altitude information				
Tilt range	±5°					
4. Scanning Laser Radar		Determines range, range rate angle, and angular rate of target with respect to OOS	2	FO/FS	20.4 kg (45 lb)	155
Range	92.5 km (50 nmi)					
Range accuracy	±10 cm or 0.02%	Determines target attitude and attitude rate with respect to line of sight of radar				
Range rate	0 to 1100 m/sec (0 to 0.6 nmi/sec)					
Range rate accuracy	±1.0 cm or 1.0%					

[a]FO = Fail Operational
FS = Fail Safe

Table 2-7. Control Avionics Component Characteristics Summary (Continued)

Component	Performance Requirements (3σ)	Function	No. per Vehicle	Redundancy Level[a]	Weight	Power (W)
5. Autocollimator		Provides intersensor alignment between the star tracker and horizon scanner	2	FO/FS	5 kg (11 lb)	5
Linear range	±30 min					
Operating distance	4.57 m (15 ft)					
Accuracy	±1%					
6. Ignition Driver Amplifier Assembly	5 on-off control moment gyros	Provides capability to fire 5 auxiliary propulsion system engines	4	NA[b]	5.4 kg (12 lb)	8
7. Engine Gimbal Servo Amplifier Assembly	4 servo amplifiers	Provides the capability to gimbal the main engine	1	FO	1.8 kg (4 lb)	12

[a]FO = Fail Operational
FS = Fail Safe

[b]One amplifier channel per engine

Table 2-8. Baseline Tug Mass Properties

Configuration	With 1360-kg Payload			Without Payload		
	Weight	Moment of Inertia: Roll	Moment of Inertia: Pitch/Yaw	Weight	Moment of Inertia: Roll	Moment of Inertia: Pitch/Yaw
Tug Full of Propellant	29,500 kg (65,000 lb)	9720 kg-m^2 (7165 slug-ft^2)	221,000 kg-m^2 (163,000 slug-ft^2)	28,100 kg (62,000 lb)	6130 kg-m^2 (4525 slug-ft^2)	80,000 kg-m^2 (59,000 slug-ft^2)
Propellant Expended	4080 kg (9000 lb)	9710 kg-m^2 (7155 slug-ft^2)	117,000 kg-m^2 (86,000 slug-ft^2)	2720 kg (6000 lb)	6110 kg-m^2 (4510 slug-ft^2)	25,800 kg-m^2 (19,000 slug-ft^2)

Table 2-9. Thruster Requirements (Auxiliary Propulsion System)

Number of Thrusters	16
Propellant	GO_2/GH_2
Thrust	134 N (30 lb_f)
Specific Impulse	3740 N-sec/kg (380 lb_f-sec/lb)
Total Impulse	781,000 N-sec (175,500 lb_f-sec)
Auxiliary Propulsion System	258 kg (568 lb)

Table 2-10. Thrust Vector Control Requirements

Control Gimbal Angle	±3 deg
Actuator Gimbal Capability	±5 deg
Engine Gimbal Rate	±5 deg/sec
Engine Control Acceleration	±1 rad/sec^2
Bandwidth	10 Hz
Duty Cycle	45 min per mission
Gimbaled Weight	135 kg (298 lb)

Table 2-11. Docking Accuracy Requirements (For Docking With Three-Axis Controlled Payload)

Centerline Miss Distance	±0.229m (±0.75 ft)
Miss Angle	±1 deg
Axial Velocity	0.0305 to 0.305 m/sec (0.1 to 1.0 ft/sec)
Lateral Velocity	±0.0915 m/sec (±0.3 ft/sec)
Angular Velocity	±0.5 deg/sec

REFERENCES

1. Unmanned Spacecraft Cost Model, Phase I Update (August 1971).

2. Solid Rocket Motor Cost Model, Aerospace Corporation Report No. ATR-73(7313-01)-4 (31 August 1972).

3. Large Solid Rocket Motor Sizing Program, Aerospace Corporation Report No. TOR-0172(2452)-3 (10 February 1972).

4. Space Transportation System Cost Methodology, Aerospace Corporation Report No. TOR-0059(6759-04)-1 (August 1970), Vols. I, II, and III.

5. Space Transportation System Cost Model, Aerospace Corporation Report No. TOR-0059(6758-04)-3 (August 1970), Vols. I and II.

6. Comparison of Earth Orbit Shuttle Costs, Aerospace Corporation Report No. TOR-0066(5758-04)-2 (March 1970).

7. Space Transportation System Management Approaches, Aerospace Corporation Report No. TOR-0059(6758-04)-4 (August 1970).

8. Aerospace Vehicle Synthesis Program, Aerospace Corporation Report No. ATR-73(7313-01)-5 (September 1972).

9. Research and Investigation on Satellite Attitude Control, General Electric Co. Report No. AFFDL-TR-64-168 (June 1965).

10. Configuration Management, Air Force Systems Command Manual No. AFSCM 375-1 (1 June 1964).

11. System Program Management Surveys, Air Force Systems Command Manual No. AFSCM 375-2 (11 June 1964).

12. System Program Office, Air Force Systems Command Manual No. AFSCM 375-3 (15 June 1964).

13. System Program Management, Air Force Systems Command Manual No. AFSCM 375-4 (16 March 1964).

14. System Engineering Procedures, Air Force Systems Command Manual No. AFSCM 375-5 (10 March 1966).

15. Development Engineering, Air Force Systems Command Manual No. AFSCM No. 375-6 (14 August 1964).

16. Management of Contractor Data, Air Force Systems Command Manual No. AFSCM 375-7 (31 March 1971).

17. Advanced Spacecraft Subsystem Cost Analysis Study, Honeywell, Inc. Report No. 21250 FR, MSC 01243 (1 December 1969).

18. C. R. Glatt, D. A. Watson, R. T. Jones, and D. S. Hague, An Introduction to Dialog: A Design Integration and Analysis Language With Open-Ended Growth Capability, Aerophysics Research Corporation, prepared under NASA Contract No. NAS 1-10692.

19. Robert E. Fulton, Jaroslaw Sobieszczanski, and Emma Jean Landrum, "An Integrated Computer System for Preliminary Design of Advanced Aircraft," AIAA 4th Aircraft Design, Flight Test, and Operations Meeting, Los Angeles, August 7-9, 1972, AIAA Paper No. 72-796.

20. Application of Engineering Cost Analysis, Sept. 1971 to Sept. 1972, Planning Research Corporation Report No. PRC-D-2087 (Contract No. NAS8-21823).

21. C. T. Davenport, "Program Model Trade Characteristics Study, Phase I Final Report," incorporated into Aerospace ATR-73(7313-01)-1 (25 August 1972), Vol. II.

22. DoD Upper Stage/Shuttle System Preliminary Design Requirements, SAMSO TR-72-195, prepared by North American Rockwell Corporation, Space Division (11 August 1972).

23. Shuttle/Agena Study, Lockheed Missile and Space Co., Space Systems Division Report No. LMSC-D152635 (25 February 1972).

24. Baseline Tug Definition Document, prepared by Preliminary Design Office, Program Development, NASA MSFC, Revision A (26 June 1972).

3. MODELING TECHNIQUES AND APPROACHES

A. INTRODUCTION

In Section 2, various modeling techniques and approaches were reviewed to assess their utility for developing a Cost/Performance Model. As a result of that review, it became apparent that a top-down approach, regressing on historical attitude control system (ACS) data, would add little to advance cost-predicting techniques. Instead, a group of control system engineers, with support from cost analysts, was chosen to develop a cost-prediction approach that reflected the views of the control engineers designing the ACS. During this conceptual phase, a number of modeling methodologies were conceived and evaluated. So that each modeling approach could be judged in a complete and objective manner, the following criteria were formulated and used to evaluate the utility of each approach:

1. The prime objective is to determine sensitivity of cost to changes in functional requirements.
2. The modeling methodology must not impose a cumbersome cost-reporting structure on the contractor.
3. The modeling methodology must estimate cost from the design and development phase through the entire program life of the system.
4. The model should be adaptable to current design procedures and tradeoff procedures.
5. The model should be capable of achieving a balanced vehicle design by a simple extension of the system methodology.

Of all the models considered during this phase, only three were developed in sufficient detail to be described in this section. The initial approaches to the modeling task considered modeling the flow of a design process. Consideration of the design process led to modeling approaches typified by the approach discussed in Section 3.B. Another modeling approach, described in Section 3.C, involved selection of equipment configurations based on system requirements. With the above approaches as prerequisites, another model, termed the "minimum model," was developed; this model is described in Section 3. D. The adjective "minimum" was used to describe this model because it considered, but did not adequately quantify, the parameters of performance, safety, cost, and schedule of an ACS. The "minimum" model was later expanded and became the Cost/Performance Model.

B. DESIGN PROCESS FLOW CHART MODEL

Initial approaches considered modeling of the design process. As a first step, an overall flow chart of the major design phases was developed. (See Figure 3-1.) A more detailed flow chart of the design process is presented in Figure 3-2. In addition, the activities performed during each major phase were considered. (See Table 3-1.)

Using the flow chart of the design process as a starting point, one could obtain a method for estimating the cost and schedule for an ACS by estimating the man-hours required to generate specific design output. A flow chart of this model approach is presented in Figure 3-3. Each subsystem requirement is an input to a serial set of blocks representing the tasks identified by the design, analysis, detailing, manufacturing, and test process flow. Each task block contains a set of functional representations of man-hours versus time associated with each block output. The man-hours-versus-time functions will, in general, be functions that peak early in time, as is typical of most programs. A simple summation gives the overall subsystem man-hours. The functional relationships could be quantified through the use of individual data constants and any constraints imposed on man-hours or schedule. Since a true design does not evolve from a sequence of independent serial paths, a more sophisticated model with feedback and coupling between requirements is necessary.

The form of the data required to develop this modeling approach imposes a cumbersome cost reporting structure on the contractor. For this reason, although the detailed flow charts provided insight into the development of schedule relationships, it was not considered useful to continue further development along these lines.

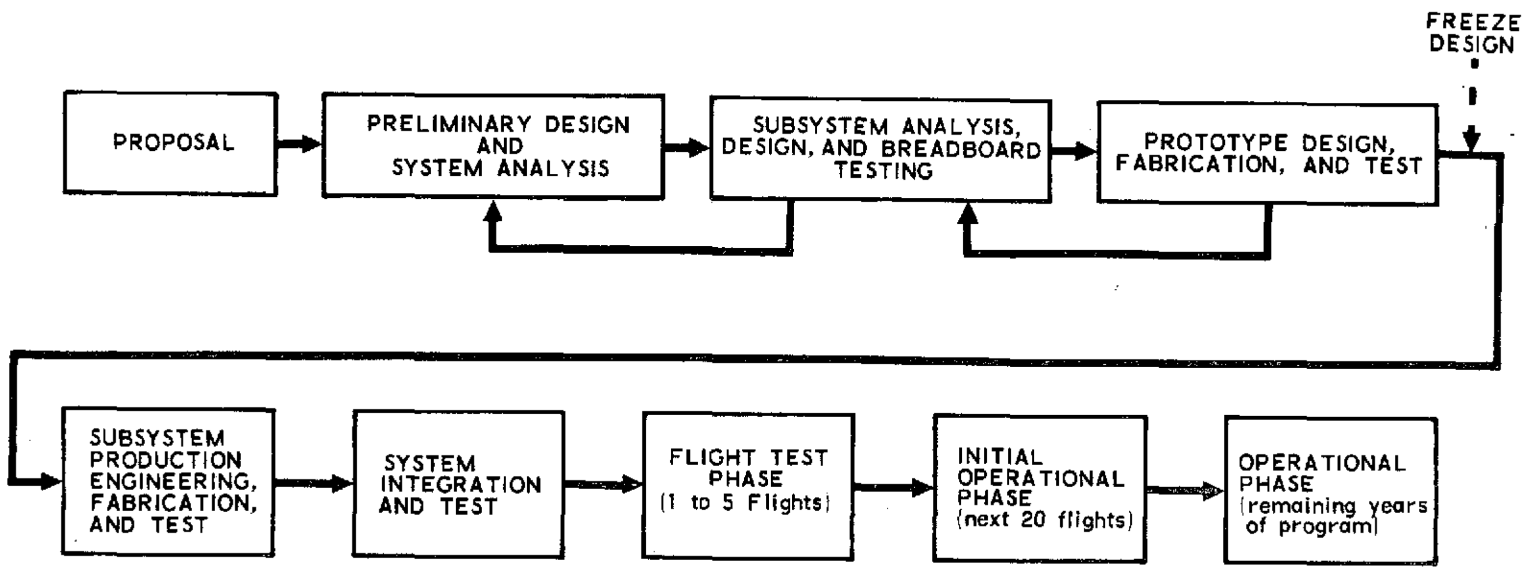

Figure 3-1. Flow Chart of Major Design Phases

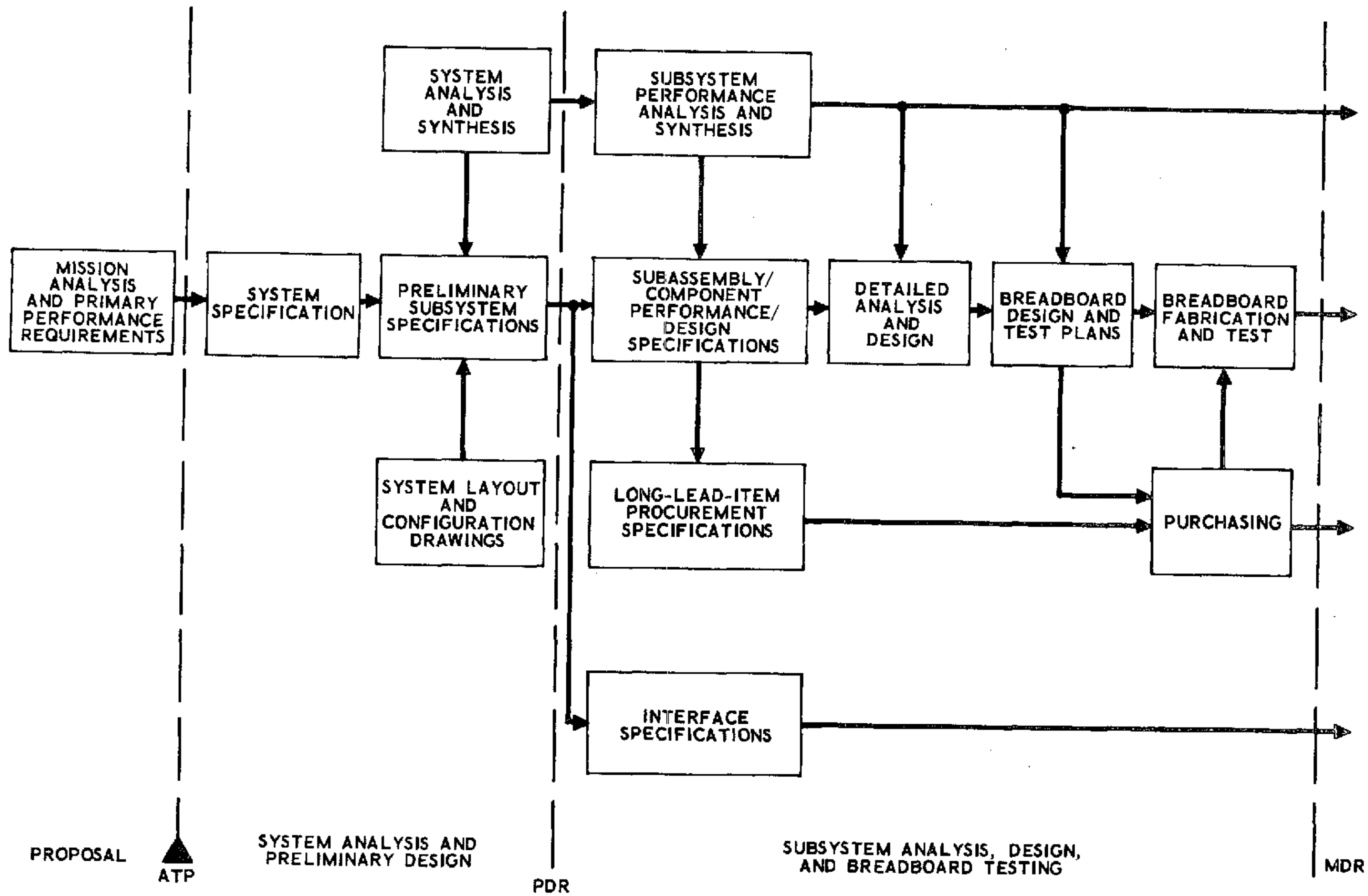

Figure 3-2. Flow Chart of the Design Process

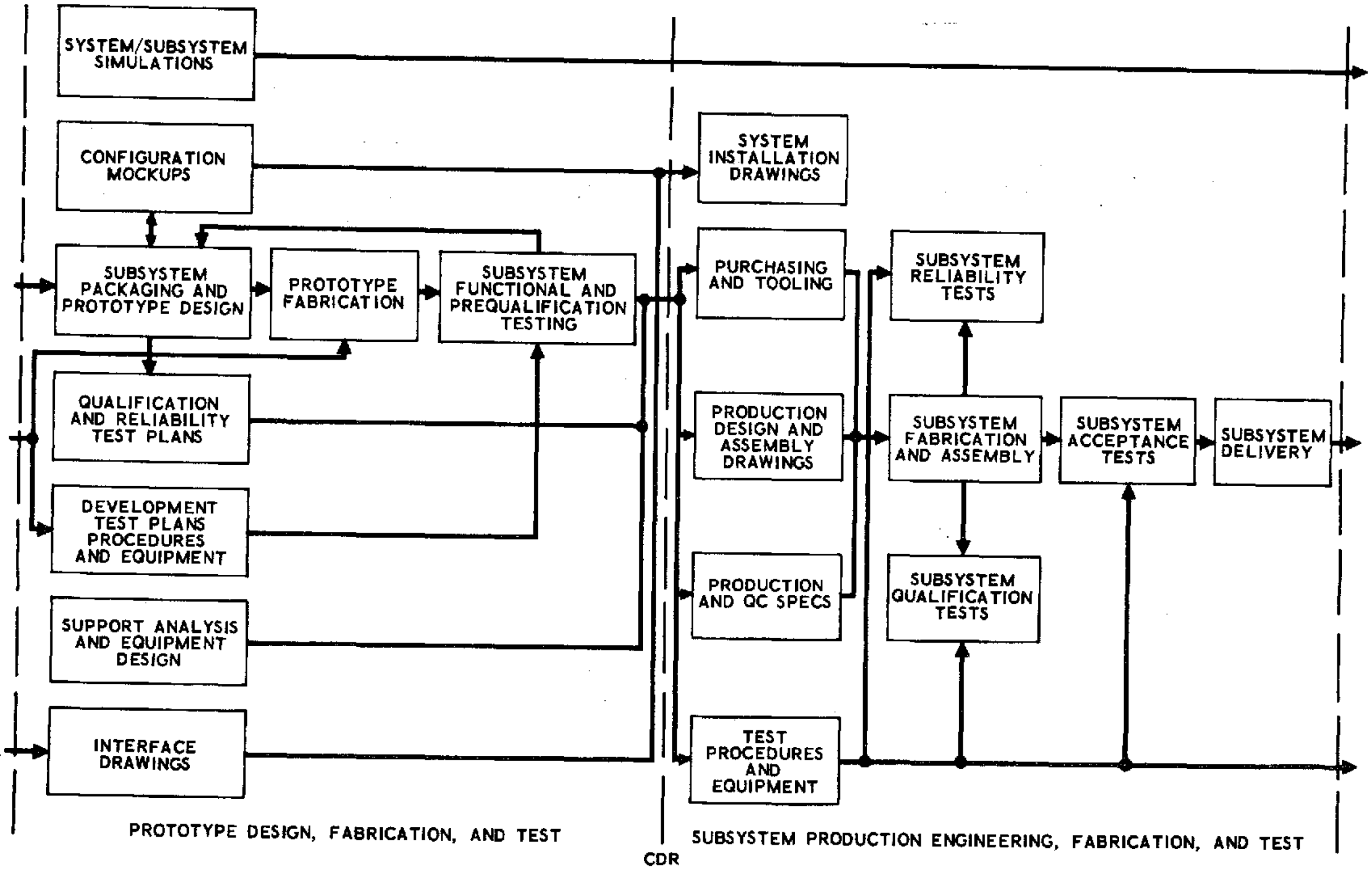

Figure 3-2. Flow Chart of the Design Process (Continued)

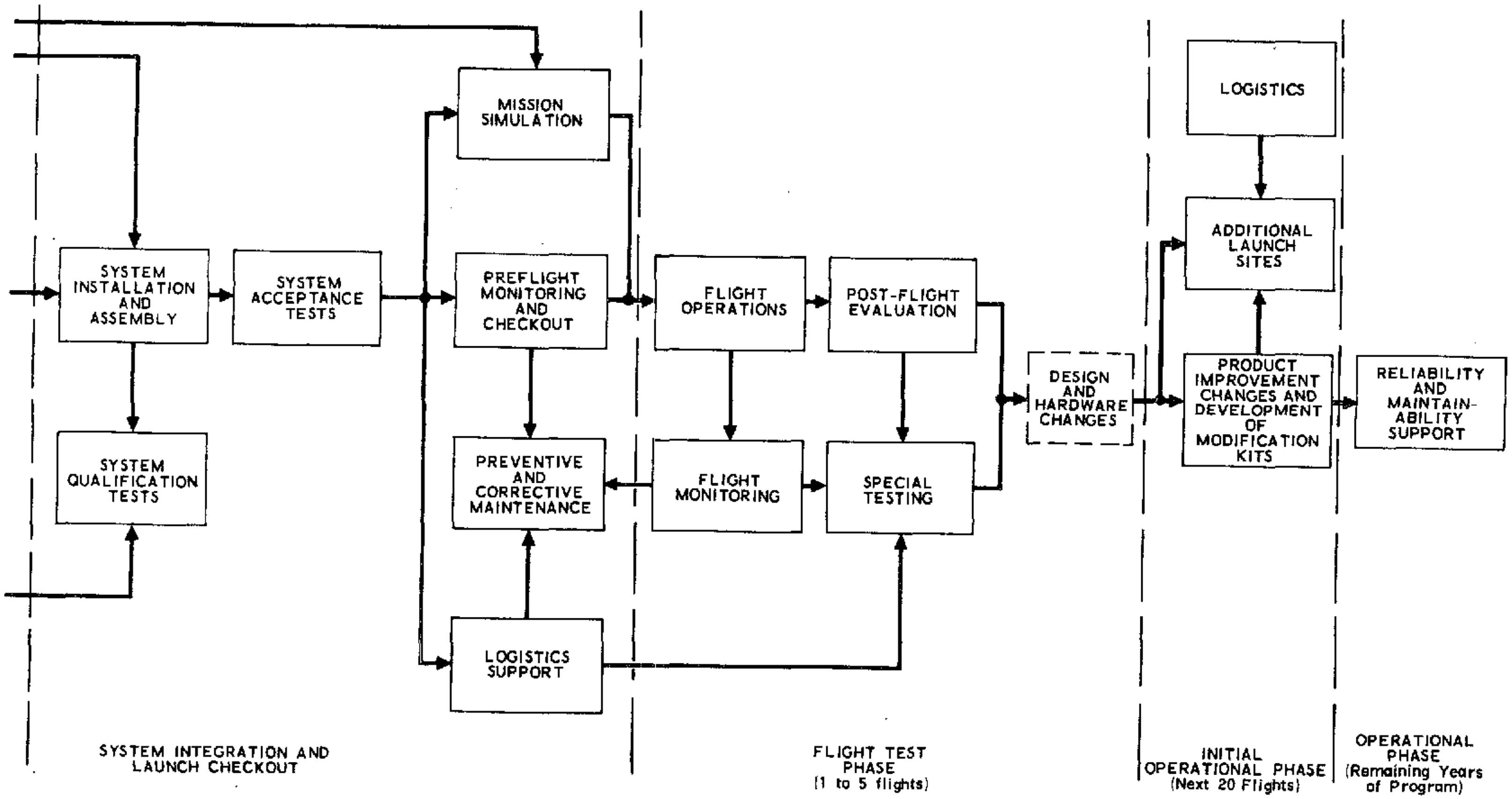

Figure 3-2. Flow Chart of the Design Process (Continued)

Table 3-1. Major Design Phases

Proposal

- Determine system requirements to satisfy payload functional requirements
- Estimate preliminary cost and schedule

Preliminary Design and System Analysis

- Program plans:
  - Master program plans
  - Subsystem specifications and requirements (end-item)
  - Test plans, manufacturing plans, quality assurance plans, reliability plans, engineering development plans
  - Interface with other subsystems, vehicle and ground support equipment
  - Subcontractor plans and specifications
  - Quality test plans
- Mechanical layouts, mathematical block diagrams, interface control diagrams, detailed drawings, long-lead items, functional block diagrams, schematics
- Analysis (stability, error, simulation, structure, thermal, reliability, circuit)
- Design (electrical, mechanical)
- Contractor liaison
- Subsystem program management

Subsystem Analysis, Design, and Breadboard Testing

- Program plans maintenance (The program plans developed during the preliminary design and system analysis must be maintained.)
- Diagrams, layouts, schematics, long-lead items
- Analysis (same categories in previous phase, with emphasis now on circuit analysis)
- Design (electrical, mechanical)

Table 3-1. Major Design Phases
(Continued)

Subsystem Analysis, Design, and Breadboard Testing (Continued)

- Breadboard fabrication and tests
- Quality assurance (box level tests)
- Product engineering and manufacturing liaison
- System test liaison

Prototype Design, Fabrication, and Test

- Prototype design and fabrication
- Prototype test

---------------- FREEZE DESIGN ----------------

Conclude whether the subsystem design will meet all requirements; if not, determine what compromises exist in terms of performance, safety, cost, and schedule. Freeze design, and begin production engineering.

Subsystem Production Engineering, Fabrication, and Test

- Production engineering, fabrication, and test
- Prove out final engineering drawings, specifications, tooling, and tests to minimize production problems

System Integration and Test

Flight Test Phase (1 to 5 flights)

Initial Operational Phase (next 20 flights)

Operational Phase (remaining years of program)

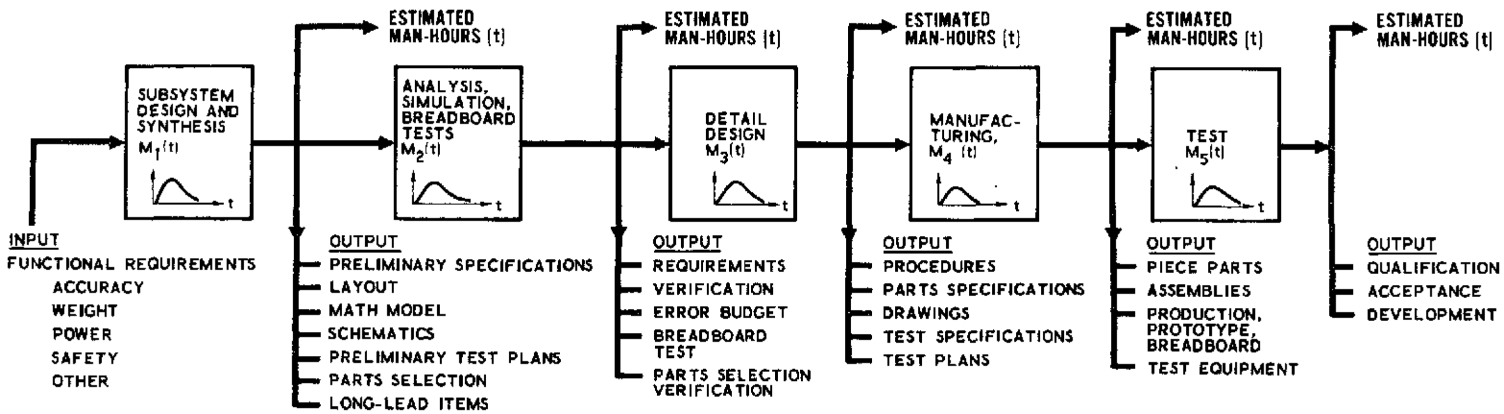

Figure 3-3. Simplified Subsystem Design Process Flow Chart

C. DESIGN SELECTION MODELS

A series of approaches was developed that attempted to model the actual design selection. (See Figure 3-4.) The concept is to enter the model with payload requirements. Component data tables are then searched to determine which attitude control sensors are capable of meeting the payload requirements. Similarly, a search is made to identify the type of applicable actuators. Typical attitude reference sensors are listed in Table 3-2; typical control actuators are listed in Table 3-3. The ACS requirements are derived from the payload requirements. Typical payload requirements are presented in Table 3-4.

In operation, the model would be employed for a preliminary sorting of components, based on accuracy. Reference accuracy would be divided into the following discrete categories (for example):

1. High accuracy (less than 0.05° at update) implies star reference, except that two-axis sun information can be obtained to this accuracy.
2. Medium accuracy (0.05° to 0.2°) permits use of earth sensors.
3. Coarse accuracy (0.2° to 2°) permits use of ion sensors.
4. Very coarse accuracy (2° to 10°) permits use of magnetometers.

Examples of control accuracy requirements and their implications might be as follows:

1. Precise pointing and tracking requirements, which imply momentum-exchange actuators
2. Jitter requirement less than 0.01°, which eliminates dual spin, unless an on-orbit balancing device is to be used.

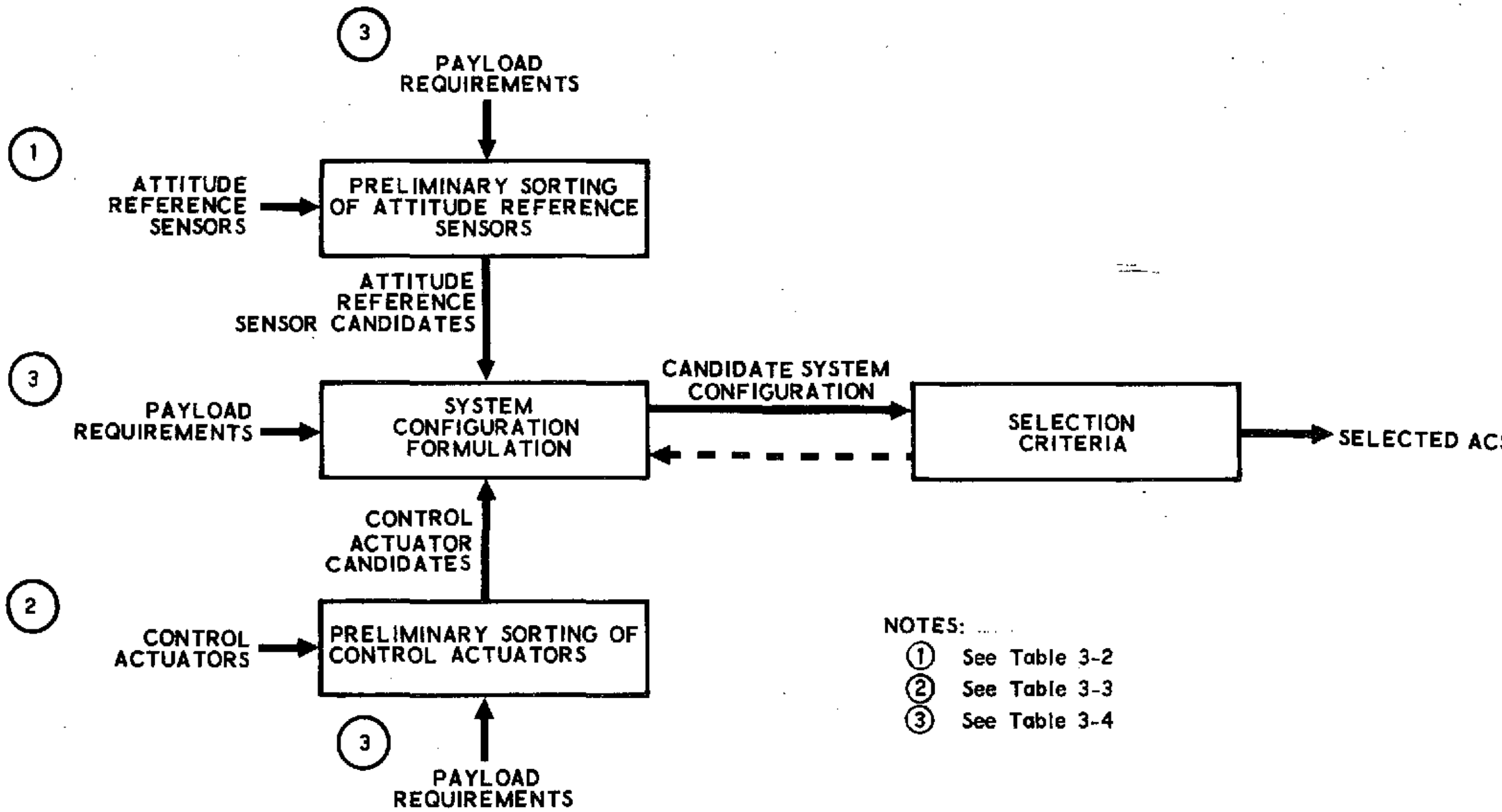

Figure 3-4. Design Selection Model

Table 3-2. Types of Attitude Reference Sensors

I. Long-Term or Update Sensors

   A. Star sensors

      1. Star tracker

         a. Electronic
         b. Gimbaled

      2. Fixed star sensor

   B. Horizon sensors

      1. Energy balance
      2. Edge tracker
      3. Scanner

   C. Sun sensors

   D. Magnetometer

   E. Ion sensor

II. Short-Term Attitude Reference

   A. Inertial

      1. Strapdown
      2. Platform

   B. Dynamics (as in spin stabilization)

   C. Math model of dynamics

Table 3-3. Types of Control Actuators

I.	Reaction Jets
II.	Reaction Wheels/Momentum Wheels
III.	Control Moment Gyros
	A. Single-gimbal
	B. Double-gimbal
IV.	Spin Stabilization
	A. Single-spin
	B. Dual-spin
V.	Gravity Gradient
VI.	Magnetic
VII.	Solar Pressure

Table 3-4. Types of Requirements

- I. Performance
  - A. Attitude orientation
    - 1. Spacecraft
      - a. Pointing
      - b. Tracking
      - c. Maneuvering
    - 2. Payloads, sensors, and appendages
      - a. Pointing
      - b. Tracking
      - c. Slewing
      - d. Scanning
  - B. Accuracy
    - 1. Control accuracy
      - a. Rate
      - b. Attitude
    - 2. Reference accuracy
      - a. Rate
      - b. Attitude
  - C. Orbit considerations
    - 1. Altitude
    - 2. Ellipticity
    - 3. Inclination
    - 4. Injection
    - 5. Stationkeeping
    - 6. Orbit adjust
  - D. Power
  - E. Weight
  - F. Volume
  - G. Autonomy
  - H. Lifetime/reliability
- II. Others

Other requirements, such as payload scanning or pointing, would be considered at this stage. For example, the payload pointing requirement would dictate the satellite orientation. Thus, if the payload is earth-pointing, the satellite would probably be earth-oriented, implying earth sensors (unless the accuracy requirement is too tight). In other cases, dissimilar multiple payload (or other subsystem) pointing requirements may require a stabilized platform to be used as a base from which the different sensors may be pointed. If the sensors have scanning requirements, the desirability of providing the scan motion with a portion of the vehicle must be considered.

Similarly, the effects of orbit requirements would be brought into the design selection. In a low-altitude earth orbit, significant control effort is required because of aerodynamic torques. The need for a low-altitude earth orbit would rule out the use of approaches such as gravity gradient, magnetic torquing, or solar torques. If orbit adjustment or stationkeeping is needed, then the ACS must be able to overcome the disturbance produced by the device used to achieve the velocity increment. This is often accomplished by spin stabilization.

This design selection model was developed somewhat further into the selection methodology depicted in Figure 3-5. Identification of standard configurations for ACSs was a necessary part of this modeling methodology. Therefore, a preliminary tabulation of standard configurations was made. (See Table 3-5.) For each system requirement, a search would be performed on all the stored standard configurations, as indicated in Table 3-6. After filtering through all control system requirements shown in Table 3-7, the remaining configurations that meet all requirements would be used as candidate configurations. In this approach, similar data tables would be developed for each sensor (e.g., earth sensor and gyro) and for each actuator (e.g., thrusters and reaction wheels). Typical component requirements are shown in Table 3-8.

The design selection models were developed further. The results of this model development generated the model described in Section 3.D.

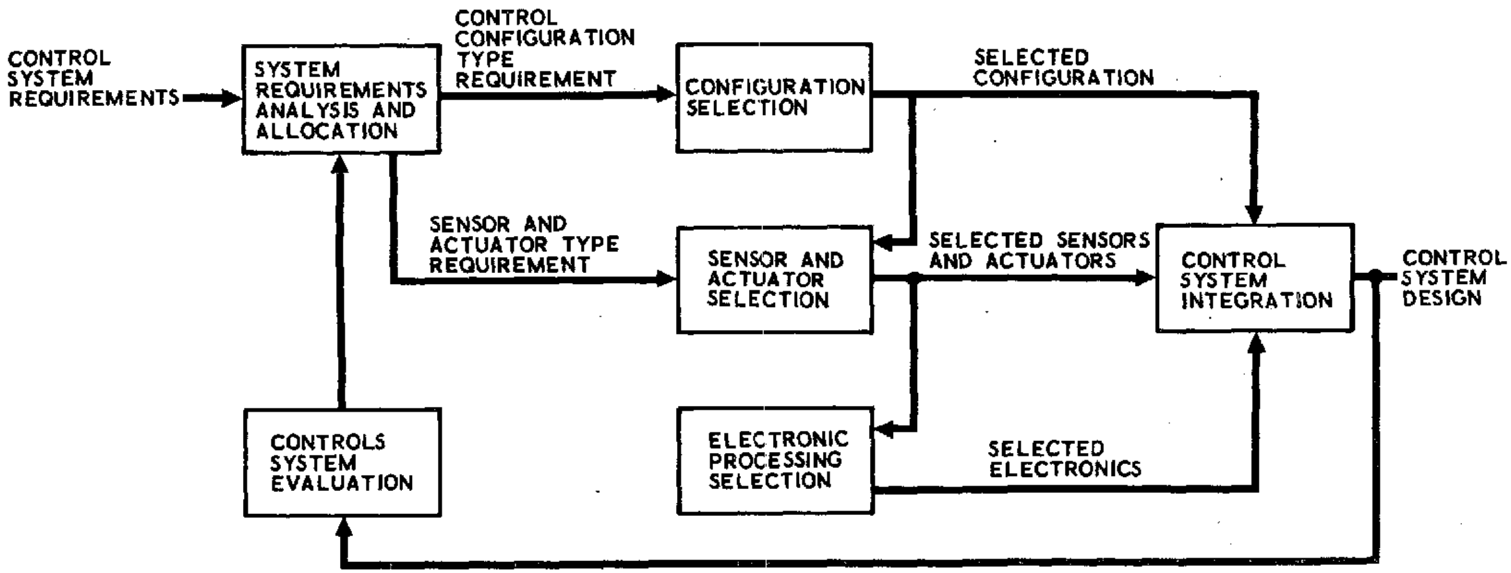

Figure 3-5. Methodology of Controls System Design from Controls System Requirements

Table 3-5. Standard ACS Configuration

Configuration No.	Configuration Components				
	Sensors	Actuators	Electronics	Processor	Comments
1	3-axis gyro reference 2-axis earth sensors	3-axis thrusters 2-axis engine gimbal actuators	Sensor processing Signal shaping Gain selection Signal conditioning (for telemetry) Thruster drives Gimbal drives		Basic Agena configuration
2	3-axis gyro reference 2-axis earth sensors Reaction wheel tachometers	3-axis thrusters 2-axis engine gimbal actuators 3-axis reaction wheels	Sensor processing Signal shaping Gain selection Signal conditioning (for telemetry) Thruster drives Gimbal drives Reaction wheels Unloading logic Wheel drives		Modified basic Agena configuration
3	3-axis gyro reference 2-axis earth sensors Control moment gyro tachometers Gimbal angle resolvers	3-axis thrusters 2-axis engine gimbal actuators 3-axis control moment gyros	Sensor processing Signal shaping Gain selection Signal conditioning (for telemetry) Thruster drives Gimbal drives Wheel drives Unloading logic (control moment gyro gimbals)		Modified basic Agena configuration
4	3-axis gyro reference 2-axis earth sensors 2-axis star tracker (gimbaled) 2-axis autocollimator	3-axis thrusters 2-axis engine gimbal actuators	Thruster drives Signal conditioning (for telemetry) Gimbal drives	Sensor processing Mode and gain Signal shaping Safety monitoring	Baseline Tug design

Table 3-5. Standard ACS Configuration (Continued)

Configuration No.	Configuration Components				
	Sensors	Actuators	Electronics	Processor	Comments
5	3-axis gyro reference 2-axis earth sensors 2-axis star tracker (gimbaled) 2-axis autocollimator Reaction wheel tachometers	3-axis thrusters 2-axis engine gimbal actuators 3-axis reaction wheels	Thruster drives Signal conditioning (for telemetry) Gimbal drives Wheel drives Reaction wheel unloading logic		Modified baseline Tug design
6	3-axis gyro reference 2-axis earth sensors 2-axis star tracker (gimbaled) 2-axis autocollimator Control moment gyro tachometers	3-axis thrusters 2-axis engine gimbal actuators 3-axis control moment gyros	Thruster drives Signal conditioning (for telemetry) Gimbal drives Wheel drives Unloading logic (control moment gyro gimbals)		Modified baseline Tug design
7	2-axis earth sensors Polaris sensor (yaw) 3-axis gyro reference	3-axis thrusters 3-axis reaction wheels	Thruster drives Wheel drives Signal conditioning (for telemetry)	Sensor processing Mode and gain switching Reaction wheel unloading logic Self-test	Primary mode of Applications Tech-nology Satellite (ATS) F and G
8	2-axis earth sensors Sun sensor and gyro (yaw) Reaction wheel tachometers	3-axis reaction wheels 2-axis thrusters (for reaction wheel unloading)	Sensor processing Wheel drives Thruster drives Unloading logic Signal shaping Signal conditioning (for telemetry)		Primary mode of Nimbus D
9	2-axis earth sensors Yaw sun sensor (on oriented array) Reaction wheel tachometers	3-axis reaction wheels 2-axis thrusters (for reaction wheel unloading)	Sensor processing Wheel drives Thruster drives Unloading logic Signal shaping Signal conditioning (for telemetry)		Normal mode of Orbiting Geophysical Observatory (OGO)

Table 3-5. Standard ACS Configuration (Continued)

Configuration No.	Configuration Components				
	Sensors	Actuators	Electronics	Processor	Comments
10	2-axis earth sensors Reaction wheel tachometers Gimbal angle resolvers	Double-gimbaled pitch momentum bias wheel 2-axis thrusters (for unloading)	Sensor processing Wheel drives Gimbal drives Thruster drives Unloading logic Signal shaping Signal conditioning (for telemetry)		Normal mode of gimbaled reaction wheel attitude stabilization package (GRASP)--TRW Comsat design
11	2-axis earth sensors Reaction wheel tachometer Gimbal angle resolver	Single-gimbal pitch bias wheel 2-axis thrusters (for unloading)	Sensor processing Wheel drive Gimbal drive Thruster drives Unloading logic Signal shaping Signal conditioning (for telemetry)		Basic normal mode of Lincoln Experimental Satellite (LES)-7
12	2-axis earth sensors Reaction wheel tachometers	Pitch momentum bias wheel 2-axis thrusters (pitch and offset roll/yaw)	Sensor processing Wheel drive Thruster drives Unloading logic (pitch only) Signal shaping Signal conditioning (for telemetry)		Canadian Technology Satellite
13	2-axis earth sensors Reaction wheel tachometers	Large pitch momentum wheel 2-axis thrusters (wheel unloading and spin axis correction) Nutation damper	Sensor processing Wheel drive Thruster drives Signal shaping (pitch only) Signal conditioning (for telemetry)		Pure pitch momentum bias stabilization

Table 3-5. Standard ACS Configuration (Continued)

Configuration No.	Configuration Components				
	Sensors	Actuators	Electronics	Processor	Comments
14	Single-axis earth sensor Single-axis spin sun sensor Reaction wheel tachometer	Large reaction wheel Transverse and spin thrusters	Sensor processing Wheel drive Thruster drives Signal shaping Signal conditioning (for telemetry)		Normal mode of 647 design
15	Spin earth sensor (2-axis) Rotor angle sensor	Despin mechanization assembly Nutation damper Thrusters (for spin axis correction)	Sensor processing Despin drive Thruster drives Signal shaping (despin loop only) Signal conditioning (for telemetry)		Normal mode of 777 and Tactical Communications Satellite (TACSAT) (dual-spin)
16	Spin sun sensor (2-axis)	Nutation damper Thrusters (for spin axis correction)	Thruster drives Signal conditioning (for telemetry)		Pure spinner with thruster
17	Spin sun sensor (2-axis)	Nutation damper Magnetic torquers	Coil drives Signal conditioning (for telemetry)		Normal mode of Space Experimental Satellite Program (SESP)-72
18		Pitch momentum bias wheel Passive damper	Wheel period timer Wheel drive (constant speed) Signal conditioning (for telemetry)		Pitch momentum bias with gravity gradient unloading

Table 3-6. Configuration Selection Matrix

Control System Requirements[a]	Standard Configurations[b]																	
	1	2	3	4	5	6	7	8	9	10	11	12	13	14	15	16	17	18
I. Acquisition																		
A. Initial position (deg)																		
1. Small (<10)	X	X	X	X	X	X	X	X	X	X	X	X	X	X	X	X	X	X
2. Limited (<90)				X	X	X				X								
3. Arbitrary				X	X	X				X								
B. Initial rate (deg/sec)																		
1. Low (<0.1)	X	X	X	X	X	X	X	X	X	X	X	X	X	X	X	X	X	X
2. Medium (0.1 to 1)	X	X	X	X	X	X				X								
3. High (>1)	X	X	X	X	X	X												
C. Acquisition time (min)																		
1. Very Long (>240)	X	X	X	X	X	X	X	X	X	X	X	X	X	X	X	X	X	X
2. Long (30 to 240)	X	X	X	X	X	X	X	X	X	X	X	X		X	X	X	X	X
3. Medium (1 to 30)	X	X	X	X	X	X	X	X	X	X								
4. Short (<1)	X	X	X	X	X	X												
II. Rate Recovery																		
A. Initial rate (deg/sec)																		
1. Low (<0.1)	X	X	X	X	X	X	X	X	X	X	X	X	X	X	X	X	X	
2. Medium (0.1 to 1)	X	X	X	X	X	X	X	X	X	X								
3. High (>1)	X	X	X	X	X	X												

[a]Control System Requirements continued in Table 3-7

[b]As defined in Table 3-5

Table 3-7. Control System Requirements for Configuration Selection

I. Acquisition
   A. Initial position
   B. Initial rate
   C. Acquisition time

II. Rate Recovery
   A. Initial rate
   B. Settling time

III. Attitude Hold
   A. Attitude reference
      1. Earth
         a. Nadir
         b. Offset
      2. Sun
         a. Center
         b. Offset
      3. Star
         a. Single star
         b. Multiple stars
      4. Inertial
   B. Orbit attitude
   C. Orbit ellipticity
      1. Near circular
      2. Medium ellipticity
      3. High ellipticity
   D. Orbit inclination
      1. Near equatorial
      2. Medium inclination
      3. Near polar

Table 3-7. Control System Requirements for Configuration Selection (Continued)

	E.	Two axes pointing accuracy	
		1.	Position
		2.	Rate
	F.	Third axis pointing accuracy	
		1.	Position
		2.	Rate
IV.	Maneuvers		
	A.	Number of axes	
	B.	Maneuver rate	
V.	Stationkeeping Control		
	A.	Disturbance torque level	
	B.	Firing duration	
VI.	Powered Flight Control		
	A.	Disturbance torque level	
	B.	Burn duration	
	C.	Thrust vector accuracy	
VII.	Reliability		
VIII.	Telemetry and Command		
	A.	Number of telemetry signals	
	B.	Number of commands	

Table 3-8. Requirements for Component Selection

I.	Earth Sensor	
	A.	Accuracy
	B.	Operational altitude
	C.	Reliability
	D.	Noise
	E.	Time constant
	F.	Scan offset capability
	G.	Number of axes sensed
	H.	Sun and moon intrusion logic
II.	Gyro	
	A.	Drift rate
	B.	Reliability
III.	Sun Sensor	
	A.	Accuracy
	B.	Reliability
IV.	Star Tracker	
	A.	Accuracy
	B.	Reliability
V.	Thruster	
	A.	Thrust level
	B.	Minimum on-time
	C.	Life
VI.	Reaction Wheel	
	A.	Peak torque
	B.	Angular momentum storage
	C.	Life

Table 3-8. Requirements for Component Selection (Continued)

VII.	Control Moment Gyro	
	A.	Peak torque
	B.	Angular momentum storage
	C.	Life
VIII.	Process Electronics (Digital)	
	A.	Memory
	B.	Word length
	C.	Cycle time
	D.	Reliability
	E.	Hardened memory
	F.	Input/output channels

D. MINIMUM MODEL

With the modeling experience obtained from the design process flow chart model described in Section 3. B, and the design selection model described in Section 3. C, the minimum model, incorporating their assets, was developed and is shown in Figure 3-6. The model was termed the "minimum model," since, as a minimum, it would consider, but did not adequately quantify, the performance, safety, cost, and schedule of an ACS.

Starting with the functional payload requirements, a sorting algorithm, as shown in Table 3-9, is used to determine an attitude control method such as gravity gradient, magnetic control, mass expulsion, momentum storage, or spin stabilization. Once the basic control method is established, various methods of configuring the design are considered. The next step is to search through component data and to select components that satisfy the performance requirements.

It is apparent that some technique must be devised for selecting the hardware. In addition, the problem of component redundancy and centralization has to be considered in the design. If the model is to be complete, it must consider the impact of the selected hardware on the other vehicle systems. At this stage of the modeling, the details for implementing the model were not established. The minimum model was expanded as described in Section 4, and became the Cost/Performance Model later used to obtain sample calculations on trade studies.

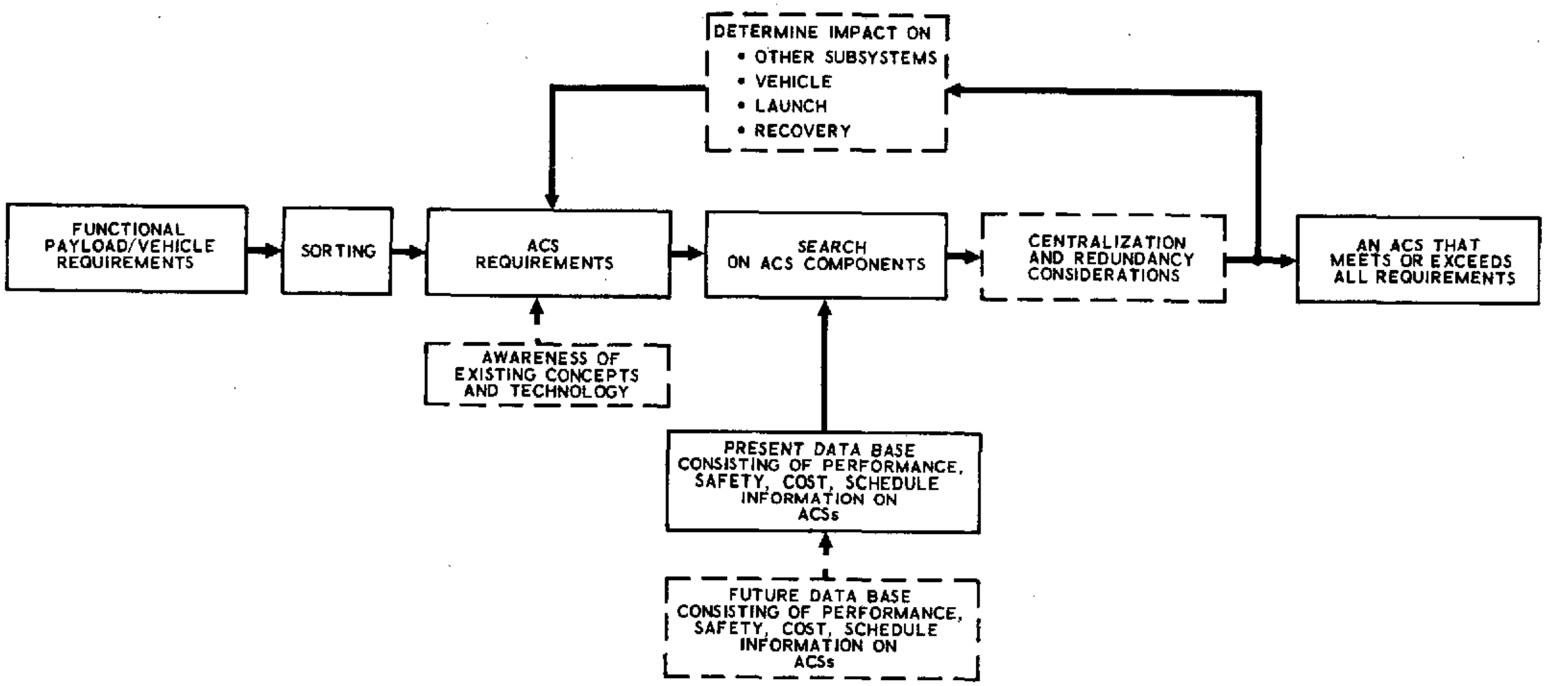

Figure 3-6. Minimum Model

Table 3-9. Sorting Matrix

Functional and Technical Requirements	Attitude Control Methods[a]				
	Gravity Gradient	Magnetic Control	Mass Expulsion	Momentum Storage[b]	Spin Stabilization
Earth Orientation	Yes	Yes	Yes	Yes	No
Inertial Orientation	No		Yes	Yes	Yes
Sun Orientation			Yes	Yes	Yes
185- to 550-km Orbits	No		Yes	Yes	Yes
550- to 37,000-km Orbits	Yes	Yes	Yes	Yes	Yes
37,000-km + Orbits	No	No	Yes	Yes	Yes
2- to 10-Deg Accuracy	Yes	Yes	Yes	Yes	Yes
0.2- to 2.0-Deg Accuracy	No	Yes	Yes	Yes	Yes
0.01- to 0.2-Deg Accuracy	No	No	Yes	Yes	Yes
0.1-Arc-Sec to 0.01-Deg Accuracy	No	No		Yes	Yes

[a]Yes: can be used
No: cannot be used
Blank: will not provide this function alone, but may be helpful

[b]Momentum storage devices cannot be used without an auxiliary torque-producing system.

4. COST/PERFORMANCE MODELING METHODOLOGY

The modeling approaches that were discussed in Section 3 did not provide quantitative relationships among the performance, safety, cost, and schedule parameters for an attitude control system (ACS). When both the top-down and bottom-up approaches were considered, it was decided that a costing methodology oriented from the bottom up could lead to a model employing quantitative expressions that could determine performance and cost sensitivities. It was realized that a set of basic equations, termed "aggregate equations," could be written that describe the performance, safety, cost, and schedule of the ACS in terms of the equipment used in a selected configuration. The equations were termed as "aggregate equations," since the independent variables that describe the ACS were "aggregated" into fundamental relationships to the elements of performance, safety, cost, and schedule. For example, the aggregate equation for the pointing accuracy of a typical three-axis ACS considers variables such as attitude sensor noise and misalignment, gyroscope drift and misalignment, signal processor noise, and control system deadband. Each of these variables is multiplied by a computed sensitivity coefficient and combined in a worst case and/or root-sum-square (RSS) manner to form the aggregate equation for the ACS pointing accuracy. One aggregate equation will be developed for each variable in Table 1-1 to form the set of aggregate equations for a particular control system configuration.

Aggregate equations in conjunction with the minimum model elements described in Section 3 were used to develop the Cost/Performance Model. The flow diagram for this model is shown in Figure 4-1. Starting with the payload functional requirements, a filtering technique (search/sort/filter) similar to that described in Section 3.C is used to determine an attitude control method (such as a gravity gradient, mass expulsion control, momentum storage, or spin stabilization) that will satisfy the functional requirements. The selection of an attitude control method is made because each different ACS configuration has its own set of aggregate equations.

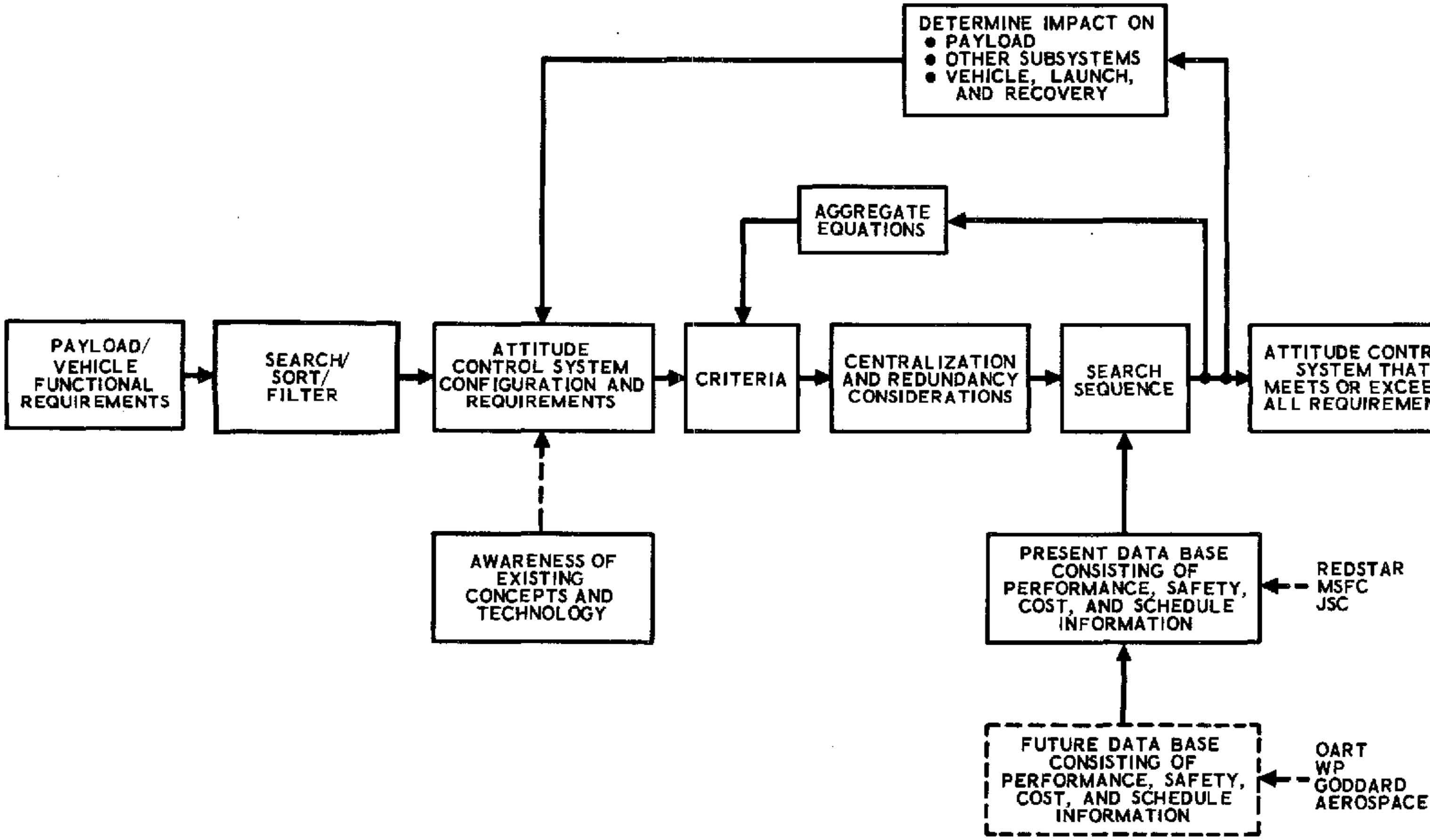

Figure 4-1. Cost/Performance Model

Once candidate control methods are determined, the type of equipment needed to mechanize the ACS can be selected by iteration. Accessing a data base consisting of all the ACS components suitable for this control method, the model first inserts the cheapest component into the pointing accuracy aggregate equation, assuming a low-cost ACS is our objective, and computes the pointing accuracy. If the pointing accuracy is poorer than desired, the model then selects the next least expensive components, iterating until the desired pointing accuracy is met. The next step is to use the safety aggregate equations to evaluate those hardware configurations that have met or exceeded the desired pointing accuracy requirement. The failure rate aggregate equations determine the necessary level (and configuration) of redundancy to satisfy the payload and mission success probability requirements. Thus, for a given configuration, a set of applicable components is chosen (based, for example, on minimum cost) from the data base that satisfies the performance and safety requirements. The next step is to compute the power dissipated by the ACS, and the weight and volume of the ACS. It would also be possible to iterate to minimize other parameters, such as weight or complexity. In addition, the total system cost and schedule can also be determined as a function of the selected equipment. One desirable feature of this aggregate equation approach is the ability to establish sensitivities to changes in requirements. One need only change the performance requirement (for example, pointing accuracy) and let the process iterate again to produce the new results.

The following sections describe the major elements of the Cost/Performance Model in detail. Section 4.A describes the search/sort/filter technique that selects an attitude control method based on a set of performance requirements; this is essentially an expansion of the technique indicated by Table 3-9. Also presented in Section 4.A are descriptions of the various control methods and their capabilities.

Section 4.B develops the more detailed information required to write performance aggregate equations for various ACS configurations. Functional block diagrams are given for attitude control configurations for several classes of vehicles. The detailed functional requirements, based on payload requirements and orbital considerations, are presented. Particular emphasis is given to a three-axis mass expulsion ACS, which is the baseline system for this study.

Sections 4.C through 4.F present the sample performance, safety, cost, and schedule aggregate equations for a specific ACS. The sample performance aggregate equations developed in this report consider the parameters of pointing accuracy, power, weight, volume, thermal specification, vibration specification, and ambient pressure specification for a three-axis mass expulsion ACS. The safety aggregate equations compute the failure rate, failure detection probability, and false alarm rate for an ACS. The cost aggregate equations determine the total cost of the ACS by considering six cost categories: design and development, build and checkout, test hardware, training and simulation, program life, and management. The schedule aggregate equations determine the amount of time required to develop an operational ACS starting with the proposal phase.

A. SEARCH/SORT/FILTER TECHNIQUE

This section discusses the methodology used to develop the search/sort/filter technique that selects an attitude control method based on a set of requirements for the ACS. In the development of the search/sort/filter technique, the usual problem of attempting to find a system that meets certain requirements was inverted. The approach is based on the existence of only a finite number of attitude control methods. Using this knowledge, one may work backward to determine what requirements each individual method meets or exceeds. Once the requirements have been tabulated for all the attitude control techniques, sorting the possible attitude control techniques by searching through the requirements is a straightforward problem. The filter output is the one or more control techniques appropriate for the mission under consideration.

Sections 4.A.1 through 4.A.4 describe the method in greater detail. First, the general requirements placed on an ACS are categorized. Second, the attitude control techniques are classified. Then, the capabilities of each technique are described. The results are summarized as a selection matrix. The section concludes with an example illustrating the search/sort/filter technique.

1. SUBSYSTEM REQUIREMENTS

All ACS requirements originate from the character of the mission and the nature of the payload. The mission and payload requirements determine the destination of the spacecraft, the duration or lifetime of the vehicle, the nominal orientation, the attitude and attitude accuracy of the ACS, and the stationkeeping and reorientation requirements. The mission and payload provide coarse estimates of vehicle size and inertia characteristics. They also determine the necessary pointing requirements for solar arrays or data telemetry. ACS requirements derived from the basic mission and payload are categorized into four groups:

a. Orbital characteristics
b. Orientation requirements
c. Accuracy requirements
d. Vehicle characteristics.

Table 4-1 subdivides these four categories into further detail.

In general, multiple control methods may seem appropriate for a given set of ACS requirements. Therefore, some rationale is necessary for choosing among the possible candidates. This rationale is provided by functional requirements; the performance specifications provide quantitative criteria for tradeoff studies in the detailed engineering analysis of the ACS. Table 4-2 illustrates a typical set of performance specifications.

2. CLASSIFICATION OF ACS METHODS

For the NASA Task 2.3 study, the attitude control methods are classified as active, semi-active, or inactive. These terms are defined by the following paragraphs.

Table 4-1. ACS Requirements

I. Orbital Characteristics
  - A. Primary Body
    1. Sun
    2. Earth
    3. Lunar or planetary
  - B. Orbital Parameters
    1. Eccentricity
    2. Semi-major axis

II. Orientation Requirements
  - A. Primary Pointing
    1. Earth
    2. Sun
    3. Inertial
    4. Lunar or planetary
  - B. Secondary Pointing
    1. Sun-oriented solar arrays
    2. Earth-pointing antenna
  - C. Required Stabilization
    1. Two axes
    2. Three axes
  - D. Stationkeeping
  - E. Reorientation

III. Accuracy Requirements
  - A. Attitude Error
  - B. Attitude Error Rate

IV. Vehicle Characteristics
  - A. Inertia (I_{min}/I_{max})
  - B. Man-rated

Table 4-2. Performance Specifications

I.	Weight and Detailed Inertial Characteristics	
II.	Reliability	
III.	Life	
IV.	Interface with Other Subsystems	
	A.	Thermal Control Subsystem
	B.	Electrical Power Subsystem
	C.	Communication Subsystem
	D.	Navigation and Guidance
	E.	Payload
	F.	Structure
	G.	Propulsion
V.	Effect of Spacecraft on Configuration	
	A.	Restriction on Choice, Location, or Field of View of Sensors
	B.	Constraint on Choice or Location of Actuators
	C.	Environmental Disturbances
	D.	Elastic Bending Modes
	E.	Dynamic Behavior

An active control method uses one or more feedback loops to maintain the vehicle attitude within specified limits. Such a closed-loop system is completely self-contained by the spacecraft. It operates by measuring the deviation of the vehicle axes from the reference orientation. These measurements are processed by suitable control logic. The output signal from the control logic energizes an actuator that torques the spacecraft toward the reference orientation.

An inactive attitude control technique directs the vehicle orientation by a passive feedback system. No sensors, no control logic, and no actuators are required by an inactive attitude control technique.

The semi-active category covers all schemes that employ some of the elements of an active control technique. This may take the form of attitude sensors so that the spacecraft orientation may be estimated by ground-based data processing. With such estimates of spacecraft attitude, it is desirable in some situations to command intermittent corrections to the spacecraft attitude over a ground station.

Nine distinct types of attitude control are considered in this section:

a. Gravity gradient
b. Solar stabilization
c. Aerodynamic stabilization
d. Magnetic stabilization
e. Spin stabilization
f. Dual-spin stabilization
g. Momentum exchange
h. Mass explusion
i. Hybrid.

Inactive and semi-active configurations are possible for attitude control techniques a through e. Methods f through h employ active or at least semi-active control methods to provide stabilization. The hybrid method is included to cover those instances when multiple sources of control torque can be used successfully in concert — for example, combined gravity gradient and magnetic stabilization. Section 4.A.3 discusses each method and describes its capabilities to meet the subsystem requirements. These descriptions provide the rationale for establishing the selection matrix.

3. DESCRIPTION OF ACS METHODS

a. Gravity Gradient

A torque results from the interaction of the earth's gravity gradient with the distributed mass of a satellite. If the satellite is designed with the maximum moment of inertia about the pitch axis and the minimum moment of inertia about the yaw axis, the gravity gradient torque aligns the vehicle to the earth's local vertical, and orbit rate coupling provides a yaw orientation. These control axes are defined in Figure D-1, Appendix D. The torque increases as the sine of twice the angle between a principal axis and the local vertical. Thus, two conditions of stable equilibrium result. In the desirable condition, the satellite points down toward the earth; in the undesirable condition, the vehicle is upside down and pointing toward space.

Transient oscillations in attitude, called librations, persist for some time because the natural period is close to the orbital period. Some form of energy dissipation in the satellite damps these initial librations and reduces the effect of perturbing torque. Energy dissipation is either mechanical or electrical in nature. In the mechanical systems, the energy loss appears in the form of fluid viscosity or a viscoelastic spring material. In electrical systems, because of vehicle motion, energy dissipation occurs (eddy current losses or hysteresis losses) from the coupling of these electrical systems to the earth's magnetic field.

There are several limitations of the gravity gradient technique:

(1) The spacecraft can only be oriented to the local vertical.

(2) The spacecraft must be in a circular or nearly circular orbit. The maximum pointing error increases as the ellipticity of the orbit for nearly circular orbits.

(3) The technique is applicable only over a limited range of altitude from approximately 550 km (300 nmi) to several earth radii. Below 550 km (300 nmi), aerodynamic effects predominate. At large distances from the earth, solar torques prevail.

(4) The method of deployment must ensure that the vehicle will be oriented right side up.

Semi-active gravity gradient control schemes attempt to overcome the problems of gravity gradient stabilization by incorporating control moment gyros or reaction wheels into the control system. This results in improved damping characteristics and an improved yaw performance of 1- to 10-deg yaw error. The Applications Technology Satellite has been chosen to evaluate gravity gradient stabilization techniques.

b. Solar Stabilization

Solar radiation pressure can be utilized to stabilize a spacecraft that has the sun as a primary reference. In the passive scheme, the spacecraft is designed so that the center of force due to the solar pressure lies behind the center of mass. Damping is provided by a passive technique.

In the semi-active category, the solar action is a vernier control to a passively stable vehicle. The Mariner C spacecraft ACS is an example of this technique. After the spacecraft is in trim for the long coasting phase of its mission, the positions of solar vanes are refined by the differential heating of their bimetallic support arms. The time constant of this heating process is chosen to provide a damping as well as a restoring torque.

c. Aerodynamic Stabilization

Satellites in low earth orbit experience significant aerodynamic forces. These forces are capable of providing two-axis orientation in pitch and yaw. The satellite is stabilized with respect to its orbital velocity vector. Weather vane stability and damping are designed into the spacecraft by choosing a configuration where the aerodynamic center of pressure is behind the center of mass. Aerodynamic forces are significant at altitudes below 550 km (300 nmi). Only moderate pointing of 1 to 10 deg is possible. The semi-active AC techniques use a momentum exchange device to provide roll control for low-accuracy, three-axis earth orientation.

d. Magnetic Stabilization

For altitudes less than approximately 22,000 km (12,000 nmi), the earth's magnetic field is strong enough to provide useful control torque when it interacts with one or more magnets mounted in a spacecraft. In a passive scheme, permanent magnets would be used to line up the spacecraft with the local direction of the magnetic field vector the same way that the magnetic needle in a compass seeks magnetic north. Damping torques would be obtained from hysteresis losses and/or eddy current losses. A semi-active configuration employs electromagnets so that the direction and strength of the spacecraft magnetic dipole is controlled by currents in the torquing coils of the electromagnet. Semi-active magnetic control systems have been used on the Tiros II and III weather satellites and on the Navy Transit IA and IB navigation satellites.

e. Spin Stabilization

Spin stabilization is used primarily at altitudes above 550 km (300 nmi). When a significant amount of spin is imparted along a prescribed axis, a satellite becomes, in effect, a gyroscope. A gyroscope is characterized by its angular momentum vector. The behavior of this vector in the presence of disturbance torques determines how adequately the gyroscopic effect may be used to stablize a spacecraft in inertial space. The angular momentum vector provides a kind of stiffening that attenuates the effect of disturbance torques on the vehicle attitude. Disturbance torques that are transverse to the spin axis precess the angular momentum vector. A transverse torque impulse results in a constant error. A constant disturbing torque gives rise to a constant vehicle rate. Disturbance torques along the spin direction modify the spin rate. In a completely inactive spin-stabilized ACS, the spin angular momentum is chosen such that the cumulative errors resulting from all disturbance torques lie below a specified tolerance. The satellite has a nutational motion about the total momentum vector when a component of momentum exists about some direction other than the spin axis. Nutational motion is removed by a number of passive damping schemes, resulting in the dissipation of rotational kinetic energy until the spacecraft finds a state of minimum energy. This implies that the spin direction must be along the axis of the maximum moment of inertia. The Tiros I weather satellite utilized inactive spin stabilization for attitude control.

Semi-active spin-stabilized ACSs employ sun and horizon sensors to detect the wanderings of the spin axis. Corrective torques are applied as required to keep the spin axis within a specified error limit. One configuration that has been used to supply reorientation and a stationkeeping capability has two mass expulsion thrusters in the ACS. One thruster is parallel to the spin axis, and, when pulsed synchronously with the spin rate, a net torque acts to precess the vehicle spin axis. The other thruster is mounted orthogonal to the spin axis. Its line of action passes through the center of mass. This thruster is pulsed synchronously with the spin rate to provide orbital velocity control for the vehicle. The Syncom Communications Satellite uses this form of semi-active attitude control.

f. Dual Spin

Dual-spin stabilization is a useful control technique at altitudes above 550 km (300 nmi), and is most commonly employed at synchronous altitude. Dual-spin satellites consist of two interconnected rotating bodies. The more slowly rotating body (usually earth-oriented) is referred to as the despun body; the other as the rotating body. This configuration has the interesting property that the maximum inertia constraint for attitude stability does not apply, providing that the despun body contains a nutation damper. In the semi-active configuration, sun sensors and earth sensors are mounted directly on the rotating body. Their outputs are telemetered to a ground station. The orientation of the vehicle is estimated from these measurements. When disturbances drive the attitude error past a prescribed tolerance, a ground-initiated control sequence actuates the spacecraft reaction jets. The thrust of these jets drives the spacecraft back to its nominal orientation.

In the active configuration, the control logic is contained onboard the spacecraft. The angular momentum of the spacecraft provides short-term stability, and the active control system maintains long-term attitude accuracy. Pointing accuracies on the order of 0.01 deg are possible. The active ACS also uses the control jets for both stationkeeping and reorientation.

Dual-spin ACSs have proven very useful in communications satellites with high pointing accuracies. The Tactical Communications Satellite is an example of a spacecraft that has employed this concept. The primary limitation of the dual-spin configuration is that the surface area on which solar cells may be mounted is not fully sun-oriented and is limited in area. Consequently, there is a limit to the quantity of available power.

g. Momentum Exchange Systems

The momentum exchange method makes it possible to design a very accurate three-axis active ACS for a spacecraft. Disturbance torques that tend to alter the vehicle attitude are counteracted by applying an equal but opposite torque to the spacecraft. The reaction torque on the momentum exchange device increases or decreases its momentum. All momentum exchange devices are capable of storing only a finite amount of momentum. When this condition is reached, they are saturated. The ACS must provide an independent source of control torque so that the saturated momentum can be dumped.

Accuracies of one-second-of-arc attitude uncertainty of the primary sensor are possible with this method. The momentum exchange devices can be used for attitude maneuvers. If a reaction jet system is present for momentum dumping, it can be used for stationkeeping. An ACS design based on the momentum exchange method is used on both the Orbiting Astronomical Observatory and the Nimbus weather satellite.

h. Mass Expulsion

In practice, mass expulsion devices take the form of cold gas, monopropellant, or bipropellant thrusters. Thrusters or reaction jets produce forces on the spacecraft. When the line of action does not pass through the center of mass, then a torque is produced. Two opposed thrusters mounted on opposite sides of the spacecraft produce control torques with no net force applied to the vehicle. These torques are used to control the vehicle attitude.

The use of thrusters results in a control system that has a limit cycle. The limit-cycle operation results in the continual depletion of fuel. The fuel consumption due to limit cycling depends on the ratio of angular rate to limit-cycle displacement. The limit-cycle amplitude and rate are determined by the ACS requirements. Hence, the propellant required depends on the mission duration.

Reaction jets have a number of distinct advantages. They can be used in several modes of spacecraft operation, for example: acquisition, maneuvering, stationkeeping, and reorientation. They can be operated all the way from minimum impulse size during unperturbed limit cycling to 100% duty cycle to counteract large transients. The primary disadvantages of the mass expulsion control technique are the limited quantity of propellant onboard the spacecraft and the maximum reliable number of valve firings.

4. EXAMPLE OF SEARCH/SORT/FILTER TECHNIQUE

The search/sort/filter matrix shown in Table 4-3 summarizes the characteristics of each attitude control technique as a function of whether it is active, semi-active, or inactive as defined in Section 4.A.2. The requirements discussed in Section 4.A.1 are listed horizontally across the top of the page. These requirements are categorized as orbital characteristics, orientation requirements, accuracy requirements, and vehicle characteristics. Each category is subdivided into as much detail as necessary to define the ACS requirements. The category of secondary pointing refers to the ability to independently point a device or sensor mounted on a spacecraft that is stabilized by the primary method. The attitude control methods are listed on the left-hand side of the table in generally increasing order of sophistication from top to bottom.

If the search/sort/filter is to be utilized, a set of ACS requirements is necessary. Then, the process commences with the gravity gradient method of attitude control. The horizontal line corresponding to the gravity gradient inactive method is followed across the page. A search is made through all requirements to determine whether this method is suitable for the mission under consideration. The process continues to sort through all the control methods and terminates when the last technique in the first column has been investigated. In the cases where several attitude control techniques satisfy the ACS requirements, a tradeoff study is used to determine the method best suited for the particular application. The performance specifications listed in Table 4-2 provide meaningful criteria for such trade studies. The following example illustrates the search/sort/filter technique.

FOLDOUT FRAME

FOLDOUT FRAME

Table 4-3. Search/Sort/Filter Matrix

Attitude Control		Attitude Control System Requirements																						
		Orbital Characteristics					Orientation Requirements										Accuracy Requirements						Vehicle Characteristics	
		Primary Body			Orbit Elements		Primary Pointing				Secondary Pointing		Stabilization				Attitude Error (°)			Attitude Error Rate(°/sec)			Inertia	
Method	Classification	Earth	Solar	Lunar or Planetary	Eccentricity (e)	Semi-Major Axis (a)	Earth	Sun	Inertial	Lunar or Planetary	Solar	Earth	2 Axis	3 Axis	Station-keeping	Attitude Maneuvers	10-1	1-0.1	<0.1	1-0.1	0.1-0.01	<0.01	I_{min}/I_{max}	Man-Rated
Gravity Gradient	Inactive	Yes	No	No	e<0.2	a<5R_o	Yes	No	No	No	No	No	Yes	No	No	No	Yes	No	No	Yes	No	No	<0.1	No
	Semi-active	Yes	No	No			Yes	No	No	No	No	Yes	Yes	Yes	No	No	Yes	No	No	Yes	No	No	<0.1	No
Solar Pressure	Inactive	Yes	Yes	No	a(1 + e) < 3AU		No	Yes	No	No	Yes	No	Yes	No	No	No	Yes	No	No	Yes	Yes	No	Near unity	No
	Semi-active	Yes	Yes	No			No	Yes	No	No	Yes	Yes	Yes	Yes	No	No	Yes	No	No	Yes	Yes	No		No
Aerodynamic Pressure	Inactive	Yes	No	No	a(1 + e) < R_o + 925 km		Yes	No	No	No	No	Yes	Yes	No	No	No	Yes	No	No	Yes	No	No	Near unity	No
	Semi-active	Yes	No	No			Yes	No	No	No	No	Yes	Yes	Yes	No	No	Yes	No	No	Yes	No	No		No
Earth's Magnetic Field	Inactive	Yes	No	No	a(1 + e) < 30, 000 km		Yes	No	No	No	No	Yes	Yes	No	No	No	Yes	No	No	Yes	Yes	No	Near unity	No
	Semi-active	Yes	No	No			Yes	No	No	No	No	Yes	Yes	No	No	No	Yes	No	No	Yes	Yes	No		No
Spin Stabilized	Inactive	Yes	Yes	Yes	Arbitrary		No	No	Yes	No	Yes	Yes	Yes	No	No	No	Yes	No	No	Yes	No	No	≤0.5	No
	Semi-active	Yes	Yes	Yes			Yes	Yes	Yes	Yes	Yes	Yes	Yes	No	Yes	Yes	Yes	No	No	Yes	No	No	≤0.5	No
Dual-Spin Stabilized	Semi-active	Yes	Yes	Yes	Arbitrary		Yes	Yes	Yes	Yes	Yes	Yes	Yes	No	No	Yes	Yes	Yes	Yes	Yes	Yes	No	Arbitrary	No
	Active	Yes	Yes	Yes			Yes	Yes	Yes	Yes	Yes	Yes	Yes	Yes	Yes	Yes	Yes	Yes	Yes	Yes	Yes	No		No
Momentum Exchange	Active	Yes	Yes	Yes	Arbitrary		Yes	Yes	Yes	Yes	Yes	Yes	Yes	Yes	Yes	Yes	Yes	Yes	Yes	Yes	Yes	Yes	Arbitrary	Yes
Mass Expulsion	Active	Yes	Yes	Yes	Arbitrary		Yes	Yes	Yes	Yes	Yes	Yes	Yes	Yes	Yes	Yes	Yes	Yes	No	Yes	Yes	No	Arbitrary	Yes
Hybrid	Active	Yes	Yes	Yes	Arbitrary		Yes	Yes	Yes	Yes	Yes	Yes	Yes	Yes	Yes	Yes	Yes	Yes	Yes	Yes	Yes	Yes	Arbitrary	Yes

R_o - earth radius

AU - astronomical units

Example: Determine an appropriate attitude control technique for an unmanned communications satellite. The satellite operates in a nearly circular synchronous earth orbit. Proper operation of the communications payload requires three-axis stabilization and a stationkeeping capability. The attitude error tolerance is 0.1 deg, and the attitude error rate tolerance is 0.005 deg/sec.

The gravity gradient, solar, and spin stabilization techniques cannot meet the accuracy requirement. Aerodynamic and magnetic stabilization are eliminated by the orbital characteristics. The dual-spin and mass expulsion techniques cannot meet the attitude error rate requirement. The momentum exchange technique is the appropriate method in this instance. The requirement for stationkeeping implies that reaction jets are included in the ACS and thus, the attitude control becomes, in effect, a hybrid method.

B. FUNCTIONAL BLOCK DIAGRAMS

The aggregate equations are a function of the particular ACS mechanization utilized. Thus, as a starting point in the modeling activity, the functional requirements must be translated into a functional block diagram, so that the ACS mechanization may be determined. For example, if a space vehicle is to have both a powered-flight and an on-orbit control capability, then a functional block diagram such as that depicted in Figure 4-2 should be drawn. The functional block diagram shows 30 elements consisting of sensors, amplifiers, shaping, compensation, thrusters, and engines. After the functional block diagrams are drawn, one must consider the issues of centralization and redundancy. As an example of centralization, the function of sensing the pitch motion of the vehicle during the on-orbit and powered-flight periods might be accomplished by the same sensor. After these steps are completed, more specific block diagrams may be drawn, from which aggregate equations can be derived.

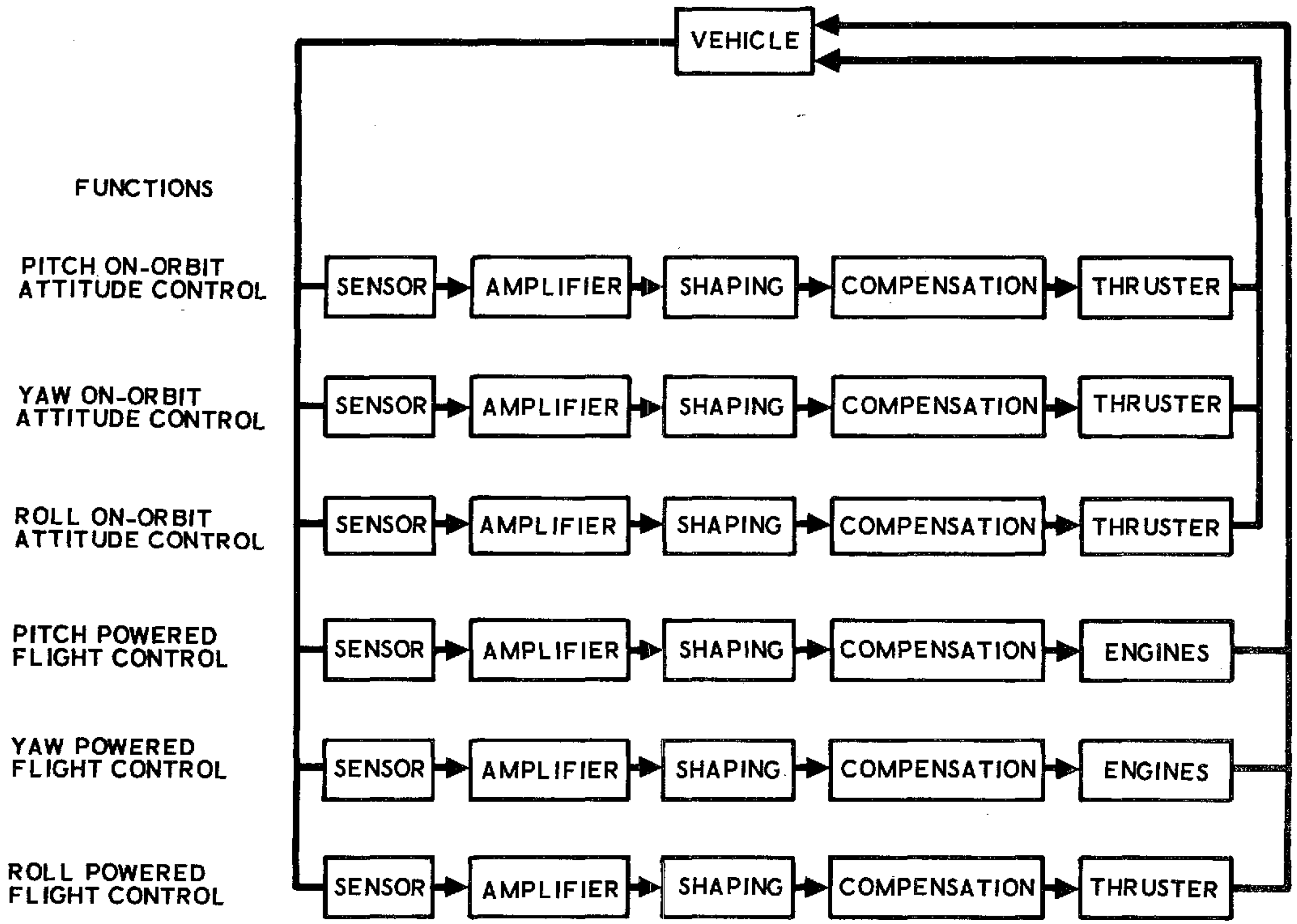

Figure 4-2. Attitude Control Functions

Four types of vehicles were considered for this study:

Class	Type of Vehicle
1	Unmanned, expendable, autonomous
2	Unmanned, reusable, autonomous
3	Manned, reusable, autonomous
4	Manned, reusable, using ground support

Table 4-4 summarizes the functional requirements of the roll, pitch, and yaw loops for these vehicles.

For the vehicles in Table 4-4, the ACS performs three basic functions:

1. Rate stabilization
2. Attitude control
3. Guidance control during powered flight.

Sections 4.B.1 through 4.B.3 discuss each of these topics in their turn. Coasting flight and powered flight above the earth's atmosphere are considered in this flight control study. Coasting flight implies the control of the spacecraft attitude while the spacecraft is orbiting a primary body such as the earth or sun. During powered flight, the attitude and the flight path of the vehicle must be controlled while thrusting. These two categories place different requirements on the ACS. The sources of reference information may not be the same, and the sources of control torques that change the vehicle attitude may be different. The overlap between these two categories of flight lies in the fact that they are both part of the same overall control system, using common equipment whenever possible.

Figure 4-3 displays the generalized functional block diagram of an active ACS. Specific examples of a dual-spin and a three-axis mass expulsion control system functional block diagram for coasting flight appear in Figures 4-4 and 4-5. The scope of the ACS includes all the functional blocks in Figures 4-3, 4-4, and 4-5, except the blocks labeled "vehicle dynamics."

Table 4-4. Functional Requirements of Three-Axis Mass Expulsion ACS

Functions	Class 1 (Unmanned, Expendable Autonomous)		Class 2 (Unmanned, Reusable Autonomous)		Class 3 (Manned, Reusable Autonomous)		Class 4 (Manned, Reusable, Using Ground Support)	
	Coasting	Powered Flight	Coasting	Powered Flight	Coasting	Powered Flight	Coasting	Powered Flight
Pitch Axis								
Damping	Yes	Yes	Yes	Yes	Yes	Yes	Yes	Yes
Attitude Hold	Yes	Yes	Yes	Yes	Yes	Yes	Yes	Yes
Reference Orientation	Yes	No	Yes	No	Yes	No	Yes	No
Pitch Program	Yes	No	Yes	No	No	No	Yes	No
Manual Input	No	No	No	No	Yes	No	Yes	No
Guidance Command	No	Yes	No	Yes	No	Yes	No	Yes
Roll Axis								
Damping	Yes	Yes	Yes	Yes	Yes	Yes	Yes	Yes
Attitude Hold	Yes	No	Yes	No	Yes	No	Yes	No
Reference Orientation	Yes	No	Yes	No	Yes	No	Yes	No
Roll Program	Yes	No	Yes	No	No	No	Yes	No
Manual Input	No	No	No	No	Yes	No	Yes	No
Guidance Command	No	Yes	No	Yes	No	Yes	No	Yes
Yaw Axis								
Damping	Yes	Yes	Yes	Yes	Yes	Yes	Yes	Yes
Attitude Hold	Yes	No	Yes	No	Yes	No	Yes	No
Reference Orientation	Yes	No	Yes	No	Yes	No	Yes	No
Yaw Program	Yes	No	Yes	No	No	No	Yes	No
Manual Input	No	No	No	No	Yes	No	Yes	No
Guidance Command	No	Yes	No	Yes	No	Yes	No	Yes

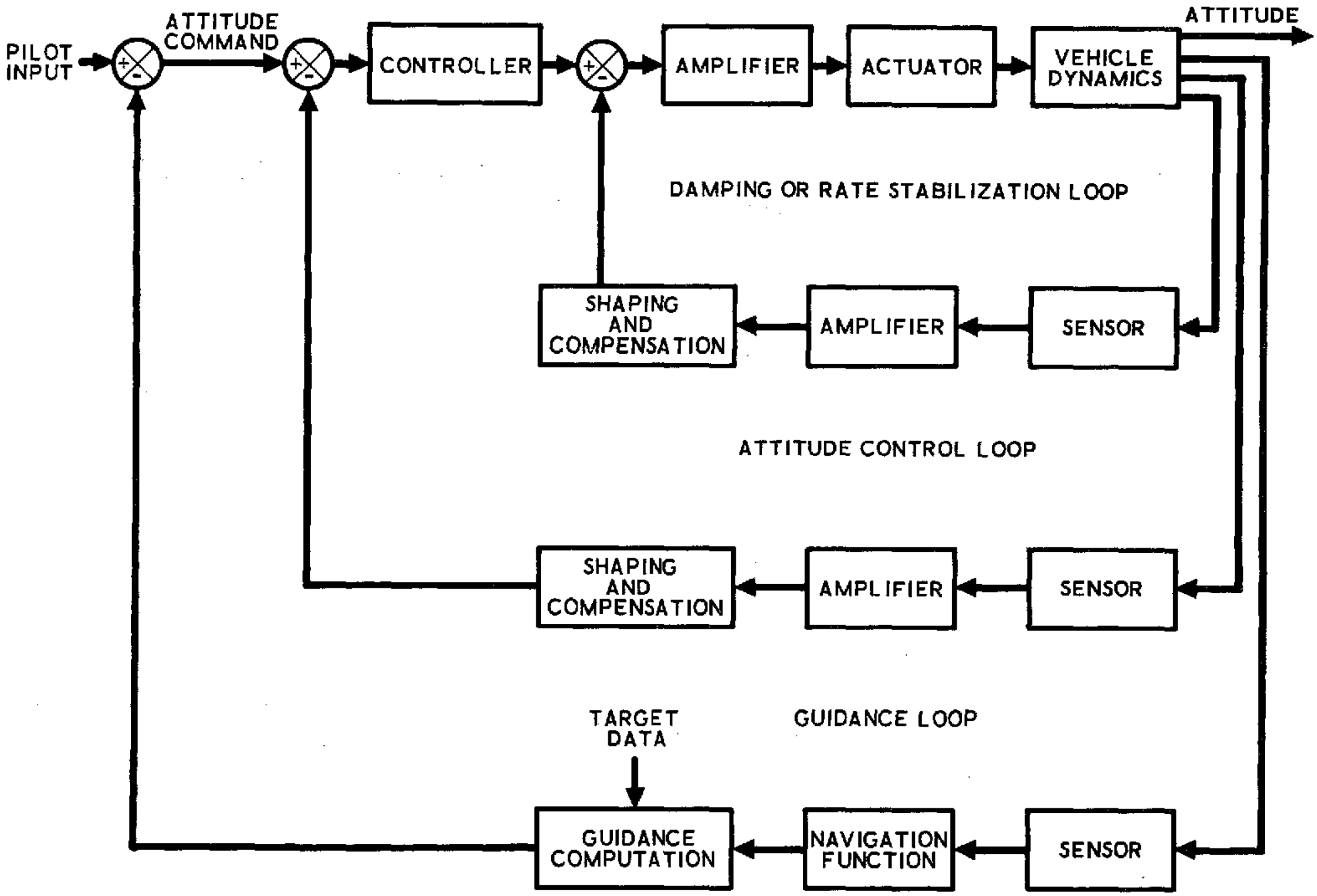

Figure 4-3. Generalized ACS Functional Block Diagram

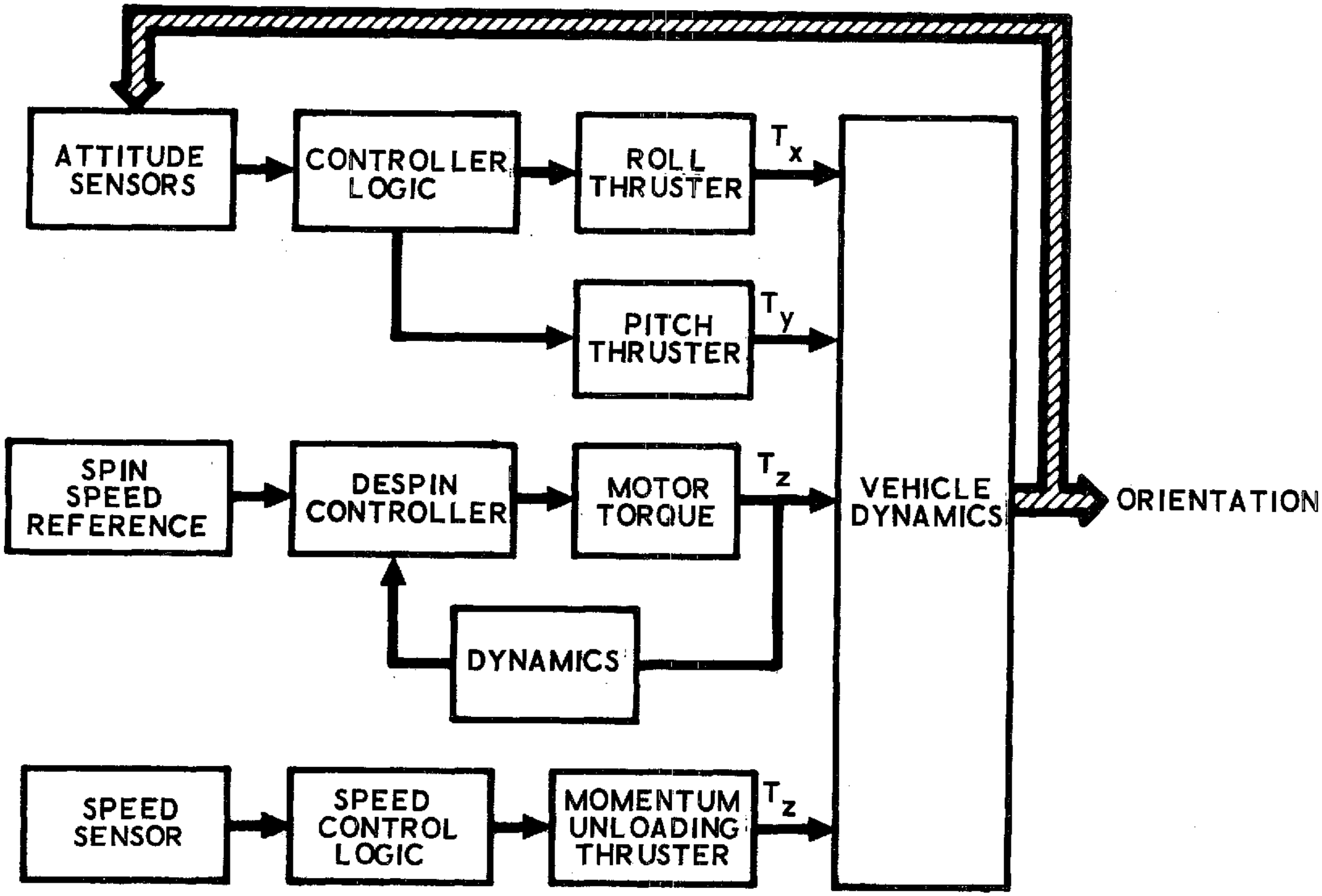

Figure 4-4. ACS Functional Block Diagram, Dual-Spin Configuration

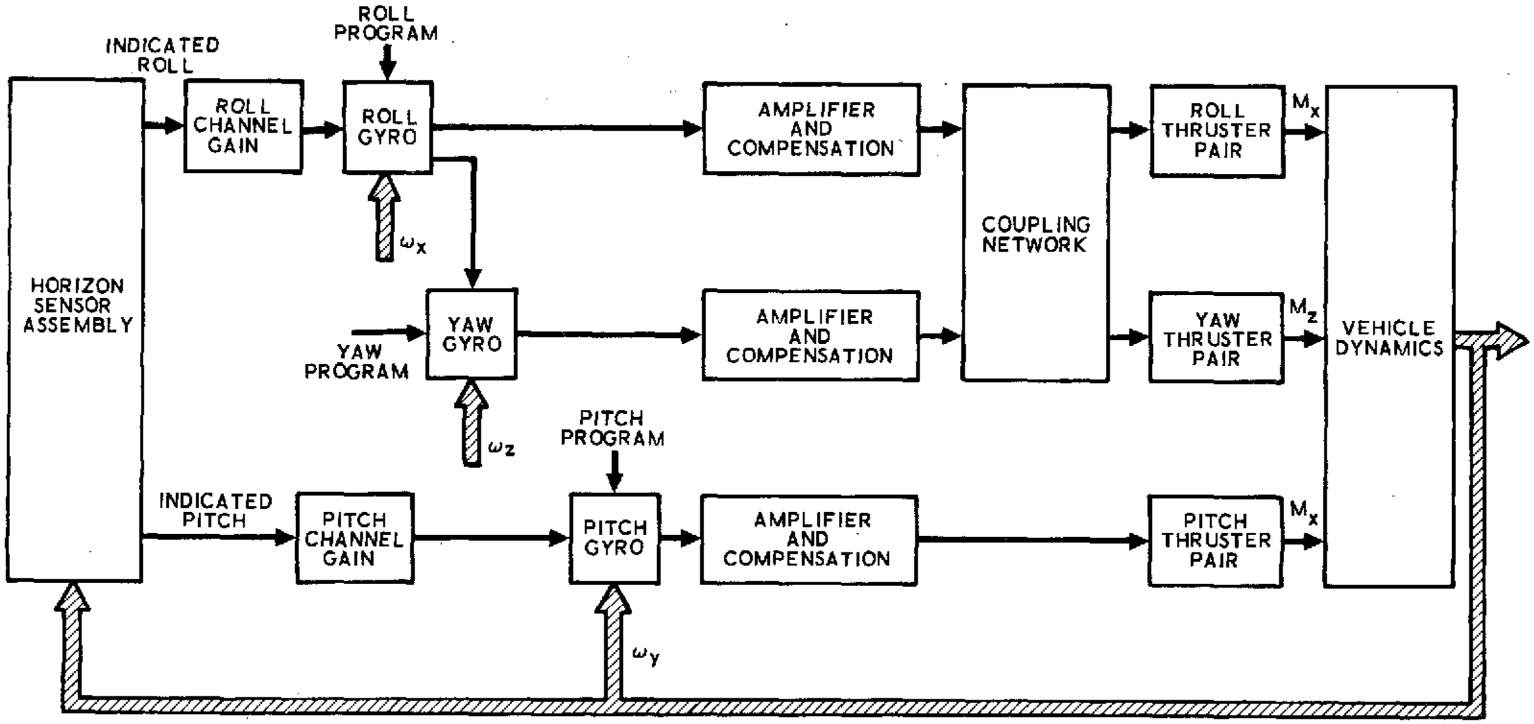

Figure 4-5. ACS Functional Block Diagram, Three-Axis Mass Expulsion Gyrocompassing Scheme

In Figure 4-3, the progression of the feedback loops from inner to outer reflects the lower requirement on the dynamic response of each successive feedback path.

Generalized functional block diagrams do not show several important features that must be considered in the design of an ACS:

1. Coupling of the control loops due to kinematic and inertial cross coupling
2. Switching functions, for example when the spacecraft transfers from the coasting-flight mode to the powered-flight mode
3. Power sources that energize the control system
4. Adaptive nature of nonlinear control loops commonly employed in an ACS
5. Redundancy that achieves a reliability commensurate with the mission requirements.

The more detailed functional diagrams of specific systems are required for this purpose and are used to develop aggregate equations.

1. RATE STABILIZATION

Rate stabilization can be mechanized by a number of techniques. The simplest manner to obtain rate information is to measure the angular velocity of the vehicle with rate gyroscopes. A rate gyro measures angular velocities with respect to inertial space. In many applications, it is desirable to stabilize the vehicle relative to a rotating coordinate system (e.g., earth reference). Under these circumstances, compensating signals must be provided that correct for the angular velocity of the noninertial coordinate frame. Several synthetic rate schemes have been developed that do not rely on rate gyros; these can vary from passive networks that differentiate the output of an attitude sensor to control systems that utilize nonlinear components to derive rate information.

2. FREE-FLIGHT ATTITUDE CONTROL

Attitude control of a space vehicle requires the ACS to perform four separate functions:

a. Identify a desired reference orientation.

b. Sense angular deviation between the reference orientation and a set of axes fixed in the vehicle.

c. Provide control torques.

d. Couple the sensor instrumentation to the control torque.

The details of each function are strongly dependent on the mission duration, required pointing accuracy, orbital geometry, and payload requirements.

Figures 4-4 and 4-5 show two configuration-oriented functional block diagrams. Figure 4-4 illustrates the dual-spin configuration, a stabilization method suitable for unmanned reusable or expendable vehicles with or without ground support. Figure 4-5 displays the functional block diagram of a three-axis mass expulsion ACS that uses a gyrocompassing scheme. A gyrocompassing configuration ACS is applicable to a space vehicle such as the Space Tug. This ACS method is acceptable also for manned or unmanned, expendable or reusable vehicles at any level of autonomy.

The following paragraphs provide some insight into the problems associated with the mechanization of each function.

For a space vehicle to execute its mission successfully, it must achieve a particular reference orientation. The reference orientation is determined by the mission objective. The mission establishes general orientation requirements, whether toward the sun, earth, or some other celestial body. Pointing requirements on solar panels and transmitting antenna also influence the reference orientation. In general, the reference orientation may be either rotating or fixed in inertial space. If orbit changes are required, several reference orientations may be required during the course of the mission.

Actuators in an ACS are torque-producing devices. The control torques produced by the actuator change the attitude of the vehicle in a prescribed manner so that the vehicle follows the reference orientation or attitude command. Two general methods are available for producing control moments: mass expulsion systems and momentum exchange systems.

On-off thrusters are the commonly employed actuators of the first category. They may be clustered to increase the net control torque applied to the vehicle and to increase the reliability of the ACS. Thrusters are of three types:

a. Cold gas, such as nitrogen
b. Monopropellant, such as hydrazine
c. Bipropellant.

The cold gas thrusters have a limited specific impulse of 785 N-sec/kg (80 lb-sec/lb_m) or less. Their tankage-to-gas-weight ratio is high. Hydrazine thrusters have a higher specific impulse of 1230 N-sec/kg (125 lb-sec/lb_m), and a favorable tankage-to-propellant ratio. Bipropellants have a high specific impulse of 2460 N-sec/kg (250 lb-sec/lb_m) or more. The selection of a particular propellant-thruster combination involves consideration of the thermal environment, mission duration, total required angular impulse, minimum impulse size, volume, and weight.

Inertia wheels and control moment gyros are two examples of momentum exchange devices. These actuators have the advantage that they need not give rise to a forced limit-cycle operation of the ACS. They use electrical energy, which may be replaced in space by a spacecraft carrying solar panels. They have the mutual disadvantage of saturation, which occurs in an inertia wheel when the wheel spins at its maximum speed relative to the spacecraft. An analogous situation arises in a control moment gyro that has been precessed through 90 deg. For either type of momentum exchange device, the ACS must make provisions to unload the momentum saturation condition by an additional independent torque-producing actuator such as an on-off thruster.

The choice between a mass expulsion or combined momentum exchange and mass expulsion torque-generating system is accomplished by a tradeoff study that considers the required pointing accuracy, performance, weight, reliability, and cost associated with each method.

The controller function is to control the spacecraft attitude. The controller performs this function by processing the signal from the attitude sensor to obtain a closed-loop input for the torque actuator. The torque produced by this input slaves the vehicle body axes to the reference orientation. This reduces the attitude sensor measurement to zero ideally. The controller is designed so that the ACS maintains the angular error between the reference and body axes below the required pointing accuracy in the presence of external and internal disturbance torques and vehicle acceleration with respect to the reference orientation. To accomplish its function throughout all phases of the mission, the controller operates in a variety of distinct modes:

a. Search Mode: The search mode represents the first operation of an ACS after the satellite has separated from the launch vehicle. The strategy in this mode is to cause the spacecraft to rotate until its attitude sensors determine the location of one or more celestial bodies.

b. Acquisition Mode: This mode is entered once the primary celestial body is within the field of view of the spacecraft sensors. If more than one celestial body is employed, the ACS may need a search and an acquisition mode for each reference body.

c. Coasting-Flight Mode: After the vehicle has acquired its desired orientation, it operates in the coasting-flight mode. If the payload does not require high pointing accuracy all the time, then suitable parameters in the ACS can be manipulated to provide both fine and coarse pointing control. In this manner, the consumption of expendables and power is minimized.

d. Reorientation Mode: This mode is required before a midcourse correction can be accomplished. It is also necessary when the ACS switches from one set of reference axes to another, for example, from local-vertical to inertial.

e. Powered-Flight Mode: Powered flight is required for midcourse corrections, orbital changes, or stationkeeping.

f. Reacquisition Mode: This mode is entered when the spacecraft switches from one reference orientation to another.

g. Backup Mode: The backup mode is necessary to achieve a reliable mission operation in the event that a failure occurs in the primary ACS.

The configuration of the signal processing for each mode is determined by a detailed design process. The signal processing for each mode is the result of a tradeoff study that analyzes and simulates the appropriate configurations of the controller, sensors, actuators, vehicle dynamics, environmental disturbances, and initial conditions.

Either digital, analog, or hybrid electronics can execute the signal processing of the controller. Analog loops are convenient for simple control systems. They efficiently implement wide bandwidth loops. Variable loop gains, time constants, and complex compensating functions are implemented with ease with digital equipment. Switching modes, for example, from coasting to powered flight or from checkout to operational, can be accomplished by accessing a program stored in the computer memory. Mode switching in an analog system requires a physical change in connections. Thus, the choice of analog or digital control affects the reliability. The cost of a digital ACS depends on whether ground-based or onboard computing is used. In either event, the computer sampling rate and quantization level must be carefully chosen.

3. POWERED-FLIGHT ATTITUDE CONTROL

The powered-flight mode of the spacecraft orientation is used to change the orbit parameters. The ACS operates during powered flight to stabilize the vehicle to the proper attitude to achieve the desired velocity change. A gimbaled engine is commonly used to provide the required propulsion. Control moments about the pitch and yaw vehicle axes result when the pitch and yaw hydraulic actuators deflect the engine thrust. Control torque about the roll axis is provided by roll thrusters whose thrust level may be greater than the level required for coasting flight. The large forces and torques applied to the spacecraft by the gimbaled engine give rise to a number of control problems that are not predominant during coasting flight. In addition to controlling the rigid body vehicle mode, the ACS must also be designed so that it does not drive lightly damped oscillatory modes unstable. Lightly damped vehicle modes arise from elastic vibration of the structure and from sloshing of the propellant in the storage tanks. These modes are excited by the torque reaction due to moving the gimbaled engine.

During powered flight, the ACS may also be coupled with the guidance loop. The vehicle acceleration during powered flight is sensed by inertial grade accelerometers. A computer resolves the measured acceleration in the desired reference frame. A navigation computer determines the vehicle's velocity by integrating the measured acceleration. The guidance computer uses the target data information and the integrated acceleration to generate steering commands for the attitude control loop. The attitude of the vehicle is commanded by the guidance loop in pitch and yaw at a rate proportional to the angular deflection about two axes of the required velocity change and the velocity to be gained. When the velocity to be gained is below a prescribed threshold, the guidance computer generates a shutdown command to the engine. Then, the ACS switches from the powered-flight operational mode to the coasting-flight mode.

C. PERFORMANCE AGGREGATE EQUATIONS

1. INTRODUCTION

The four variables that define a subsystem are the performance, safety, cost, and schedule parameters. These general parameters were each subdivided into specific parameters as shown in Table 1-1. Under the heading of "technical characteristics," this study considers as an example the on-orbit pointing accuracy of a three-axis, earth-pointing, mass expulsion ACS. The pointing accuracy aggregate equations presented in Section 4.C.2 relate the pointing accuracy to the error characteristics of the

ACS components. The fuel consumption of the ACS must also be considered, since it is a major contributor to the weight and volume of the ACS. The fuel consumption aggregate equations are presented in Section 4.C.3. The remaining performance parameters listed in Table 1-1 are power, weight, volume, vibration specification, temperature specification, and pressure specification. Sections 4. C. 4 through 4. C. 9 present the aggregate equations developed thus far for these parameters.

The prime objective of this section is to develop a set of performance aggregate equations for an ACS. It was necessary to computerize some of these equations to facilitate their use in a trade study. The particular aggregate equations used in the sample computer simulation are described in Section 5.

2. ON-ORBIT ACCURACY AGGREGATE EQUATIONS

The aggregate equations presented in this section are for a Tug-type vehicle with a three-axis mass expulsion ACS, using horizon scanners for pitch and roll reference and gyrocompassing for yaw reference. The particular mechanization of this type of ACS that is treated in this section is that used on an Agena-type vehicle (Ref. 1). The vehicle attitude is sensed by a three-axis body-mounted inertial reference unit containing rate integrating gyros that are referenced to local vertical/orbit plane (LV/OP) coordinates by horizon scanners and gyrocompassing. The control axes are defined in Figure D-1, Appendix D. The vehicle is maintained in a fixed attitude with respect to the LV/OP with a pitch program, where the orbital pitchover rate is achieved by programming the appropriate signal into the pitch gyro. The horizon scanners bound the effect of gyro drift, thereby keeping the vertical axis of the vehicle aligned with the center of the earth. The block diagrams for the attitude reference unit mechanization are shown in Figure 4-6.

The equation for attitude error on a control axis consists of two parts, the attitude reference error and the control system deadband. The equations for pitch, yaw, and roll attitude reference error for a near-circular orbit are derived in Section 1 of Appendix D. The attitude error due

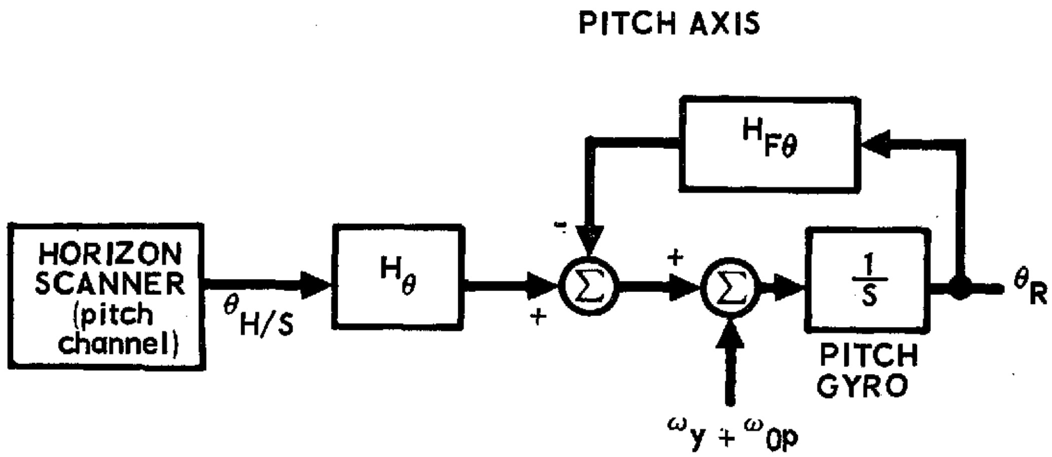

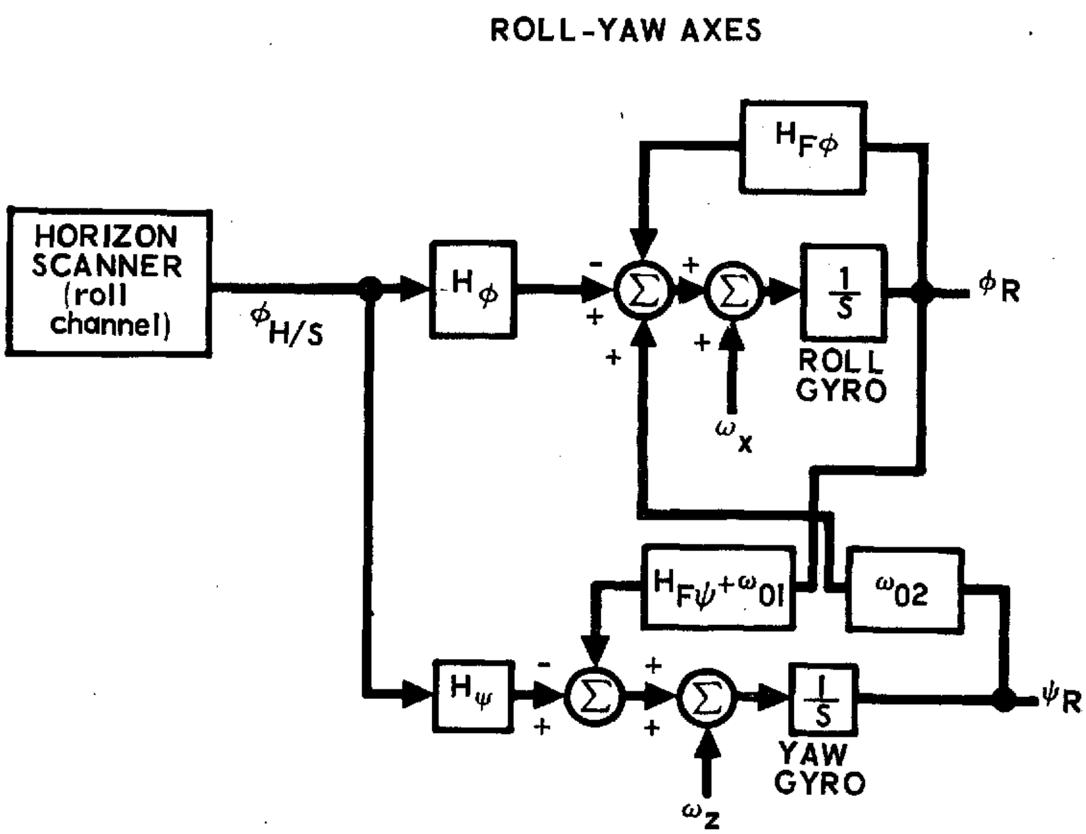

Figure 4-6. Attitude Reference Unit

to the control deadband consists of two parts: the nominal deadband setting and the error in the nominal deadband setting. This can be expressed as

$$\theta_{DB} = \theta_{DBN} + (\theta_{DB})_\epsilon \tag{4-1}$$

where

θ_{DBN} = nominal control deadband
$(\theta_{DB})_\epsilon$ = deadband tolerance

The form of the expression for total attitude error is the sum of the nominal deadband setting and the RSS value of all the other terms representing variation about the nominal deadband.

$$E_\theta = \theta_{DBN} + \left[(\text{Attitude reference error})^2 + (\theta_{DB})_\epsilon^2\right]^{1/2} \tag{4-2}$$

Thus, the on-orbit accuracy aggregate equations for pitch, roll, and yaw are

$$\text{Pitch:}\quad E_\theta \cong \theta_{DBN} + \Big\{P_{\theta N} + (\theta_N H_\theta/H_{F\theta})^2 + (\theta_H H_\theta/H_{F\theta})^2 + \left[(\omega_{0p} - \omega_0)/H_{F\theta}\right]^2 + (\theta_A)^2 + (\theta_{DB})_\epsilon^2\Big\}^{1/2} \tag{4-3}$$

$$\text{Roll:}\quad E_\phi \cong \phi_{DBN} + \left[P_{\phi N} + (\phi_N G_1)^2 + (\phi_H G_1)^2 + (\phi_A)^2 + (\phi_{DB})_\epsilon^2\right]^{1/2} \tag{4-4}$$

$$\text{Yaw:}\quad E_\psi \cong \psi_{DBN} + \left[(\theta_{YG}\,\omega_0\,G_3)^2 + (\dot{\psi}_D G_3)^2 + (\theta_{RG}\,\omega_0/\omega_{02})^2 + (\dot{\phi}_D/\omega_{02})^2 + (\phi_N G_2)^2 + (\psi_A)^2 + (\psi_{DB})_\epsilon^2\right]^{1/2} \tag{4-5}$$

where

$$G_1 = H_\psi/(H_{F\psi} + \omega_{01})$$
$$G_2 = [H_\psi H_{F\phi} - H_\phi (H_{F\psi} + \omega_{01}]/\omega_{02} (H_{F\psi} + \omega_{01})$$
$$G_3 = H_{F\phi}/\omega_{02} (H_{F\psi} + \omega_{01})$$

The sensitivity terms are

H_θ = pitch horizon scanner gain

H_ϕ = roll horizon scanner gain to roll axis

H_ψ = roll horizon scanner gain to yaw axis

$H_{F\theta}$ = pitch feedback gain

$H_{F\phi}$ = roll feedback gain

$(H_{F\psi} + \omega_{01})$ = roll-to-yaw coupling gain

ω_{02} = yaw-to-roll coupling gain

ω_0 = true orbital pitchover rate.

The error terms are

<u>Pitch axis</u>

$P_{\theta N}$ = filtered pitch horizon scanner noise power [defined in Eq. (4-6)]

θ_N = pitch horizon scanner null error

θ_H = pitch horizon anomalies

$(\omega_{0p} - \omega_0)$ = programmed pitchover rate error

θ_A = vehicle alignment in pitch

θ_{DBN} = pitch deadband setting

$(\theta_{DB})_\epsilon$ = pitch deadband tolerance

Roll axis

$P_{\phi N}$ = filtered roll horizon scanner noise power [defined in Eq. (4-7)]

ϕ_N = roll horizon scanner null error

ϕ_H = roll horizon anomalies

ϕ_A = vehicle alignment in roll

ϕ_{DBN} = roll deadband setting

$(\phi_{DB})_\epsilon$ = roll deadband tolerance

Yaw axis

θ_{YG} = pitch misalignment of yaw gyro

$\dot{\psi}_D$ = G-insensitive drift of yaw gyro

θ_{RG} = pitch misalignment of roll gyro

$\dot{\phi}_D$ = G-insensitive drift of roll gyro

ϕ_N = roll horizon scanner null error

ψ_A = vehicle alignment in yaw

ψ_{DBN} = yaw deadband setting

$(\psi_{DB})_\epsilon$ = yaw deadband tolerance

The expressions for the filtered pitch and roll horizon scanner noise power are

$$P_{\theta N} = \int_0^\infty \frac{S_\theta(\omega)\, H_\theta^{\,2}}{\omega^2 + H_{F\theta}^{\,2}}\, d\omega \tag{4-6}$$

$$P_{\phi N} = \int_0^\infty \frac{S_\phi(\omega)\, [\omega^2 H_\phi^2 + \omega_{02}^2 H_\psi^2]}{\omega^4 + \omega^2 \left(H_{F\phi}^2 - 2H_\phi/G_3\right) + H_\phi^2/G_3^2}\, d\omega \tag{4-7}$$

where S_θ and S_ϕ are the pitch and roll horizon scanner output noise power spectra.

3. PROPELLANT CONSUMPTION AGGREGATE EQUATIONS

Propellant consumption can be broadly classified into two categories:

a. Propellant consumption proportional to the spacecraft activity (such as number of maneuvers)

b. Propellant consumption proportional to the spacecraft life.

The total propellant consumption is the sum of categories a and b. In principle, one might want to subtract from category b the time the spacecraft is particularly active (such as maneuvering time). However, since such activity times are usually small, compared to the total spacecraft lifetime, the propellant consumption for category b is usually computed by neglecting the time spent during maneuvers. The total propellant consumption is conservatively given by

$$W_T = W_R + \sum_N W_M + W_{LC} + W_D + W_V \tag{4-8}$$

where

W_R = rate recovery propellant consumption

W_M = single-maneuver propellant consumption

N = number of maneuvers

W_{LC} = limit-cycle propellant consumption

W_D = disturbance-torque propellant consumption

W_V = powered-flight ΔV propellant consumption.

Sections 4.C.3.a through 4.C.3.c present the aggregate equations for ACS propellant consumption due to rate recovery and maneuvers, limit-cycle operation, and disturbance torques, including the torques during powered flight. Section 4.C.3.d gives the aggregate equation for propellant consumption for the ΔV during powered flight. Also included for convenience are tables of replacement characteristics for various engines and thrusters. The derivations of the aggregate equations are given in Section 2 of Appendix D.

a. Rate Recovery Propellant Consumption

At various times during the spacecraft life, the control system must stabilize the spacecraft from moderately high initial rates. Moderately high means that the spacecraft control system tends to operate linearly because the effects of a deadzone are negligible. For this type of vehicle, the aggregate equation for rate recovery propellant consumption is

$$W_R = \sum_{i=1}^{3} I_i\, G_i \left|\dot{\theta}_{oi}\right| / \ell_i\, I_{sp} \tag{4-9}$$

where

I_i = vehicle inertia about ith control axis
ℓ_i = thruster moment arm for ith control axis
I_{sp} = specific impulse
$\dot{\theta}_{oi}$ = initial rate about ith control axis

and

$$G_i = (1 + 2e^{-\eta_i/2} + e^{-\eta_i})/(1 + e^{-\eta_i}) \tag{4-10}$$

$$\begin{aligned} \eta_i &= 2\pi/(1 - \zeta_i^2)^{1/2} && \text{for } \zeta_i < 1 \\ \eta_i &= 0 && \text{for } \zeta_i \geq 1 \end{aligned} \tag{4-11}$$

where ζ_i is the control system damping for the ith control axis as defined in Section 2 of Appendix D.

The propellant consumption for additional maneuvers that may be performed by the spacecraft during its lifetime must be added to that given by Eq. (4-9). The consumption for each additional maneuver may be obtained by

$$W_M = \sum_{i=1}^{3} 2I_i \, G_i |\dot{\theta}_{Mi}| / \ell_i \, I_{sp} \tag{4-12}$$

where $\dot{\theta}_{Mi}$ is the maneuver rate about the ith control axis, and the factor of two accounts for rate increments at the start and end of a maneuver.

b. Limit-Cycle Propellant Consumption

The aggregate equation for limit-cycle propellant consumption in the absence of external torques is given in Eq. (4-13). The consumption with external torques may be computed conservatively by adding the limit-cycle propellant consumption to that given in Section 4.C.3.c for disturbance-torque propellant consumption.

$$W_{LC} = \sum_{i=1}^{3} I_i (\Delta\dot{\theta}_i)^2 \, t_L / 6 \, \ell_i \, I_{sp} \, D_i' \tag{4-13}$$

$$D_i' = D_i - 2\theta_{npi}/3 \tag{4-14}$$

where

I_i = vehicle inertia about ith control axis

ℓ_i = thruster momentum arm for ith control axis

I_{sp} = specific impulse

$\Delta\dot{\theta}_i$ = rate increment from one thruster pulse on ith control axis

D_i' = effective deadband width for ith control axis

D_i = deadband setting for ith control axis

θ_{npi} = peak attitude reference noise for ith control axis

t_L = vehicle lifetime.

c. Disturbance-Torque Propellant Consumption

The aggregate equation for worst case disturbance-torque propellant consumption is

$$W_D = \sum_{i=1}^{3} [(t_L/\ell_i I_{sp}) (T_{Gi} + T_{Ai} + T_{Mi} + T_{Si}) + (t_P/\ell_i I_{sp}) T_{Pi}] \quad (4\text{-}15)$$

where

ℓ_i = thruster moment arm for ith control axis

I_{sp} = specific impulse

t_L = vehicle lifetime

t_P = time of powered flight

T_{Gi} = gravity gradient torque about ith control axis

T_{Ai} = aerodynamic torque about ith control axis

T_{Mi} = magnetic torque about ith control axis

T_{Si} = solar torque about ith control axis

T_{Pi} = torque during powered flight about ith control axis.

Equation (4-15) gives worst case propellant consumption because the time variability of the torque terms has not been considered. This variability cannot be considered unless the particular spacecraft configuration, spacecraft attitude, and orbital parameters are defined. Expressions for the disturbance torques are given in Section 2 of Appendix D.

d. Powered-Flight ΔV

The aggregate equation for powered-flight ΔV propellant consumption is

$$W_V = W_E [\exp(\Delta V/I_{sp}) - 1] \quad (4\text{-}16)$$

where

W_E = weight of vehicle without fuel

ΔV = velocity change

I_{sp} = specific impulse[1] (N-sec/kg)

Expressions for ΔV for a typical mission profile are given in Section 2 of Appendix D.

Because of current NASA interest in the Tug, which has a powered-flight capability, vehicles similar to the baseline Tug vehicle were examined. There are three vehicles with flight capability very similar to the baseline Tug vehicle: Agena, Transtage, and Centaur. Their characteristics are shown in Table 4-5. Possible main engine candidates are shown in Tables 4-6 and 4-7; possible ACS engine candidates are shown in Table 4-8.

4. POWER AGGREGATE EQUATIONS

These equations determine the amount of power that must be supplied to the ACS by the power conditioning subsystem. Both average and peak power must be considered. Average power is computed by summing the average power used by each component that satisfies the pointing accuracy requirements. Peak power requirements are a function of time, and may be computed by adding the power-versus-time functions for all components. In addition, resistive losses, which are a function of the cabling characteristics, must be considered. The power aggregate equations are

$$\text{Average Power} = (1 + \delta) \sum \text{Component Average Power}$$

$$\text{Peak Power } (t) = (1 + \delta) \sum \text{Component Peak Power } (t)$$

where

$\delta = f$ (cabling characteristics)

[1] If I_{sp} in $lb\text{-}sec/lb_m$ is used, it must be multiplied by g (acceleration due to gravity) before substitution into Eq. (4-15).

Table 4-5. Upper Stage Characteristics

Main Engine Characteristics	Vehicle Designation (Manufacturer, Model) Agena (Bell, 8096)	Transtage (Aerojet, 10-138)	Centaur (P&W, RL10A-3)
Thrust F, N (lb)	71,168 (16,000)	36,251 (8150)	66,720 (15,000)
Burn time t_b, sec	240	500	470
Mode of Cooling	Regenerative oxidizer	Ablation	Regenerative fuel
Fuel	UDMH[a]	50/50[b]	LH_2
Oxidizer	IRFNA[c]	N_2O_4	LO_2
Mixture Ratio, O/F[d]	2.58	2.0	5.0
Chamber Pressure P_c, N/m^2 (psia)	3.49×10^6 (506)	0.745×10^6 (108)	2.07×10^6 (300)
Chamber Temperature T_c, °C	2727	2804	2924
Exhaust Temperature, °C	802	1097	836
Specific Impulse I, N-sec/kg (sec)	2940 (298)	2980 (303)	4200 (426)
Nozzle Expansion Ratio ϵ	45	40	40
Overall Length L, m (in.)	2.1 (83)	2.06 (81)	1.71 (67.5)
Maximum Diameter D, m (in.)	0.83 (32.5)	1.21 (47.4)	0.98 (38.7)
Total Dry Weight W, kg (lb)	134 (296)	96 (211)	134 (296)
Ignition Mode	Hypergolic	Hypergolic	Spark
Propellant Feed	Turbopump	He pressure	Turbopump
Restart Capability	Dual	Multiple	3, with throttling 100:1
Power Requirement, continuous W	113	NA[e]	NA[e]
Engine Life, sec	1330	500	2820
Storage Life, yr	2	NA[e]	3
Thrust Vector Control	±5° hydraulic gimbal	None	±4° gimbal

[a]UDMH = unsymmetrical dimethylhydrazine

[b]50/50 = 50% UDMH, 50% N_2H_4

[c]IRFNA = inhibited red fuming nitric acid, 2% H_2O, 84.6% HNO_3, 13.4% N_2O_4, 0.7% HF inhibitor

[d]O/F = weight of oxidizer/weight of fuel

[e]NA = not available

Table 4-5. Upper Stage Characteristics (Continued)

Attitude Control Propulsion Characteristics	Vehicle Designation (Manufacturer)		
	Agena (NA)[a]	Transtage (Rocket Research Corp.)	Centaur (Bell)
Propellant	N_2/Fr-14 (cold gas)	N_2H_4	H_2O_2
Type of Pressurization	Pressure regulated	N_2 pressure blowdown	N_2 pressure regulated
F (multilevels), N (lb)	44.5/2.2 (10/0.5)	111 (25)	13.3/222 (3/50)
Storage Pressure, N/m^2 (psia)	2.48×10^7 (3600)	2.21×10^7 (3200)	
P_c, N/m^2 (psia)	$6.9 \times 10^5/3.4 \times 10^4$ (100/5)	2.06×10^6 to 6.9×10^5 (300 to 100)	1.31×10^6 (190)
T_c, °C	21	899	699
I, N-sec/kg (sec)	670 (68)	2260 (230)	1530 (155)
ϵ	45	50	15
L, m (in.)	Integral cluster of 3	0.13 (5.2)	17.0 (6.7)
D, m (in.)	NA[a]	0.064 (2.5)	0.04/0.046 (1.6/1.8)
W, kg (lb)	NA[a]	0.54 (1.2)	0.68/1.36 (1.5/3.0)
Ignition	DNA[b]	Catalyst	Catalyst
Restarts	DNA[b]	Multiple	900
Minimum Impulse Bit, N-sec (lb-sec)	0.044 (0.01)	0.556 (0.125)	1.34 (0.3)
Power, continuous W	NA[a]	NA[a]	24

[a]NA = not available
[b]DNA = does not apply

Table 4-6. Possible Candidates

	Manufacturer, Model		
Engine	Agena	Transtage	Centaur
Main	Aerojet 10-137	Aerojet 10-104 Aerojet 10-118 Rocketdyne G-1 TRW LEMDE	Aerojet 10-137 Rocketdyne G-1 TRW LEMDE
ACS	Cold gas	Marquardt Advent Bell 8441 Aerojet Rocketdyne	RRC TRW Hughes (electrolysis) Rocketdyne

Table 4-7. Main Engine Replacement Characteristics

Main Engine Characteristics	Manufacturer (Model)				
	Aerojet (10-118)	Aerojet (10-104)	Aerojet (10-137)	TRW (LEMDE)	Rocketdyne (G-1)
F, N (lb)	33,964 (7575)	35,095 (7890)	95,632 (21,500)	46,704 (10,500)	53,376 (12,000)
t_b, sec	170	290	750	1030	338
Mode of Cooling	Regenerative oxidizer	Regenerative oxidizer	Ablation and Radiation	Ablation and Radiation	Regenerative fuel
Fuel	UDMH[a]	UDMH[a]	50/50[b]	50/50[b]	N_2H_4
Oxidizer	IRFNA[c]	IRFNA[c]	N_2O_4	N_2O_4	LF_2
O/F[d]	2.8	2.8	2.0	1.6	1.6
P_c, N/m^2 (psia)	1.42×10^6 (206)	1.42×10^6 (206)	0.69×10^6 (100)	0.758×10^6 (110)	1.03×10^6 (150)
T_c, °C	2727	2727	2808	2808	3871
I, N-sec/kg (sec)	2630 (267)	2740 (278)	3140 (319)	3000 (305)	3270 (332)
ϵ	20	40	62.5	47.5	20
L, m (in.)	4.85 (191)	1.8 (71)	3.35 (132)	216 (85)	1.6 (63)
D_{max}, m (in.)	0.81 (32)	0.84 (33)	2.5 (98)	1.5 (59)	0.91 (36)
W, kg (lb)	61 (135)[e]	452 (997)[f]	352 (777)[f]	159 (350)[f]	401 (885)[f]
Propellant Feed	He pressure regulated	He pressure regulated	He pressure regulated	He pressure regulated	He pressure regulated
Ignition	Hypergolic	Hypergolic	Hypergolic	Hypergolic	Hypergolic
Restarts	None	None	50	20	2
Thrust Vector Control	Hydraulic gimbal	Hydraulic gimbal	Hydraulic gimbal	Gimbal 10:1 throttling	Electromechanical gimbal
ACS	Ullage gas	N_2 gas	None	None	None
Storage Life, yr	2.5		3	5	
Development Status	Delta launch vehicle	Ablestar	Apollo service module	LEM descent	Nomad experimental

[a] UDMH = unsymmetrical dimethylhydrazine

[b] 50/50 = 50% UDMH, 50% N_2H_4

[c] IRFNA = inhibited red fuming nitric acid, 2% H_2O, 84.6% HNO_3, 13.4% N_2O_4, 0.7% HF inhibitor

[d] O/F = weight of oxidizer/weight of fuel

[e] Chamber and injector

[f] Overall engine

Table 4-8. Attitude Control Thruster Characteristics

Attitude Control Thruster Characteristics	Manufacturer							
	Marquardt	RRC	Bell	TRW	Aerojet	Hughes	Rocketdyne	Rocketdyne
F, N (lb)	111 (25)	8.9 (2)	111 (25)	13.3 (3)	111 (25)	6.7 (1.5)	111 (25)	111 (25)
t_b, sec	5400	Unlimited	3000	4000	5700	30	140	360
Mode of Cooling	Radiation	Radiation	Radiation	Radiation	Radiation	Radiation and heat sink	Ablation	Ablation
Fuel	25% N_2H_4	N_2H_4	MMH[a]	N_2H_4	50/50[b]	H_2O electrolysis	50/50[b]	50/50[b]
Oxidizer	N_2O_4	DNA[c]	N_2O_4	DNA[c]	N_2O_4	DNA[c]	N_2O_4	N_2O_4
O/F[d]	1.47	Mono	1.6	Mono	1.55	8	1.56	1.56
P_c, N/m^2 (psia)	1.28×10^6 (185)	1.03×10^6 (150)	0.552×10^6 (80)	1.28×10^6 to 0.793×10^6 (185 to 115)	NA[e]	1.03×10^5 (15)	1.03×10^6 (150)	0.98×10^6 (142)
T_c, °C (°F)	2816 (5100)	899 (1650)	3116 (5640)	871 (1600)	2808 (5086)	2504 (4540)	2808 (5086)	2808 (5086)
I, N-sec/kg (sec)	2960 (300)	2220 (225)	2760 (280)	2220 (225)	2790 (283)	3450 (350)	2910 (295)	2960 (300)
ϵ	40	50	40	40	30	40	60	60
L_e, m (in.)	0.25 (10)	0.076 (3)	0.269 (10.6)	0.11 (4.3)	0.297 (11.7)	0.076 (3)	0.21 (8.3)	0.28 (11)
D_{max}, m (in.)	0.1 (4)	0.025 (1)	0.076 (3)	0.025 (1.0)	0.16 (6.2)	0.04 (1.6)	0.083 (3.3)	0.12 (4.8)
W_e, kg (lb)	1.2 (2.7)	0.23 (0.50)	1.4 (3.0)	0.24 (0.54)	2.1 (4.6)	0.68 (1.5)	1.32 (2.9)	3.67 (8.1)
Propellant Feed	Pressurized	Pressurized	Pressurized	Pressurized blowdown	Pressurized	Self pressurized blowdown	N_2 pressure regulated	N_2 pressure regulated
Ignition	Hypergolic	Catalyst	Hypergolic	Catalyst	Hypergolic	Spark	Hypergolic	Hypergolic
Development Status	Advent	Internal research and development	Internal research and development	Comsat	Internal research and development	Development	Former Transtage	Former Transtage
Storage Life, yr	3	Unlimited	10	2	NA[e]	1	1	1
Restarts	Unlimited	Unlimited	50,000	5000	67,000	Yes	540	650
Power, continuous W	60	NA[e]	NA[e]	10	NA[e]	30[f]	NA[e]	NA[e]
Minimum Impulse, N-sec (lb-sec)	0.535 (0.12)	0.04 (0.01)	1.11 (0.25)	NA[e]	NA[e]	NA[e]	NA[e]	NA[e]

[a]MMH = monomethylhydrazine = CH_3NHNH_2

[b]UDMH = unsymmetrical dimethylhydrazine

[c]DNA = does not apply

[d]O/F = weight of oxidizer/weight of fuel

[e]NA = not available

[f]Does not include electrolysis power

An aggregate equation must be written relating δ to the cabling characteristics to quantify the power aggregate equations.

5. WEIGHT AGGREGATE EQUATION

The weight aggregate equation can be expressed as the sum of the weights of components that satisfy pointing accuracy requirements, plus the weights of the lines, cables, connectors, fixtures, and hold structure. Also, the weight of the propellant (as determined by the propellant consumption aggregate equations), reserve propellant, and tankage must be included.

$$W = \sum \text{Component Weight} + f_1 \text{ (lines, cables, connectors)}$$
$$+ f_2 \text{ (fixture, structure)} + f_3 \text{ (propellant)}$$

The parameters contributing to the total weight of the ACS have been identified in the above equation. Aggregate equations incorporating these parameters must be written to quantify the total weight aggregate equation.

6. VOLUME AGGREGATE EQUATION

The volume aggregate equation can be expressed as the sum of the volumes of the components that satisfy the pointing accuracy requirement, divided by a packing efficiency factor. This factor accounts for the fact that the components are of various shapes and there must necessarily be some empty space. In addition, the volume associated with temperature control (cold plates, shrouds, etc.), lines, cables, and connectors must be considered.

$$\text{Volume} = \frac{1}{\eta} \sum \text{Component Volume} + f_1 \text{ (thermal control)}$$
$$+ f_2 \text{ (lines, cables, connectors)}$$

where

η = packing efficiency factor

The parameters contributing to the total volume of the ACS have been identified in the above equation. Aggregate equations incorporating these parameters must be written to quantify the total volume aggregate equation.

7. SPECIFICATION AGGREGATE EQUATIONS

In the study, the approach taken to develop preliminary specifications on vibration, temperature, and ambient pressure was the viewpoint of the ACS designer. Thus, these items are not treated as requirements imposed on the ACS, rather as ACS capabilities. The selected components used to mechanize the best system are then examined to determine the system capability.

In vehicle design, compromises must be made; obviously, further development of this model must provide for iterations to examine these preliminary specifications, compare them to predicted vehicle capabilities, and select alternate components to improve ACS capabilities, if necessary. This approach clearly shows the impact of increased vehicle requirements and provides a balance between those requirements imposed on the ACS and other vehicle systems.

a. Vibration Specification Aggregate Equation

The vibration specification aggregate equation, as a function of frequency, can be expressed as the minimum, at each frequency, of all the vibration specifications for components that satisfy the pointing accuracy requirement. The vibration specification aggregate equation can be written as

$$\text{Vibration Spec (freq)} = \text{Min}\left\{\text{Vibration Spec (freq) of Components}\right\}$$

b. Temperature Specification Aggregate Equations

The maximum temperature specification aggregate equation can be expressed as the minimum of all maximum temperature specifications for components that satisfy the pointing accuracy requirement, and similarly for the minimum temperature specification. The temperature aggregate equations can be written as

$$\text{Max Temp Spec} = \text{Min}\left\{\text{Max Temp Spec of Components}\right\}$$

$$\text{Min Temp Spec} = \text{Max}\left\{\text{Min Temp Spec of Components}\right\}$$

c. Ambient Pressure Specification Aggregate Equation

The ambient pressure specification aggregate equation can be expressed as the minimum of all ambient pressure specifications for components that satisfy the pointing accuracy requirement. The ambient pressure specification aggregate equation can be written as

$$\text{Ambient Pressure Spec} = \text{Min}\left\{\text{Ambient Pressure Spec of Components}\right\}$$

D. SAFETY AGGREGATE EQUATIONS

1. INTRODUCTION

As a result of satisfying the performance aggregate equations, one will have a finite number of ACS configurations with hardware selected to meet the steady-state pointing accuracy requirements. The next step is to develop the three sets of equations under the main heading of safety. The three categories of aggregate equations to be discussed are the failure rate, failure detection probability, and false alarm probability aggregate equations.

The basic ACS considered consists of four elements: sensor, signal processor, actuator, and energy source. The analysis was performed for each of the following variations of the basic system:

a. The basic system alone, referred to as the single-string ACS, since no redundancy exists. A monitoring system is also included for purposes of status determination.

b. One ACS in the active (operating) mode with a complete ACS in a standby mode as a backup, together with necessary monitoring and switching equipment.

c. Three ACSs in the active mode with a voter monitoring their performance with capability to censor any faulty ACS.

For each of the configurations being considered, the following characteristics were derived (see Section 3 of Appendix D) using standard probabilistic techniques:

a. Failure Rate: The failure rate for each configuration was determined on a module-by-module basis. (A module is represented by a single box in the reliability diagrams.) The module failure rate information was then combined by standard techniques (Ref. 2) into a reliability model expressing the probability of equipment survival (reliability) as a function of time and module failure rates. The failure rate equations assume that all necessary failure detection monitoring is performed.

b. Failure Detection Probability: Expressions for the probability of detecting a failure were derived using failure rates for the monitoring and switching system.

c. False Alarm Rates: The overall failure rates for the monitoring and switching equipment were reduced to consider only those failure modes that would result in an incorrect failure indication or an untimely actuation of the switching system. Again, using standard techniques, the probability of such an event occurring was derived as a function of time and the partial failure rates.

2. FAILURE RATE AGGREGATE EQUATIONS

a. Single-String ACS

The system failure rate is the sum of the individual module failure rates, and the system reliability $R_S(t)$ is given by

$$R_S(t) = e^{-\lambda_a t} \tag{4-17}$$

where

$$\lambda_a = \sum_{i=1}^{N} \lambda_i \tag{4-18}$$

for N modules, and the individual module failure rates λ_i are functions of part failure rates, duty cycles, environmental stress factors, and dormancy factors, as given in Section 3 of Appendix D.

It is evident that successful ACS operation requires successful functioning of each module, i.e., there is no redundancy, and each module constitutes a single-point failure hazard.

b. Active ACS with Switched Standby ACS

The system reliability is a function of the individual ACS module failure rates and the modes of failure of the monitor and switch.

$$R_S(t) = e^{-(\lambda_{s_1}+\lambda_{s_2})t} \Bigg\{ e^{-(\lambda_a+\lambda_{s_3}+\lambda_{m_1})t} + \frac{(\lambda_a + \lambda_{s_3} + \lambda_{m_1})}{(q\lambda_a + \lambda_{s_3} + \lambda_{m_1} + \lambda_{s_4} + \lambda_{m_2} - \lambda_{m_3} - \lambda_{s_5})} e^{-(\lambda_a+\lambda_{m_3}+\lambda_{s_5})t} \times \left[1 - e^{-(q\lambda_a+\lambda_{s_3}+\lambda_{m_1}+\lambda_{s_4}+\lambda_{m_2}-\lambda_{m_3}-\lambda_{s_5})t}\right]\Bigg\} \quad (4\text{-}19)$$

where

λ_{s_1} = rate of switch failures open

λ_{s_2} = rate of switch failures common, i.e., both ACSs actuated

λ_{m_1} = rate of monitor prematurely commanding switch to change states

λ_{s_3} = rate of switch changing state without command from monitor

λ_{s_4} = rate of switch failing to actuate on command

λ_{m_2} = rate of monitor failing to detect failure of active unit

λ_{m_3} = rate of monitor commanding switching from standby unit back to disabled active unit

λ_{s_5} = rate of switch changing state to put failed active unit on line, without command from monitor

λ_a = the active single-string failure rate as given in Eq. (4-18)

$q\lambda_a$ = the standby string failure rate as given in Section 3 of Appendix D.

c. Triply Active ACS with Voting

In the model considered here, the monitor signal processors are triply redundant (active) to reduce the impact of failure there. That is, each ACS has its own monitor signal processor, the outputs of which are acted on by the voter. The system reliability for this configuration is

$$R_S(t) = e^{-\lambda_v t}\left[1 - (1 - e^{-(\lambda_a+\lambda_{sp})t})^3\right] \tag{4-20}$$

where

λ_a = the active single-string failure rate as given in Eq. (4-18)

λ_v = the failure rate of the voter/switch

λ_{sp} = the failure rate of one monitor signal processor.

3. FAILURE DETECTION PROBABILITY AGGREGATE EQUATIONS

a. Single-String ACS

The expression for failure detection probability is

$$P_D(t) \cong \frac{n}{N} \exp(- \sum_{i=1}^{n} \lambda_{mi} t) \tag{4-21}$$

where

n = number of parameters monitored

N = total number of functional parameters

λ_{mi} = failure rate of that portion of the monitoring system assigned to the ith parameter monitored.

b. Active ACS with Switched Standby ACS

The expression for failure detection probability is

$$P_D(t) \cong \left[\frac{N(n + n') - nn'}{N^2}\right] \exp(- \sum_{i=1}^{n+n'} \lambda_{mi} t) \qquad (4\text{-}22)$$

where

n = number of monitored parameters of the active ACS

n' = number of monitored parameters of the backup ACS while on standby,

and the other terms are as previously defined.

c. Triply Active ACS with Voting

The expression for failure detection probability is

$$P_D(t) \cong \frac{3n}{3N} e^{-(\lambda_v - \lambda_s)t} \qquad (4\text{-}23)$$

where

n = number of monitored parameters of each ACS

N = total number of functional parameters of each ACS

$(\lambda_v - \lambda_s)$ = failure rate of voter only, excluding the switch.

4. FALSE ALARM RATE AGGREGATE EQUATIONS

The false alarm rate refers to the frequency of failures:

a. In the sensor/signal processor, which make up the monitoring subsystem, resulting in a command to the switch to change state

b. In the system selection switch, which results in a state change without a command.

The result of such a failure is that an active, properly functioning ACS is switched off-line, or erroneous status reports would go to the user and sacrifice of mission objectives would result. If ACS redundancy is still available, then this situation will not degrade performance immediately, but will likely result in a shortened mission duration. However, if ACS redundancy has been invalidated through previous failures, inadvertent switching will degrade mission performance.

a. Single-String ACS

The probability of false alarm P_F is given by

$$P_F(t) = 1 - e^{-\lambda_{m_F} t} \qquad (4\text{-}24)$$

where λ_{m_F} is that portion of the monitoring system failure rate linked to a false alarm condition, specifically, that portion associated with a false status signal of failure being issued.

b. Active ACS with Switched Standby ACS

The probability of a false alarm is given by

$$P_F(t) = 1 - e^{-(\lambda_{m_F} + \lambda_{s_F})t} \qquad (4\text{-}25)$$

where λ_{s_F} is that portion of the switch failure rate linked to a change of state without a command from the monitor subsystem.

c. Triply Active ACS with Voting

The probability of false alarm is given by

$$P_F(t) = 1 - e^{-(3\lambda_{sp_F} + \lambda_{v_F})t} \qquad (4\text{-}26)$$

where λ_{sp_F} is that portion of the signal processor failure rate associated with a false indication of failure in one of the three ACSs and λ_{v_F} is that portion of the voter failure rate that results in the censoring of one or more ACS inputs when the inputs are, in fact, acceptable.

E. COST AGGREGATE EQUATIONS

1. INTRODUCTION

Two costing techniques are presented in this section. The first costing technique developed cost aggregate equations from a data base structure consisting of a work breakdown structure (WBS), subdivision of work (SOW) and the elements of cost (EOC) approach. The above cost structure is similar, but not identical to the REDSTAR data base described in Section 2.B. The second costing technique developed cost aggregate equations based on the cost of the ACS components selected to satisfy the performance and safety requirements. This second technique, the one selected for computer implementation in this task, requires cost data to be formatted in a specific format, i.e., the format of Table 1-1.

The objective of the cost aggregate equations is to determine the total cost of an ACS. The total cost of a system is subdivided by the SOW. The SOW described in the REDSTAR data base divides the total cost of a system into four cost categories:

a. Design, development, test, and evaluation
b. Non-recurring investment
c. Recurring investment
d. Operations.

The total cost of an ACS, for both costing techniques, has been divided into the following more descriptive cost categories:

a. Design and development (D&D)
b. Build and checkout (B&C/O)
c. Test hardware (TH)

d. Training and simulation (TS)
e. Program life (PL)
f. Management (MGMT).

Each of these six cost categories can be found within the REDSTAR data base. The purpose of this breakdown is to determine the sensitivity of each of these six cost categories to changes in performance and safety requirements.

2. COST AGGREGATE EQUATIONS - WBS/SOW/EOC APPROACH

This section presents the six cost aggregate equations developed using cost analysis. The form of these cost aggregate equations is based on many years of costing experience.

The WBS/SOW/EOC approach for developing cost aggregate equations requires having detailed cost data in a format similar to the REDSTAR data base described in Section 2.B.1. The form of the cost aggregate equations is a product of a labor rate multiplied by the number of hours required to complete a specific activity. The six cost categories for which cost aggregate equations were developed are

a. Design and development
b. Build and checkout
c. Test hardware
d. Training and simulation
e. Program life
f. Management.

The costs being considered in this section are theoretical first unit costs.

The first cost aggregate equation, design and development cost, is described by the following sum:

$$\text{Design and Development Cost} = ED + TL + GSE + MU + TE + TO$$

where

ED = engineering design cost

TL = tooling cost

GSE = ground support equipment cost

MU = mockups cost

TE = test equipment cost

TO = test operation cost.

Each of these six costs is described by an equation. The engineering design cost equation is described as

$$ED = (C_E)\ [MHPS + (MH/D)\ (ND) + MHSC + MHSE + MHDR] + LT$$

where

C_E = engineering labor rate

$MHPS$ = man-hours to prepare specifications and parts lists

MH/D = man-hours per drawings and diagrams

ND = number of engineering drawings and wiring diagrams

$MHSC$ = subcontractor and vendor coordination man-hours

$MHSE$ = systems engineering and integration man-hours

$MHDR$ = data reduction and report preparation man-hours

LT = laboratory test models, breadboards, and material costs.

The tooling cost equation is described as

$$TL = (C_{E+M})\ (MHTL) + MTL$$

where

C_{E+M} = weighted average of engineering and manufacturing labor rates

$MHTL$ = man-hours for tooling design and manufacture

MTL = tooling material cost.

The ground support equipment cost equation is described as

$$GSE = (C_{E+M}) (MHGSE) + MGSE$$

where

MHGSE = ground support equipment man-hours

MGSE = ground support material cost.

The mockups cost equation is described as

$$MU = (NMU) (PS) (STFU)$$

where

NMU = number of mockups

PS = constant percent

STFU = system theoretical first-unit cost (defined under build and checkout).

The test equipment cost equation is described as

$$TE = [(NFTH)^{b} + NGTH] (STFU) [1 + PS]$$

where

NFTH = number of flight test subsystem equipment items

NGTH = equivalent number of ground test subsystem equipment items

b = slope of learning curve.

The test operation cost equation is described as

$$TO = (C_{E+M}) [(NGT) (MH/GT) + (NFT) (MH/FT)]$$

$$+ (NGT) (M/GT) + (NFT) (M/FT)$$

where

NGT = number of ground tests
MH/GT = man-hours per ground test
NFT = number of flight tests
MH/FT = man-hours per flight test
M/GT = material costs per ground test
M/FT = material costs per flight test.

The build and checkout cost aggregate equation can be described as

$$B\&C/O = STFU = \text{System Theoretical First-Unit Cost}$$

$$STFU = (C_M)\,(MH/STFU) + (M/STFU)$$

where

C_M = manufacturing labor rate
$MH/STFU$ = man-hour per system theoretical first unit
$M/STFU$ = material cost per system theoretical first unit.

The test hardware cost aggregate equation can be described as

$$TH = (C_E)\,(DMHTH) + (C_M)\,(PMHTH) + MTH$$

where

C_E = engineering labor rate
$DMHTH$ = test hardware design man-hours
C_M = manufacturing labor rate
$PMHTH$ = test hardware production man-hours
MTH = test hardware material cost

The training and simulation cost aggregate equation can be described as

$$TS = (C_T)\ (NTR) + (N)\ (PS)\ (STFU)$$

where

C_T = training cost per trainee
NTR = number of trainees
N = number of simulations
PS = constant percent
STFU = system theoretical first-unit cost.

The program life cost aggregate equation can be described as

$$PL = OH + S + LO$$

where

OH = operational hardware cost
S = spares cost
LO = launch operations cost.

The operational hardware cost equation can be described as

$$OH = (STFU)\ (QS)^b + TLS + ES$$

where

STFU = system theoretical first-unit cost
QS = program quantities
b = slope of learning curve
TLS = tooling support cost
ES = engineering support cost.

The spares cost equations can be described as

$$S = (P)\ (OH)$$

where

P = constant percent

OH = operational hardware cost.

The launch operations cost equation can be described as

$$LO = (LO/Y)\ (NYO)$$

where

LO/Y = launch operations costs per year

NYO = number of years of operation.

The last cost aggregate equation to be described is the management cost aggregate equation. The management cost aggregate equation can be described as

$$MGMT = (0.05)\ [D\&D + TE + TS] + (0.03)\ (PL)$$

The preceding cost aggregate equations, to be useful tools for estimating the ACS cost in the preliminary design phase, require data in a very detailed or WBS format. Unfortunately, such data is not available until a design has progressed into its intermediate phase because, while the dependent variables on the left side of the above cost aggregate equations correspond to the REDSTAR data base, the independent variables on the right side of the equations are not readily available in the preliminary design phase. An alternate costing technique, based on the costs of the ACS components selected to satisfy the performance and safety requirements, is described in Section 4.E.3. This alternate technique, which is used in the Cost/Performance Model, can be used to obtain preliminary cost estimates as a function of the preliminary ACS configurations.

3. COST AGGREGATE EQUATIONS - COMPONENT COST APPROACH

The second costing technique, termed the "component cost approach," develops cost aggregate equations based on the cost of the ACS components selected via the performance and safety aggregate equations and requirements. This costing technique requires that each ACS component have cost data available in a specific format, i.e., Table 1-1 format. The ACS considered in this study consists of four major subsystems: sensors, signal processors, actuators, and energy sources (see Figure 4-7).

The total cost of an ACS is the sum of its non-recurring cost and its recurring cost. The non-recurring costs are described in Section 4.E.3.a and the recurring costs, in Section 4.E.3.b.

a. Non-Recurring Costs

The total non-recurring cost is the sum of the non-recurring material cost and the non-recurring system engineering cost. The form of the non-recurring material cost aggregate equation is a sum of the non-recurring costs of the ACS components, multiplied by an inflation factor. The first non-recurring material cost aggregate equation, the design and development non-recurring cost, is described as

$$ACS(D\&D)_{NR} = I[S(D\&D)_{NR} + SP(D\&D)_{NR} + A(D\&D)_{NR} + E(D\&D)_{NR}]$$

where

$ACS(D\&D)_{NR}$ = ACS design and development non-recurring material cost

$S(D\&D)_{NR}$ = sensor design and development non-recurring material cost

$SP(D\&D)_{NR}$ = signal processor design and development non-curring material cost

$A(D\&D)_{NR}$ = actuator design and development non-recurring material cost

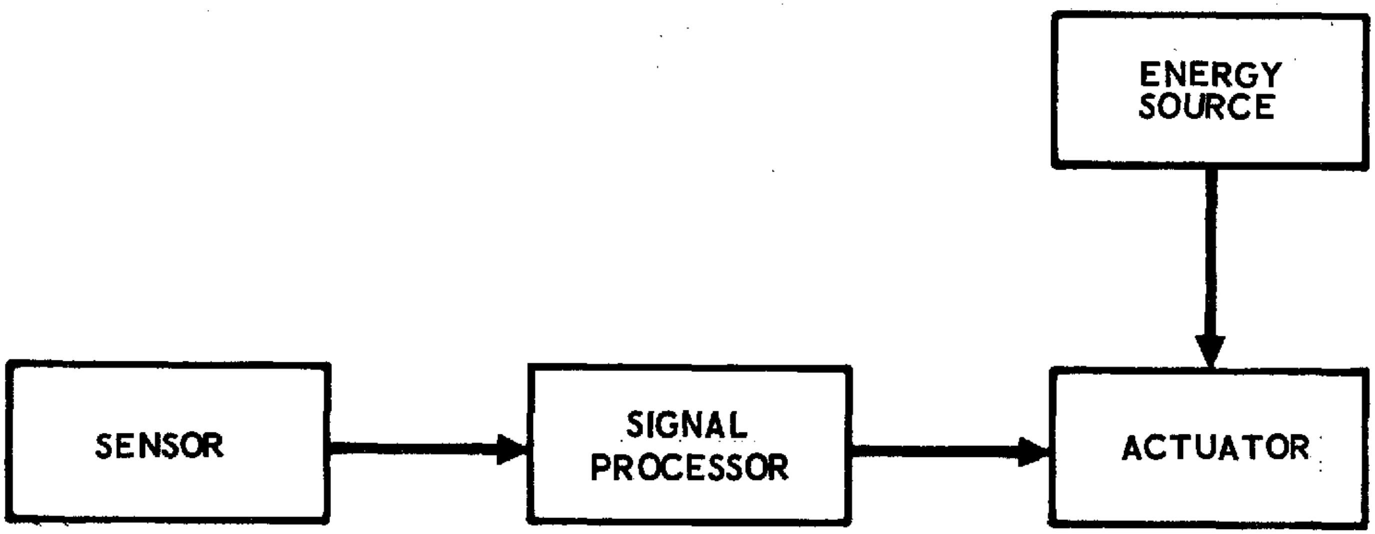

Figure 4-7. Attitude Control System

$E(D\&D)_{NR}$ = energy source design and development non-recurring material cost

I = inflation factor.

The cost inputs on the right side of the above equation are available in Table 1-1. This fact increases the utility of this costing technique as compared to the previous costing technique.

Similarly, the other four non-recurring material cost aggregate equations can be written as follows:

$$ACS(B\&C/O)_{NR} = I[S(B\&C/O)_{NR} + SP(B\&C/O)_{NR} + A(B\&C/O)_{NR} + E(B\&C/O)_{NR}$$

where $ACS(B\&C/O)_{NR}$ = ACS build and checkout non-recurring material cost;

$$ACS(TH)_{NR} = I[S(TH)_{NR} + SP(TH)_{NR} + A(TH)_{NR} + E(TH)_{NR}]$$

where $ACS(TH)_{NR}$ = ACS test hardware non-recurring material cost;

$$ACS(T\&S)_{NR} = I[S(T\&S)_{NR} + SP(T\&S)_{NR} + A(T\&S)_{NR} + E(T\&S)_{NR}]$$

where $ACS(T\&S)_{NR}$ = ACS training and simulation non-recurring material cost; and

$$ACS(PL)_{NR} = I[S(PL)_{NR} + SP(PL)_{NR} + A(PL)_{NR} + E(PL)_{NR}]$$

where $ACS(PL)_{NR}$ = ACS program life non-recurring material cost.

The total non-recurring material cost of an ACS is the sum of the non-recurring material costs for the design and development, build and checkout, test hardware, and program life. The total ACS non-recurring material cost aggregate equation can be written as

$$(ACS)_{NR} = ACS(D\&D)_{NR} + ACS(B\&C/O)_{NR} + ACS(TH)_{NR} + ACS(T\&S)_{NR} + ACS(PL)_{NR}$$

where $(ACS)_{NR}$ = total ACS non-recurring material cost.

To obtain the total ACS non-recurring cost, one must add the total non-recurring system engineering cost to the total non-recurring material cost. The total non-recurring system engineering cost can be described as

$$(TSE)_{NR} = P_{T_{NR}} [(TSE)_{NR} + (ACS)_{NR}]^{*}$$

where

$(TSE)_{NR}$ = total non-recurring system engineering cost

$(ACS)_{NR}$ = total non-recurring material cost

$P_{T_{NR}}$ = fixed percent = 0.484*.

The system engineering cost during the design and development phase can be described as

$$SE(D\&D)_{NR} = P_1[(TSE)_{NR} + (ACS)_{NR}]$$

where P_1 = fixed percent = 0.404.*

In a similar manner, the system engineering cost during the other four phases can be described as follows

*The form of the non-recurring system engineering aggregate equation and the percentages were obtained from the Honeywell cost analysis (Ref. 3).

$$SE(B\&C/O)_{NR} = P_2[(TSE)_{NR} + (ACS)_{NR}]$$

where $P_2 = 0.067^*$;

$$SE(TH)_{NR} = P_3[(TSE)_{NR} + (ACS)_{NR}]$$

where $P_3 = 0.013^*$;

$$SE(T\&S)_{NR} = P_4[(TSE)_{NR} + (ACS)_{NR}]$$

where P_4 = negligible*; and

$$SE(PL)_{NR} = P_5[(TSE)_{NR} + (ACS)_{NR}]$$

where P_5 = negligible.*

The total non-recurring cost T_{NR} can be described by the sum

$$T_{NR} = (ACS)_{NR} + (TSE)_{NR}$$

b. Recurring Costs

The total recurring cost is the sum of the recurring material costs and the recurring system engineering cost. The form of the recurring material cost aggregate equations is the sum of the recurring cost of the ACS components multiplied by an inflation factor. The first recurring material cost aggregate equation, design and development recurring cost, is described as

*The form of the non-recurring system engineering aggregate equation and the percentages were obtained from the Honeywell cost analysis (Ref. 3).

$$ACS(D\&D)_R = I[S(D\&D)_R + SP(D\&D)_R + A(D\&D)_R + E(D\&D)_R]$$

where

$ACS(D\&D)_R$ = ACS recurring design and development material cost

$S(D\&D)_R$ = sensor recurring design and development cost

$SP(D\&D)_R$ = signal processor recurring design and development cost

$A(D\&D)_R$ = actuator recurring design and development cost

$E(D\&D)_R$ = energy source recurring design and development cost

I = inflation factor.

In a similar manner, the other four recurring material cost aggregate equations can be written as follows

$$ACS(B\&C/O)_R = I[S(B\&C/O)_R + SP(B\&C/O)_R + A(B\&C/O)_R + E(B\&C/O)_R]$$

where $ACS(B\&C/O)_R$ = ACS recurring build and checkout material cost;

$$ACS(TH)_R = I[S(TH)_R + SP(TH)_R + A(TH)_R + E(TH)_R]$$

where $ACS(TH)_R$ = ACS recurring test hardware material cost;

$$ACS(T\&S)_R = I[S(T\&S)_R + SP(T\&S)_R + A(T\&S)_R + E(T\&S)_R]$$

where $ACS(T\&S)_R$ = ACS recurring training and simulation material cost; and

$$ACS(PL)_R = I[S(PL)_R + SP(PL)_R + A(PL)_R + E(PL)_R]$$

where $ACS(PL)_R$ = ACS recurring program life material cost.

The total recurring material cost of an ACS is the sum of the recurring material costs for the design and development, build and checkout, test hardware, and program life. The total ACS recurring material cost aggregate equation can be written as

$$(ACS)_R = ACS(D\&D)_R + ACS(B\&C/O)_R + ACS(TH)_R + ACS(T\&S)_R + ACS(PL)_R$$

where $(ACS)_R$ = total ACS recurring material cost.

To obtain the total ACS recurring cost, one must add the total recurring system engineering cost to the total recurring material cost. The total recurring system engineering cost can be described as

$$(TSE)_R = P_{T_R}[TSE_R + (ACS)_R]$$

where

$(TSE)_R$ = total recurring system engineering cost
$(ACS)_R$ = total recurring material cost
P_{T_R} = fixed percent.

The total ACS recurring cost T_R can be described by the sum

$$T_R = (ACS)_R + (TSE)_R$$

The total cost T of a single ACS (less management) is the sum of the total recurring cost and the non-recurring cost:

$$T = T_{NR} + T_R$$

If more than one ACS is produced, it is necessary to add a learning factor to the recurring system engineering cost. The derivation of the learning curve used in the computer simulation is described in Appendix C.

The only remaining cost item is the management cost. Management cost can be expressed as a percent of total ACS cost:

$$\text{Management} = p(\text{Management} + T)$$

where p = fixed percent.

The component cost approach was the costing technique selected for use in the computer simulation. The reason for this choice is that component cost data in a Table 1-1 format appears easier to obtain than very detailed or WBS format data in the preliminary design phase of a program.

F. SCHEDULE AGGREGATE EQUATIONS

1. INTRODUCTION

This section presents the schedule aggregate equations that determine, in terms of performance and safety parameters, the amount of series time required, starting from the proposal phase, to develop an operational ACS. Instead of developing one schedule aggregate equation for the total program life of an ACS, which would be a formidable task, it was decided that separate schedule aggregate equations for each major phase of the life cycle of an ACS would be more tractable. The life cycle of most systems can be divided into the following nine major phases:

a. Proposal
b. Preliminary design and system analysis
c. Subsystem analysis, design, and breadboard testing
d. Prototype design, fabrication, and test
e. Subsystem production engineering, fabrication, and test
f. System integration and test
g. Flight test phase (1 to 5 flights)

h. Initial operational phase (6 to 20 flights)

i. Operational phase (remaining flights).

Before quantitative relationships could be developed that would relate schedule to performance and safety parameters, it was necessary to identify the pertinent schedule parameters involved in each of the nine major phases. The first schedule parameters considered were sequence restraints, man-loading limitations, production quantity, production rate, and delivery span. It was very difficult to write schedule aggregate equations using only these five parameters; thus, other parameters affecting schedules were identified. Table 4-9 depicts the schedule analysis matrices consisting of all pertinent parameters that impact schedule. In addition to identifying and listing the schedule parameters in a matrix format, flow charts of the major life-cycle activities were used to show the interrelationships between life-cycle activities (see Figure 4-8).

The technique developed to estimate the amount of time necessary for completing a particular life-cycle activity is to estimate the necessary manpower, in man-months, required to complete a particular life-cycle activity, and then to divide the estimate by the average number of men available for performing that activity. This technique can be expressed in a simple equation:

$$T_S = MP/M$$

where

T_S = series time to complete a specific design phase (months)

MP = manpower needed to complete a specific design phase (man-months)

M = average number of men available during a specific phase (men).

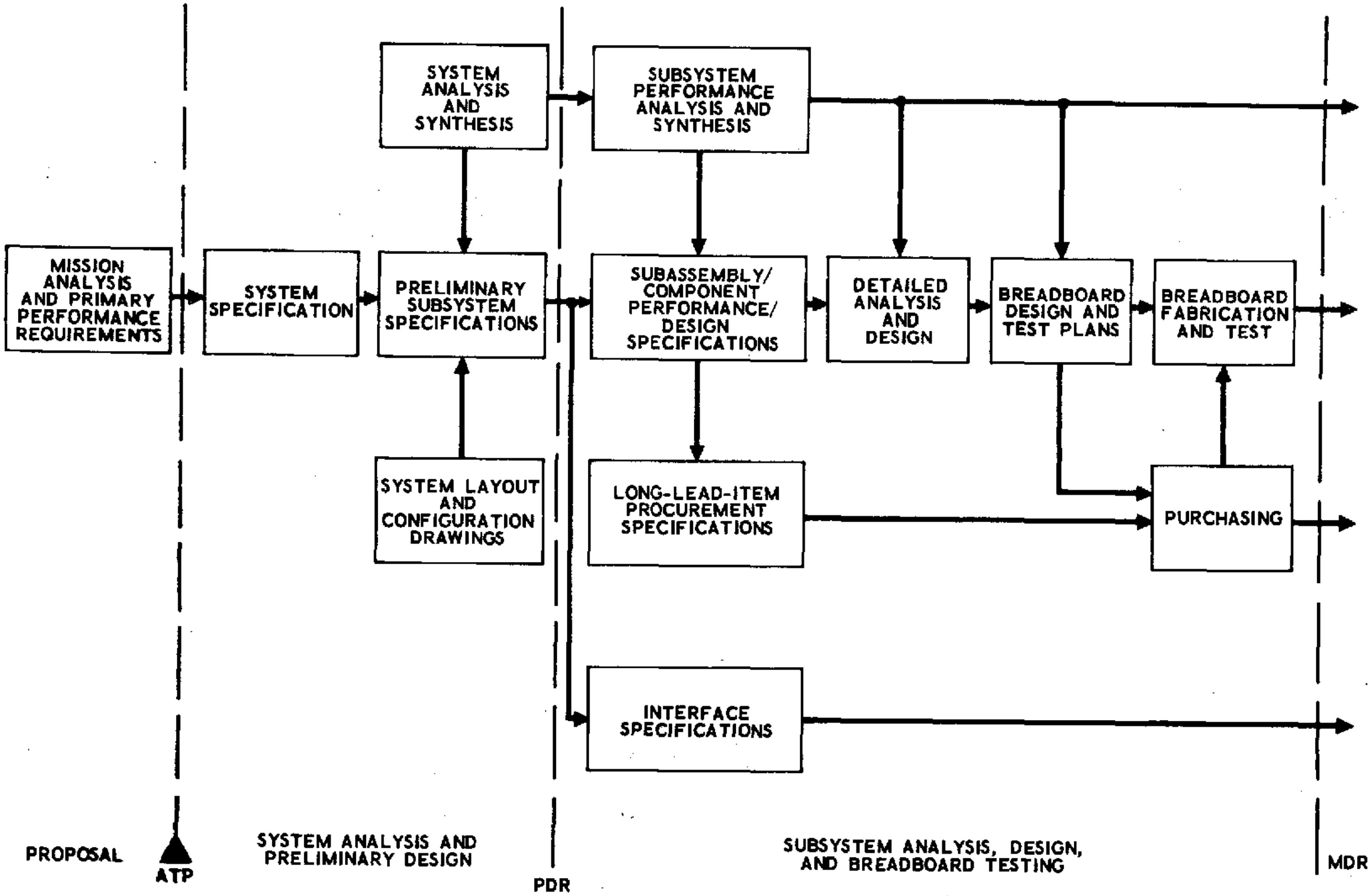

Figure 4-8. Attitude Control System (Life-Cycle Activities)

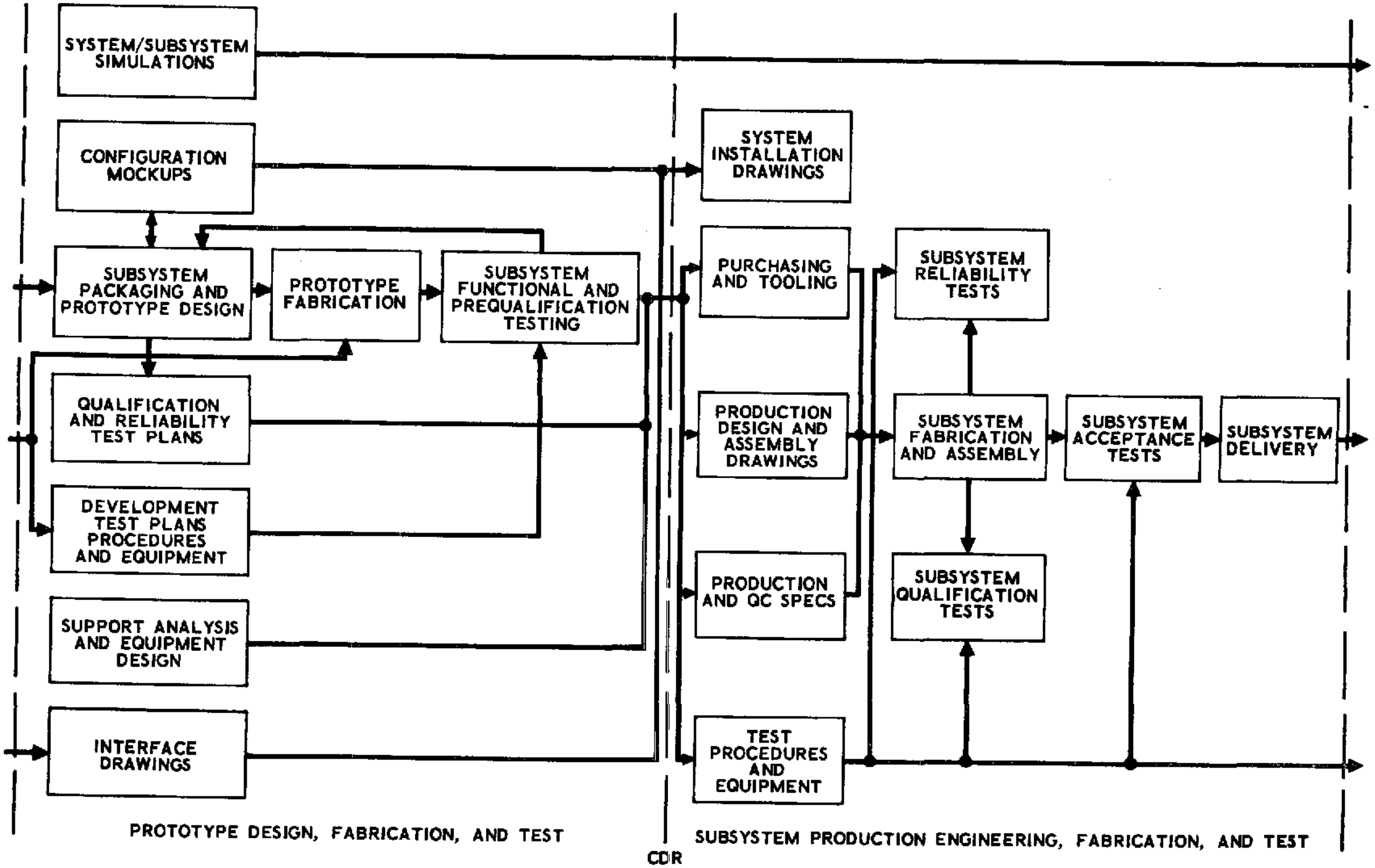

Figure 4-8. Attitude Control System (Life-Cycle Activities) (Continued)

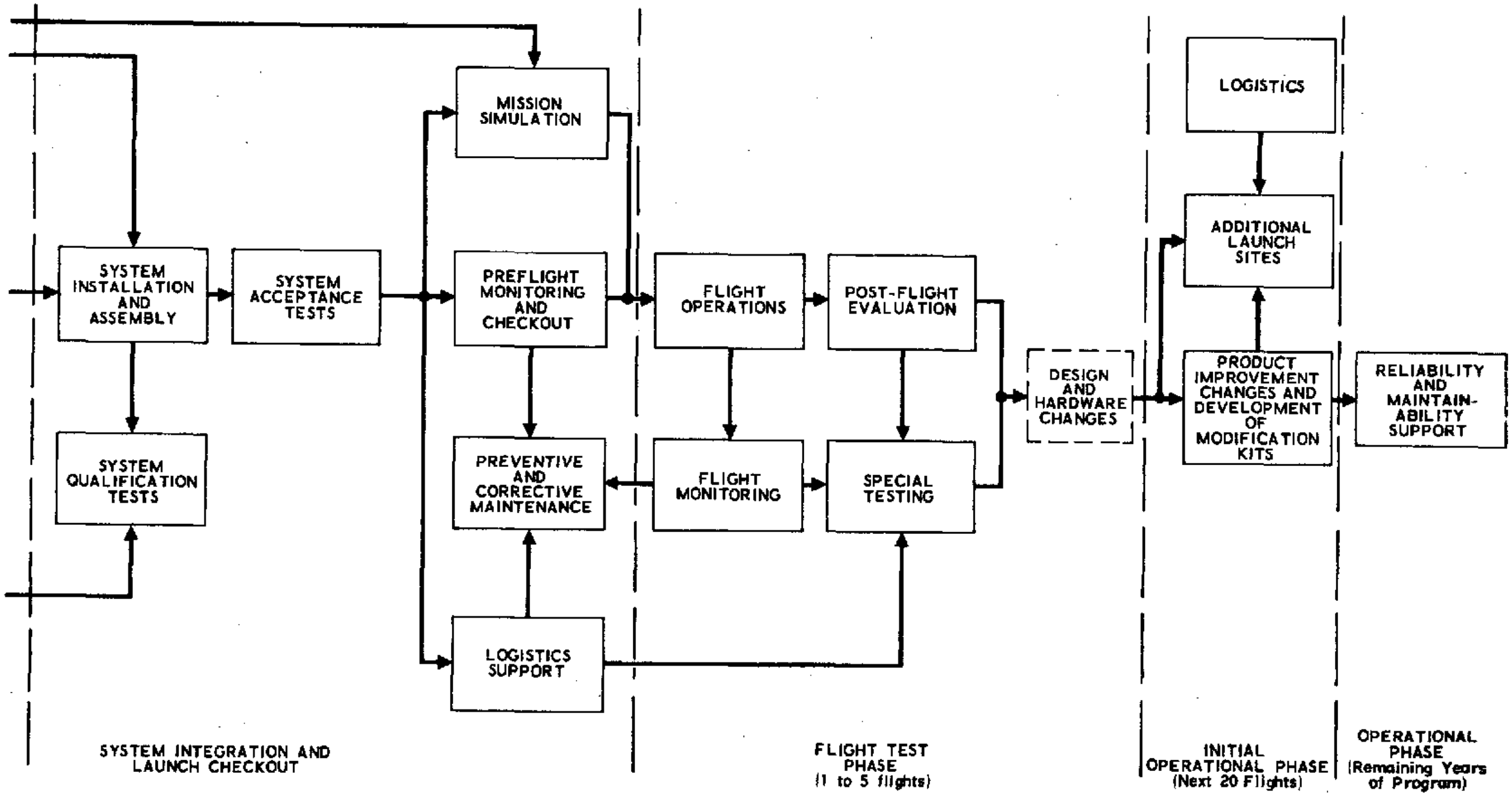

Figure 4-8. Attitude Control System (Life-Cycle Activities) (Continued)

Table 4-9. Attitude Control System Schedule Analysis Matrix

Phase	Activity	Typical Products	Schedule Considerations and Constraints			
			Sequence Restraints (Prerequisites)	Man-Loading Limitations	Production Quantity/ Production Rate/ Delivery Span	Other Factors Affecting Length of Accomplishment
Proposal	Mission analysis and primary performance requirements	Orbit characteristics Gross vehicle sizing Propulsion Weight Power Payload characteristics Guidance and navigation accuracies Mission event timelines	Basic mission purpose and objective definition RFP or contract go-ahead (normally) Required mission launch dates	Skill related - no significant constraints		Type of mission Complexity of orbit maneuvers Mission duration Mission requirements (payload, etc.) Characteristics of other stages Performance Design Prior application Level of development Management factors Contracting status Status of program approval
Preliminary Design and System Analysis	Preparation of system specifications and preliminary subsystem specifications System analyses and syntheses System layout and configuration drawings	Initial system and subsystem performance, design and verification requirements Functional requirements Reliability, maintainability Environmental requirements Preliminary physical features Development, reliability, and qualification test requirements Stability and sensitivity analyses Subsystem configuration layouts Support policies and philosophies	Basic vehicle definition Size envelopes Weight allocation Functions and accuracies Launch site selection	Some parallel activities after system specification prepared	Will affect reliability verification requirements[a]	Required control accuracies Severity of mission environment No. of interfaces and extent of definition Power Guidance and navigation Telemetry Environmental control Structures No. of participating contractors No. of control loops Redundancy requirements Reusability considerations

[a] Applies only to production quantity

Table 4-9. Attitude Control System Schedule Analysis Matrix (Continued)

Phase	Activity	Typical Products	Schedule Considerations and Constraints			
			Sequence Restraints (Prerequisites)	Man-Loading Limitations	Production Quantity/ Production Rate/ Delivery Span	Other Factors Affecting Length of Accomplishment
Subsystem Analysis and Design	Preparation of subsystem/component performance/design specifications Preparation of interface specifications Subsystem performance analyses and syntheses Long-lead item procurement specifications Detailed circuit analyses and designs	Subsystem/component performance/design and verification requirements Make-or-buy decision Functional interface requirements Performance Environment requirements Interface verification requirements Schematic and drawings	System/subsystem performance requirements System configuration layouts Identification of participating contractors		Will affect reliability verification requirements[a]	Same as above In-house fabrication vs subcontract
Breadboard Test	Breadboard design and test plans Breadboard fabrication and tests Purchasing	Breadboard and required functional verification	Breadboard layouts and required functional verification Initial verification of subsystem and component functional operation Initiation of long-lead item purchases	Physical layout for test No. and type of functional verifications (i.e., no. of disciplines involved) Fabrication/assembly physical limitations		Required accuracy and tolerances Degree of initial verification required No. and type of interfaces Anticipated environment (e.g., EMC, temperature) No. of major high reliability parts Type of component and degree of prior use/application (screening requirements)

[a] Applies only to production quantity

Table 4-9. Attitude Control System Schedule Analysis Matrix (Continued)

Phase	Activity	Typical Products	Schedule Considerations and Constraints			
			Sequence Restraints (Prerequisites)	Man-Loading Limitations	Production Quantity/ Production Rate/ Delivery Span	Other Factors Affecting Length of Accomplishment
Prototype Design, Fabrication, and Test	Subsystem package and prototype design System/sub-system simulations Support analysis and equipment design Configuration mockups Interface drawings Qualification and reliability test plans Development test plans, procedures, and equipment Prototype fabrication Subsystem functional and prequalification testing	Tested prototype design Functional Selected environments Initial software requirements Definition of physical interfaces Qualification and reliability test sequences, schedules and equipment requirements Definition of check-out and maintenance requirements and equipment Initial spares analysis	Program development decision (if required) Breadboard test Finalized interface specifications Sequence requirements Test sequencing requirements (i.e., ambient check-out prior to environment; temperature soak; etc.) Test equipment/ chamber available Required assembly sequence	Fabrication/ assembly physical constraints and sequencing Test sequencing requirements	Will affect support analysis and equipment[a] Checkout equipment configuration no. and location Transport analysis and equipment Quantity and schedule of spares	Required ACS accuracies and tolerances Type and severity of anticipated environments No. of environments No. of outputs to be checked Type of components and degree of prior use/ application State of interfacing sub-system and contractor design/testing Extent of breadboard verification accomplished Complexity of interfaces

[a] Applies only to production quantity

Table 4-9. Attitude Control System Schedule Analysis Matrix (Continued)

Phase	Activity	Typical Products	Schedule Considerations and Constraints			
			Sequence Restraints (Prerequisites)	Man-Loading Limitations	Production Quantity/ Production Rate/ Delivery Span	Other Factors Affecting Length of Accomplishment
Subsystem Production Engineering, Fabrication, and Test	Production design and assembly drawings Production and QC specifications Qualification, reliability, and acceptance test procedures and equipment Purchasing and tooling (including facilities) Subsystem fabrication and assembly Subsystem qualification and reliability testing Subsystem acceptance tests Subsystem delivery	Delivery of accepted production subsystem configuration resulting from qualification and reliability testing (including spares and ground equipment)	Signed interface drawings Production go-ahead decision Complete qualification prior to acceptance Assembly sequence requirements Test sequencing requirements Test equipment/ facility availability Personnel training	Test facility physical limitations Test sequence Assembly area physical limitations Skill mix availability	Tooling configuration and setup heavily dependent upon production quantity, production rate, and delivery span[a] Tooling sophistication Station no. and configuration Inspection procedures Assembly automation degree Facility space requirements Personnel no.	Required production tolerances Degree of acceptable post-acceptance test No., type, and severity of environment Degree of previous part use/application (extent of qualification/reliability testing) Complexity and type of interfaces No. of outputs to be checked Cleanliness requirements

[a]Applies to all three categories

Table 4-9. Attitude Control System Schedule Analysis Matrix (Continued)

Phase	Activity	Typical Products	Schedule Considerations and Constraints			
			Sequence Restraints (Prerequisites)	Man-Loading Limitations	Production Quantity/ Production Rate/ Delivery Span	Other Factors Affecting Length of Accomplishment
System Integration	System installation and assembly System qualification tests System acceptance tests	Delivery of accepted production system configuration resulting from system qualification testing	Receipt of accepted subsystem assemblies Complete qualification prior to acceptance Assembly sequence requirements Test sequencing requirements Test equipment facility availability Personnel training	Test facility physical limitations Assembly area physical limitations Skill mix availability Vehicle space limitations	Same as subsystem production engineering, fabrication, and test[a]	Required assembly tolerance Degree and type of inspection Cleanliness requirements Complexity and type of interfaces Degree of previous application of assembly Type and automation of testing Location of assembly site Location of test site Number of subsystems

[a]Applies to all three categories

Table 4-9. Attitude Control System Schedule Analysis Matrix (Continued)

Phase	Activity	Typical Products	Schedule Considerations and Constraints: Sequence Restraints (Prerequisites)	Man-Loading Limitations	Production Quantity/ Production Rate/ Delivery Span	Other Factors Affecting Length of Accomplishment
Launch Checkout and Flight Test	Preflight monitoring and checkout Mission simulation Flight operations Flight monitoring Post-flight evaluation Special testing Logistic support Preventive and corrective maintenance	Accomplishment of mission objectives Problem evaluation Implementation of required design changes	Receipt of accepted system Launch complex supply and checkout Facilities Expendables Ground checkout equipment Trained personnel	Vehicle servicing and checkout sequencing requirements Vehicle checkout area physical characteristics Skill and mix of available manpower	Launch rate will influence structure of launch complex and checkout[a] High rate will require higher degree of automation[a] Multi-pad complex if checkout servicing time > launch rate-significant manpower impact[a] Potential subsystem or system storage if checkout servicing and launch rate > most efficient production rate[a]	Location of launch site Mission characteristics Degree and type of problem areas Required change verification Maintenance philosophy and policy Organization Field Depot Extent and type on ground mission simulation Complexity of subsystem and interfaces Checkout policy Degree of automation Integral vs remote No. of launch pads No. of test sets Reusability

[a] Applies only to delivery span

Manpower aggregate equations were written to estimate the required manpower; as a starting point, the equations used all the parameters identified in the schedule analysis matrices and life-cycle flow charts. Since the proposal phase in most of the designs reviewed was approximately 3 months, independent of functional requirement, the first life-cycle activity for which aggregate equations will be developed is the preliminary design and system analysis phase.

2. PRELIMINARY DESIGN AND SYSTEM ANALYSIS AGGREGATE EQUATION

The preliminary design and system analysis phase begins with the authorization to proceed (ATP) and ends with the preliminary design review (PDR). The first step in developing a manpower aggregate equation for the preliminary design and system analysis phase was to list the major activities of this phase. The schedule analysis matrices and flow charts developed in the previous section were used as a master list from which to select those activities pertinent to the preliminary design and system analysis phase. Table 4-10, developed by a panel of control engineers with many years of program experience, lists the major activities performed during this phase. The list will be used throughout the other seven life-cycle phases, except for minor additions or deletions.

The first major activity in Table 4-10 is the program plans activity. The manpower aggregate equation for this activity was estimated by the panel of control engineers to be a constant, 27 man-months, independent of functional requirements.

The second major activity in Table 4-10 consists of developing layouts, diagrams, schematics, etc. The manpower aggregate equation for each task is shown in Table 4-11. The forms of the equation and the coefficients were estimated by the panel of control engineers, using previous ACS manpower program requirements.

Table 4-10. Major Activities During Preliminary Design System Analysis Phase

I.	Program plans
	A. Master program plans
	B. Subsystem specifications and requirements
	C. Test plans, manufacturing plans, quality assurance plans, reliability plans, engineering development plans
	D. Interfaces with other subsystem, vehicle, and ground support equipment
	E. Subcontractor plans and specifications
	F. Quality test plans
II.	Mechanical layouts, mathematical block diagrams, interface control diagrams, detailed drawings, long-lead items, functional block diagrams, schematics
III.	Analyses (stability, error, simulation, structural, thermal, reliability, circuit)
IV.	Design (electrical, mechanical, test hardware, tooling)
V.	Contractor liaison
VI.	Subsystem program management

If the schedule aggregate equations are to be implemented, the values for the independent variables must be selected. The value for N_S can be determined by comparing the cost of a single-string, active/standby, and triply redundant configuration that have met the performance and safety requirement and by using, for example, the cheapest configuration for the value of N_S. The other values, i.e., $N_{C/S}$ and $N_{B/S}$, must be selected by the system designer; by an iteration technique, he can compute the sensitivity of schedule time to these parameters.

Table 4-11. Manpower Aggregate Equations for Layouts, Diagrams, and Schematics

Task	Task Aggregate Equation (man-months)
Mathematical Block Diagrams	$0.2\ N_{C/S}\ N_S$
Interface Control Diagrams	$0.3\ N_{C/S}\ N_S$
Mechanical Layouts	$0.5\ N_{B/S}\ N_S$
Detailed Drawings	$0.5\ N_{B/S}\ N_S$
Long-Lead Items	$1.0\ N_{B/S}$
Functional Block Diagrams	$0.1\ N_{B/S}\ N_S$
Schematics	$1.0\ N_{B/S}$

where

N_S = number of ACS modules, $N_S = \begin{cases} 1 = \text{single-string} \\ 2 = \text{active/standby} \\ 3 = \text{triply redundant} \end{cases}$

$N_{C/S}$ = number of control functions per ACS module

$N_{B/S}$ = number of boxes per ACS module

The third major activity in Table 4-10 consists of analyses. The manpower aggregate equation for each task is shown in Table 4-12.

Table 4-12. Manpower Aggregate Equations for Analyses

Task	Task Aggregate Equation (man-months)
Stability Analysis	$1.0\ N_{C/S}\ N_S$
Error Analysis	$1.0\ N_{C/S}\ N_S$
Simulations	$1.0\ N_{C/S}\ N_S$
Structural Analysis	$1.0\ N_{C/S}\ N_S$
Thermal Analysis	$0.5\ N_{C/S}\ N_S$
Reliability Analysis	$0.5\ N_{B/S}$
Circuit Analysis	$1.0\ N_{C/S}\ N_S$

The fourth major activity in Table 4-10 consists of design activities. The manpower aggregate equation for each task is shown in Table 4-13.

Table 4-13. Manpower Aggregate Equations for Design Activities

Task	Task Aggregate Equation (man-months)
Electrical Design	$1.0\ N_{C/S}\ N_S$
Mechanical Design	$2.0\ N_{B/S}$
Test Hardware Design	$0.5\ N_{B/S}$
Tooling Design	$0.5\ N_{B/S}$

The last two major activities in Table 4-10, contractor liaison and subsystem program management, will each require a manpower of 3 man-months.

The manpower aggregate equation for the preliminary design and system analysis phase can be described as the sum of the task aggregate equations for each activity performed during the phase:

$$MP_1 = 33 \text{ man-months} + 7.0\, N_{C/S}\, N_S + 1.1\, N_{B/S}\, N_S + 5.5\, N_{B/S}$$

where MP_1 = preliminary design and system analysis manpower.

To illustrate the use of this manpower aggregate equation for determining schedules, assume that a three-axis ACS (i.e., $N_{C/S} = 3$, three control functions per ACS module) is to be mechanized to have triple redundancy and is to be packaged in four boxes per ACS module (i.e., $N_{B/S} = 4$). Substituting these numbers in the above manpower aggregate equation, one obtains a manpower requirement of 104.2 man-months. To estimate the amount of time needed to complete the preliminary design and system analysis phase, one must estimate the average number of men available during the phase. Assuming that one has 20 men available, then the time to complete this phase will be 5.21 months.

3. SUBSYSTEM ANALYSIS, DESIGN, AND BREADBOARD TESTING AGGREGATE EQUATIONS

The subsystem analysis, design, and breadboard testing phase begins with the completion of the PDR and ends with the midterm design review (MDR).

Table 4-14 lists the major activities performed during the subsystem analysis, design, and breadboard testing phase.

The first major activity in Table 4-14 is the program plans maintenance. The manpower aggregate equation for this activity was estimated by the panel of control engineers to be a constant, 6 man-months, independent of functional requirements.

Table 4-14. Major Activities During Subsystem Analysis, Design, and Breadboard Testing Phase

I.	Program plans maintenance (The program plans developed during the preliminary design and system analysis phase must be maintained.)
II.	Diagrams, layouts, schematics, long-lead items
III.	Analyses (same tasks as in preliminary design and system analysis phase with emphasis now on circuit analysis)
IV.	Design (electrical, mechanical, tooling, test hardware)
V.	Breadboard fabrication and tests
VI.	Quality assurance
VII.	Product engineering and manufacturing liaison
VIII.	System test liaison
IX.	Contractor liaison
X.	Subsystem program management

The second major activity in Table 4-14 consists of developing layouts, diagrams, schematics, etc. The manpower aggregate equation for each task is shown in Table 4-15.

Table 4-15. Manpower Aggregate Equations for Layouts, Diagrams, and Schematics

Task	Task Aggregate Equation (man-months)
Mathematical Block Diagrams	$0.1\ N_{C/S}\ N_S$
Interface Control Diagrams	$0.15\ N_{C/S}\ N_S$
Mechanical Layouts	$0.25\ N_{B/S}\ N_S$
Detailed Drawings	$0.25\ N_{B/S}\ N_S$
Long-Lead Items	$1.0\ N_{B/S}$
Functional Block Diagrams	$0.1\ N_{B/S}\ N_S$
Schematics	$3.0\ N_{B/S}$

where

$$N_S = \text{number of ACS modules},\quad N_S = \begin{cases} 1 = \text{single-string} \\ 2 = \text{active/standby} \\ 3 = \text{triply redundant} \end{cases}$$

$N_{C/S}$ = number of control functions per ACS module

$N_{B/S}$ = number of boxes per ACS module

The third major activity in Table 4-14 consists of analyses. The manpower aggregate equation for each task is shown in Table 4-16.

Table 4-16. Manpower Aggregate Equations for Analyses

Task	Task Aggregate Equation (man-months)
Stability Analysis	$1.0\ N_{C/S}\ N_S$
Error Analysis	$1.0\ N_{C/S}\ N_S$
Simulations	$1.0\ N_{C/S}\ N_S$
Structural Analysis	$1.0\ N_{C/S}\ N_S$
Thermal Analysis	$1.0\ N_{C/S}\ N_S$
Reliability Analysis	$0.5\ N_{B/S}$
Circuit Analysis	$3.0\ N_{B/S}\ N_S$

The fourth major activity in Table 4-14 consists of design activities. The manpower aggregate equation for each task is shown in Table 4-17.

Table 4-17. Manpower Aggregate Equations for Design Activities

Task	Task Aggregate Equation (man-months)
Electrical Design	$8.0\ N_{C/S}\ N_S$
Mechanical Design	$4.0\ N_{B/S}$
Tool Design	$0.5\ N_{B/S}$
Test Hardware Design	$0.5\ N_{B/S}$

The fifth major activity in Table 4-14 is the breadboard fabrication and tests. The manpower aggregate equation for this activity can be described by

$$MP(\text{breadboard fabrication and tests}) = 1.0\ N_{SI/B}\ N_B + 0.5\ N_{SO/B}\ N_B$$

where

$N_{SI/B}$ = number of input signals per box
$N_{SO/B}$ = number of output signals per box
N_B = number of boxes per ACS module.

The sixth major activity in Table 4-14 is the quality assurance activity. The manpower aggregate equation for this activity can be described as

$$MP(\text{quality assurance}) = 3.0\ N_{B/S}$$

The last two major activities in Table 4-14, product engineering and manufacturing liaison, and system test liaison — will each require a manpower of 6 man-months.

The manpower aggregate equation for the subsystem analysis, design, and breadboard testing phase can be described as the sum of the task aggregate equations for each activity performed during the phase.

$$MP_2 = 18 \text{ man-months} + 13.25\ N_{C/S}\ N_S + 3.6\ N_{B/S}\ N_S + 12.5\ N_{B/S} + 1.0\ N_{SI/B}\ N_B + 0.5\ N_{SO/B}\ N_B$$

where MP_2 = subsystem analysis, design, and breadboard testing manpower.

4. PROTOTYPE DESIGN, FABRICATION, AND TEST AGGREGATE EQUATION

The prototype design, fabrication and test phase begins with the MDR and ends with the critical design review (CDR). The output of this design phase consists of two engineering models. The first engineering model undergoes a qualification test and remains with the contractor. The second engineering model undergoes an acceptance test and is used for simulation purposes; it also remains with the contractor.

Table 4-18 lists the major activities performed during the prototype design, fabrication, and test phase.

Table 4-18. Major Activities During Prototype Design, Fabrication, and Test Phase

I.	Program plans maintenance (The program plans that were developed during the preliminary design and system analysis phase and that continued through the subsystem analysis, design, and breadboard testing must be maintained.)
II.	Diagrams, layouts, schematics, long-lead items
III.	Analyses (same categories as in the preliminary design and system analysis phase, with emphasis now on worst case circuit analyses)
IV.	Design (electrical, mechanical, tooling, test hardware)
V.	Engineering model fabrication and test
VI.	Quality assurance
VII.	Packaging engineering and manufacturing liaison
VIII.	System test liaison
IX.	Contractor liaison
X.	Subsystem program management

The first major activity in Table 4-18 is the program plans maintenance. The manpower aggregate equation for this activity was estimated by the panel of control engineers to be a constant, 12 man-months, independent of functional requirements.

The second major activity in Table 4-18 consists of developing layouts, diagrams, schematics, etc. The manpower aggregate equation for each task is shown in Table 4-19.

Table 4-19. Manpower Aggregate Equations for Layouts, Diagrams, and Schematics

Task	Task Aggregate Equation (man-months)
Mathematical Block Diagrams	$0.1\ N_{C/S}\ N_S$
Interface Control Diagrams	$0.3\ N_{C/S}\ N_S$
Mechanical Layouts	$0.15\ N_{B/S}\ N_S$
Detailed Drawings	$4.0\ N_{B/S}\ N_S$
Long-Lead Items	$0.5\ N_{B/S}\ N_S$
Functional Block Diagrams	$0.1\ N_{B/S}\ N_S$
Schematics	$1.0\ N_{B/S}\ N_S$

The third major activity in Table 4-18 consists of analyses. The manpower aggregate equation for each task is shown in Table 4-20.

Table 4-20. Manpower Aggregate Equations for Analyses

Task	Task Aggregate Equation (man-months)
Stability Analysis	$1.0\ N_{C/S}\ N_S$
Error Analysis	$1.0\ N_{C/S}\ N_S$
Simulations	$2.0\ N_{C/S}\ N_S$
Structural Analysis	$1.0\ N_{C/S}\ N_S$
Thermal Analysis	$1.5\ N_{C/S}\ N_S$
Reliability Analysis	$1.5\ N_{C/S}\ N_S$
Circuit Analysis	$3.0\ N_{C/S}\ N_S$

The fourth major activity in Table 4-18 consists of design activities. The manpower aggregate equation for each task is shown in Table 4-21.

Table 4-21. Manpower Aggregate Equations for Design Activities

Task	Task Aggregate Equation (man-months)
Electrical Design	$2.0\ N_{C/S}\ N_S$
Mechanical Design	$3.0\ N_{C/S}\ N_S$
Test Hardware Design	$3.0\ N_{C/S}\ N_S$
Tooling Design	$3.0\ N_{C/S}\ N_S$

The fifth major activity in Table 4-18 consists of the engineering model fabrication and test phase. The manpower aggregate equation for this activity can be described by

$$MP_a = (1 + K_p)\,(1 + K_r)\,(2N_{SI/B}\,N_{B/S} + 1N_{SO/B}\,N_{B/S})$$

where

MP_a = engineering model fabrication and test manpower
$N_{SI/B}$ = number of input signals per box
$N_{SO/B}$ = number of output signals per box.

Accuracy Ranges	K_p
2° to 10°	0
0.2° to 2°	0.2
0.02° to 0.2°	0.4

Reliability Ranges	K_r
0.7 to 0.5	0
0.9 to 0.7	0.05
0.999 to 0.9	0.10

The manpower aggregate equation for the sixth major activity, quality assurance, can be described by

$$MP(\text{quality assurance}) = 3.0\ N_{B/S}$$

The manpower aggregate equation for the seventh major activity, packaging engineering and manufacturing liaison, can be described by

$$MP(\text{packaging engineering and manufacturing liaison}) = 4.0\ N_{B/S}$$

The manpower aggregate equation for the eighth activity, system test liaison, was estimated by a panel of control engineers to be a constant, 6 man-months.

The last two major activities, contractor liaison and subsystem program management, will each require a manpower of 6 man-months.

The manpower aggregate equation for the prototype design, fabrication, and test phase can be described as the sum of the task aggregate equation for each activity performed during the phase:

$$MP_3 = 24 \text{ man-months} + 11.4\, N_{C/S}\, N_S + 4.25\, N_{B/S}\, N_S + 8.5\, N_{B/S} + (1 + K_p)(1 + K_r)(2.0\, N_{SI/B}\, N_{B/S} + 1.0\, N_{SO/B}\, N_{B/S})$$

where MP_3 = prototype design, fabrication, and test manpower.

5. SUBSYSTEM PRODUCTION ENGINEERING, FABRICATION, AND TEST AGGREGATE EQUATIONS

The subsystem production engineering, fabrication, and test phase begins with the completion of the CDR and ends with the fabrication and qualification testing of two ACSs. The first qualification unit is subjected to the acceptance and qualification tests. The second qualification unit is subjected to acceptance tests and is used in a vehicle level acceptance test.

Table 4-22 lists the major activities performed during the subsystem production engineering, fabrication, and test phase.

Table 4-22. Major Activities During Subsystem Production Engineering, Fabrication, and Test Phase

I.	Program plans maintenance (The program plans developed during the preliminary design and system analysis phase must be maintained.)
II.	Diagrams, layouts, schematics, long-lead items
III.	Analyses
IV.	Design (electrical, mechanical, tooling, test hardware)
V.	Production engineering, fabrication, and test
VI.	Quality assurance
VII.	Packaging engineering and manufacturing liaison
VIII.	System test liaison
IX.	Contractor liaison
X.	Subsystem program management

The first major activity is the program plans maintenance. The manpower aggregate equation for this activity was estimated by the panel of control engineers to be a constant, 12 man-months, independent of functional requirements.

The second activity consists of developing interface control diagrams and detailed drawings. The manpower aggregate equation for each task is shown in Table 4-23.

Table 4-23. Manpower Aggregate Equations for Interface Control Diagrams and Detailed Drawings

Task	Task Aggregate Equation (man-months)
Interface Control Diagrams	$0.3\ N_{C/S}\ N_S$
Detailed Drawing	$0.3\ N_{C/S}\ N_S$

The third activity consists of analyses. The manpower aggregate equation for each task is shown in Table 4-24.

Table 4-24. Manpower Aggregate Equations for Analyses

Task	Task Aggregate Equation (man-months)
Stability Analysis	$0.3\ N_{C/S}\ N_S$
Error Analysis	$0.3\ N_{C/S}\ N_S$
Simulations	$0.3\ N_{C/S}\ N_S$
Structural Analysis	$0.3\ N_{C/S}\ N_S$
Thermal Analysis	$0.3\ N_{C/S}\ N_S$
Reliability Analysis	$0.1\ N_{B/S}$
Circuit Analysis	$0.5\ N_{B/S}\ N_S$

The fourth activity consists of design activities. The manpower aggregate equation for each task is shown in Table 4-25.

Table 4-25. Manpower Aggregate Equations for Design Activities

Task	Task Aggregate Equation (man-months)
Electrical Design	$4.0\ N_{C/S}\ N_S$
Mechanical Design	$2.0\ N_{B/S}$
Test Hardware Design	$2.0\ N_{B/S}$
Tooling Design	$2.0\ N_{B/S}$

The manpower aggregate equation for the production engineering, fabrication, and test phase can be described by

$$\text{MP(production engineering, fabrication, and test)} = 12\ N_{B/S}\ N_S$$

The manpower aggregate equation for quality assurance can be described by

$$\text{MP(quality assurance)} = 2.0\ N_{B/S}$$

The manpower aggregate equation for the packaging engineering and manufacturing liaison can be described by

$$\text{MP(packaging engineering and manufacturing liaison)} = 2.0\ N_{B/S}$$

The manpower aggregate equations for each of the last three activities, namely, system test liaison, contractor liaison, and subsystem program management were estimated to be a constant, namely, 6 man-months.

The manpower aggregate equation for the subsystem production engineering, fabrication, and test phase can be described as the sum of the task aggregate equations for each activity performed during the phase

$$MP_4 = 30 \text{ man-months} + 6.1\, N_{C/S}\, N_S + 12.5\, N_{B/S}\, N_S + 10.1\, N_{B/S}$$

where MP_4 = subsystem production engineering, fabrication, and test manpower.

6. SYSTEM INTEGRATION AND TEST AGGREGATE EQUATIONS

The system integration and test phase consists of integrating the ACS into the space vehicle and performing an acceptance test on the ACS after this integration.

Table 4-26 lists the major activities performed during the system integration and test phase.

Table 4-26. Major Activities During System Integration and Test

I.	Program plans maintenance
II.	System integration
III.	Tests
IV.	Contractor liaison
V.	Subsystem program management

The first major activity is the program plans maintenance. The manpower aggregate equation for this activity was estimated to be a constant, 6 man-months.

The manpower aggregate equation for the system integration phase can be described by

$$MP(\text{system integration}) = 0.2\, N_{B/S}\, N_S$$

The manpower aggregate equation for the test phase can be described as

$$MP(\text{tests}) = (1 + K_m)\,(1 + K_p)\,(1 + K_r)\,(0.1\, N_{SI/B}\, N_{B/S} + 0.3\, N_{SO/B}\, N_{B/S})$$

where

j	K_m
1	0
2	0.1
3	0.15
4	0.2
5	0.25

K_p and K_r are defined in Section 4.F.4 and j is the number of operational modes of the ACS.

The last two activities, namely, contractor liaison and subsystem program management, will each require a manpower of 6 man-months.

The manpower aggregate equation for the system integration and test phase can be described as the sum of the task aggregate equation for each activity performed during the phase:

$$MP_5 = 18 \text{ man-months} + 0.2\, N_{B/S}\, N_S + (1 + K_m)\,(1 + K_p)\,(1 + K_r)$$
$$\times\, (0.1\, N_{SI/B}\, N_{B/S} + 0.3\, N_{SO/B}\, N_{B/S})$$

where MP_5 = system integration and test manpower.

REFERENCES

1. Standard Agena Space Vehicle Technical Description, Lockheed Report No. LMSC-A397890 (1 December 1964).

2. Reliability Stress and Failure Rate Data for Electronic Equipment, Bureau of Naval Weapons, Department of the Navy MIL-HDBK-217A (1 December 1965).

3. Advanced Spacecraft Subsystem Cost Analysis Study, Honeywell, Inc. Report No. 21250FR, MSC-01243 (1 December 1969).

5. COST/PERFORMANCE SIMULATION

A. INTRODUCTION

This section describes the Cost/Performance Simulation used to perform sample attitude control system (ACS) cost/performance calculations on a Tug-type vehicle as a practical example of implementing the methods developed by this study. As the simulation consists of extensive interaction among aggregate equations and the addition of certain auxiliary equations, the simulation is described to place sample calculations in proper perspective and to provide insight into various ways of tailoring the simulation program to individual study requirements. It is also intended to show a general implementation approach for vehicle subsystems other than the ACS and to provide a core for the construction of an overall vehicular simulation.

B. SIMULATION DESCRIPTION

The simulation implementing the Cost/Performance Model is formulated to be adaptable; i. e., it may be upgraded as a project progresses from the conceptual phase through design and development stages. Thus, as increasingly definitive ACS configuration and data base material become available during the design process, individual Cost/Performance Model data base inputs and aggregate equations may be changed to reflect the normal progression of various design and development tasks. It is also anticipated that the basic interactions and interfaces among major simulation modules will require only a minor amount of change, thereby maintaining the utility of the simulation as a viable, short-reaction-time tool to support management decisions.

With this approach in mind, initial aggregate equations used in performance, cost, safety, and schedule portions of the simulation may be general and may reflect implementation of a single baseline ACS. In this case, all possible combinations of candidate components within the four major ACS modules are automatically tested against ACS design criteria, and results are presented according to operator-selectable sort criteria. In this early or conceptual phase application of the Cost/Performance Simulation, data bases may well be relatively incomplete or inaccurate; therefore, sensitivity studies of the baseline system are much more useful than absolute performance, cost, safety, and schedule figures. However, as work progresses and specific ACS designs emerge with increasing definition of their supporting data bases, absolute ACS assessments will become more meaningful.

1. INITIALIZATION

Figure 5-1 is an overview of the ACS Cost/Performance Simulation. As shown in the chart, entry of model variables and matrices initializes the program. A complex data base results from the many inputs required to define various ACS configurations. Therefore, the program is structured to allow entry of a stored data base, followed by easy program data base modifications or additions.

Following the first initialization phase (consisting of data base entry and modification), data are provided for the various performance, safety (reliability), cost, and schedule criteria to be used in the program during execution. For example, performance criteria such as the required coast flight attitude control accuracy in roll, pitch, and yaw axes are the inputs during this second phase of the program initialization procedure. These inputs are used to evaluate acceptability of specific ACS configurations during execution of aggregate equations in the performance module of the program. A similar input specifies a required ACS mission reliability and sets a criterion for acceptance of each candidate ACS configuration during program execution of safety aggregate equations. Final inputs prior to program execution provide sort criteria to format program outputs by ranking acceptable ACS configurations according to cost, reliability, accuracy, or any other criterion calculable, using aggregate equations implemented in the simulation.

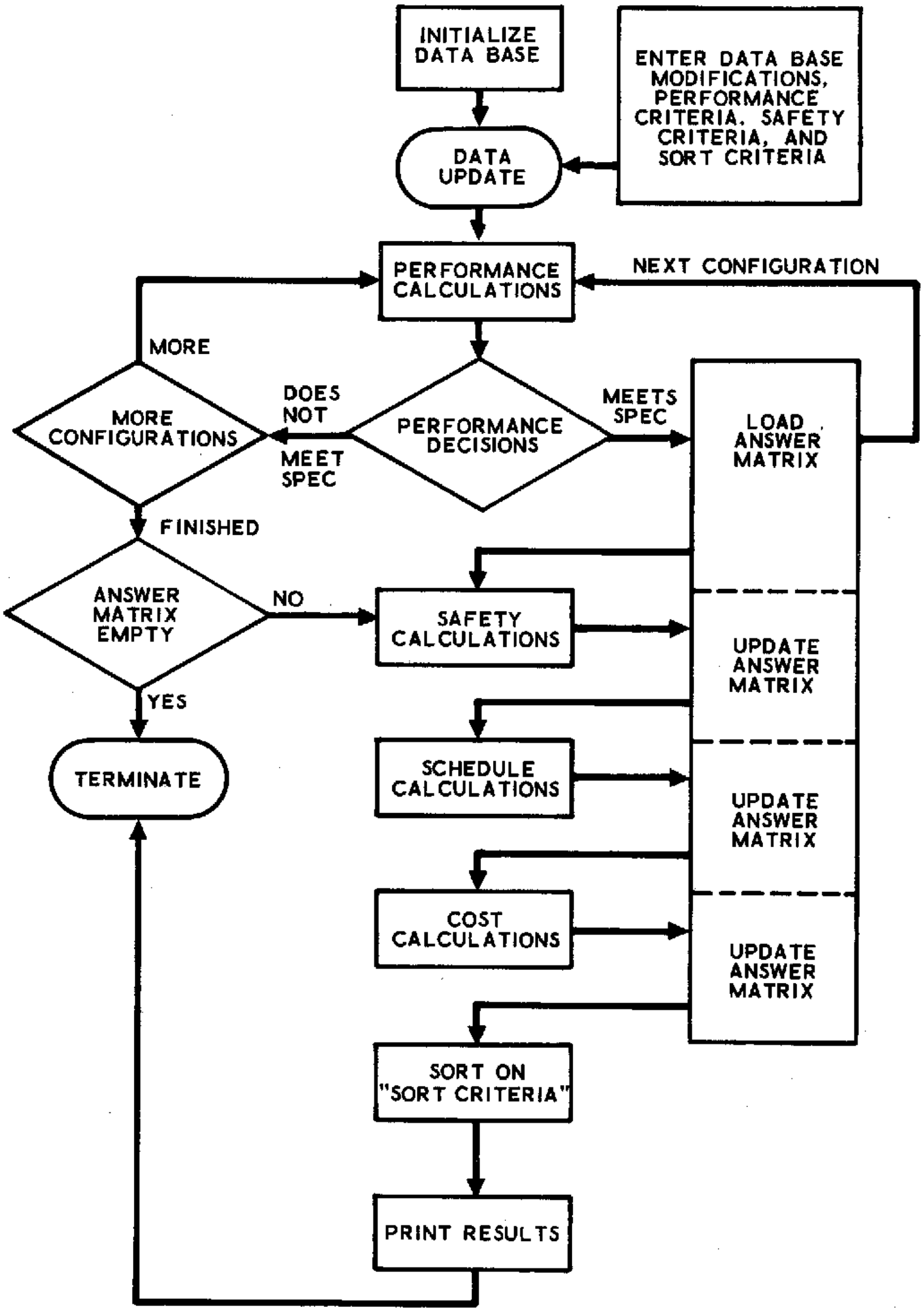

Figure 5-1. Cost/Performance Simulation Overview

Upon completion of the ACS requirements phase of initialization, the program begins execution of performance aggregate equations and decisions described in Section 5. B. 2.

2. PERFORMANCE MODULE

In the performance module of the Cost/Performance Simulation, the acceptability of each candidate ACS is evaluated by comparing calculated ACS performance, as determined by performance aggregate equations, to required ACS performance parameters entered during program initialization. The flow of calculations in this module may be relatively simple, such as those shown in Figure 5-1, or they may be more complex and essentially represent a basic error analysis of a particular ACS configuration. In general, use of the simulation during early conceptual phases of a program would rest on several baseline ACSs, with each specific baseline defined by a separate set of aggregate equations. Later applications would be based on a single ACS configuration, requiring a single set of performance aggregate equations. As mentioned previously, the program is structured to accept these intermodule changes without disrupting the basic intramodule interactions that form the basis of the Cost/Performance Simulation.

The program, as it presently exists, implements an early version of the performance aggregate equations, which vary in some details from those in Section 4. For example, major aggregate equations, such as the coast flight ACS accuracy equation, are implemented, while total ACS weight, volume, and power are obtained by simply summing component contributions without using a factor to account for cables, lines, or other ancillary equipment. Vibration, temperature, pressure, and schedule relationships are not included at this stage.

Regardless of the level of sophistication of the performance aggregate equations, all ACS configurations passing the performance criteria are stored in the answer matrix. This matrix maintains a dynamic record of ACS configurations that have met or surpassed criteria entered by the operator during program initialization.

The answer matrix is structured so that each column represents a particular ACS configuration and each row represents a total system attribute. Examples of answer matrix attributes are total ACS system weight or an identifier of a particular data base component that is a part of a specific ACS configuration. Thus, the first row of all answer matrix columns could identify a particular inertial measurement unit (IMU); the second row, a horizon sensor; the third, a star reference; the fourth, the system weight; and so on. While some row entries may be the same for different columns, each column will represent a distinct combination of row entries and hence a unique ACS configuration.

Calculation of total system attributes peculiar to each ACS configuration is accomplished by using answer matrix pointers that refer to attributes of each component stored in the data base matrix. (The data base matrix is similar in structure to the answer matrix, except that columns list individual component attributes in each row, rather than system attributes.) For example, the total weight of a specific ACS configuration stored in the first column of the answer matrix is presently calculated by summing the weight of each ACS component stored in the data base matrix that is listed in the first column of the answer matrix. Other calculations, such as the one for total system cost, use individual component attributes as inputs to one or more aggregate equations, which then calculate the total system attribute.

This multilevel matrix approach to identification of system and component attributes is illustrated in Figure 5-2. It is typical of discrete event simulation languages and particularly efficient in limiting the size of matrices by minimizing storage of redundant information in the computer.

Following assessment of performance, each ACS configuration meeting requirements and stored as an answer matrix entry is subjected to evaluation using a set of safety aggregate equations as detailed in Section 5. B. 3.

3. SAFETY MODULE

The safety aggregate equation module immediately follows implementation of the performance module in the sequence of operations performed during execution of the Cost/Performance Simulation. All ACS configurations

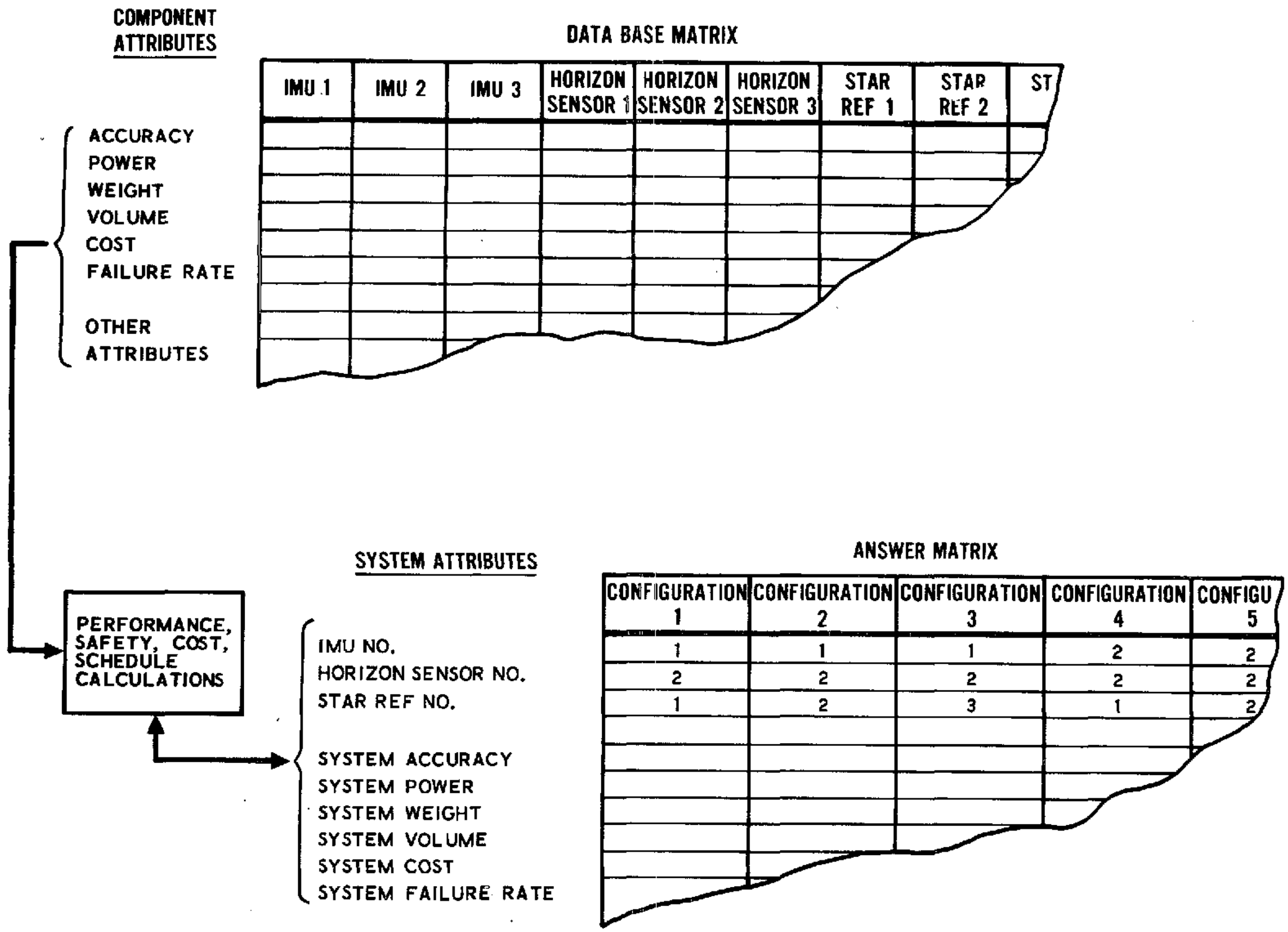

Figure 5-2. Data Base/Answer Matrix Configuration

that have successfully passed performance criteria and have been stored in the answer matrix are screened by the safety module as indicated in Figure 5-3.

As shown in the figure, three distinct ACS mechanizations are assessed by the safety aggregate equations:

a. Single-string ACS
b. Active/standby string ACS
c. Triply redundant ACS with voting

All ACS configurations stored in the answer matrix are first evaluated for their reliability in a single-string mechanization. Those systems not meeting reliability criteria are upgraded by paralleling the lowest reliability module in the ACS sensor, processor, actuator, energy source module string. The total reliability of the improved system is then recalculated and checked for compliance with reliability specifications. If the system is still unacceptable, paralleling of the weakest module continues. (The weakest module may or may not be the same module paralleled previously.) This process is continued until the system is acceptable or until a module exceeds triple redundancy, at which point the program rejects the configuration as unacceptable in a single-string mechanization and proceeds to evaluate the next configuration. Should the system meet reliability criteria, failure detection probability and false alarm probability are calculated for the configuration and the system is stored in the answer matrix as an acceptable single-string mechanization.

After evaluating all configurations stored in the answer matrix for compliance with reliability criteria when mechanized as a single-string ACS, the program proceeds to evaluate each configuration in an active/standby ACS mechanization. As before, paralleling of modules is allowed to upgrade reliability of the active/standby mechanizations, and individual modules are held to maximums of triple redundancy. Systems meeting reliability criteria have failure detection and false alarm probabilities calculated and are then stored in the answer matrix as an acceptable active/standby mechanization.

Following evaluation of all answer matrix entries as active/standby mechanizations, the program evaluates each entry in the answer matrix

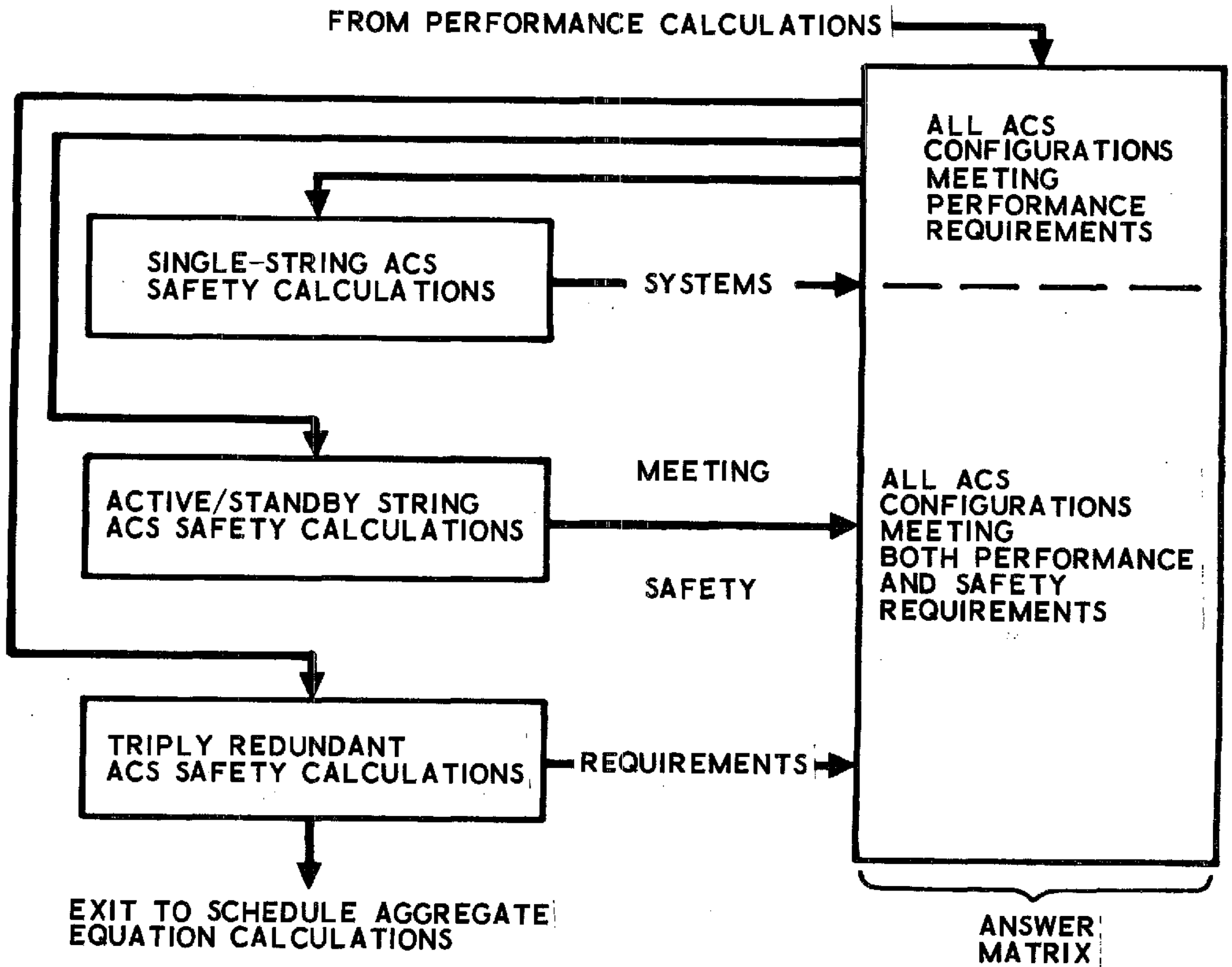

Figure 5-3. Flow Chart Overview of Safety Aggregate Equation Calculations

mechanized as triply redundant ACS strings with voting. In this mechanization, upgrading of individual modules by paralleling is not allowed, as the total ACS already consists of triply redundant systems. Other calculations proceed in a manner similar to previously described mechanizations.

Detailed flow charts of the procedures described above and shown as major program blocks in Figure 5-3 are given in Figures 5-4 through 5-7.

Configurations not meeting reliability criteria after safety module processing are deleted from the answer matrix, and the program processes schedule and cost aggregate equations described in Section 5. B. 4.

4. SCHEDULE AND COST MODULE

Schedule and cost calculations are straightforward implementations of the schedule/cost aggregate equations; however, the present program does not implement schedule equations. Present plans include presenting schedule results as charts showing major program milestones for each configuration stored in the answer matrix. Each chart would be keyed to the printout of other information for the particular configuration it represents; the total package would represent complete assessment results of all ACS configurations meeting performance and safety criteria. For ease in evaluating various ACS configurations, printouts are ordered according to sort criteria previously entered by the operator.

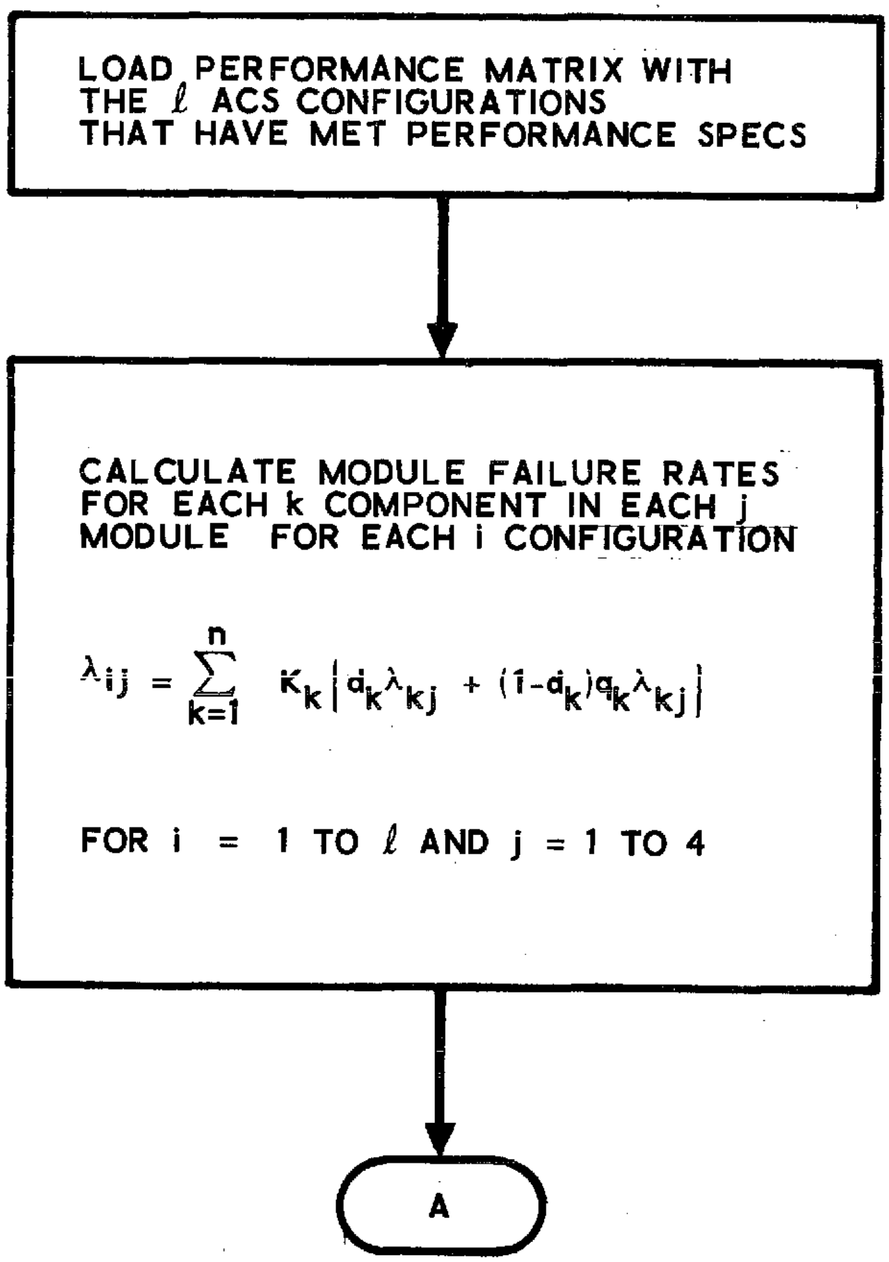

Figure 5-4. Failure Rates, Active System

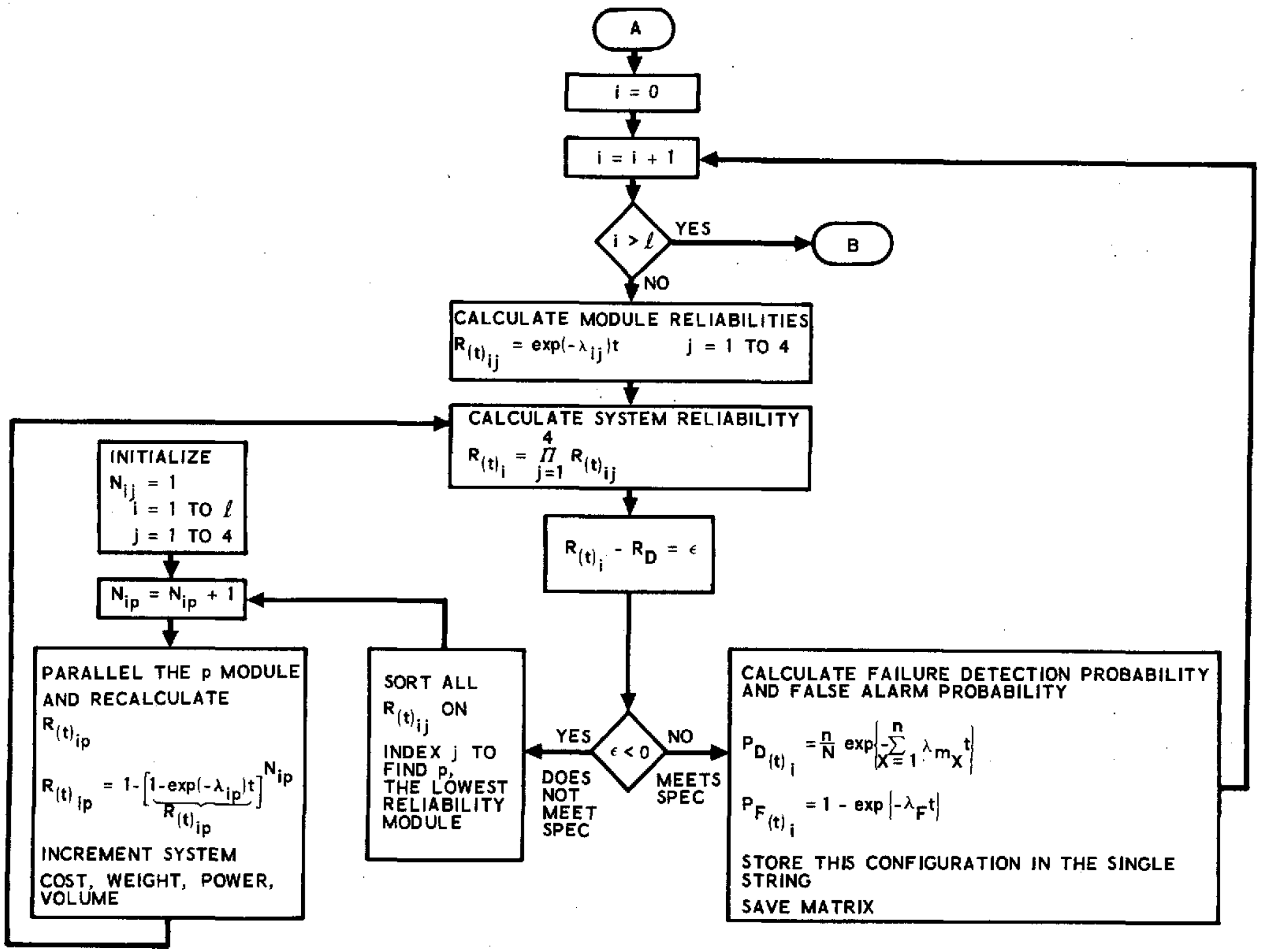

Figure 5-5. Single-String ACS

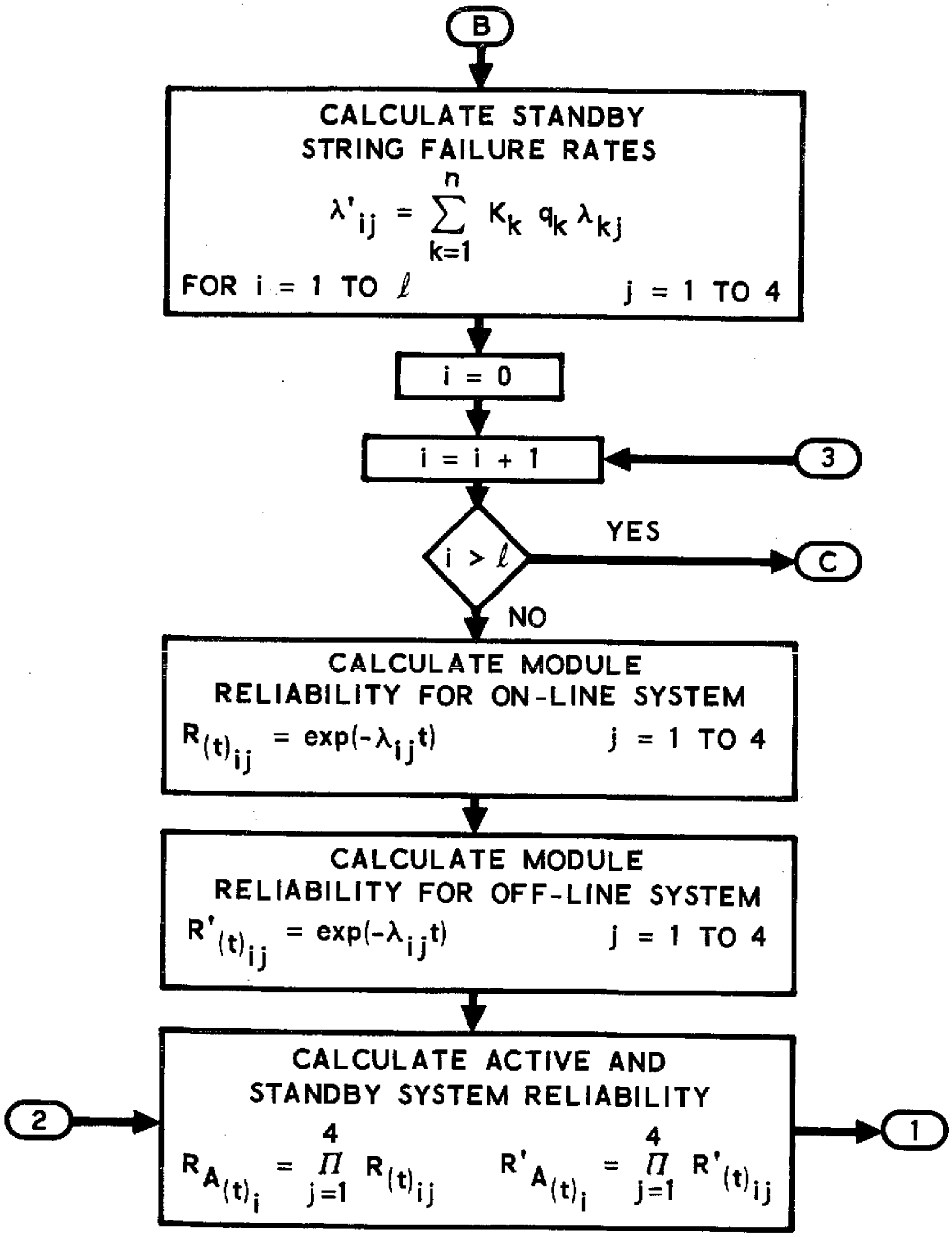

Figure 5-6. Active ACS, Standby ACS

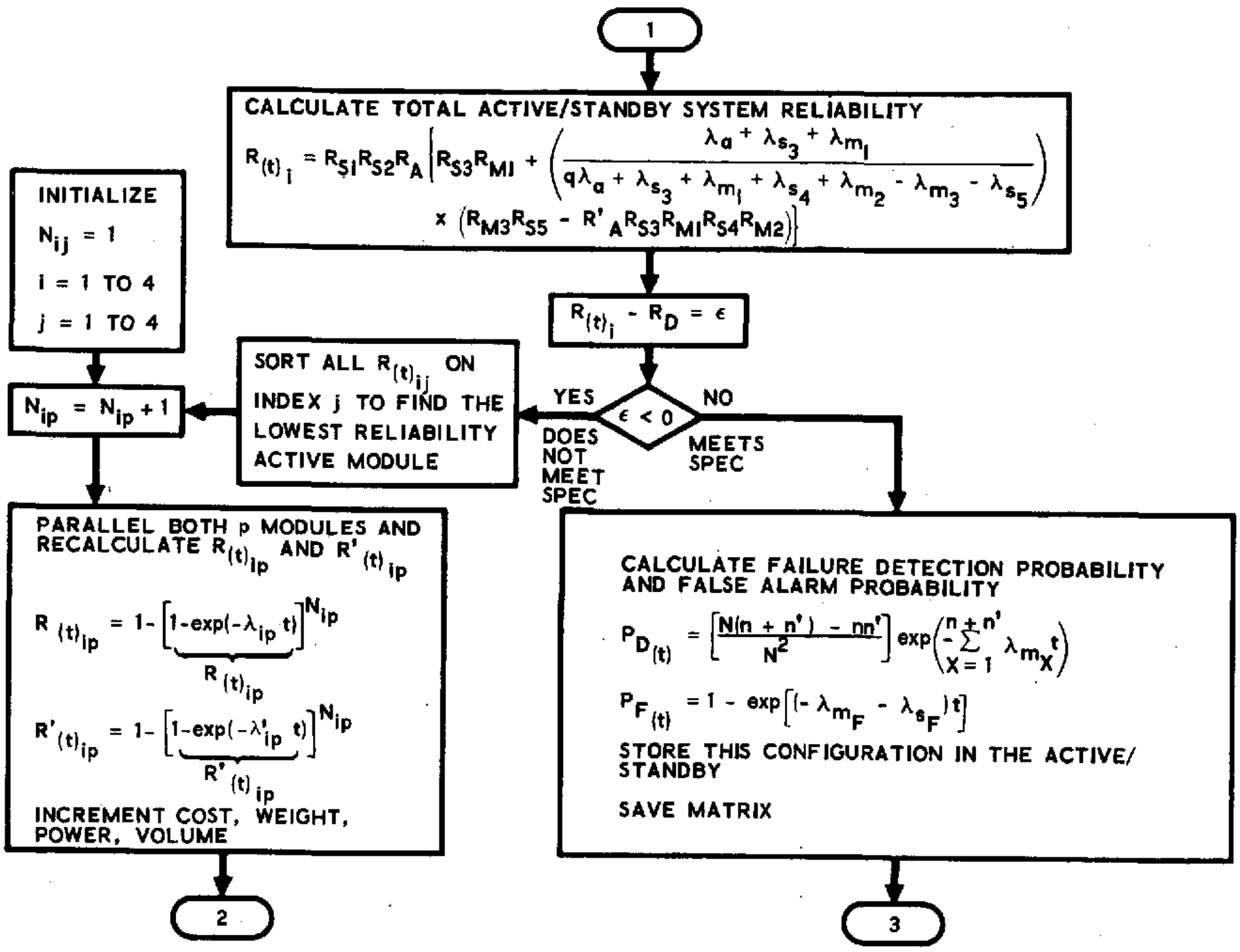

Figure 5-6. Active ACS, Standby ACS (Continued)

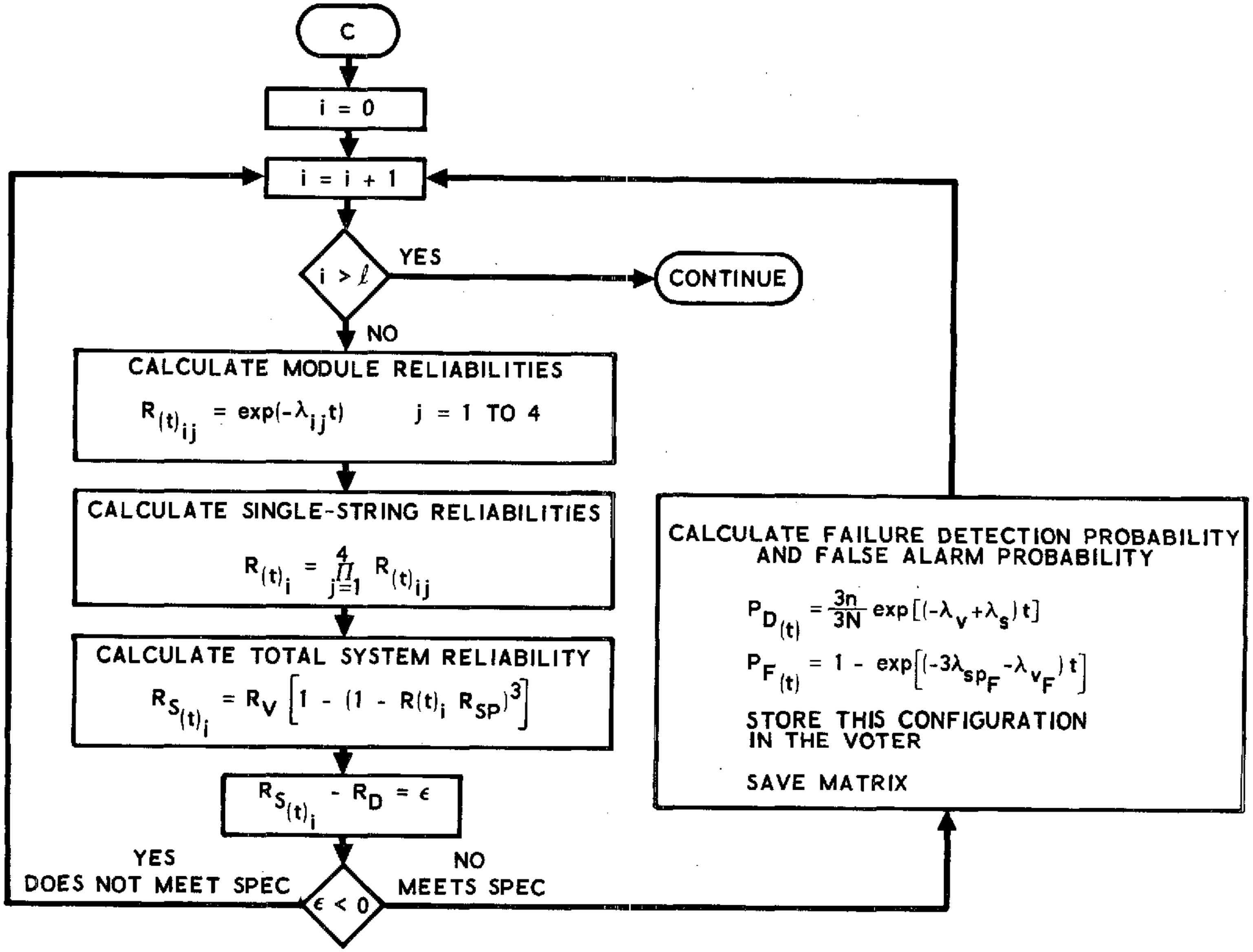

Figure 5-7. Triply Active ACS With Voting

6. ACS COMPONENT DATA BASE

One objective of this task was to develop a component data base format for use with the aggregate equations for the ACS, but also sufficiently general for use with the aggregate equations for other space vehicle systems. After data format inputs were obtained from both cost and performance specialists, the Table 1-1 data format was formulated, and some ACS component data were gathered. A partial list of this data is presented in Tables 6-1 through 6-13. The component data used in the cost/performance computer study are shown in Appendix C.

Table 6-1. Attitude Control System Component Data (Electromagnets)

		Electromagnets		
1.0.0	PERFORMANCE	Boeing Part No. 223-10036-2 (S-3 Program)	MSFC Estimate for LST Mission	LMSC Estimate for LST
1.1.0	Technical Characteristics	Magnetic Residual Moment = 150 pole-cm Linearity ±1% Magnet Moment 150,000 pole-cm	$M = 4.5 \times 10^6$ pole-cm	$M = 0.6 \times 10^6$ pole-cm
1.2.0	Power	4.9 W	10 W max	10 W
1.3.0	Weight	2.3 kg (5 lb)	28.1 kg (62 lb)	5.0 kg (11 lb)
1.4.0	Volume	$0.00052\ m^3$ ($32\ in.^3$)	$0.00188\ m^3$ ($115\ in.^3$)	$0.00074\ m^3$ ($45\ in.^3$)
1.5.0	Vibration Specification	Random: 19.7 g rms overall	NA[a]	NA[a]
1.6.0	Temperature Specification (radiation and conduction)	0°C to +60°C	NA[a]	NA[a]
1.7.0	Ambient Pressure Specification	$0.00133\ N/m^2$ (10^{-5} Torr)	NA[a]	NA[a]

[a]NA = not available

Table 6-1. Attitude Control System Component Data (Electromagnets) (Continued)

2.0.0 SAFETY AND HAZARDS	Electromagnets		
	Boeing Part No. 223-10036-2 (S-3 Program)	MSFC Estimate for LST Mission	LMSC Estimate for LST
2.1.0 Failure Rate	6.9×10^{-7}/hr	1.1×10^{-6}/hr	NA[a]
2.1.1 Number of Single Point Failures 2.1.2 Number of Double Point Failures	NA[a]	NA[a]	NA[a]
2.2.0 Failure Detection Probability	0	0	0
2.3.0 False Alarm Probability	0	0	0
2.4.0 Destructive Potential (TNT equivalence)	0	0	0

[a]NA = not available

Table 6-2. Attitude Control System Component Data (Rate Gyro Assembly)

	Rate Gyro Assembly (backup)	
1.0.0 PERFORMANCE	LMSC RGA CCA 2794 (P50 Program)	Timex RGP 402035-0 (STP 72-2)
1.1.0 Technical Characteristics	Threshold 0.0009 rad/sec Rate Range ± 0.1047 rad/sec 3-Axis uses 3 Mod CD 040 Timex Rate Gyros	Threshold 0.00003 rad/sec Rate Range ± 0.349 rad/sec 3-Axis uses 3 IG10 Timex Rate Gyros
1.2.0 Power	Running 20 W max Starting 30 W max	Running 20 W max Starting 25 W max
1.3.0 Weight	1.4 kg (3 lb)	1.4 kg (3 lb)
1.4.0 Volume	0.00061 m^3 (37 $in.^3$)	0.00100 m^3 (61 $in.^3$)
1.5.0 Vibration Specification	Random: Survival 13.9 g rms	Random: Survival 18.5 g rms
1.6.0 Temperature Specification (radiation and conduction)	NA[a]	-12°C to + 49°C for Qual
1.7.0 Ambient Pressure Specification	0.00133 N/m^2 (10^{-5} Torr)	0.0133 N/m^2 (10^{-4} Torr)

[a]NA = not available

Table 6-2. Attitude Control System Component Data (Rate Gyro Assembly) (Continued)

2.0.0 SAFETY AND HAZARDS	Rate Gyro Assembly (backup)	
	LMSC RGA CCA 2794 (P50 Program)	Timex RGP 402035-0 (STP 72-2)
2.1.0 Failure Rate	100×10^{-6}/hr	4.6×10^{-6}/hr
2.1.1 Number of Single Point Failures 2.1.2 Number of Double Point Failures	NA[a]	NA[a]
2.2.0 Failure Detection Probability	0	0
2.3.0 False Alarm Probability	0	0
2.4.0 Destructive Potential (TNT equivalence)	0	0

[a]NA = not available

Table 6-3. Attitude Control System Component Data (Digital Computers)

1.0.0 PERFORMANCE	Digital Computers		
	RCA "MARC" 5D Model Microcomputer	Honeywell HDC 301	Autonetics D216
1.1.0 Technical Characteristics	Speed: Addition = 4.7 μsec Mult = 49/μsec CPU + 8K R/W Memory + I/O Electronics	Speed: Addition = 5.0 μsec Mult = 21.0 μsec CPU + 8K R/W Memory + I/O Electronics	Speed: Addition = 2.5 μsec Mult = 13.75 μsec CPU + 8K R/W Memory + I/O Electronics
1.2.0 Power	4.2 W	5 to 20 W	32 W
1.3.0 Weight	3.1 kg (6.9 lb)	1.4 to 3.2 kg (3 to 7 lb)	2.7 kg (6.0 lb)
1.4.0 Volume	0.00521 m^3 (318 in.^{3})	0.00241 m^3 (147 in.^{3})	0.00410 m^3 (250 in.^{3}) (Does not include power conversion electronics)
1.5.0 Vibration Specification	NA[a]	NA[a]	NA[a]
1.6.0 Temperature Specification (radiation and conduction)	NA[a]	NA[a]	NA[a]
1.7.0 Ambient Pressure Specification	NA[a]	NA[a]	NA[a]

[a]NA = not available

Table 6-3. Attitude Control System Component Data (Digital Computers) (Continued)

2.0.0 SAFETY AND HAZARDS	Digital Computers		
	RCA "MARC" 5D Model Microcomputer	Honeywell HDC 301	Autonetics D216
2.1.0 Failure Rate	5.7×10^{-6}/hr	63.5×10^{-6}/hr	191×10^{-6}/hr
2.1.1 Number of Single Point Failures 2.1.2 Number of Double Point Failures	NA[a]	NA[a]	NA[a]
2.2.0 Failure Detection Probability	0	0	0
2.3.0 False Alarm Probability	0	0	0
2.4.0 Destructive Potential (TNT equivalence)	0	0	0

[a]NA = not available

Table 6-4. Attitude Control System Component Data (Reaction Wheels)

1.0.0 PERFORMANCE	Reaction Wheels		
	Sperry Model 35 RWA	Sperry Model 45Q RWA	Bendix OAO Type 1880272
1.1.0 Technical Characteristics	Speed 2400 to 4100 rpm $407 \leq H \leq 678$ N-m-sec	Speed 5200 rpm $13.6 \leq H \leq 122$ N-m-sec	Speed 1200 rpm H = 2.8 N-m-sec at 900 rpm
1.2.0 Power	10 W at 3600 rpm 88 W max during run-up	10 W at 5200 rpm	3.3 W at stall
1.3.0 Weight	31.0 kg (68.5 lb)	9.1 kg (20 lb)	4.5 kg (10 lb)
1.4.0 Volume	0.0781 m^3 (4770 $in.^3$)	0.0290 m^3 (1770 $in.^3$)	0.006 m^3 (366 $in.^3$)
1.5.0 Vibration Specification	Random: 19.5 grms	NA[a]	NA[a]
1.6.0 Temperature Specification (radiation and conduction)	-40°C to + 77°C	NA[a]	NA[a]
1.7.0 Ambient Pressure Specification	NA[a]	NA[a]	NA[a]

[a]NA = not available

Table 6-4. Attitude Control System Component Data (Reaction Wheels) (Continued)

2.0.0 SAFETY AND HAZARDS	Reaction Wheels		
	Sperry Model 35 RWA	Sperry Model 45Q RWA	Bendix OAO Type 1880272
2.1.0 Failure Rate	0.55×10^{-6}/hr	Life 4 yr	NA[a]
2.1.1 Number of Single Point Failures 2.1.2 Number of Double Point Failures	NA[a]	NA[a]	NA[a]
2.2.0 Failure Detection Probability	0	0	0
2.3.0 False Alarm Probability	0	0	0
2.4.0 Destructive Potential (TNT equivalence)	0	0	0

[a]NA = not available

Table 6-5. Attitude Control System Component Data (Control Moment Gyros)

1.0.0 PERFORMANCE	Control Moment Gyros: Northrop CMG-II	Control Moment Gyros: Bendix CMG + Electronics Assy for HEAO	Control Moment Gyros: Sperry Model 75 CMG
1.1.0 Technical Characteristics	Bias $< 4.86 \times 10^{-7}$ rad/sec Unbal: $<9.72 \times 10^{-7}$ (rad/sec)/g Single gimbal floated. H = 8.95 N-m-sec	Wheel: speed control ±1% Gimbal: drift = 1.75×10^{-4} rad/sec Single gimbal H = 610 N-m-sec	Double gimbal H = 102 N-m-sec
1.2.0 Power	Wheel 9 W (no heaters)	Gimbal: 40 W max Wheel: 200 W max during run-up 16 W max on orbit	Power: 45 W peak
1.3.0 Weight	10.4 kg (23 lb)	81.6 kg (180 lb) including mounting ring	15.9 kg (35 lb)
1.4.0 Volume	0.00463 m^3 (283 $in.^3$)	0.292 m^3 (17,800 $in.^3$)	0.062 m^3 (3800 $in.^3$) estimated
1.5.0 Vibration Specification	Sine: 0.3 to 10 g for 5 to 3,000 Hz Rand: 7.7 g rms	Sine: 1.0 g peak 10 to 50 Hz 9 min/axis	NA[a]
1.6.0 Temperature Specification (radiation and conduction)	-18°C to + 38°C	NA[a]	NA[a]
1.7.0 Ambient Pressure Specification	0 to 207×10^3 N/m^2 (0 to 30 psia)	NA[a]	NA[a]

[a]NA = not available

Table 6-5. Attitude Control System Component Data (Control Moment Gyros) (Continued)

2.0.0 SAFETY AND HAZARDS	Control Moment Gyros		
	Northrop CMG-II	Bendix CMG + Electronics Assy for HEAO	Sperry Model 75 CMG
2.1.0 Failure Rate	Life 20, 000 hrs	1.1×10^{-6}/hr	NA[a]
2.1.1 Number of Single Point Failures 2.1.2 Number of Double Point Failures	NA[a]	NA[a]	NA[a]
2.2.0 Failure Detection Probability	0	0	0
2.3.0 False Alarm Probability	0	0	0
2.4.0 Destructive Potential (TNT equivalence)	0	0	0

[a]NA = not available

Table 6-6. Attitude Control System Component Data (Sun Sensors)

1.0.0 PERFORMANCE	Sun Sensors (heads only)		
	Bendix Fine Angle Sensor No. 1818823	Adcole Aspect Sensor No. 1401	Adcole Aspect Sensor No. 1301
1.1.0 Technical Characteristics	Accuracy: 24×10^{-6} rad (3σ assumed) Null seeker type 2-axis total FOV ±10 deg	Accuracy: 4.4×10^{-3} rad (3σ) Digital 8-bit outputs FOV 128° × 128°	Accuracy: 4.4×10^{-3} rad (3σ) Digital 7-bit output Modulation - spin of spacecraft
1.2.0 Power	None required	None required	None required
1.3.0 Weight	0.85 kg (1.88 lb)	0.10 kg (0.22 lb)	0.044 kg (0.095 lb)
1.4.0 Volume	54×10^{-5} m^3 (33 $in.^3$)	5.2×10^{-5} m^3 (3.2 $in.^3$)	2.2×10^{-5} m^3 (1.33 $in.^3$)
1.5.0 Vibration Specification	NA[a]	NA[a]	NA[a]
1.6.0 Temperature Specification (radiation and conduction)	-55°C to + 50°C	NA[a]	NA[a]
1.7.0 Ambient Pressure Specification	NA[a]	NA[a]	NA[a]

[a]NA = not available

Table 6-6. Attitude Control System Component Data (Sun Sensors) (Continued)

2.0.0 SAFETY AND HAZARDS	Sun Sensors		
	Bendix Fine Angle Sensor No. 1818823	Adcole Aspect Sensor No. 1401	Adcole Aspect Sensor No. 1301
2.1.0 Failure Rate	NA[a]	NA[a]	NA[a]
2.1.1 Number of Single Point Failures 2.1.2 Number of Double Point Failures	NA[a]	NA[a]	NA[a]
2.2.0 Failure Detection Probability	0	0	0
2.3.0 False Alarm Probability	0	0	0
2.4.0 Destructive Potential (TNT equivalence)	0	0	0

[a]NA = not available

Table 6-7. Attitude Control System Component Data (Magnetometers)

1.0.0 PERFORMANCE	Magnetometers (sensor and electronics)	
	Schonstedt SAM-63C-1 (S-3 Program)	Dalmo Victor Part 76974 (OAO Program)
1.1.0 Technical Characteristics	Accuracy ±0.044 rad (3σ) Linearity ±0.1% of null 3-axis flux gate	Linearity ±3% 3-axis flux gate
1.2.0 Power	1.1 W max	NA[a]
1.3.0 Weight	0.91 kg (2.0 lb)	4.1 kg (9 lb)
1.4.0 Volume	0.0028 m^3 (169 $in.^3$)	0.00458 m^3 (275 $in.^3$)
1.5.0 Vibration Specification	Random: 19.7 g rms during boost	NA[a]
1.6.0 Temperature Specification (radiation and conduction)	Sensor: -20°C to + 53°C Electronics: -5.5°C to + 45°C	NA[a]
1.7.0 Ambient Pressure Specification	1.333×10^{-3} N/m^2 (10^{-5} Torr)	NA[a]

[a]NA = not available

Table 6-7. Attitude Control System Component Data (Magnetometers) (Continued)

2.0.0 SAFETY AND HAZARDS	Magnetometers: Schonstedt SAM-63C-1 (S-3 Program)	Magnetometers: Dalmo Victor Part 76974 (OAO Program)
2.1.0 Failure Rate	1.4×10^{-6}/hr	NA[a]
2.1.1 Number of Single Point Failures 2.1.2 Number of Double Point Failures	NA[a]	NA[a]
2.2.0 Failure Detection Probability	0	0
2.3.0 False Alarm Probability	0	0
2.4.0 Destructive Potential (TNT equivalence)	0	0

[a]NA = not available

Table 6-8. Attitude Control System Component Data (Inertial Reference Assembly)

1.0.0 PERFORMANCE	Inertial Reference Assembly LMSC's ARA CCA No. 3006
1.1.0 Technical Characteristics	Non-accel sensitive drift = 1.7×10^{-6} rad/sec for 2 mo 3-axis 3 SDF 2564 gyros with necessary electronics for rate and attitude sensing
1.2.0 Power	25 W max at 46°C 50 W max at 4°C 135 W max during warmup
1.3.0 Weight	10 kg (22 lb)
1.4.0 Volume	0.009 m^3 (545 $in.^3$)
1.5.0 Vibration Specification	Random: performance 7.68 g rms Survival 18.5 g rms
1.6.0 Temperature Specification (radiation and conduction)	Baseplate 4°C to 49°C
1.7.0 Ambient Pressure Specification	1.333×10^{-6} N/m^2 (10^{-8} Torr)

Table 6-8. Attitude Control System Component Data (Inertial Reference Assembly) (Continued)

2.0.0 SAFETY AND HAZARDS	Inertial Reference Assembly LMSC's ARA CCA No. 3006
2.1.0 Failure Rate	40×10^{-6}/hr
2.1.1 Number of Single Point Failures 2.1.2 Number of Double Point Failures	NA[a]
2.2.0 Failure Detection Probability	0
2.3.0 False Alarm Probability	0
2.4.0 Destructive Potential (TNT equivalence)	0

[a]NA = not available

Table 6-9. Attitude Control System Component Data (Fixed Head Star Trackers)

1.0.0 PERFORMANCE	Fixed Head Star Trackers (head + electronics)		
	OAO Boresighted Star Tracker ITT	ITT OAO Electro-Optical Sensing Head	TRW Solid State Star Field Scanner Pioneer F/G
1.1.0 Technical Characteristics	Accuracy: 22.6×10^{-6} rad (3σ) M = +4 Electronics scanning $1° \times 1°$ FOV 2-axis analog outputs	Accuracy: 131×10^{-6} rad (3σ) M = +2.5 Electronic scanning $1° \times 1°$ FOV 2-axis analog outputs	Accuracy: 0.009 rad (3σ) Canopus FOV $0.5° \times 40°$
1.2.0 Power	7.7 W	4.5 W	0.5 W
1.3.0 Weight	10.4 kg (23 lb)	2.7 kg (6 lb)	1.1 kg (2.5 lb)
1.4.0 Volume	0.013 m^3 (795 $in.^3$)	0.0025 m^3 (155 $in.^3$)	0.0027 m^3 (166 $in.^3$) + sunshade
1.5.0 Vibration Specification	NA[a]	NA[a]	NA[a]
1.6.0 Temperature Specification (radiation and conduction)	NA[a]	NA[a]	NA[a]
1.7.0 Ambient Pressure Specification	NA[a]	NA[a]	NA[a]

[a]NA = not available

Table 6-9. Attitude Control System Component Data (Fixed Head Star Trackers) (Continued)

2.0.0 SAFETY AND HAZARDS	Fixed Head Star Trackers (head + electronics)		
	OAO Boresighted Star Tracker ITT	ITT-OAO Electro-Optical Sensing Head	TRW Solid State Star Field Sensor Pioneer F/G
2.1.0 Failure Rate	NA[a]	NA[a]	0.76×10^{-6}/hr
2.1.1 Number of Single Point Failures 2.1.2 Number of Double Point Failures	NA[a]	NA[a]	NA[a]
2.2.0 Failure Detection Probability	0	0	0
2.3.0 False Alarm Probability	0	0	0
2.4.0 Destructive Potential (TNT equivalence)	0	0	0

[a]NA = not available

Table 6-10. Attitude Control System Component Data (Earth Sensor Assemblies)

1.0.0 PERFORMANCE	Earth Sensor Assemblies (including electronics)		
	TRW FLTSATCOM	Barnes Model 13-210	Barnes Model 13-181X
1.1.0 Technical Characteristics	Accuracy 0.87×10^{-3} rad (3σ) 2-axis sweep through	Accuracy 1.75×10^{-3} rad (3σ) Horizon crossing indicator (spinning) 1-axis	Accuracy 0.026 to 0.035 rad (3σ) Radiation balance 1-axis
1.2.0 Power	5 W (av)	1.35 W (av)	0.5 W (av)
1.3.0 Weight	2.7 kg (5.9 lb)	0.91 kg (2.0 lb)	1.4 kg (3.0 lb)
1.4.0 Volume	0.005 m^3 (322 $in.^3$)	0.0018 m^3 (110 $in.^3$)	0.0017 m^3 (104 $in.^3$)
1.5.0 Vibration Specification	NA[a]	25 g rms random (survival)	NA[a]
1.6.0 Temperature Specification (radiation and conduction)	-18°C to + 54°C (design goal)	-20°C to + 60°C	-20°C to + 60°C
1.7.0 Ambient Pressure Specification	NA[a]	6.7×10^{-3} N/m^2 (5×10^{-5} Torr)	1.333×10^{-3} N/m^2 (10^{-5} Torr)

[a]NA = not available

Table 6-10. Attitude Control System Component Data (Earth Sensor Assemblies) (Continued)

2.0.0 SAFETY AND HAZARDS	Earth Sensor Assemblies (including electronics)		
	TRW FLTSATCOM	Barnes Model 13-210	Barnes Model 13-181X
2.1.0 Failure Rate	10.1×10^{-6}/hr	1.1×10^{-6}/hr	3.5×10^{-6}/hr
2.1.1 Number of Single Point Failures 2.1.2 Number of Double Point Failures	NA[a]	NA[a]	NA[a]
2.2.0 Failure Detection Probability	0	0	0
2.3.0 False Alarm Probability	0	0	0
2.4.0 Destructive Potential (TNT equivalence)	0	0	0

[a]NA = not available

Table 6-11. Attitude Control System Component Data (Interface Electronics)

1.0.0 PERFORMANCE	Interface Electronics MSFC Estimate for LST Mission
1.1.0 Technical Characteristics	Switches various sensors and actuators on line as required. Provides fault detection and isolation. Provides command implementation. Provides backup circuitry.
1.2.0 Power	3 W (av)
1.3.0 Weight	4.5 kg (10.0 lb)
1.4.0 Volume	0.0084 m^3 (514 $in.^3$)
1.5.0 Vibration Specification	NA[a]
1.6.0 Temperature Specification (radiation and conduction)	NA[a]
1.7.0 Ambient Pressure Specification	NA[a]

[a]NA = not available

Table 6-11. Attitude Control System Component Data (Interface Electronics) (Continued)

	Interface Electronics
2.0.0 SAFETY AND HAZARDS	MSFC Estimate for LST Mission
2.1.0 Failure Rate	1.0×10^{-6}/hr
2.1.1 Number of Single Point Failures 2.1.2 Number of Double Point Failures	NA[a]
2.2.0 Failure Detection Probability	0
2.3.0 False Alarm Probability	0
2.4.0 Destructive Potential (TNT equivalence)	0

[a]NA = not available

Table 6-12. Attitude Control System Component Data (Reaction Control Subsystem Electronics)

1.0.0 PERFORMANCE	Reaction Control Subsystem Electronics
	MSFC Estimate for LST Mission
1.1.0 Technical Characteristics	Drives solenoids of reaction control jets.
1.2.0 Power	Average power is negligible.
1.3.0 Weight	2.7 kg (6.0 lb)
1.4.0 Volume	0.0054 m^3 (328 $in.^3$)
1.5.0 Vibration Specification	NA[a]
1.6.0 Temperature Specification (radiation and conduction)	NA[a]
1.7.0 Ambient Pressure Specification	NA[a]

[a]NA = not available

Table 6-12. Attitude Control System Component Data (Reaction Control Subsystem Electronics) (Continued)

2.0.0 SAFETY AND HAZARDS	Reaction Control Subsystem Electronics
	MSFC Estimate for LST Mission
2.1.0 Failure Rate	0.01×10^{-6}/hr
2.1.1 Number of Single Point Failures 2.1.2 Number of Double Point Failures	NA[a]
2.2.0 Failure Detection Probability	0
2.3.0 False Alarm Probability	0
2.4.0 Destructive Potential (TNT equivalence)	0

[a]NA = not available

Table 6-13. Attitude Control System Component Data (Reaction Control Jet Thrust Levels)

1.0.0 PERFORMANCE	Reaction Control Jet Thrust Levels
	Agena Thrusters[a]
1.1.0 Technical Characteristics	Selectable at 2.224 N (0.5 lb) or 44.48 N (10.0 lb) by dual press. reg
1.2.0 Type	Monopropellant cold gas (N_2)
1.3.0 ISP	590 N - sec/kg (60 lb_f - sec/lb_m)

[a] Typical of thrusters suitable for spectrum of NASA Payload Missions

7. POWER CONDITIONING SUBSYSTEM

A. INTRODUCTION

A generalized guideline for the development of a power conditioning subsystem for the attitude control system (ACS) is presented in this section. A power conditioning subsystem is defined as the functional blocks that receive raw spacecraft power, and convert and condition it to a usable form. The subsystem does not include energy conversion devices such as batteries and solar arrays. Conversion and conditioning would involve DC/DC or DC/AC conversion and would include voltage regulation. The terms "power system" and "power supply" are used interchangeably with "power conditioning subsystem."

This guideline is general; it is intended as a system view of functional blocks to identify the basic concept. From this generalized system viewpoint, where the detailed circuit design is left to the circuit designer, it examines the following:

1. Development of a generalized expression for overall efficiency as a function of power supply efficiency, coupling networks, and cabling resistances
2. Effects of transfer losses on regulation
3. Weight and volume estimation.

B. POWER SYSTEM DESIGN GUIDELINES

A representative power system, as shown in Figure 7-1, considered the following characteristics as a minimum:

1. Voltage outputs
2. Efficiency
3. Average or peak power
4. Weight
5. Volume
6. Regulation.

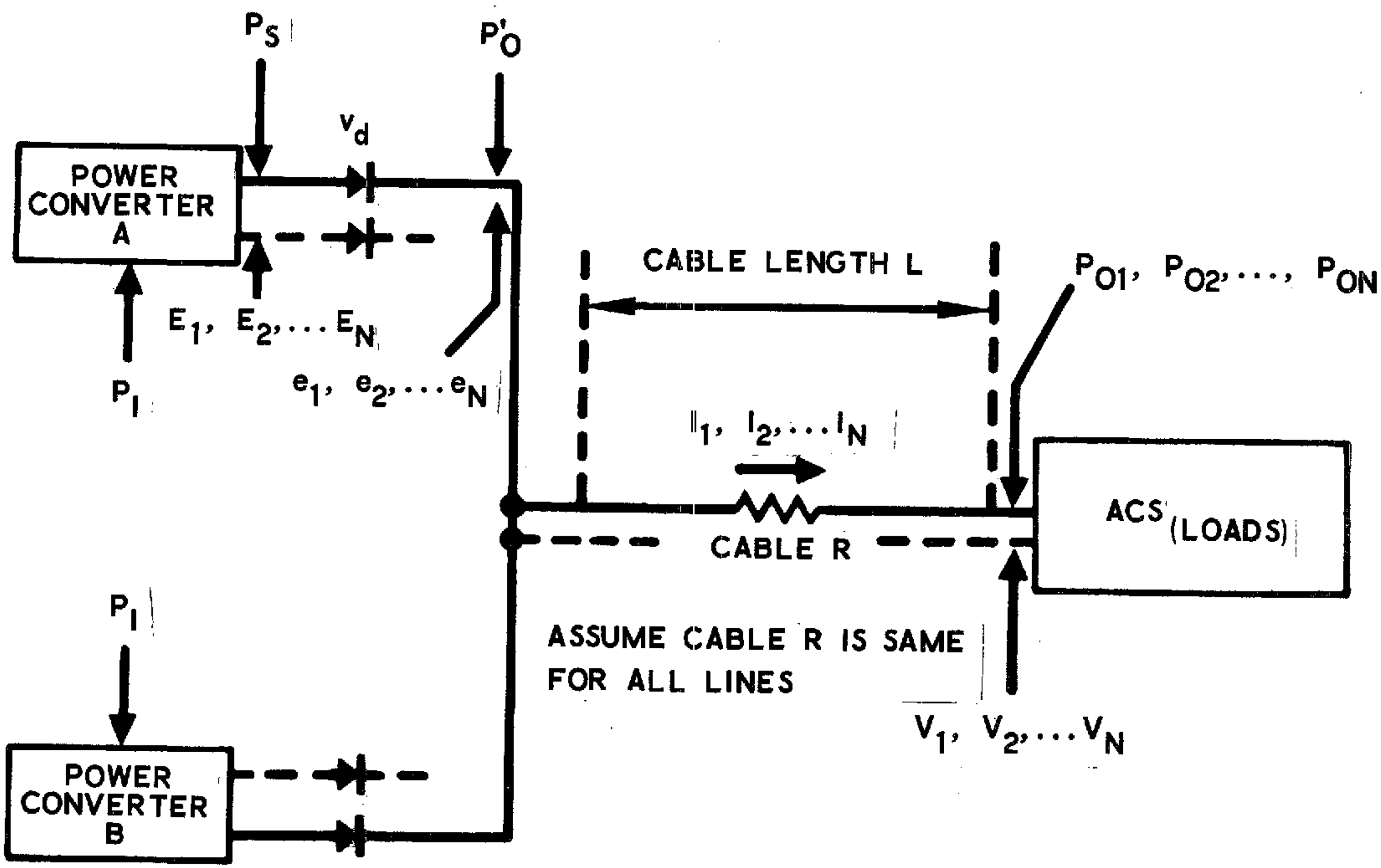

Figure 7-1. Power System

For design optimization, design guidelines considered tradeoffs between such factors as desired efficiencies, power requirements, weight, and volume. The first step in defining an approach for the ACS power supply system is to consider efficiency, and then to relate power requirements with weight and volume. This is in view of the overall system perspective where source, power conditioning, and load requirements are considered simultaneously.

1. EFFICIENCY

Power system efficiency depends on the following factors:

a. Efficiency of power converter

b. Efficiency of redundancy coupling networks

c. Losses in cabling.

Referring to Figure 7-1, the following terms are defined:

$V_1, V_2, \ldots V_N$ = voltages at ACS

$E_1, E_2, \ldots E_N$ = output voltages at power converter

$e_1, e_2, \ldots e_N$ = output voltages at diode summing point

$I_1, I_2, \ldots I_N$ = current outputs

$P_{O1}, P_{O2}, \ldots P_{ON}$ = powers at the ACS loads

P_O' = power output at diode summing point

P_I = power input to power converters

P_S = power output of power converters

$m_1, m_2, \ldots m_N$ = cable voltage drops

R = cable resistance

v_d = diode voltage drop

The overall system efficiency η_t is given by

$$\eta_t = P_O / P_I$$

where

$$P_O = \sum_{i=1}^{N} P_{Oi}$$

The overall efficiency may be expressed as the product of the previously mentioned factors

$$\eta_t = \eta_1 \eta_2 \eta_3$$

where

η_1 = power converter efficiency
η_2 = redundancy coupling network efficiency
η_3 = efficiency of power transfer through cabling

$$\eta_1 = P_S / P_I$$

$$\eta_2 = P'_O / P_S$$

The efficiency of power transfer is

efficiency = 1 - (summation of series losses)/(input power)

Writing η_2 in this form,

$$\eta_2 = 1 - \left[\sum_{i=1}^{N} (v_d I_i) \right] / P_S$$

Assuming v_d is constant for all diodes in the coupling network,

$$\eta_2 = 1 - v_d \left(\sum_{i=1}^{N} I_i \right) / P_S$$

But

$$P_S = \sum_{i=1}^{N} E_i \, I_i$$

and

$$\sum_{i=1}^{N} E_i \, I_i = \sum_{i=1}^{N} (V_i + v_d + m_i) \, I_i$$

$$= \sum_{i=1}^{N} P_{Oi} + \sum_{i=1}^{N} (v_d + m_i) \, I_i$$

giving

$$\eta_2 = 1 - v_d \left(\sum_{i=1}^{N} I_i \right) / \left[\sum_{i=1}^{N} P_{Oi} + \sum_{i=1}^{N} (v_d + m_i) \, I_i \right]$$

Similarly for η_3

$$\eta_3 = P_O / P'_O$$

$$\eta_3 = 1 - \left(\sum_{i=1}^{N} I_i^2 R \right) / P'_O = 1 - \left[\sum_{i=1}^{N} \left(m_i^2 / R \right) \right] / P'_O$$

Assuming the cable resistance is constant for all lines,

$$\eta_3 = 1 - \frac{1}{R}\left(\sum_{i=1}^{N} m_i^2\right)/P'_O$$

$$P'_O = \sum_{i=1}^{N} e_i I_i$$

$$\sum_{i=1}^{N} e_i I_i = \sum_{i=1}^{N} (V_i + m_i) I_i = \sum_{i=1}^{N} P_{Oi} + \sum_{i=1}^{N} m_i I_i$$

$$\eta_3 = 1 - \frac{1}{R}\left(\sum_{i=1}^{N} m_i^2\right)/\left[\sum_{i=1}^{N} P_{Oi} + \sum_{i=1}^{N} m_i I_i\right]$$

The final expression for η_t then is

$$\eta_t = \eta_1 \left[1 - \frac{v_d \sum_{i=1}^{N} I_i}{\sum_{i=1}^{N} P_{Oi} + \sum_{i=1}^{N} (v_d + m_i) I_i}\right]\left[1 - \frac{\sum_{i=1}^{N} m_i^2}{R\left(\sum_{i=1}^{N} P_{Oi} + \sum_{i=1}^{N} m_i I_i\right)}\right]$$

2. REGULATION

Since a typical system contains digital and/or analog circuits using the same power supply voltage, it becomes apparent that any current fluctuations on any line will produce voltage fluctuations that are coupled to all the circuits. These voltage fluctuations, which represent reduced regulation, are dependent upon the common line impedance through which the load currents flow. Thus,

$$\text{Reg}_L = \Delta V/V = R\Delta I/V = \rho L \Delta I/AV \qquad (7\text{-}1)$$

where Reg_L = regulation resulting from line impedance R for a load change ΔI.

This would be added to the regulation of the power supply. Since certain networks may require tightly regulated voltages (sensors, for example), it would be wise to investigate the regulation on those lines, and ensure, by proper cable design, that line resistance does not degrade the regulation to a point that would be detrimental to the operation of those circuits. In addition, the changes in current drawn by a particular circuit not only produce voltage fluctuations on the distribution line, but, because of the complex impedance of the power supply bus, also produce transient voltages. In systems that experience rapid changes in load current, the transients produced are much more significant than the simple resistive (IR) drop. A transient analysis would evaluate the effects of these voltage transients, and would be part of the detailed design effort when the hardware orientation is established. These analyses would, in effect, be part of the electromagnetic interference (EMI) considerations normally investigated during spacecraft system design.

The overall regulation of the power system would depend on the design requirements of the loads. As implied above, however, since the overall regulation would include the regulation of the power supply itself (converter and regulator), as well as the effects of cabling resistances, the power supply regulation must be considered in light of the overall requirements. In other words,

$$Syst_{reg} \approx PS_{reg} + Cb_{reg} \tag{7-2}$$

or,

$$PS_{reg} \approx Syst_{reg} - Cb_{reg} \tag{7-3}$$

where

PS_{reg} = regulation of the power supply

$Syst_{reg}$ = overall system regulation

Cb_{reg} = regulation due to cable resistance effects

Cb_{reg} is the regulation described by Eq. (7-1).

Table 7-1, from Ref. 1, shows general performance of various types of regulators, and illustrates relative characteristics of ripple, noise, reliability, etc.

3. WEIGHT AND VOLUME

The rapidly increasing use of microelectronic circuits in the design of regulators and of DC/DC converters and inverters contributes to the reduction of power supply weight and volume. The use of higher frequencies, providing that resultant EMI characteristics are kept within acceptable limits, allows the use of smaller components (filters, transformers, etc.). Limitations also exist for the use of ICs, such as power-handling abilities, and the inability to microminiaturize power transistors and transformers. Other factors subject to compromise or tradeoff include

a. AC or DC output
b. Types of oscillators
c. Oscillator frequency
d. Heat sinking
e. Regulation
f. Efficiency.

Generalized graphs resulting from studies of typical power supply parameter data can be used as a tool for estimating weight and volume versus load capabilities. These graphs represent typical supplies designed in the past and empirical data collected by various agencies. The curves, from Ref. 2, reflect the effects of load capabilities, regulation, and efficiency on the parameters mentioned above, and ultimately on weight and volume.

Table 7-1. General Performance of Regulators[a]

Type	Pulse Width	Boost	Phase	Buck Boost	Series
Efficiency (%)					
V in: 20	96	93	88	90	97
V in: 32	92	96	86	89	60
Regulation (%)	±1/2	±1/2	±1/2	±1/2	±0.1
Output Voltage	20 max	31 min	Any	Any	19 max
Common Grounds	Yes	Yes	Isolation	Isolation	Yes
Output Impedance (mΩ)	20	20	Varies with f to 50	20	1
Ripple (mV)	100	150	100	150	1
Induced Noise	High	Low or high	High	Very High	Min
Audio Susceptibility	200:1	20:1 200:1	20:1	100:1	400:1
Cost	High	High	Medium[b]	Highest	Lowest
Outputs	1	1	Many	Many	1
Reliability	Good	Good	Good	Good	Best
Weight (kg)	0.91	0.91	1.1	1.1	0.45[c]
Output	DC	DC	AC or DC	DC	DC

[a] Assume input voltages of 20 to 32 V.

[b] Depends on frequency response.

[c] Depends on heat sink.

They are reproduced as Figures 7-2 through 7-8. Figure 7-9 shows typical effects of operating frequency on transformer weight.

Table 7-2, also from Ref. 2, summarizes the data of Figures 7-2 and 7-3 in two categories: medium power (150 W to 1 kW) and low power (less than 150 W).

Figure 7-10, from Ref. 3, shows a curve relating weight per power to power output of a typical power conditioner. This curve covers power outputs from about 3 to several thousand W; it was developed from analytical data, vendor data, and data from existing hardware by a study conducted in 1971. This curve essentially agrees with Figure 7-3, but covers a wider power range.

C. SUMMARY

A discussion of the basic power conditioning system concept has been presented to familiarize the reader with three basic parameters (from an overall system viewpoint):

1. Efficiency
2. Regulation
3. Weight and volume estimation (versus power and efficiency requirements).

An attempt was made to relate these parameters to external considerations, i.e., cabling and coupling network losses. The basic converter/regulator was presented as a functional block with a given efficiency, and the overall (converter/coupling/cabling) efficiency was given as a function of transfer losses (DC series losses).

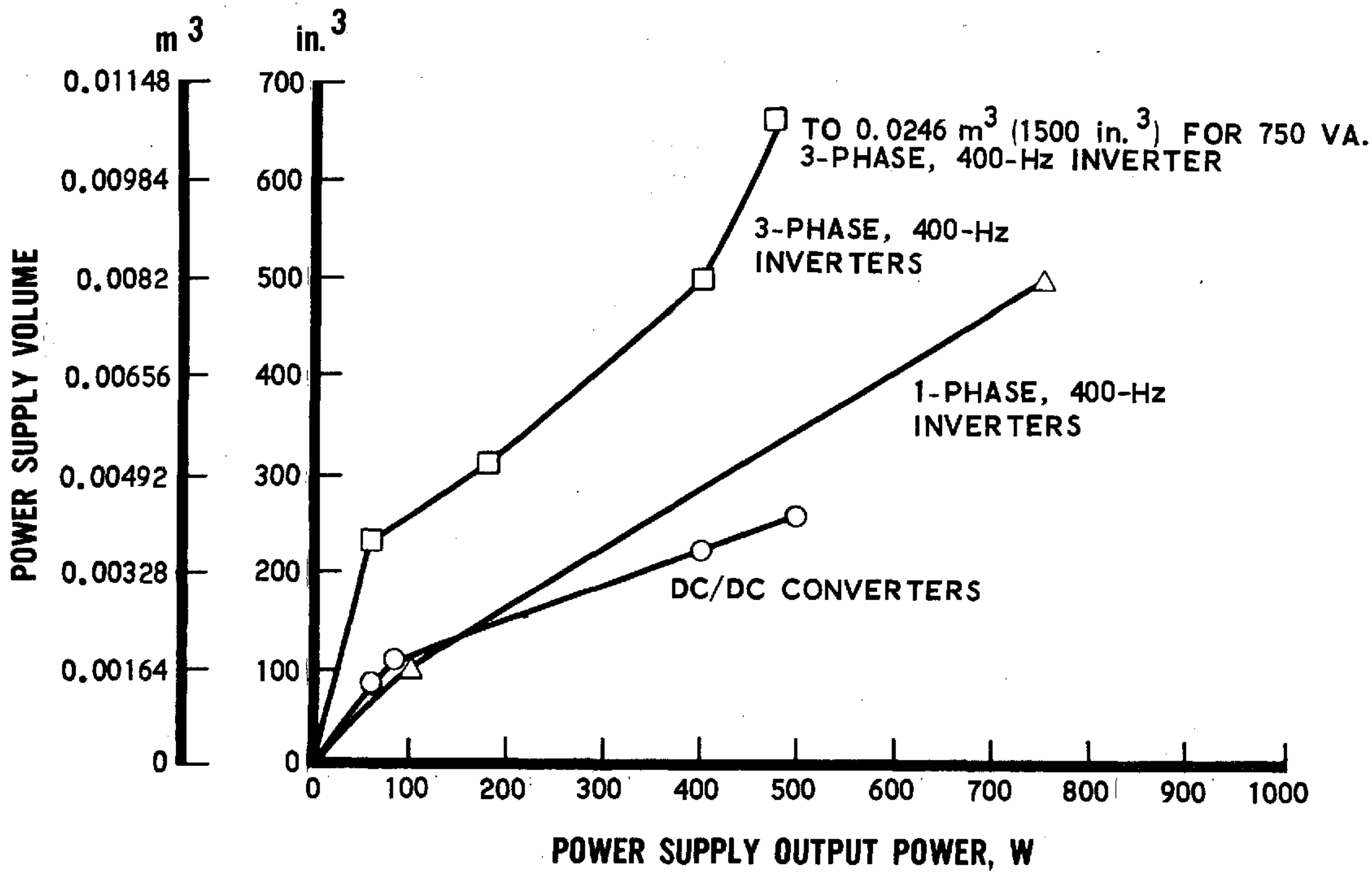

Figure 7-2. Power Supply Volume vs Power Supply Output Power

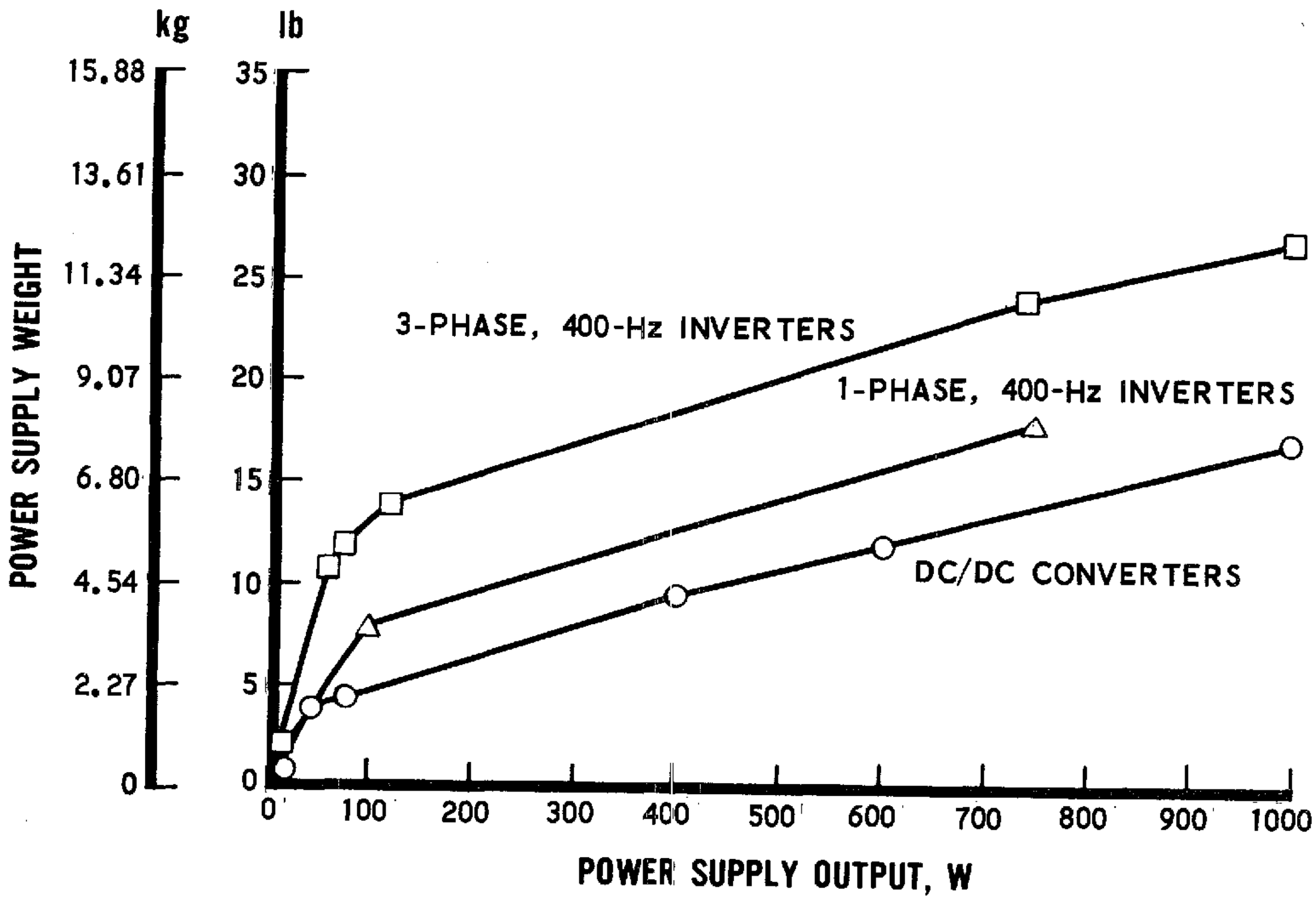

Figure 7-3. Power Supply Weight vs Power Supply Output Power

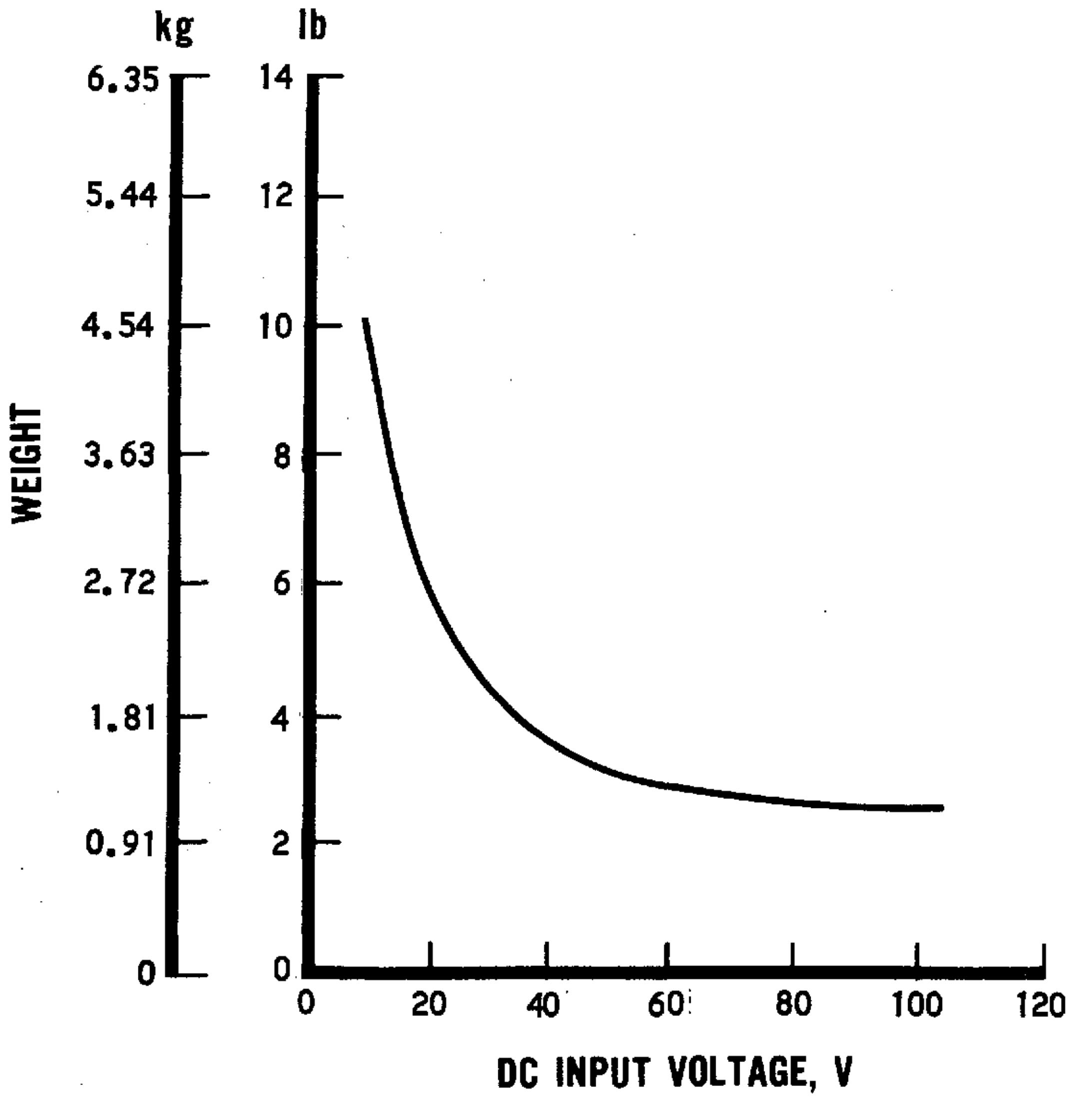

Figure 7-4. Weight vs Input Voltage for Typical 70-W DC/DC Converter

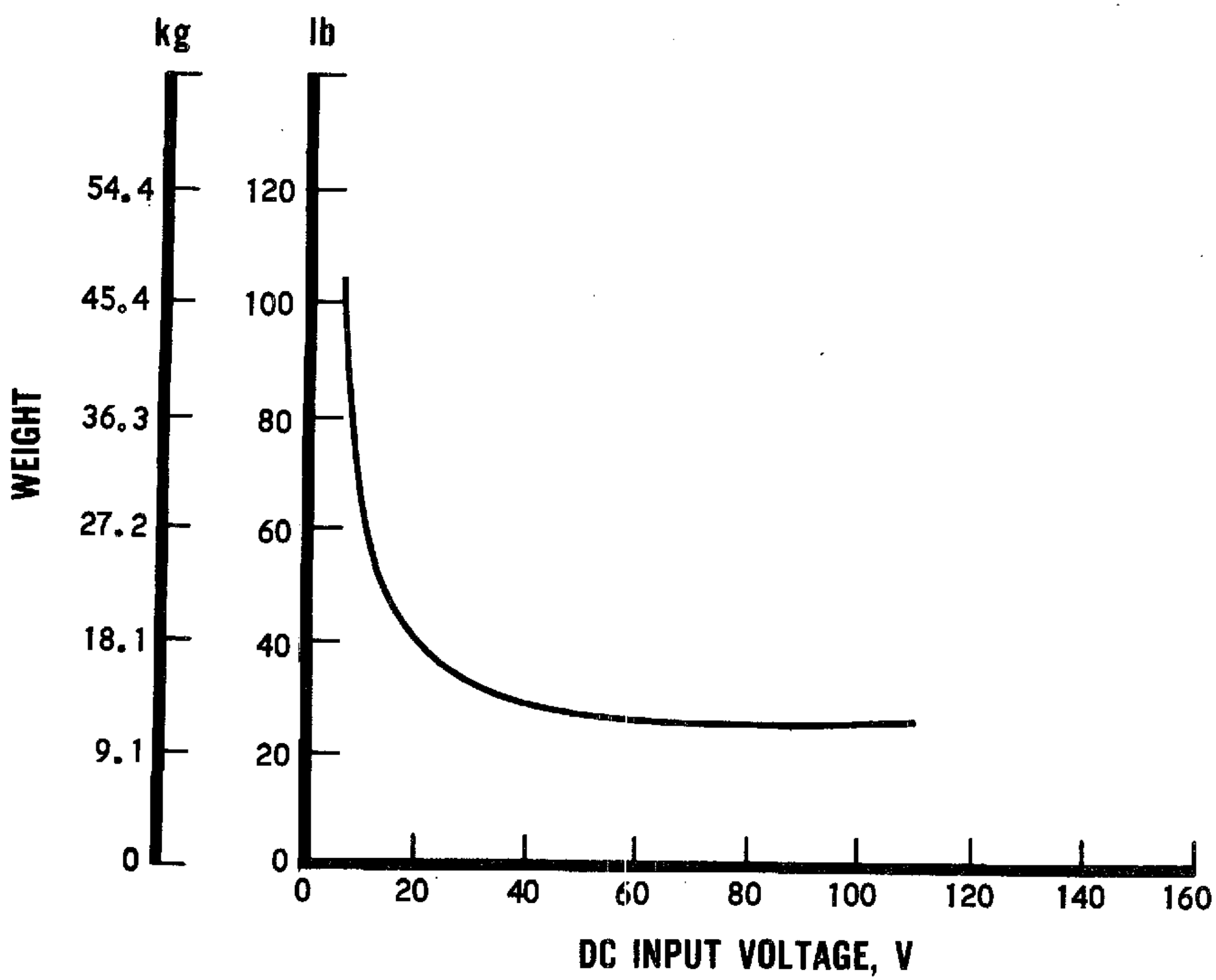

Figure 7-5. Weight vs Design Input Voltage for a 400-Hz, 3-Phase, 115-V, 1.25 KVA Static Inverter

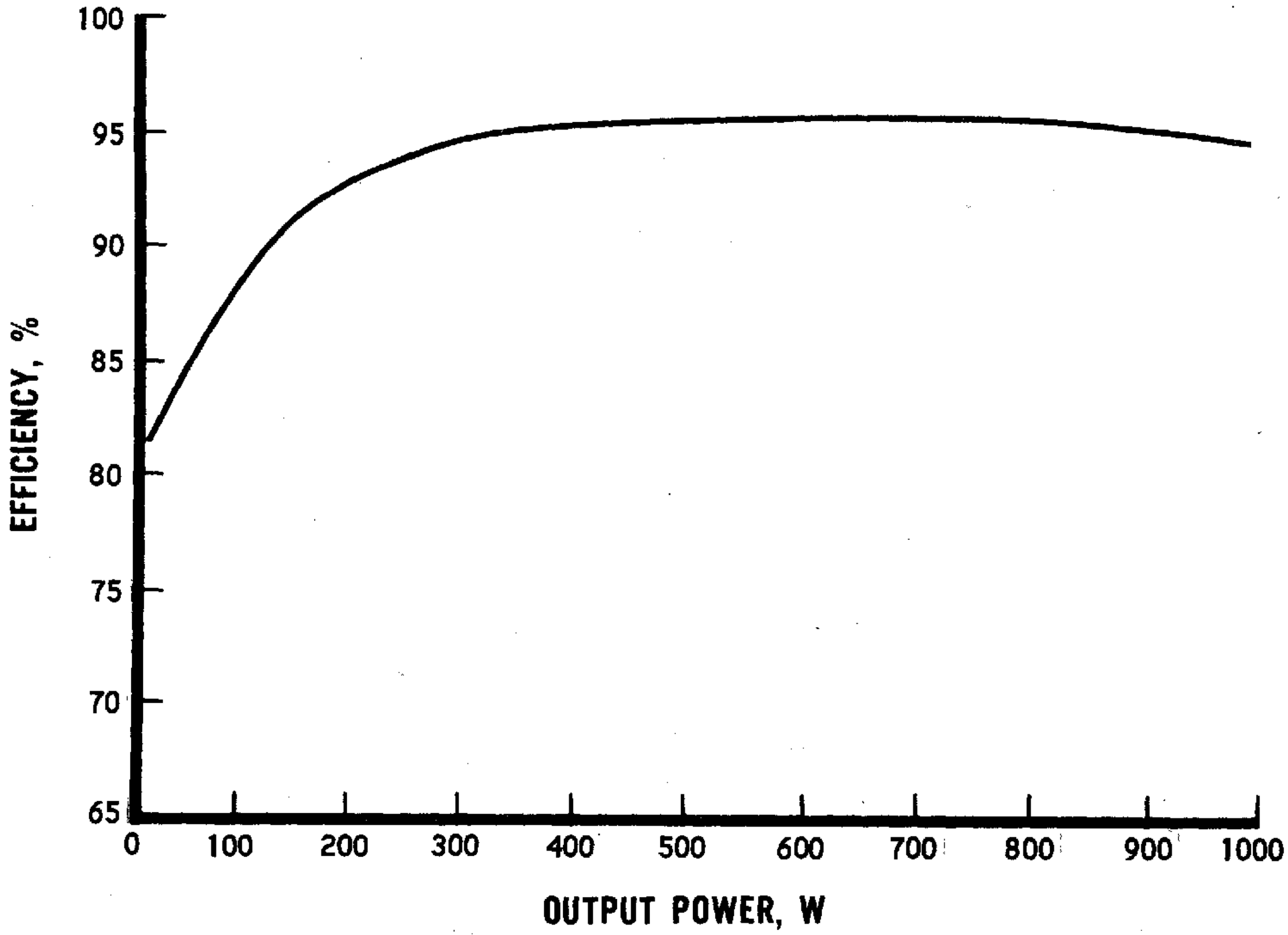

Figure 7-6. Typical DC Voltage Regulator Efficiency vs Output Power

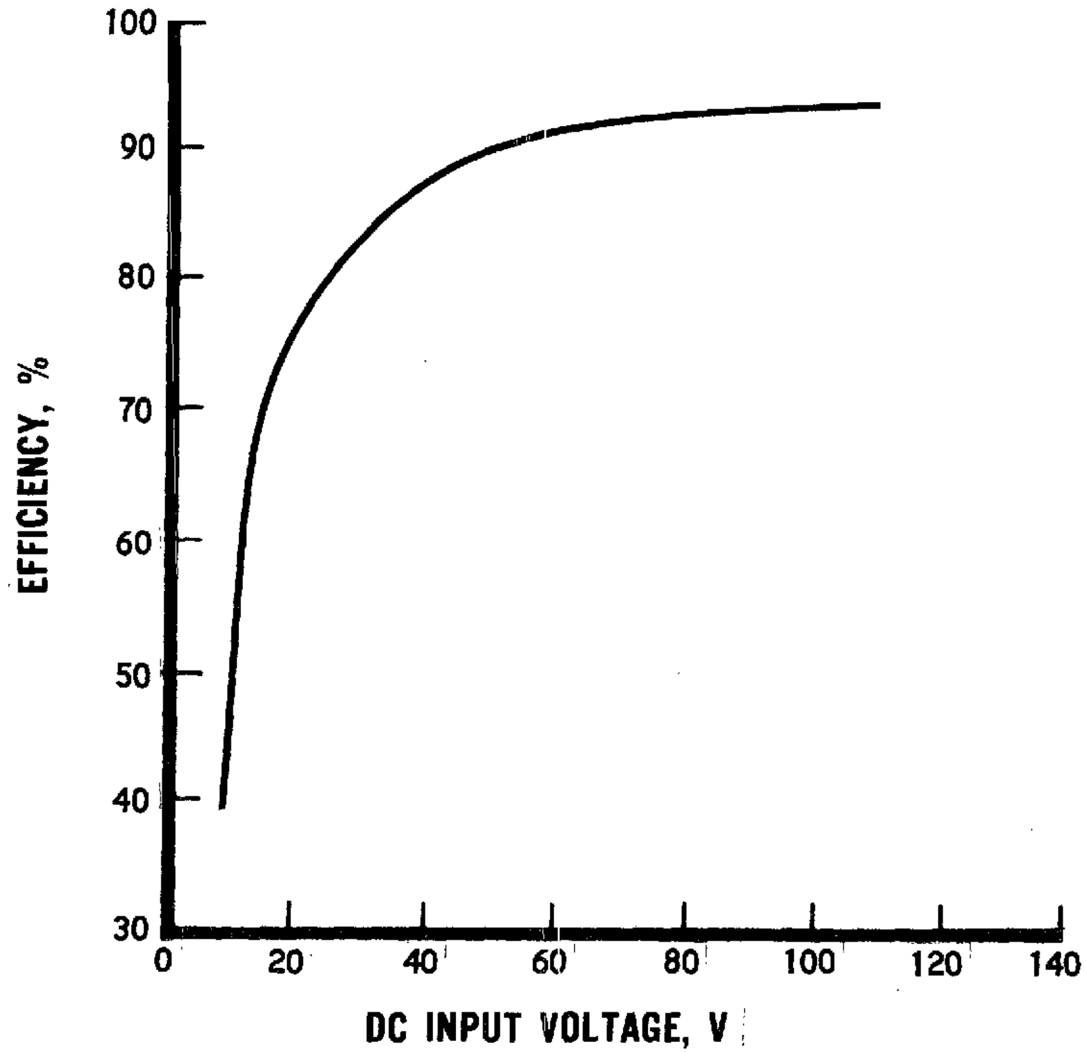

Figure 7-7. Efficiency vs Input Voltage for a Typical 70-W DC/DC Converter

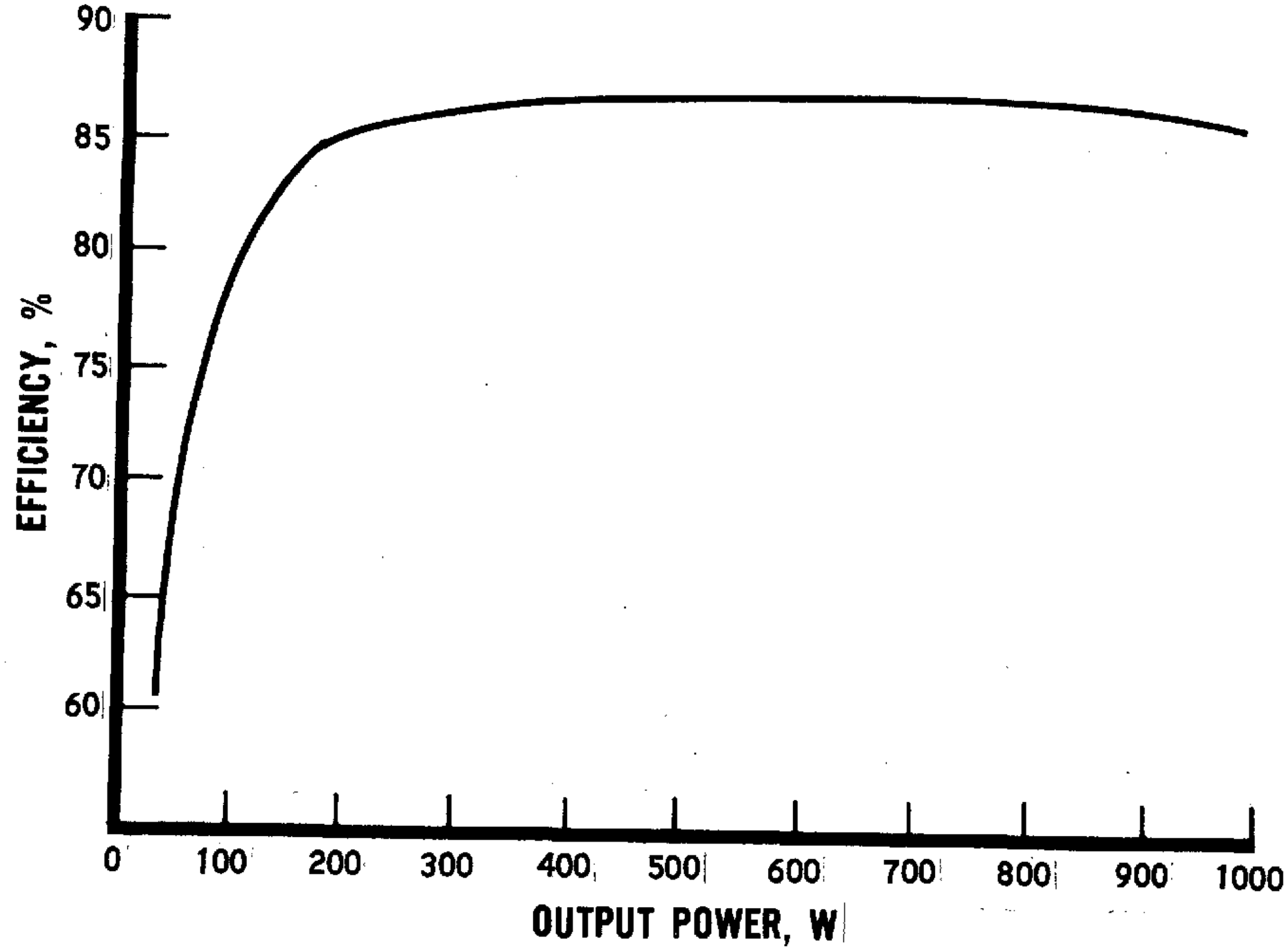

Figure 7-8. Typical 3-Phase, 400-Hz Inverter Efficiency vs Output Power

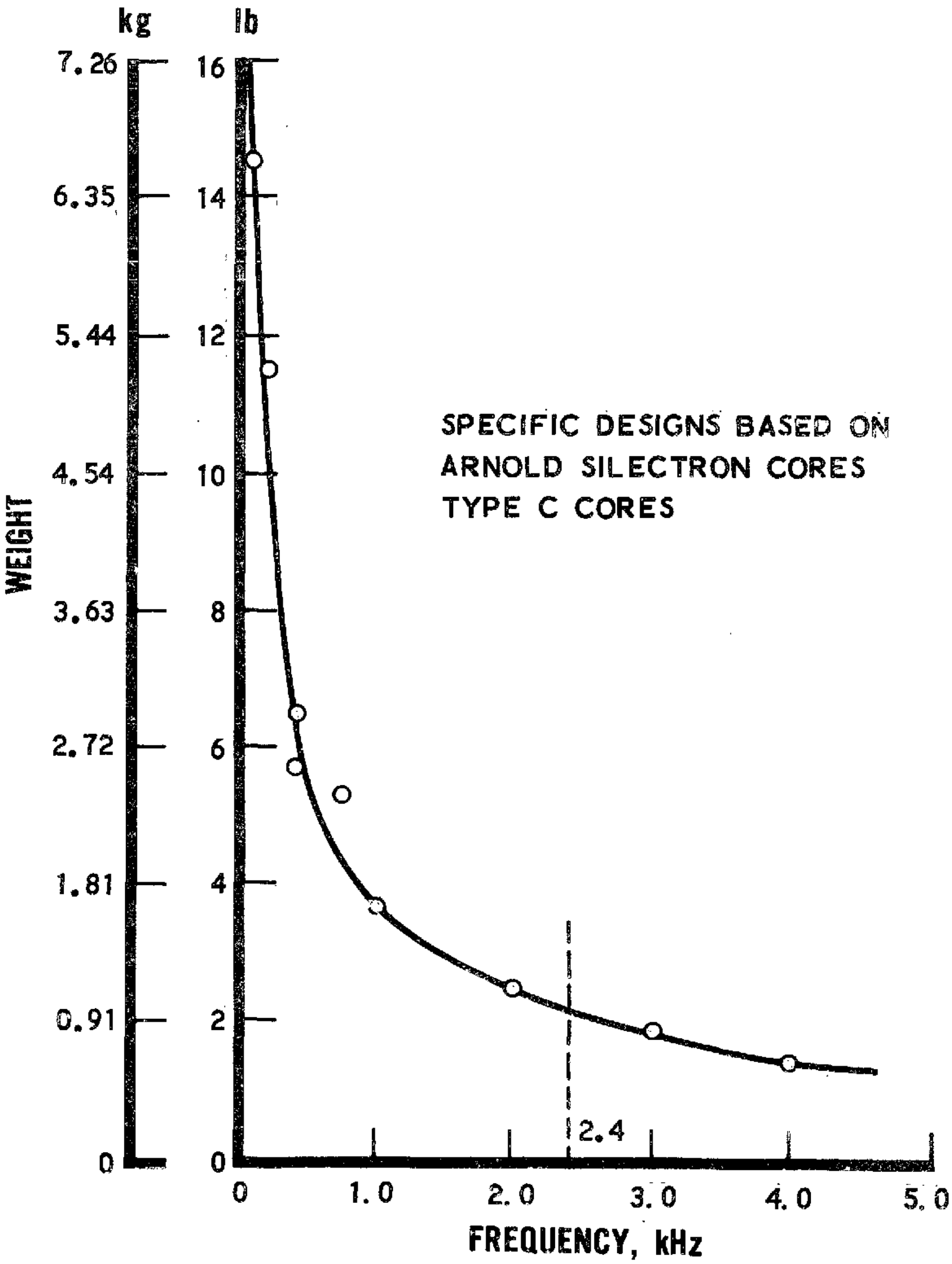

Figure 7-9. Transformer Weight (200-W Output, 97% Efficiency) vs Operating Frequency

Table 7-2. Power/Weight and Power/Volume Data Summarization

Component	Medium Power (150 W to 1 kW)		Low Power (<150 W)	
	W/kg (W/lb)	W/m^3 ($W/in.^3$)	W/kg (W/lb)	W/m^3 ($W/in.^3$)
DC/DC Converter Regulators	99.2 (45)	1.2×10^5 (2)	22 (10)	4.9×10^4 (0.8)
1-Phase, 400-Hz Inverters	91.7 (41.6)	7.6×10^4 (1.25)	17 (7.7)	6.1×10^4 (1)
3-Phase, 400-Hz Inverters	68.3 (~31)	3.6×10^4 (~0.6)	12.1 (5.5)	1.5×10^4 (0.25)

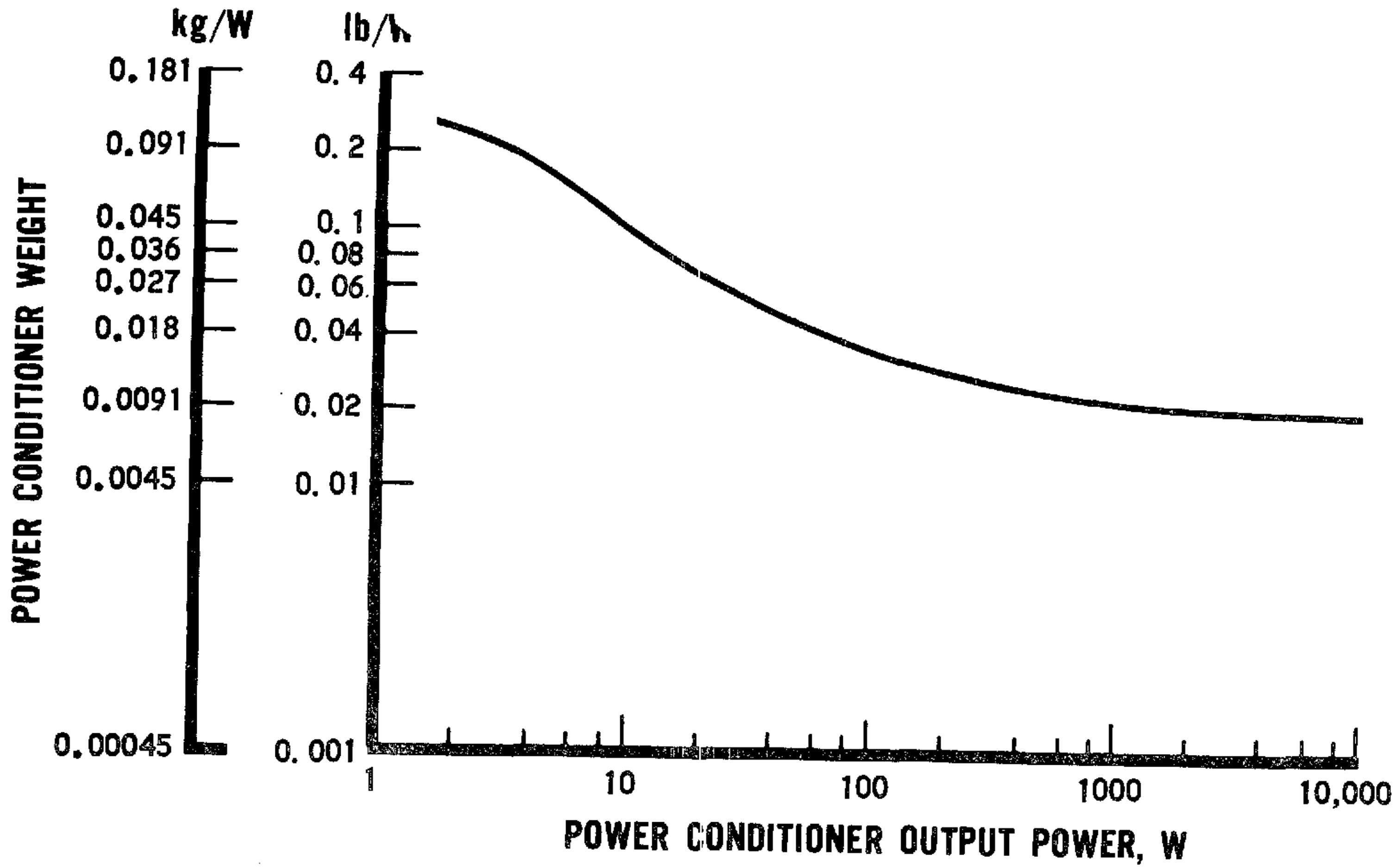

Figure 7-10. Power Conditioner Weight Curve

REFERENCES

1. J. W. Bates, "Power Conditioning System Design," WESCON 1965 Technical Papers, Part III.

2. E. R. Hnatek, Design of Solid-State Power Supplies, (Van Nostrand-Reinhold Co., 1971).

3. W. B. Collins and D. R. Newell, "Power Conditioning Requirements and Trade-Off Considerations for the Space Shuttle," IEEE Power Conditioning Specialists Conference, 1971.

8. THERMAL CONTROL SUBSYSTEM

A. INTRODUCTION

As part of NASA Task 2.3, a number of separate but related studies were undertaken to define system and component characteristics for use in synthesizing analytical models to derive system cost. As part of a general framework, this subtask provides the thermal considerations that influence the design, synthesis, and eventual cost of a spaceborne guidance, navigation, and control (GNC) subsystem. Specifically, this subtask identifies the thermal "drivers," or parameters, that influence the design and operation of typical GNC components, and discusses the rationale for using various thermal margins.

To define the key thermal drivers, one must understand the following concepts:

1. Basic thermal control subsystem (TCS) design philosophy, which includes thermal design margins (e.g., design temperature margins and heater power margins)
2. TCS design logic from the standpoint of the spacecraft contractor integrating the various payloads and vehicle subsystems, such as GNC; telemetry, tracking, and command (TTC); and power
3. Logic or procedure for specifying temperature requirements from the subsystem level.

B. DESIGN PHILOSOPHY

The purpose of the spacecraft TCS is to provide a relatively benign environment for the proper functioning of the other subsystems. Failure of the TCS often produces synergistic results: a loss of the TCS may result in the failure of other subsystems.

A study of failures/anomalies occurring on selected Air Force programs (Ref. 1) was conducted to identify common underlying causes and to determine corrective actions. The failures/anomalies included such items as overheating of components, thermal runaway of batteries, and inaccuracies in temperature predictions due to improper analysis and simulation. The study showed that 11.6% of the failures/anomalies were directly attributable to thermal design. It also showed that a significant number of failures/ anomalies were due to inadequate thermal design resulting from insufficient thermal margins in the TCS design.

Two factors determine the thermal adequacy of a TCS:

1. Magnitude of temperature margin
2. Fidelity of thermal model used in temperature prediction.

In a thermal analysis, thermal margins must be defined and specified in the design requirements of the system to account for uncertainties in the modeling of the system, errors in the solution methods, and uncertainties in the data used. Based on studies correlating analytical temperature predictions and flight data, the temperature accuracy of an analytical thermal model has been estimated as follows (Ref. 2):

Standard Deviation (σ)	Percent of Confidence	Temperature Accuracy (°C)	
		Unverified Analytical Predictions	Predictions Verified by Testing
1.0	68	8	5.5
1.4	85	12	8
2.0	95	17	11
3.0	99	25	17

Because of the shortcomings of analytical predictions, it is strongly recommended that all spacecraft equipment be designed and tested with a 17°C margin, i.e., all components shall perform satisfactorily 17°C above the maximum predicted temperature and 17°C below the minimum predicted temperature. Obviously, there are always exceptions, in which case a "sensitivity-analysis" or "statistical analysis (Monte Carlo)" shall be performed. These analytical techniques allow the analyst to identify the key parameters that affect a given temperature and therefore, can be used to quantify the magnitude of uncertainty in the analysis to enhance the confidence level in achieving the predicted values.

In an active TCS, where electrical or mechanical devices (e.g., heaters and mechanical refrigerators) are utilized to effect temperature control, the energy to drive these control devices should include a 25% margin. For example, if heaters are utilized to meet the lower temperature limit of a component in an extremely cold environment, the heater should be sized such that only 75% of its rated capacity is being used to maintain temperature control. In the case of a refrigerator, only 75% of the cooling capacity should be required to effect temperature control in an extremely hot environment. The philosophy of the 25% capacity/capability margin should be utilized for all active control devices such as louvers, heat pipes, and fluid loops.

C. DESIGN LOGIC

This section examines the parameters required to define various TCS techniques that have been utilized to provide and maintain temperature control for all kinds of spacecraft; i.e., from a simple passive control system (e.g., Explorer), where only surface coatings and insulation are used to effect temperature control, to the more complex active control systems (e.g., Skylab), where multiple heat transport loops have been utilized to provide and maintain temperatures. Table 8-1 lists some of the TCS techniques used or considered in previous spacecraft design. The names and/or groupings of the various TCS techniques shown were coined in an attempt to categorize TCS into increasing levels of complexity (which would implicitly reflect increasing cost). However, affixing explicit cost correlations is beyond the scope of this subtask.

Two approaches are used to design a subsystem or component TCS. The first approach defines the temperature range for optimum subsystem or component performance. This requirement and the requirements of other subsystems are then specified for the design of the overall spacecraft TCS. The second approach assumes an overall TCS with its implicit temperature

Table 8-1. Spacecraft TCS Techniques

Passive TCS
Coatings
Insulation
Modified Passive TCS
Heaters
Heat pipe (conductors)
Phase change
Semi-Active TCS
Louvers
Diode
Isothermalizer heat pipe
Active TCS
Radiator loop
Transport loop
Others (special TCS)
Cryogenic coolers
Expendable coolants

limits, and then designs the subsystem or component to operate within these limits.

Figure 8-1 is a typical flow diagram of the logic used to select a TCS. The minimum input requirements for preliminary TCS design include

1. Spacecraft configuration (e. g., a spin-stabilized cylindrical spacecraft or a three-axis stabilized rectangular spacecraft)
2. Orbital data (e. g., sun-synchronous low earth orbit)
3. Preliminary equipment temperature limits based on best available data
4. Preliminary equipment duty cycle (i. e., heat dissipation as a function of time).

Inputs 1 and 2 are used to assess the environmental heat loads. Inputs 3 and 4 are used to define a TCS technique to satisfy the equipment thermal requirements in extremely cold and hot environments.

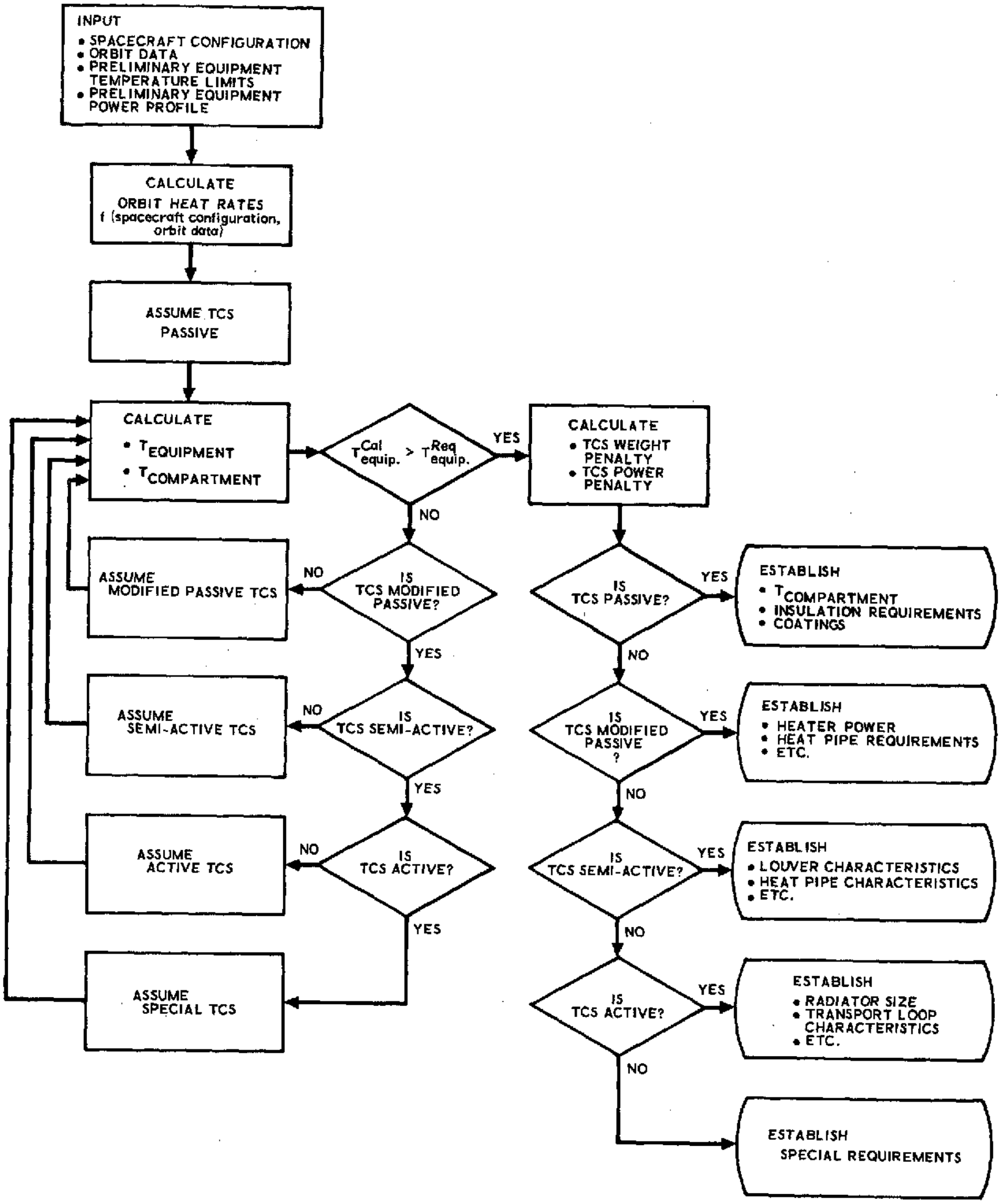

Figure 8-1. Preliminary Spacecraft TCS Configuration

In configuring a preliminary TCS, one generally starts with the simple passive technique, and gradually increases the complexity of the system until every thermal requirement has been satisfied. As TCS complexity increases, more requirements must be defined and established. For example, if a passive TCS adequately meets the spacecraft thermal requirements, the output from Figure 8-1 would be a definition of insulation requirement, thermal costing requirement, and compartment temperatures. However, if a louver is required, the louver requirements must also be defined.

Figure 8-2 shows the logic sometimes used in specifying the design temperature limits for various spacecraft subsystems and components. This approach is utilized to update and/or modify components. For example, in a spacecraft program, where modifications are implemented in block changes, an updated GNC system may be implemented with no change in the TCS. In this example, the updated GNC system must be designed to function in the existing spacecraft TCS environment.

The logic in Figure 8-2 is more usefully applied to perform TCS tradeoff studies on the subsystem level prior to subsystem integration into the spacecraft. The drivers required to perform the subsystem TCS tradeoff studies are presented in Table 8-2. Two types of drivers are identified: spacecraft drivers (i. e., spacecraft-peculiar parameters), and component drivers (i. e., component-peculiar parameters).

After identifying the general TCS drivers in Table 8-2, one can qualitatively specify the drivers for individual components utilized in a given subsystem. Table 8-3 lists the drivers necessary to characterize or specify the thermal requirement of specific components used in a GNC system. For example, the drivers that must be specified to define the thermal characteristic of a rate gyro assembly are duty cycle, thermal capacitance, and temperature limits.

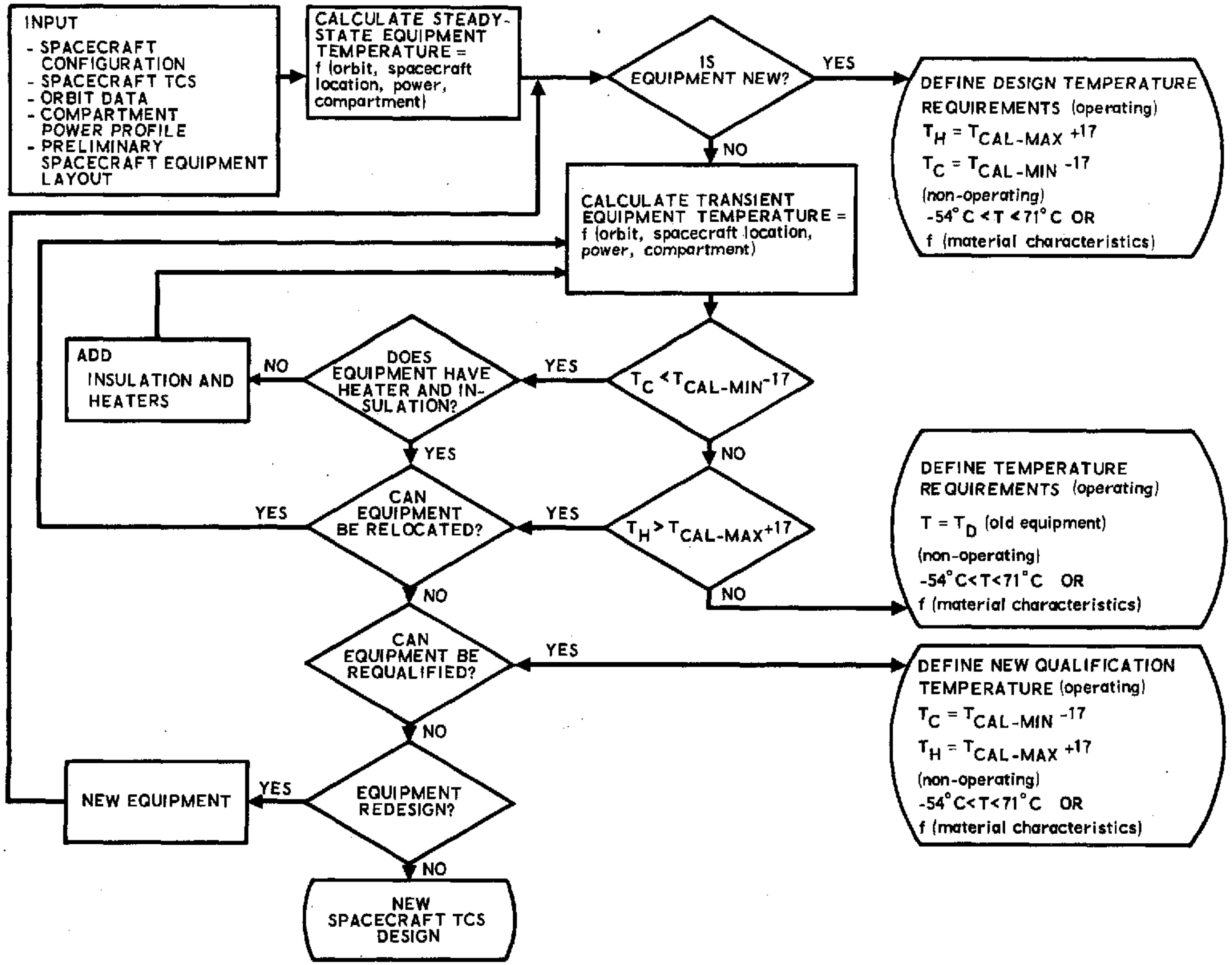

Figure 8-2. Component Design Temperature Requirements

Table 8-2. Drivers Required for Subsystem TCS Tradeoff Studies

Spacecraft Drivers
Location
Defined by subsystem
Integrator's choice
Equipment Interaction
Other subsystems
Other components
Component Drivers
Power Profile (duty cycle)
$f(\theta)$
$f(T)$
Constant
Thermal Capacitance
Weight
Material
General assembly
Heat Transfer Mode
Base conduction
Radiation from housing
$dT/d\theta\|_{max}$
During operation
During warmup/cool-down
Temperatures
Operating limits
Non-operating limits

Table 8-3. GNC Component TCS Drivers[a]

GNC Components	Spacecraft Drivers		Component Drivers				
	Location	Equipment Interaction	Duty Cycle (power level)	Thermal Capacitance	Temperature	dT/dθ	Heat Transfer Mode
Electromagnets					X		
Rate Gyro Assembly			X	X	X		
Computers			X		X		
Reaction Wheels	X				X		
Control Moment Gyro			X	X	X		
Sun Sensors	X				X		
Magnetometers Sensor and Electronics	X		X		X		
Inertial Reference Assembly	X	X	X	X	X	X	X
Star Trackers Head and Electronics	X		X		X		X
Earth Sensor Assembly Electronics	X		X		X		X
Reaction Control Assembly	X	X	X		X		
Electronics							
Jet Thrusters							
Fluids							

[a]X signifies the primary spacecraft and component drivers.

REFERENCES

1. W. C. Williams, Design, Test, and Human/Procedural Working Group Summary Report (U), Aerospace Corporation Report No. TOR-0073(3421-01)-1 (4 December 1972).

2. R. Stark, Thermal Testing of Spacecraft, Aerospace Corporation Report No. TOR-0172(2441-01)-4 (7 September 1971).

C4

C4

9. GROUND SUPPORT EQUIPMENT

A. INTRODUCTION

The ACS-peculiar ground support equipment (GSE) must be analyzed to the same level of detail as the attitude control system (ACS) to determine the total impact of the ACS on the cost and schedule of a program, as well as on the safety and confidence of successfully completing all mission objectives. The final testing of the ACS not only impacts the cost and schedule through design of test hardware production, but also interacts significantly with the safety and performance requirements of the payload.

The GSE and the ACS function together; this functional relationship was studied. As the modeling develops in future phases, the interface requirements between the ACS and the GSE will be quantified by aggregate equations and data items within the model. As a first step, a satellite system was examined to establish the nature of the requirements placed on the GSE by ACS components. These requirements were identified for earth sensors, sun sensors, rate gyros, and reaction wheels. The requirements for these items, based on a sample ACS, are described below to demonstrate the interrelationship between the GSE requirements and to serve as a basis for further effort to quantify these relationships in aggregate equations.

B. ACS TEST SET

The ACS test set provides functional testing of the satellite ACS and monitors the subsystem performance. A typical test set provides simulation of signals from the earth sensor, the sun sensor, and the rate gyro rates to the satellite subsystem; it may also monitor and control the speed of the reaction wheel or other ACS components. The ACS test set may be manually operated or automated. A functional schematic block diagram of a sample ACS test set is shown in Figure 9-1. The ACS test set is required to simulate the performance of the sensors and to introduce these signals into the ACS realistically so that the control can be evaluated and the ACS response can be monitored.

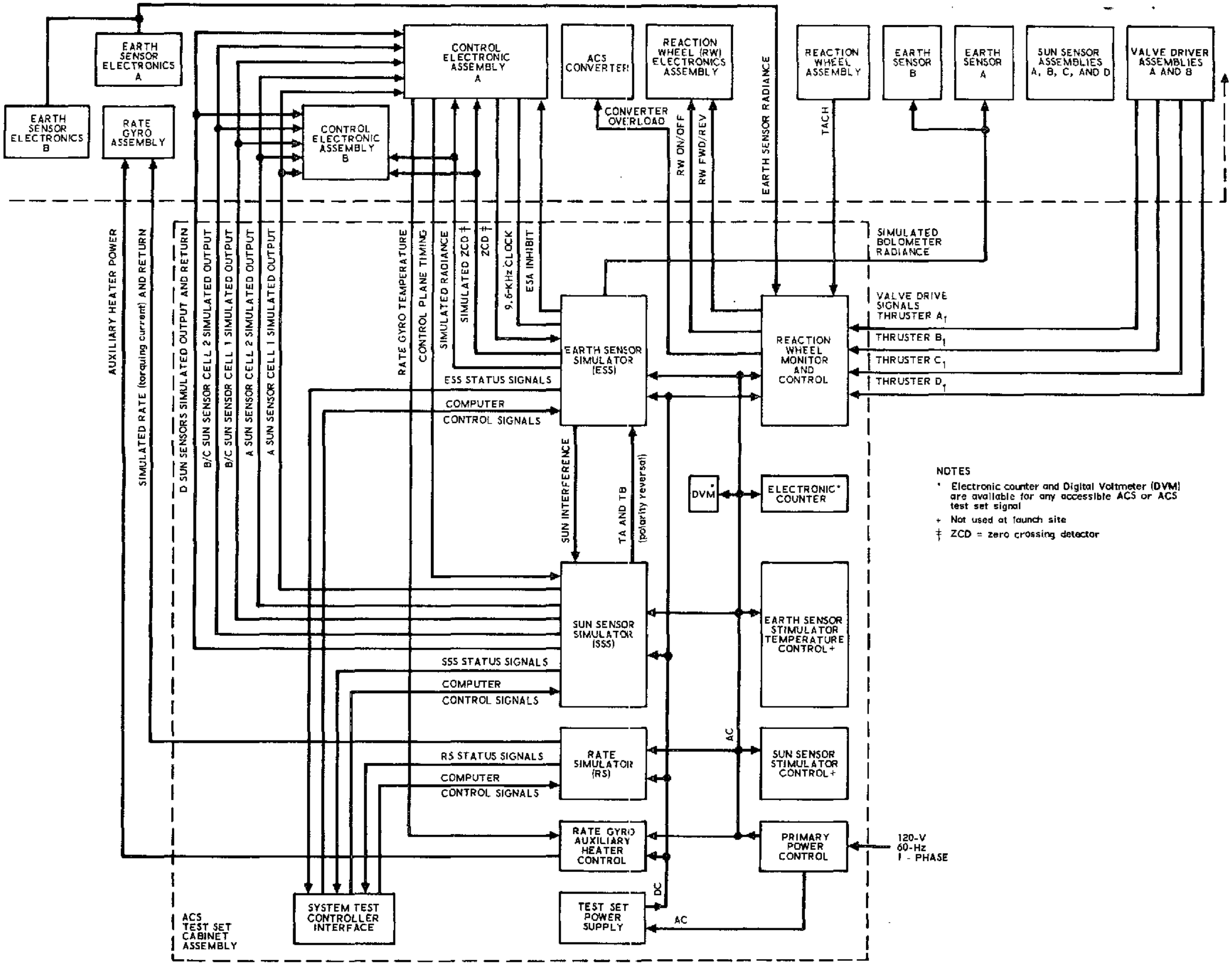

Figure 9-1. Sample ACS Test Set Block Diagram

1. EARTH SENSOR TEST SET

The earth sensor assembly (ESA) of the sample ACS scans about a null axis 8.7 deg from the spacecraft spin axis and provides logic level outputs to the control electronic assembly (CEA), indicating null axis and actual horizon crossing. The scan rate is accurately stabilized so that the time between null and horizon crossing may be interpreted as an angular pointing error.

The test set must provide a number of modes for simulating the signals of the two ACS earth sensors for this case. The signals that must be generated to simulate earth sensor outputs are all pulses with 5- to 10-μsec rise and fall times.

a. Earth Sensor Output Simulation

The radiance logic and the zero crossing outputs of the earth sensor must be simulated to permit ACS testing without using an earth sensor. In this mode, the test set causes the ACS ESA inhibit signal to attain a logic zero level. This will result in the ESA outputs to the CEA.

b. Bolometer Signal Simulation

The bolometer radiance signal must be simulated to permit ACS and/or earth sensor testing without stimulating the earth sensor under test with infrared radiation. In a system with two active earth sensors, the test set must be capable of simulating the signals of both earth sensors simultaneously in both of these modes. The test set must provide signals simulating the radiance logic and the zero crossing signal outputs of the ESA. Except for the pulse duration, the characteristics of both signals are identical.

c. Bolometer Earth Radiance Simulation

The test set must provide a signal that simulates the bolometer radiance signal of the earth viewed by the earth sensor. This test signal is applied to the preamplifier test inputs of both earth sensors. The clock signal is used as basic timing in generating the simulated bolometer earth radiance signal. In addition, the leading edge of the ACS zero crossing signal is used as a timing reference for the positive transition of the test signal.

d. Sun Radiance Simulation

The test set provides a simulated sun radiance pulse that, on command, can be inserted in the simulated earth radiance pulse train. When commanded, the simulated sun radiance pulse must occur at the appropriate time once during each simulated spin period.

e. Moon Radiance Simulation

The test set must also provide a simulated moon radiance signal that, on command, can be inserted in a similar manner to that indicated for the sun radiance pulse.

2. SUN SENSOR TEST SET

A sun sensor assembly (SSA) in the sample system incorporates two vertical slits on the face and corresponding apertures on the back, with solar cells mounted behind the apertures to detect the time at which the sun line crosses the slip plane (via the summed cell outputs) and to measure the sun aspect angle at that time (via the differenced outputs). The aspect signal is used in sun acquisition, and the crossing signal is used for timing in earth as well as sun acquisition.

The test set must generate signals that simulate the two output signals of the sun sensor solar cells and the output of the single sun sensor solar cell. In the normal mode, the test set simulates approximately in synchronism with the simulated sun radiance pulse from the earth sensor.

The amplitudes of the simulated outputs of each solar cell are equal for a simulated aspect angle of zero. For a positive simulated aspect angle, the amplitude of the signal simulating the output of solar cell 1 increases, and the amplitude of the signal simulating the output of solar cell 2 of the same sun sensor decreases at the same rate. For negative simulated aspect angles, the changes in amplitudes of the simulation signals are of opposite polarity, but of equal magnitude. The range of aspect angles required to be simulated is ±5.5 deg.

The test set must provide a means of varying the amplitude of each simulated output of the sun sensors so that the threshold of each individual channel of the ACS sun sensor processor may be measured.

3. RATE GYRO TEST SET

The rate gyro assembly (RGA) in the sample ACS provides rate information for use only during acquisition. The test set must generate a signal that simulates constant angular rates being applied to the ACS rate gyro. These signals take the form of the constant DC currents transmitted to the rate gyro torquer. The magnitude and polarity of the signal must be selectable. The power furnishing this signal is isolated from ground.

The test set is required to supply power to the rate gyro auxiliary heater and to provide a display that permits reading the gyro temperature to within 2.8°C. Full power is applied until the gyro temperature signal indicates that a gyro temperature of 54.5 ±2.8°C has been attained. At the indicated temperature, the power is automatically reduced to a pre-adjusted level within the range 1.5 to 3.0 W. If the gyro temperature signal increases to a temperature of 68.5 ±2.8°C, the test automatically interrupts the power applied to the auxiliary heater.

4. REACTION WHEEL TEST SET

The reaction wheel assembly (RWA) provides the angular momentum necessary to cancel the momentum developed by the spacecraft. It receives drive signals for its squirrel-cage induction motor from the reaction wheel electronics assembly (RWEA) and sends a once-per-revolution tachometer pulse to the RWEA for speed computation. The RWEA maintains the speed of the reaction wheel at a preset value based on the CEA clock input.

a. Monitoring and Control of Reaction Wheel

The test set is required to have a monitoring and a combined monitoring and control mode for the reaction wheel.

b. Monitoring Mode

The test set must allow the operator to determine the reaction-wheel speed within 1 part in 2×10^4 at any speed greater than 1000 rpm by processing the tachometer hardline signal and then measuring the period of the signal with the test set electronic counter.

c. Monitoring and Control Mode

The test set provides a means of manually switching wheel power off by driving the ACS disable (DIS) signal to a zero logic state. When the test set allows the DIS signal to reach a logic one level (open circuit), wheel power is controlled by the ACS.

d. Wheel Power Reversal

The test set provides a method of causing the RWEA to reverse one phase of the reaction wheel drive power to reduce wheel rundown time after operation at normal speeds. The test set provides this capability by automatically driving the ACS reversal (REV) signal to a zero logic state when the conditions requiring drive power reversal exist.

e. Wheel Power Interruption as a Result of Overspeed Detection

The test set must cause wheel power to be interrupted automatically whenever the reaction wheel speed, as indicated by the tachometer output, exceeds 3700 rpm. If this event occurs, the reaction wheel is allowed to coast to a stop, rather than braking as specified for deceleration after normal speed operation.

5. THRUSTER VALVE DRIVER TEST SET

The valve driver assemblies (VDAs) amplify the pulse commands from the CEA, and activate valves by grounding the thruster solenoid return lines. The VDAs also enable the appropriate thrusters upon command from the CEA, by connecting the high sides of the solenoids to the spacecraft bus by a relay.

The test set provides a means for conditioning the hardline valve commands for spin jets and control jets suitable for application via hardline digital telemetry unit.

C. POWER SUPPLY AND AC CONTROL TEST SET

The test set contains a power supply for furnishing various DC voltages required for operation of its components.

Provision is made for controlling the application of primary power to the ACS test set. The provision incorporates overload protection of the ACS test set console. Instantaneous cutoff of facility power must not adversely affect the console, nor cause the test set to adversely affect any satellite equipment. The test set may not be reenergized automatically upon restoration of primary power after an interruption.

APPENDIX A

STUDY 2.3 SYSTEM COST/PERFORMANCE ANALYSIS

The following Statement of Work is extracted from Request for Proposal No. W10-12296-DHC-3:

2.3 Systems Cost/Performance Analysis

Background

As the space program matures into an applications industry (with a supporting effort of exploratory and experimental activities) greater emphasis will be placed on improving the ability to predict the effect of program requirements on cost and schedules. These predictions will be needed as users commit funds and as programs proceed through the operational phases.

The objective of the overall effort, of which this study comprises one part, is to assist NASA in the generation and maintenance of program models and methodology. The program models will include a consistent and compatible set of performance, weight, cost and schedule interrelationships to be used in the evaluation of proposed and on-going space vehicle programs.

This vehicle program model methodology will be applicable to (expendable and reusable) launch vehicles, orbital propulsion stages, space stations, payloads and other vehicles. A secondary objective is to provide, to a limited extent, insight into DOD decision making criteria and data requirements with the intent to making the NASA-developed program models and methodology suitable for use in the evaluation of potential joint NASA/DOD programs.

The efforts under this task will be directed at the analysis of the interrelationships between and within the performance, weight, safety, cost and schedule parameters; and providing assistance where required, in the formulation of NASA cost models. When a degree of understanding of these parameters has been achieved and the basis for the individual models (cost models, weight models, etc.) is accepted then a Program Model can be developed by NASA which combines these characteristics and their interrelationships.

Emphasis will be placed on relating with quantitative expressions the interrelationships by understanding the effect of the proposed vehicle characteristics on the material and manpower demands. Technical feasibility and levels of risk or uncertainty effects on the parameters along with support requirements will be considered. Subsystem data will be stressed.

Aerospace experience with the following two activities will be utilized: (a) the development of the Solid Rocket Motor Program Model which combines performance, weight and cost factors, and (b) the reprogramming of the vehicle synthesis program using MSC cost equations, in support of NASw-2301 task 2.3 during the fiscal 72 year.

The NASA experience with ODIN and IPAD programs will be incorporated in the following studies. The contractor shall perform analysis in areas typified by the task listing below:

2.3.1 Definition of Program Model Parameters

2.3.1.1 The interrelationships between and within performance, weight, safety, cost and schedule factors will be determined and quantified for typical subsystems such as the following: Electric Power, Attitude Control (shall include the Attitude Control Propulsion system and the Attitude Control Command and Sensing system), and the Environmental Control System.

2.3.1.2 The contractor shall identify those parameters which are likely to be of interest in the accomplishment of trade studies for subsystems.

2.3.1.3 Functional block diagrams for each subsystem investigated shall be developed for four classes of space vehicles, of increasing system complexity and interactions: i.e., unmanned, expendable, autonomous vehicles; unmanned, reusable, autonomous vehicles; manned, reusable, autonomous vehicles; and manned, reusable vehicles using ground support systems.

2.3.1.4 Typical functional relationships between space vehicle systems and supporting systems shall be identified and characterized. Using these relationships quantitative expressions will be developed.

2.3.2 Support of NASA Program Model Development Activities

The contractor shall provide support to NASA in development of NASA program models. NASA low cost payload, payload effects and tug studies results will be utilized in conducting these studies. Typical analysis tasks are listed below:

2.3.2.1 Review existing program models in performance, weight, cost and scheduling areas and provide an assessment of their strengths and limitations.

2.3.2.2 The contractor shall review existing CER's and recommend to NASA those CER's which require updating due to new analyses of historical cost data, and those CER's which require modification of the principal independent variable. Specific CER's will be updated at NASA's request.

2.3.2.3 Provide an assessment of the use of program models for program control purposes, and provide a discussion of alternative display/interrogation techniques.

2.3.2.4 Provide an informal assessment of DOD program model capabilities and requirements, and highlight potential areas of conflict or incompatibility with the projected NASA program models.

APPENDIX B

TASK 2.3 DETAILED TASK PLAN

1. SUBTASK DESCRIPTION

This plan presents the detailed subtasks to be performed in developing a modeling technique to interrelate the parameters of performance, safety, cost, and scheduling. The parameters defined in Table B-1 will be considered for their utility in the modeling effort. The objective is to develop a methodology that permits calculation of these parameters for an attitude control system (ACS) meeting given functional requirements and to permit tradeoffs among these parameters. Because of the nature of a task to develop a new analytical technique, detailed planning is only possible for about 3 months in advance. Details of the work to be done after December 1972 will be developed as the task progresses.

This task consists of the subtasks detailed below. The relationship of these tasks is given in Figure B-1. The schedule is shown in Figure B-2. Manpower distribution is shown in Table B-2.

a. TASK 2.3.1: DEFINITION OF MODEL PARAMETERS

(1) Subtask 1: Develop Flow Chart of Design Process

A series of flow charts will be developed to represent the thought processes performed during the evolvement of a design. The flow should begin with the functional requirements, and should develop downward to component level. These flow charts will satisfy the "functional block diagram" task of the statement of work (SOW), since the design thought process will depend in part on the system functional mechanization.

This subtask will be developed in four parts noted below. At the conclusion of this subtask, a preliminary program model will have evolved.

Table B-1. Definition of Parameters

Performance
Functional requirements
Technical characteristics: accuracy, drift, etc.
Power
Volume
Weight
Vibration specification: GRMS random
Temperature specifications: conduction environment
Ambient pressure specification: radiation environment
Safety
Failure rate - qualification requirements
Failure detection: detection technique, false alarm rate
Cost
Total cost to customer in time (manpower) and material
Design and development
Build and checkout
Test equipment
Training and simulation
Maintenance
Management
Schedule
Sequence restraint
Man-loading limitation

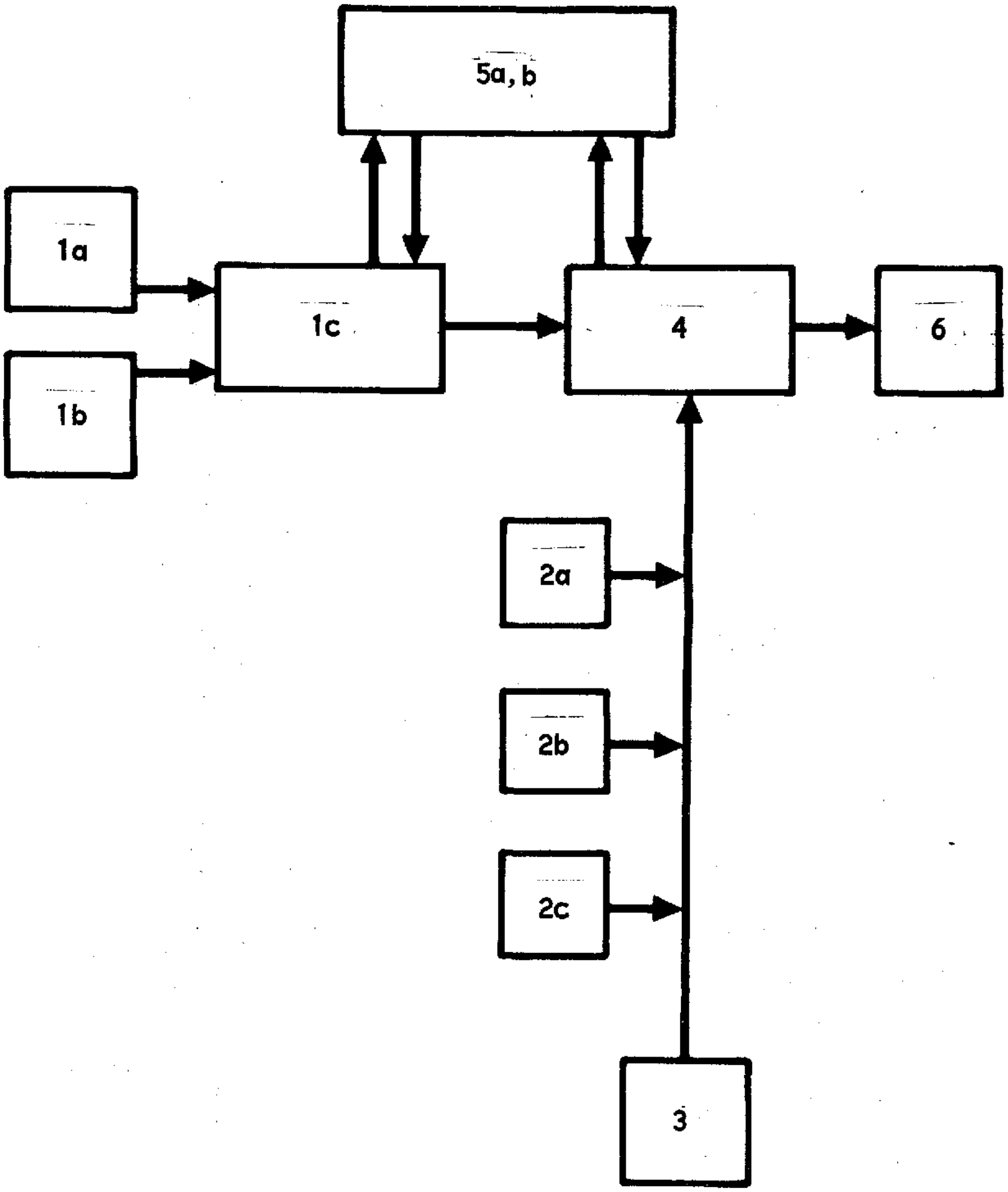

Figure B-1. Subtask Relationship

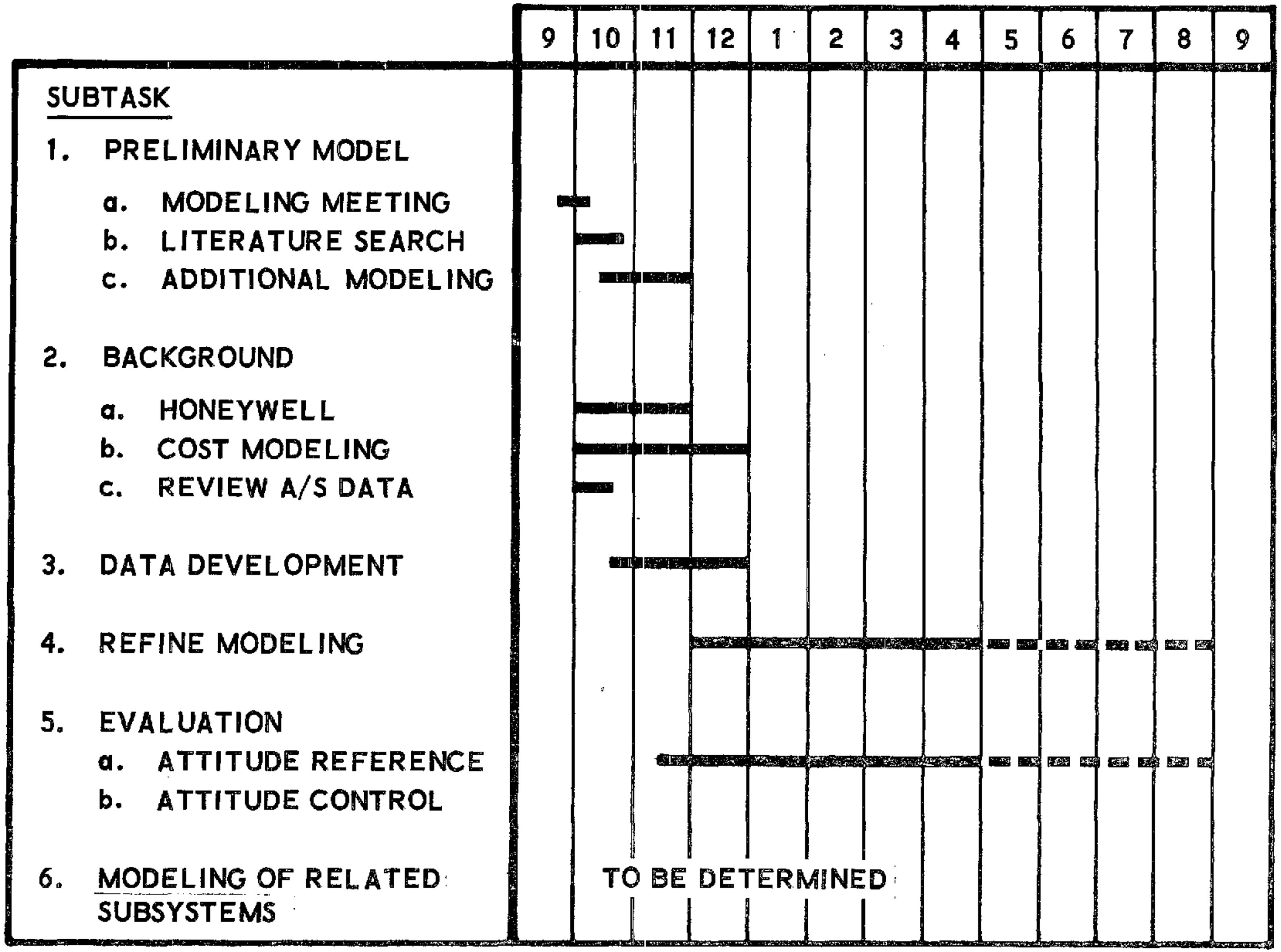

Figure B-2. Preliminary Schedule

Table B-2. Manpower Distribution

Subtask	Title	Member-of-Technical-Staff Distribution (%)
Task 2.3.1	Definition of program model parameters	
Subtask 1	Develop flow chart of design process	13
Subtask 2	Develop background information	7
Subtask 3	Develop data	10
Subtask 4	Refine flow chart of design process	25
Subtask 5	Model test cases	15
Subtask 6	Model related subsystems	20
TOTAL		90
Task 2.3.2	Support of NASA program model development activities	10
TOTAL		100

(a) In meetings, a small number of senior engineers will lay out a flow chart of the design process as applied to ACSs. The goal of this model is to develop, from the functional requirements, the detailed reasoning path that leads a designer to the component selection level. These flow charts will be developed for the ACS for an unmanned, expendable vehicle in this prelininary phase. While the major attention will be specifically for ACSs, cognizance of interface requirements with other subsystems (such as environmental control, power, and communications) will be maintained.

(b) A literature search will identify published versions of the "proper" design process for equipment similar to an ACS. This information will be used to further develop the flow charts prepared under Subtask 1(a).

(c) Modeling of costs and schedules loosely related to the functional block diagram of the design process will be investigated. Many requirements for a design do not appear in the thought process described in the flow charts. Examples are type of drawing format imposed, level of management control imposed, and reporting and documentation requirements of the contract. Emphasis will be placed on relating such elements to the flow charts to form a more comprehensive model.

(2) Subtask 2: Develop Background Information

This subtask will review and develop information on the more traditional cost estimating models in existence at The Aerospace Corporation and elsewhere to support the other modeling efforts of this task. It will consist of the following parts:

(a) Review, understand, and attempt to build on the work performed by Honeywell, Inc. in their attitude control costing study.

(b) Review other available cost modeling tools, such as the Unmanned Spacecraft Model and the Solid Rocket Motor Program Model to determine strengths, weaknesses, and applicability of these approaches to the task under consideration.

(c) Review general cost data available within The Aerospace Corporation and the NASA REDSTAR data base, and its ACS data.

(3) Subtask 3: Develop Data

This subtask will compile the data selected from the review of the Aerospace and NASA data base performed under Subtask 2(c). This data, together with the data base available in the Honeywell study, will form the basis for testing the modeling efforts under Subtasks 1 and 4. It is believed that the Honeywell data base will prove the most useful for this purpose.

(4) Subtask 4: Refine Flow Chart of Design Process

This subtask will develop refinements for the modeling technique based on the preliminary modeling of Subtask 1 and other information. The refinements to the preliminary model will emphasize the incorporation of the non-design-oriented elements defined in Subtask 1(c). Also included in this subtask is ascertaining the relationship of cost and schedule parameters to the design thought processes. In addition, traditional cost modeling techniques will be used where they appear to be beneficial. Another possible refinement would be to include some dynamic features into the model.

(5) Subtask 5: Model Test Cases

As the flow charting of the design process develops, an attempt will be made to devise test cases to assess the validity of the model. As stated earlier, it is believed that the data base obtained from the Honeywell study will be the most useful for this purpose. If other data appears beneficial, either available data will be employed, or the need for additional data will be identified from other NASA contracts.

(6) Subtask 6: Model Related Subsystems

The current opinion is that modeling related subsystems will not be useful for one of the following reasons:

(a) The entire task budget will be usefully expended in the ACS modeling task.

(b) The modeling task will have encountered sufficient difficulties that modeling other subsystems does not appear profitable.

If these conditions do not prevail, modeling of the design process for related subsystems will be investigated using the same methodology developed for ACSs.

b. TASK 2.3.2: SUPPORT OF NASA PROGRAM MODEL DEVELOPMENT ACTIVITIES

This task is planned as a level of effort support to NASA in the development of NASA program models as specifically requested by NASA. This effort will be based on existing program models and methodology, rather than the new methodology under consideration in Task 2.3.1.

2. REVIEW MEETING

Because of the nature of this task, which develops new analytical approaches along lines previously developed by the study director, frequent review meetings are scheduled early in the task. At the present time, only the quarterly reviews are scheduled late in the task. Additional review meetings will be scheduled between these quarterly reviews, if required. Review meetings are anticipated on approximately the following dates:

a. 19 October 1972
b. 8 November 1972
c. 22 November 1972[1]
d. 15 December 1972
e. 17 January 1973[1]
f. 15 March 1973[1]
g. 27 September 1973[1]

3. DELIVERABLE ITEMS

The deliverable items will consist of the following:

a. Monthly letter progress reports

[1] Joint Task Review Meetings

b. Midterm and final presentations describing general activities and achievements of the task

c. Final report, which will discuss the modeling techniques evolved and the degree of achievement of the goal of developing a more effective means of evaluating and controlling program costs. The degree of success achieved and the degree to which the resulting modeling technique should be programmed for a computer will be evaluated. The modeling technique developed will be presented in flow chart form.

APPENDIX C

TUG ACS SIMULATION STUDIES

1. INTRODUCTION

This section presents results of a preliminary Tug attitude control system (ACS) trade study obtained using the Cost/Performance Simulation described in Section 5. The preliminary nature of these results arises from two considerations: first, much of the simulation data base is itself preliminary, having been taken from Tug contractor documents representing a very early stage of tug development; and, second, the Cost/Performance Model has not been fully verified against other cost/performance models. Therefore, the following Tug trade studies should be considered primarily a demonstration of the Cost/Performance Simulation and a starting point for future trade studies following refinement of the simulation and its data base.

2. TUG ACS TRADE STUDY DATA BASE

The simulation data base used for trade studies is presented in Tables C-1 through C-6 with data formatted according to the description of the data base matrix in Section 5, and with component attributes formatted according to the data base described in Section 6.

As various contractor-defined candidate ACSs depend primarily on sensor configurations and on specific sensors used in each configuration, most of the data base is concerned with sensor characteristics. Thus, Table C-1 lists attributes of specific inertial measurement units (IMUs); Table C-2 presents attributes of specific horizon sensors; and Table C-3 is concerned with star reference characteristics. Each table lists attributes for three sensors, presenting 27 possible ACS combinations for a single-string mechanization, 27 active/standby mechanizations, and 27 triply redundant/voting mechanizations; in total, 81 possible ACSs are presented. All safety parameter values in Tables C-1 through C-6 were engineering estimates and were not contractor-defined.

Table C-1. IMU Data Base

Attribute No.	Attribute	Program Mnemonic	Attribute Units	Comments	IMU 1 (Current Strapdown)	IMU 2 (Developmental Strapdown)	IMU 3 (Current Gimbaled)
1	Manufacturer, System				Hamilton Standard, DIG	MIT, DODEC	Delco, Carousel
2	Type			Strapdown, gimbal	Strapdown	Strapdown	Gimbal
3	Alignment accuracy		rad		0.0007	0.00014	0.00021
4	Drift rate		rad/sec		0.14×10^{-6}	1.2×10^{-6}	0.48×10^{-6}
5	Power		W		82	325	125
6	Weight		kg (lb)		22.2 (49)	55.4 (122)	20.4 (45)
7	Volume		m^3 (ft^3)		0.017 (0.6)	0.045 (1.6)	0.052 (1.84)
8	Vibration						
9	Temperature 1			Radiation			
10	Temperature 2			Conduction			
11	Pressure						
12	Failure rate 1		failures/hr	Active mode	1.42×10^{-4}	2×10^{-5}	2.198×10^{-4}
13	Failure rate 2		failures/hr	Dormant mode	1.42×10^{-4}	2×10^{-5}	2.198×10^{-4}
14	No. of parameters monitored 1				15	15	15
15	No. of parameters monitored 2				5	5	5
16	Parameter total				20	20	20
17	Failure rate 3		failures/hr		1×10^{-6}	1×10^{-6}	1×10^{-6}
18	Failure rate 4		failures/hr		1×10^{-6}	1×10^{-6}	1×10^{-6}
19	Failure rate 5		failures/hr		1×10^{-6}	1×10^{-6}	1×10^{-6}
20	Failure rate 6		failures/hr		1×10^{-6}	1×10^{-6}	1×10^{-6}
21	Failure rate 7		failures/hr		1×10^{-6}	1×10^{-6}	1×10^{-6}
22	Failure rate 8		failures/hr		1×10^{-6}	1×10^{-6}	1×10^{-6}
23	Failure rate 9		failures/hr		1×10^{-6}	1×10^{-6}	1×10^{-6}
24	Failure rate 10		failures/hr		1×10^{-6}	1×10^{-6}	1×10^{-6}
25	Failure rate 11		failures/hr		1×10^{-6}	1×10^{-6}	1×10^{-6}
26	Cost 1		\$	Hardware design, development, test, and evaluation	1.5×10^{6}	2.5×10^{6}	5×10^{6}
27	Cost 2		\$	Software design, development, test, and evaluation			
28	Cost 3		\$	Unit cost	120×10^{3}	420×10^{3}	200×10^{3}
29	Time 1		months	Prototype development time			
30	Time 2						

Table C-2. Horizon Sensor Data Base

Attribute No.	Attribute	Program Mnemonic	Attribute Units	Comments	Horizon Sensor 1	Horizon Sensor 2	Horizon Sensor 3
1	Manufacturer, system				Barnes, 13-192	Quantic, IV	TRW, MOBS
2	Type			Conical scan/edge track	Conical scan	Edge track	Edge track
3	Accuracy		rad		0.0017	0.001	0.0014
4							
5	Power		W		8.5	30	20
6	Weight		kg (lb)		7.9 (17.5)	31.8 (70)	12.7 (28)
7	Volume		m^3 (ft^3)				
8	Vibration						
9	Temperature 1			Radiation			
10	Temperature 2			Conduction			
11	Pressure						
12	Failure rate 1		failures/hr	Active mode	1.54×10^{-5}	0.77×10^{-6}	1×10^{-6}
13	Failure rate 2		failures/hr	Dormant mode	1.54×10^{-5}	0.77×10^{-6}	1×10^{-6}
14	No. of parameters monitored 1				15	15	15
15	No. of parameters monitored 2				5	5	5
16	Parameter total				20	20	20
17	Failure rate 3		failures/hr		1×10^{-6}	1×10^{-6}	1×10^{-6}
18	Failure rate 4		failures/hr		1×10^{-6}	1×10^{-6}	1×10^{-6}
19	Failure rate 5		failures/hr		1×10^{-6}	1×10^{-6}	1×10^{-6}
20	Failure rate 6		failures/hr		1×10^{-6}	1×10^{-6}	1×10^{-6}
21	Failure rate 7		failures/hr		1×10^{-6}	1×10^{-6}	1×10^{-6}
22	Failure rate 8		failures/hr		1×10^{-6}	1×10^{-6}	1×10^{-6}
23	Failure rate 9		failures/hr		1×10^{-6}	1×10^{-6}	1×10^{-6}
24	Failure rate 10		failures/hr		1×10^{-6}	1×10^{-6}	1×10^{-6}
25	Failure rate 11		failures/hr		1×10^{-6}	1×10^{-6}	1×10^{-6}
26	Cost 1		$	Hardware design, development, test, and evaluation	0.87×10^{6}	2×10^{6}	1×10^{6}
27	Cost 2		$	Software design, development, test, and evaluation			
28	Cost 3		$	Unit cost	150×10^{3}	441×10^{3}	405.8×10^{3}
29	Time 1		months				
30	Time 2						

Table C-3. Star Reference Data Base

Attribute No.	Attribute	Program Mnemonic	Attribute Units	Comments	Star Reference 1	Star Reference 2	Star Reference 3
1	Manufacturer, system				Kollsman	Bendix	Honeywell
2	Type			Strapdown, gimbal	Gimbal	Gimbal	Strapdown
3	Update accuracy		rad		0.00007	0.0002	0.0009
4							
5	Power		W		23	32	6
6	Weight		kg (lb)		13.6 (30)	15.9 (35)	5.4 (12)
7	Volume		m^3 (ft^3)		0.028 (1)	0.034 (1.2)	0.017 (0.6)
8	Vibration						
9	Temperature 1			Radiation			
10	Temperature 2			Conduction			
11	Pressure						
12	Failure rate 1		failures/hr	Active mode	8.5×10^{-5}	1.23×10^{-4}	1.136×10^{-5}
13	Failure rate 2		failures/hr	Dormant mode	8.5×10^{-5}	1.23×10^{-4}	1.136×10^{-5}
14	No. of parameters monitored 1				15	15	15
15	No. of parameters monitored 2				5	5	5
16	Parameter total				20	20	20
17	Failure rate 3		failures/hr		1×10^{-6}	1×10^{-6}	1×10^{-6}
18	Failure rate 4		failures/hr		1×10^{-6}	1×10^{-6}	1×10^{-6}
19	Failure rate 5		failures/hr		1×10^{-6}	1×10^{-6}	1×10^{-6}
20	Failure rate 6		failures/hr		1×10^{-6}	1×10^{-6}	1×10^{-6}
21	Failure rate 7		failures/hr		1×10^{-6}	1×10^{-6}	1×10^{-6}
22	Failure rate 8		failures/hr		1×10^{-6}	1×10^{-6}	1×10^{-6}
23	Failure rate 9		failures/hr		1×10^{-6}	1×10^{-6}	1×10^{-6}
24	Failure rate 10		failures/hr		1×10^{-6}	1×10^{-6}	1×10^{-6}
25	Failure rate 11		failures/hr		1×10^{-6}	1×10^{-6}	1×10^{-6}
26	Cost 1		$	Hardware design, development, test, and evaluation	0.582×10^6	0.4×10^6	0.3×10^6
27	Cost 2		$	Software design, development, test, and evaluation			
28	Cost 3		$	Unit cost (no. of units)	66.4×10^3	178.7×10^3	170.1×10^3
29	Time 1		months				
30	Time 2						

Table C-4. Processor Data Base

Attribute No.	Attribute	Program Mnemonic	Attribute Units	Comments	Central Processor and Control Logic
1					
2					
3					
4					
5	Power		W		120
6	Weight		kg (lb)		27.2 (60)
7	Volume		m^3 (ft^3)		0.057 (2)
8	Vibration				
9	Temperature 1				
10	Temperature 2				
11	Pressure				
12	Failure rate 1		failures/hr		10^{-3}
13	Failure rate 2		failures/hr		15
14	No. of parameters monitored 1				5
15	No. of parameters monitored 2				20
16	Parameter total				
17	Failure rate 3		failures/hr		1×10^{-6}
18	Failure rate 4		failures/hr		1×10^{-6}
19	Failure rate 5		failures/hr		1×10^{-6}
20	Failure rate 6		failures/hr		1×10^{-6}
21	Failure rate 7		failures/hr		1×10^{-6}
22	Failure rate 8		failures/hr		1×10^{-6}
23	Failure rate 9		failures/hr		1×10^{-6}
24	Failure rate 10		failures/hr		1×10^{-6}
25	Failure rate 11		failures/hr		1×10^{-6}
26	Cost 1				1×10^{6}
27	Cost 2				14.4×10^{6}
28	Cost 3				200×10^{3}
29	Time 1				
30	Time 2				

Table C-5. Actuator Data Base

Attribute No.	Attribute	Program Mnemonic	Attribute Units	Comments	Actuator
1					
2					
3					
4					
5	Power		W		20
6	Weight		kg (lb)		22.7 (50)
7	Volume		m^3 (ft^3)		0.057 (2)
8	Vibration				
9	Temperature 1				
10	Temperature 2				
11	Pressure				
12	Failure rate 1		failures/hr		3×10^{-3}
13	Failure rate 2		failures/hr		15
14	No. of parameters monitored 1				5
15	No. of parameters monitored 2				20
16	Parameter total				
17	Failure rate 3		failures/hr		1×10^{-6}
18	Failure rate 4		failures/hr		1×10^{-6}
19	Failure rate 5		failures/hr		1×10^{-6}
20	Failure rate 6		failures/hr		1×10^{-6}
21	Failure rate 7		failures/hr		1×10^{-6}
22	Failure rate 8		failures/hr		1×10^{-6}
23	Failure rate 9		failures/hr		1×10^{-6}
24	Failure rate 10		failures/hr		1×10^{-6}
25	Failure rate 11		failures/hr		1×10^{-6}
26	Cost 1				1×10^{6}
27	Cost 2				
28	Cost 3				100×10^{3}
29	Time 1				
30	Time 2				

Table C-6. Energy Source Data Base

Attribute No.	Attribute	Program Mnemonic	Attribute Units	Comments	Energy Source: Tank	Energy Source: Regulator	Energy Source: Lines
1							
2							
3							
4							
5	Power		W			20	
6	Weight		kg (lb)		22.7 (50)	4.5 (10)	22.7 (50)
7	Volume		m^3 (ft^3)		0.057 (2)	0.0057 (0.2)	0.0057 (0.2)
8	Vibration						
9	Temperature 1						
10	Temperature 2						
11	Pressure						
12	Failure rate 1		failures/hr		1×10^{-8}	3×10^{-7}	2×10^{-7}
13	Failure rate 2		failures/hr		15	15	15
14	No. of parameters monitored 1				5	5	5
15	No. of parameters monitored 2				20	20	20
16	Parameter total						
17	Failure rate 3		failures/hr		1×10^{-6}	1×10^{-6}	1×10^{-6}
18	Failure rate 4		failures/hr		1×10^{-6}	1×10^{-6}	1×10^{-6}
19	Failure rate 5		failures/hr		1×10^{-6}	1×10^{-6}	1×10^{-6}
20	Failure rate 6		failures/hr		1×10^{-6}	1×10^{-6}	1×10^{-6}
21	Failure rate 7		failures/hr		1×10^{-6}	1×10^{-6}	1×10^{-6}
22	Failure rate 8		failures/hr		1×10^{-6}	1×10^{-6}	1×10^{-6}
23	Failure rate 9		failures/hr		1×10^{-6}	1×10^{-6}	1×10^{-6}
24	Failure rate 10		failures/hr		1×10^{-6}	1×10^{-6}	1×10^{-6}
25	Failure rate 11		failures/hr		1×10^{-6}	1×10^{-6}	1×10^{-6}
26	Cost 1				1×10^{6}	1×10^{6}	1×10^{4}
27	Cost 2						
28	Cost 3				1×10^{4}	1×10^{4}	1×10^{3}
29	Time 1						
30	Time 2						

The specific sensors selected represent typical sensors currently available within industry. For example, Table C-1 lists attributes of a current strapdown IMU, a developmental strapdown IMU, and a current gimbaled IMU. Similarly, conical scan and edge tracker horizon sensors are represented, while both gimbaled and strapdown star references are listed.

Attributes for the Processor Module, the Actuator Module, and the Energy Source Module are presented in Tables C-4 through C-6, with each module limited to a single entry, due primarily to the lack of available data.

3. TUG ACS TRADEOFF CONFIGURATION/MECHANIZATIONS

The Cost/Performance Simulation is programmed to consider all combinations of data base components in configuring systems processed by the performance aggregate equations. Systems consisting of component combinations that meet or exceed the performance criteria are designated as acceptable configurations and are stored in the answer matrix for processing by the safety aggregate equations. As each acceptable configuration is mechanized and processed by the safety equations as a single-string ACS, answer matrix attributes are updated as described in Section 5. Similarly, each of the same configurations is processed by the safety equations as an active/standby and a triply redundant/voting ACS. Thus, for each acceptable configuration, three separate ACS mechanizations are formed and stored in the answer matrix.

Section C. 4 presents trade results, showing system cost versus system weight and system autonomy, for each mechanization of each configuration described above. In addition, voting versus standby redundancy, and gimbaled versus strapdown IMU systems are compared.

As previously mentioned, autonomy is ranked as a trade study result. Table C-7 represents four levels of autonomy as defined by NASA. These four levels represent a much broader definition than is used in the trade results presented in this report. The definition of Table C-7 encompasses not only the ACS, but also other areas, such as the communication, rendezvous and docking, and telemetry subsystems that are outside the scope of the present Cost/Performance Model.

Table C-7. Space Tug System Levels of Autonomy

<u>Level I Autonomy</u>
Completely independent of any man-made inputs after separation (such as beacons, orbiter and ground)
Onboard measurements and calculations that enable mission to be completed in its entirety, including all Tug and payload operations
Final onboard rendezvous and docking capability
Command uplink override capability and telemetry downlink
<u>Level II Autonomy</u>
Ground or navigation satellite beacons (either required to serve multiple users) acceptable
Level I autonomy required for those orbits where ground or satellite beacons do not provide satisfactory state determinations
Final onboard rendezvous and docking capability
Command uplink override capability, including payload status, redirection, and retargeting of mission with telemetry downlink
<u>Level III Autonomy</u>
Ground stations providing state update during entire mission
Onboard calculations performed for mission completion
Final rendezvous made by onboard capability
Final docking with ground support
Command and telemetry capability
<u>Level IV Autonomy</u>
All phases controlled from the ground
Calculations performed primarily on the ground (such as main burn and midcourse - duration and direction)
Ground controlling final rendezvous and docking
Command and telemetry capability

The definition used in this report quantifies autonomy as ACS failure detection probability, and this depends entirely on the calculation of failure detection probability made in the safety aggregate equation module. Thus, while the failure detection probability may differ among single-string, active/standby, and triply redundant mechanizations of each ACS configuration, no provision is made in the safety aggregate equations to determine if these calculations are performed onboard or by a ground computer. (The provision could be added in future refinements of the safety aggregate equations.) Thus, while failure detection probabilities provide for a means for quantifying autonomy, and do indeed measure the self-capability of the system to determine its operational capability, they do so in a limited manner. In effect, failure detection probability provides a means of quantifying the autonomy of each ACS mechanization within each of the major categories listed in Table C-7.

4. TUG ACS TRADE STUDY EXAMPLES

An example for a baseline three-axis mass expulsion ACS presented in this section was obtained using the Cost/Performance Simulation described in Section 5 with the performance criterion of pointing accuracy set at 0.7 deg, and the reliability specification set at 0.97 over a mission time of 4 hr. All results represent a build of 20 ACSs using data given in Tables C-1 through C-6; all possible combinations of ACS represented by these data passed the performance criterion. Thus, 27 separate ACS configurations or 81 ACS mechanizations are represented by the following material.

a. SYSTEM COST AND WEIGHT VERSUS SYSTEM MECHANIZATION

Broad types of system mechanizations are compared on a cost basis by averaging the cost of all single-string ACS and comparing them to averaged active/standby and averaged triply redundant system costs. System weights are also averaged in a similar manner; the results are presented in Table C-8.

The results shown in Table C-8, indicating incremental costs and weights, are reasonable with each additional ACS string, adding a cost and weight penalty approximately equal to the basic single-strong figures.

Results are compared to SAMSO/Aerospace cost estimating relationships (CERs) developed for unmanned spacecraft to judge the validity of absolute cost and weight numbers (Ref. 1).

Table C-8. System Cost and Weight

Type of Mechanization	Cost[a] (millions of dollars)	Weight[b] (kg)
Single-String	151	189
Active/Standby	239	377
Triply Redundant	327	565

[a]Average cost of 27 configurations
[b]Average weight of 27 configurations

The CERs used are given in Eqs. (C-1) and (C-2).

$$\text{DDTE Cost} = (4.015)(IF)[2190. + (25.3)WT] \tag{C-1}$$

$$\text{First Article Cost} = (3.48)(IF)[28.9 + 9.45\ WT] \tag{C-2}$$

where

DDTE Cost = design, development, test, and evaluation costs in thousands of dollars

IF = inflation factor, using 1971 as a base year = 1.114

WT = weight in kilograms

Since Eq. (C-2) gives first article cost, and cost/performance results are for a build of 20 units, a learning curve must be applied to the SAMSO/Aerospace CER to obtain the total cost of 20 units. The following material presents a brief explanation of the learning curve used to convert first article cost to the cost of 20 units.

(1) Learning Curve Derivation

An exponentially decreasing cost per unit is assumed as given in Eq. (C-3).

$$c_n = K_1(\text{FAC}) + K_2(\text{FAC}) \exp\left[-K_3(n-1)\right] \qquad \text{(C-3)}$$

where

c_n = cost of the nth unit

FAC = first article cost

also defined

SAC = stabilized last article cost

P = ratio of SAC to FAC

Stabilized last article cost is the cost per unit that would result for the last unit of a large build of systems where costs no longer decrease due to the learning process.

Constants K_1 and K_2 are evaluated by setting c_n = FAC for n = 1 and c_n = SAC for large n. The result is Eq. (C-4).

$$c_n = (\text{FAC}) \left\{P + (1-P) \exp\left[-K_3(n-1)\right]\right\} \qquad \text{(C-4)}$$

To find C_T, the total cost of N units, c_n is summed over N units.

$$C_T = \sum_{n=1}^{N} c_n \qquad \text{(C-5)}$$

Equation (C-5) is a geometric series with a "common ratio" of e^{-K_3}. The sum may be written in terms of the first term, the number of terms, and the common ratio. The final result is given by Eq. (C-6).

$$C_T = (FAC)\left\{NP + (1 - P)\left[\frac{1 - \exp(-K_3 N)}{1 - \exp(-K_3)}\right]\right\} \qquad \text{(C-6)}$$

If one uses Eq. (C-6), given FAC and N, values must be chosen for P and K_3. For example, past history may show that the per-unit cost for a large build of a certain type of system stabilizes at 80% of first article cost after many systems are built. This would set P = 0.8.

The constant K_3 determines the rate at which the cost per unit stabilizes. If 95% of the difference between FAC and SAC is to vanish by the thirteenth unit, K_3 must satisfy $-K_3 (13 - 1) = 3$, since $\exp[-3] \cong 0.05$.

For values of P and K_3 in the above example, the per-unit and total cost expressions are given by Eqs. (C-7) and (C-8).

$$c_n = (FAC)\left\{0.8 + 0.2 \exp\left[\frac{-(n-1)}{4}\right]\right\} \qquad \text{(C-7)}$$

$$C_T = (FAC)\left\{0.8N + 0.2\left[\frac{1 - \exp\left(-\frac{N}{4}\right)}{1 - \exp\left(-\frac{1}{4}\right)}\right]\right\} \qquad \text{(C-8)}$$

(2) Cost/Performance - CER Comparison

Figure C-1 compares the results of the cost/performance figures given in Table C-8 with CERs given in Eqs. (C-1) and (C-2). Equation (C-8) was used to find the cost for 20 ACSs, using first article cost calculated from Eq. (C-2).

As seen in Figure C-1, the Cost/Performance Model exhibits a lower slope in the cost-weight plane than does the SAMSO/Aerospace model, with the two models showing the same costs for systems weighing approximately 187 kg. When the preliminary nature of the cost/performance data base is considered, it is concluded that agreement between the two models is acceptable. Also, it is anticipated that the cost/performance curve may

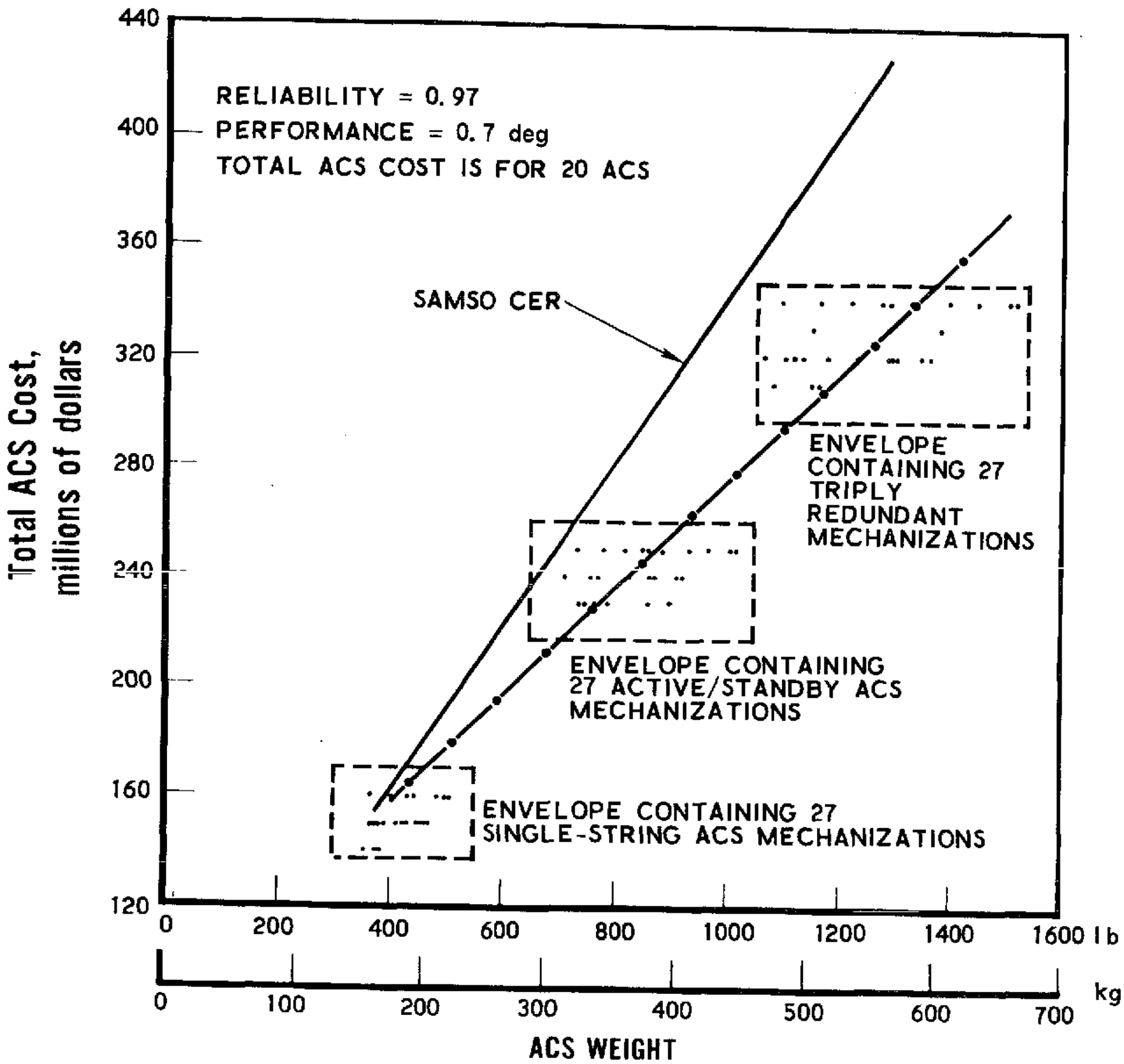

Figure C-1. Total ACS Cost vs ACS Weight rise as the model is refined and additional cost factors are included. Note that the Cost/Performance Model emphasizes the fact that the cost-to-weight relationship for real systems is a set of discrete points with gaps, rather than the continuous curve implied by the CER.

b. COST OF VOTING VERSUS STANDBY REDUNDANCY

The dollar and weight/cost of an additional string in the ACS to implement voting, instead of standby redundancy, may be seen in Figure C-1. The results of the computer run show that the dual string mechanizations generate reliabilities of approximately 0.9996, while triply redundant mechanizations give 0.99999 reliable systems. (See Figure C-2.) Due to the preliminary nature of the data base, no conclusions regarding these results should be drawn at this time.

c. GIMBALED-VERSUS-STRAPDOWN SYSTEMS

Average system cost, weight, and volume figures show very little sensitivity to gimbaled versus strapdown IMU implementations with typical costs of 150 million dollars, weights of approximately 195 kg, and volumes of 0.31 m^3 per ACS string for either gimbaled or strapdown IMUs. It is concluded that insensitivity to IMU type in this case is attributed to the fact that IMU power, weight, and volume contributions represent a relatively small percentage of system totals.

d. SYSTEM AUTONOMY

As mentioned in Section 2, system autonomy is quantified as system failure detection probability. Calculation of failure detection probability depends on knowledge of the total number of ACS parameters that must be monitored to ensure detection of a failure, and on knowledge of parameters actually monitored and of monitor system failure rates. As none of these data are available at the present time, realistic assessment of system autonomy is impossible. However, purely as a demonstration, values were assumed for these parameters and results are presented below. Parameter values used are given in Tables C-1 through C-6.

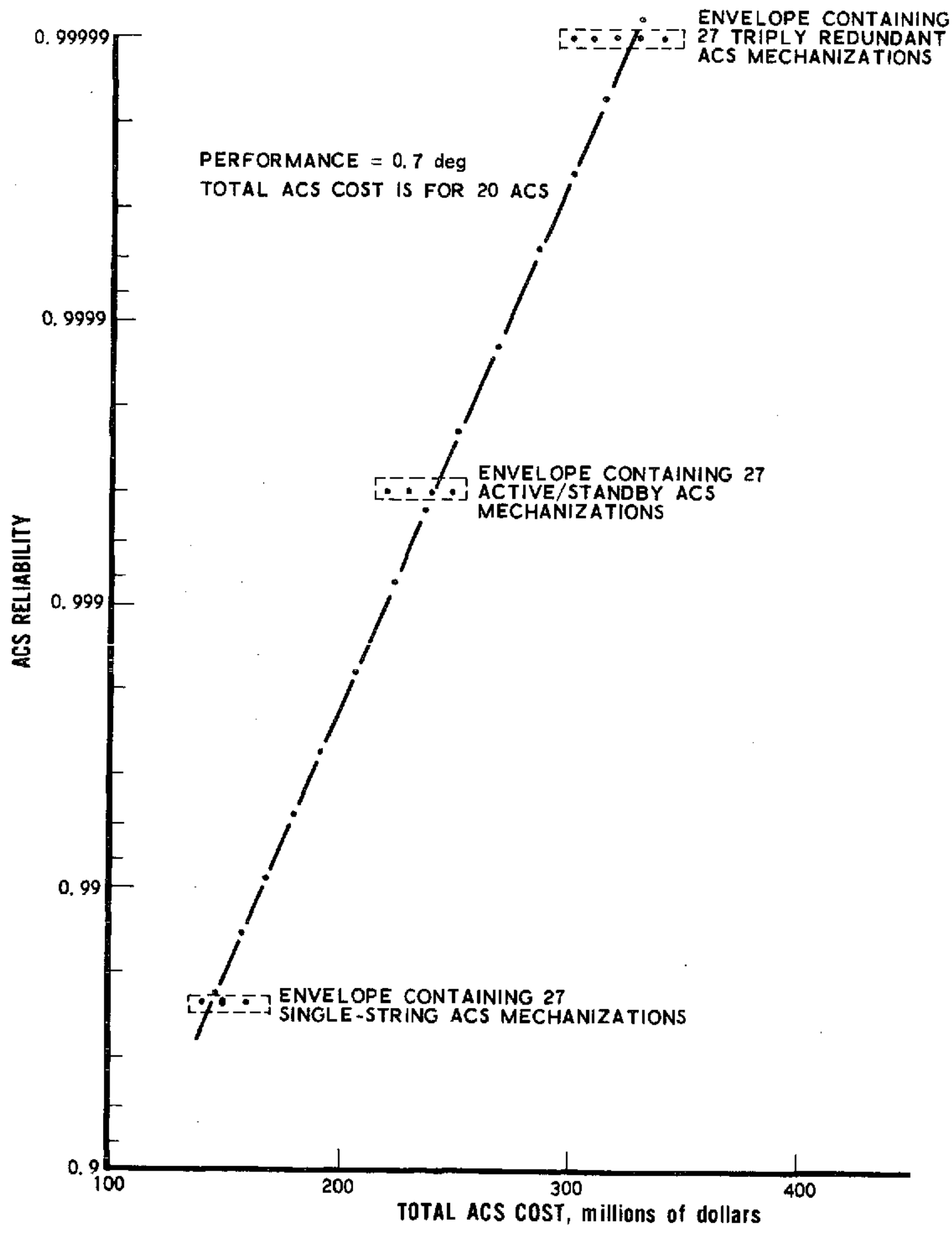

Figure C-2. ACS Reliability vs Total ACS Cost

If one assumes that, out of the 20 parameters required to ensure failure detection, 15 per component are monitored on active strings and 5 per component are monitored on standby strings, and that all monitor system failure rates are 10^{-6} failures per hr, the following failure detection probabilities (FDPs) result:

Single-string:	FDP ≅ 0.75
Active/standby:	FDP ≅ 0.45
Triply redundant:	FDP ≅ 0.75

The inputs giving the above results were selected to exercise the computational algorithms and are not representative of a real system. In a single-string configuration, it is likely that no parameters would be monitored, giving an FDP of zero. In a triply redundant system, the presence of the voter output implies that all parameters are monitored, giving an FDP of near unity.

REFERENCE

1. Unmanned Spacecraft Cost Model, Phase I Update, August 1971.

APPENDIX D

SUPPORTING ANALYSES

1. ON-ORBIT POINTING ACCURACY AGGREGATE EQUATIONS

This appendix derives the error equations for the attitude reference system for an Agena-type attitude control system (ACS). The spacecraft control axes are defined in Figure D-1.

The vehicle pitch axis pointing error θ_ϵ will be defined as

$$\theta_\epsilon = \theta_R - \theta \tag{D-1}$$

where

θ_R = vehicle pitch control reference

θ = pitch attitude with respect to local vertical

The vehicle pitch control reference can be expressed in terms of the gyroscope, horizon sensor, electronics, and mechanization parameters. Referring to Figure 4-6, one can write the following Laplace transform expression for $\theta_R(S)$:

$$\theta_R(S) = \frac{H_\theta \, \theta_{H/S}(S) + (\omega_{0p}(S) + \omega_y(S))}{S + H_{F_\theta}} \tag{D-2}$$

where

H_θ = pitch horizon sensor gain

H_{F_θ} = pitch decoupling gain

$\theta_{H/S}$ = pitch horizon sensor reference

ω_{0p} = preprogrammed orbit rate

ω_y = pitch axis body rate

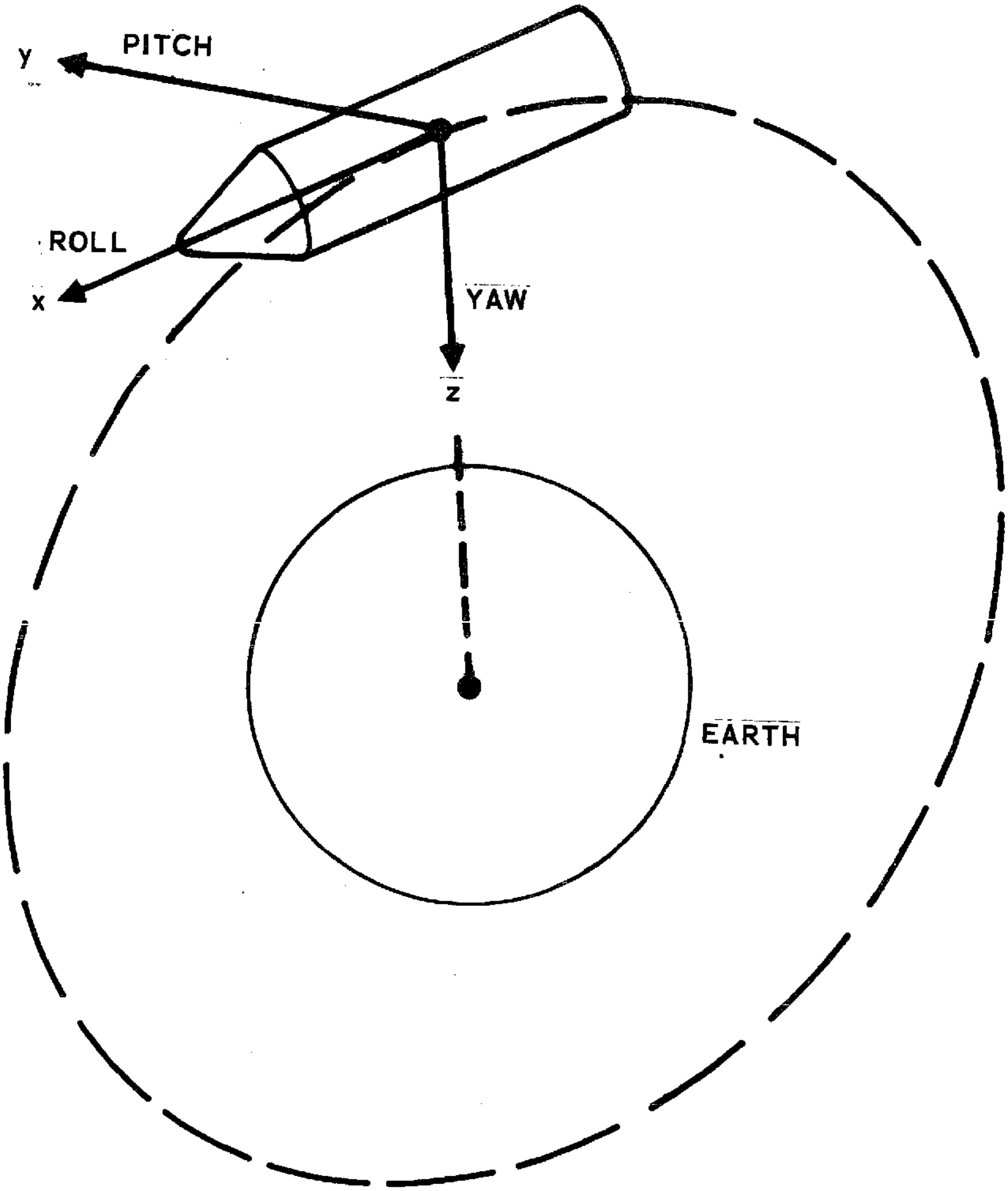

Figure D-1. Spacecraft Coordinates

The horizon sensor reference $\theta_{H/S}$ can be expressed as

$$\theta_{H/S} = \theta + (\theta_{H/S})_\epsilon \tag{D-3}$$

where

$(\theta_{H/S})_\epsilon$ = horizon sensor error.

The pitch axis body rate ω_y can be expressed as

$$\omega_y = \dot{\theta} - \omega_0 + (\dot{\theta}_g)_\epsilon \tag{D-4}$$

where

ω_0 = local vertical orbit rate

$(\dot{\theta}_g)_\epsilon$ = pitch gyro error.

Substituting Eqs. (D-2), (D-3), and (D-4) into Eq. (D-1), the pitch pointing error can be expressed as

$$\theta_\epsilon(S) = \frac{(H_\theta - H_{F_\theta})\,\theta + H_\theta(\theta_{H/S})_\epsilon + (\omega_{0p} - \omega_0) + (\dot{\theta}_g)_\epsilon}{S + H_{F_\theta}} \tag{D-5}$$

The steady-state pitch pointing error can be expressed as

$$\begin{aligned} \theta_{ss\epsilon}(S) &= \lim_{S \to 0} S\,\theta_\epsilon(S) \\ &= [(H_\theta - H_{F_\theta})/H_{F_\theta}]\,\theta + [H_\theta/H_{F_\theta}]\,(\theta_{H/S})_\epsilon \\ &\quad + [1/H_{F_\theta}]\,(\omega_{0p} - \omega_0) + [1/H_{F_\theta}]\,(\dot{\theta}_g)_\epsilon \end{aligned} \tag{D-6}$$

Four major error sources contribute to the pitch pointing error: gyroscope, horizon sensor, electronics, and those associated with the mechanization. Using Eq. (D-6) as a starting point to indicate how sensitivity coefficients are determined, one can develop a complete set of error sources, multipliers, and sensitivity coefficients, as shown in Table D-1. Similarly, the equations for the roll and yaw axes can be determined. The roll axis errors are shown in Table D-2, and the yaw axis errors are shown in Table D-3.

The error terms used in the pointing accuracy aggregate equations are indicated in the tables by asterisks. Additionally, the terms for roll and yaw gyro alignment in Table D-3 were linearized by substituting the orbital rate ω_0 for the vehicle pitch rate ω_y in the multiplier.

2. PROPELLANT CONSUMPTION AGGREGATE EQUATIONS

a. RATE REDUCTION AND MANEUVERS

At various times during spacecraft life, the control system must stabilize the spacecraft from moderately high initial rates. Moderately high means that the spacecraft control system tends to operate linearly because the effects of a deadzone are negligible (except that the settling time is increased by the amount of time needed to traverse the deadzone). This is especially the case for a spacecraft (like the Agena) with pulse modulator controllers.

A simple model of a pulse modulator is a hysteresis switch with a lag network in the feedback. If the feedback lag network transfer function is

$$\frac{K_M}{\tau_M S + 1}$$

then the modulator can be linearized via the equivalent transfer function

$$K(\tau S + 1)$$

Table D-1. Pitch Axis Steady-State Errors

Error Sources	Multiplier	Sensitivity Coefficient
Pitch Gyroscope		
Linearity	ω_y	$1/H_{F_\theta}$
Roll alignment	ω_x	$1/H_{F_\theta}$
Yaw alignment	ω_z	$1/H_{F_\theta}$
G-insensitive drift	1	$1/H_{F_\theta}$
Horizon Sensor (pitch channel)		
Linearity	θ	H_θ/H_{F_θ}
Alignment	1	H_θ/H_{F_θ}
Noise*	$f_1(j\omega)$	H_θ/H_{F_θ}
Null*	1	H_θ/H_{F_θ}
Horizon anomalies*	1	H_θ/H_{F_θ}
Electronics		
Electronic gain mismatch	θ	$1/H_{F_\theta}$
Mechanization		
Euler cross coupling	$\phi\dot{\psi}$	$1/H_{F_\theta}$
Orbit rate mismatch* $(\omega_{0p} - \omega_0)$	1	$1/H_{F_\theta}$
Vehicle alignment*	1	1

*Major error sources

Table D-2. Roll Axis Steady-State Errors

Error Source	Multiplier	Sensitivity Coefficient
Yaw Gyroscope		
Linearity	ω_x	$1/(H_{F_\psi} + \omega_{01})$
Pitch alignment	ω_y	$1/(H_{F_\psi} + \omega_{01})$
Yaw alignment	ω_z	$1/(H_{F_\psi} + \omega_{01})$
G-insensitive drift	1	$1/(H_{F_\psi} + \omega_{01})$
Horizon Sensor (roll channel)		
Linearity	ϕ	$H_\psi/(H_{F_\psi} + \omega_{01})$
Alignment	1	$H_\psi/(H_{F_\psi} + \omega_{01})$
Noise*	$f_2(j\omega)$	$H_\psi/(H_{F_\psi} + \omega_{01})$
Null*	1	$H_\psi/(H_{F_\psi} + \omega_{01})$
Horizon anomalies*	1	$H_\psi/(H_{F_\psi} + \omega_{01})$
Electronics		
Electronic gain mismatch		
Roll electronics	$\dot{\phi}$	$1/[\omega_{02}(H_{F_\psi} + \omega_{01})]$
Yaw electronics	ϕ	$1/(H_{F_\psi} + \omega_{01})$
Cross coupling gain	$\dot{\psi}$	$1/[\omega_{02}(H_{F_\psi} + \omega_{01})]$
Mechanization		
Euler cross coupling	$\phi\dot{\theta}$	$1/(H_{F_\psi} + \omega_{01})$
Orbit rate mismatch $(\omega_0 - \omega_{01})$	ϕ	$1/(H_{F_\psi} + \omega_{01})$
$(\omega_{02} - \omega_0)$	$\dot{\psi}$	$1/\omega_{02}(H_{F_\psi} + \omega_{01})$
Vehicle alignment*	1	1

*Major error sources

Table D-3. Yaw Axis Steady-State Errors

Error Sources	Multiplier	Sensitivity Coefficient
Yaw Gyroscope		
Linearity	ω_z	$H_{F_\phi}/[\omega_{02}(H_{F_\psi} + \omega_{01})]$
Pitch alignment*	ω_y	$H_{F_\phi}/[\omega_{02}(H_{F_\psi} + \omega_{01})]$
Roll alignment	ω_x	$H_{F_\phi}/[\omega_{02}(H_{F_\psi} + \omega_{01})]$
G-insensitive drift*	1	$H_{F_\phi}/[\omega_{02}(H_{F_\psi} + \omega_{01})]$
Roll Gyroscope		
Linearity	ω_x	$1/\omega_{02}$
Pitch alignment*	ω_y	$1/\omega_{02}$
Yaw alignment	ω_z	$1/\omega_{02}$
G-insensitive drift*	1	$1/\omega_{02}$
Horizon Sensor (roll channel)		
Linearity	ϕ	$\dfrac{H_\psi H_{F_\phi} - H_\phi(H_{F_\psi} + \omega_{01})}{\omega_{02}(H_{F_\psi} + \omega_{01})}$
Alignment	1	$\dfrac{H_\psi H_{F_\phi} - H_\phi(H_{F_\psi} + \omega_{01})}{\omega_{02}(H_{F_\psi} + \omega_{01})}$
Noise	$f_3(j\omega)$	$\dfrac{H_\psi H_{F_\phi} - H_\phi(H_{F_\psi} + \omega_{01})}{\omega_{02}(H_{F_\psi} + \omega_{01})}$
Null*	1	$\dfrac{H_\psi H_{F_\phi} - H_\phi(H_{F_\psi} + \omega_{01})}{\omega_{02}(H_{F_\psi} + \omega_{01})}$
Horizon anomalies	1	$\dfrac{H_\psi H_{F_\phi} - H_\phi(H_{F_\psi} + \omega_{01})}{\omega_{02}(H_{F_\psi} + \omega_{01})}$

*Major error sources

Table D-3. Yaw Axis Steady-State Errors (Continued)

Error Sources	Multiplier	Sensitivity Coefficient
Electronics		
Electronic gain mismatch		
Roll electronics	ϕ	$1/[\omega_{02}(H_{F_\psi} + \omega_{01})]$
Yaw electronics	$\dot{\phi}$	$1/[\omega_{02}(H_{F_\psi} + \omega_{01})]$
Cross coupling ω_{02}	$\dot{\psi}$	
Mechanization		
Euler cross coupling	$\phi\dot{\theta}$	$H_{F_\phi}/[\omega_{02}(H_{F_\psi} + \omega_{01})]$
Euler cross coupling	$\theta\dot{\psi}$	$1/\omega_{02}$
Orbit rate mismatch		
$(\omega_{02} - \omega_0)$	ψ	$1/\omega_{02}$
$(\omega_0 - \omega_{01})$	ϕ	$H_\phi/[\omega_{02}(H_{F_\psi} + \omega_{01})]$
Vehicle alignment*	1	1

*Major error sources

where

$$K = 1/K_M$$

and

$$\tau = \tau_M.$$

Alternately, we can consider a linear controller with a rate gain of K and a rate gain divided by a position gain of τ. Then, again, the controller transfer function is $K(\tau S + 1)$. Under these assumptions, the spacecraft control loop for each axis can be represented as a second-order transfer function with natural frequency ω given by

$$\omega = (K/I)^{1/2}$$

and damping ratio ζ given by

$$\zeta = \omega\tau/2$$

where I is the inertia of the spacecraft axis under consideration.

When the response of the second-order loop to an impulsive torque (equivalently, an initial rate error) is considered, it is found that the absolute rate variation during convergence from an initial angular rate of $\dot{\theta}_0$ is

$$G_\zeta|\dot{\theta}_0| \qquad \text{(rad/sec)}$$

where

$$G_\zeta = (1 + 2e^{-\eta/2} + e^{-\eta})/(1 + e^{-\eta})$$

and

$$\eta = 2\pi/(1 - \zeta^2)^{1/2} \qquad \text{for} \qquad \zeta^2 < 1.$$

Absolute rate variation is defined as the sum of the absolute difference between successive rate peaks. Thus, if the initial rate is $\dot{\theta}_0$, the peak overshoot rate is $\dot{\theta}_1$, and the peak reversed overshoot is $\dot{\theta}_2$, then the absolute rate variation during the cycle is

$$|\dot{\theta}_1 - \dot{\theta}_0| + |\dot{\theta}_2 - \dot{\theta}_1|$$

The reason for computing the absolute rate variation is that the propellant required to remove a spacecraft rate (i.e., to remove spacecraft angular momentum) is independent of the sign of the rate.

The angular impulse required to stop the initial angular rate of $\dot{\theta}_0$ is the absolute rate variation times the inertia about the axis under consideration:

$$I\, G_\zeta |\dot{\theta}_0| \qquad \text{(N-m-sec)}$$

The linear impulse required is the angular impulse divided by the effective control lever arm ℓ:

$$\frac{I\, G_\zeta |\dot{\theta}_0|}{\ell} \qquad \text{(N-sec)}$$

It is assumed that the angular impulse is removed via thrusters that produce a control force at lever arm ℓ about the center of mass of the spacecraft. If the propellant specific impulse is I_{sp} (N-sec/kg), then the weight of propellant required to remove an initial rate of $\dot{\theta}_0$ on one control axis is

$$W_R = \frac{I\, G_\zeta |\dot{\theta}_0|}{\ell\, I_{sp}} \qquad \text{(kg)}$$

This is the propellant weight required, for example, to null a rate of $\dot{\theta}_0$ induced by the powered-flight controller at powered-flight termination.

If a maneuver is executed by inducing a rate $\dot{\theta}_0$ (e.g., by torquing a gyro), keeping this rate for a time t_m (where $\theta_m = \dot{\theta}_0 t_m$ is the maneuver angle), then the propellant consumption for the maneuver is

$$\frac{2I\,G\zeta|\dot{\theta}_0|}{\ell\,I_{sp}}$$

The factor 2 accounts for the initial rate error of $-\dot{\theta}_0$ at the start of the maneuver (when gyro torquing was begun), and a rate error of $+\dot{\theta}_0$ at the end of the maneuver (when gyro torquing was stopped). If there are N maneuvers, all at the rate $\dot{\theta}_0$ and all with the same spacecraft and controller parameters, the propellant weight required per control axis is

$$W_M = \frac{2N\,I\,G\zeta|\dot{\theta}_0|}{\ell\,I_{sp}}$$

If the maneuver occurs about more than one axis, the maneuvers about the separate axes are considered as separate maneuvers; this assumes that the maneuver angles and rates are small enough so that "Euler coupling" can be neglected.

b. COASTING FLIGHT

During the spacecraft life, when it is essentially quiescent, the propellant consumption is that required to maintain the spacecraft attitude at some fixed roll, pitch, and yaw orientation angles of ϕ_0, θ_0, ψ_0 (these angles are assumed "small," as in the case of earth pointing at a fixed target close to nadir). The propellant required during this attitude hold period can be conservatively estimated as the <u>sum</u> of two parts:

(1) Propellant consumption for limit-cycle motion

(2) Propellant consumption to counteract environmental disturbance torques.

A less conservative assumption would be to assume that (because of the disturbance torques), the controller operates almost always at one edge of the deadzone, so that only propellant consumption to counteract disturbance torques must be considered. However, if the control thruster impulse bit is large, and the disturbance torques are small, the propellant consumption is very nearly the propellant consumption for limit-cycle motion. Since generally (1) or (2) is small compared to the other, it is logical to add the two contributions to get a conservative bound.

(1) <u>Limit-Cycle Propellant Consumption</u>

If the change in spacecraft rate per minimum impulse bit thruster firing is $\Delta\dot{\theta}$ (so that the minimum impulse bit is $I\,\Delta\dot{\theta}$), and if the spacecraft is in a symmetric limit cycle, then the symmetric limit-cycle period is

$$P_{SLC} = 8D/\Delta\dot{\theta}$$

where D is the deadzone. Symmetric limit cycle means that the spacecraft rotates with a rate of $+\Delta\dot{\theta}/2$ from $\theta = -D$ to $\theta = +D$, then a thruster pulse is fired that changes the rate to $-\Delta\dot{\theta}/2$, then the spacecraft rotates with a rate of $-\Delta\dot{\theta}/2$ from $\theta = D$ to $\theta = -D$, another pulse is fired that changes the rate back to $+\Delta\dot{\theta}/2$, and the process continues.

Since two pulses are fired every period, the symmetric limit-cycle firing duty cycle γ_{SLC} is (in the absence of noise)

$$\gamma_{SLC} = 2/P_{SLC} = \Delta\dot{\theta}/4D \qquad \text{(no noise)}$$

There is usually some noise in the control signal that actuates the control thrusters. The effect of this noise is usually to reduce the deadzone effectively to D' where

$$D' \approx D - 2n_p/3$$

where n_p is the peak amplitude of the signal noise. The above approximation assumes that the controller (e.g., pulse modulator) has been designed properly, so as to avoid multiple firings at the edge of the deadzone. Thus, the symmetric limit-cycle duty cycle is better represented by

$$\gamma_{SLC} = \Delta\dot{\theta}/4D'$$

and D' reduces to D as $n_p \to 0$.

However, γ_{SLC} is too conservative an estimate of the firing duty cycle, because the spacecraft is usually not in a symmetric limit cycle. In fact, generally the duty cycle γ is lower than γ_{SLC}. If the rate from $\theta = -D$ to $\theta = +D$ is denoted by $\dot{\theta}_+ > 0$, and the rate from $\theta = +D$ to $\theta = -D$ is denoted by $\theta_- < 0$, then

$$\Delta\dot{\theta} = \dot{\theta}_+ - \dot{\theta}_-$$

and the limit cycle period P is given by

$$P = 2D' \, \Delta\theta/\dot{\theta}_+(\Delta\dot{\theta} - \dot{\theta}_+)$$

This reduces to P_{SLC} when $\dot{\theta}_+ = \Delta\dot{\theta}/2$. Thus, the firing duty cycle is

$$\gamma = 2/P = \dot{\theta}_+(\Delta\dot{\theta} - \dot{\theta}_+)/D' \, \Delta\dot{\theta}$$

Now $\dot{\theta}_+$ may have any value between 0 and $\Delta\dot{\theta}$, and all values in this range are equally probable. In fact, in the presence of an arbitrarily small disturbance torque, $\dot{\theta}_+$ will actually slowly range through this region at a rate proportional to the (small) disturbance torque. Thus, the average firing duty cycle $\overline{\gamma}$ can be computed from

$$\bar{\gamma} = \frac{1}{\Delta\dot{\theta}} \int_0^{\Delta\dot{\theta}} \gamma d\dot{\theta}_+$$

$$= \frac{1}{D'(\Delta\dot{\theta})^2} \int_0^{\Delta\dot{\theta}} (\Delta\dot{\theta}\ \dot{\theta}_+ - \theta_+^2)\ d\dot{\theta}_+$$

$$= \frac{\Delta\dot{\theta}}{6D'}$$

$$= \frac{2\gamma_{SLC}}{3}$$

Thus, the average limit-cycle firing duty cycle is 2/3 of the symmetric limit-cycle firing duty cycle.

Since each firing represents the angular impulse consumption ΔH of

$$\Delta H = I\ \Delta\dot{\theta} \qquad \text{(N-m-sec)}$$

the limit-cycle angular impulse consumption for a spacecraft lifetime t_L is

$$\bar{\gamma}\ \Delta H\ t_L \qquad \text{(N-m-sec)}$$

Dividing by the effective lever arm ℓ yields the linear impulse consumption

$$\frac{\bar{\gamma}\ \Delta H\ t_L}{\ell} \qquad \text{(N-sec)}$$

and dividing by the propellant specific impulse I_{sp} yields the propellant limit-cycle weight consumption W_{LC} given by

$$W_{LC} = \frac{\bar{\gamma}\ \Delta H\ t_L}{\ell\ I_{sp}} \qquad \text{(kg)}$$

Substituting the expressions

$$\overline{\gamma} = \frac{2}{3} \cdot \frac{\Delta\dot{\theta}}{4D'}$$

$$\Delta H = I \, \Delta\dot{\theta}$$

the propellant consumption (per control axis) is

$$W_{LC} = \frac{I(\Delta\dot{\theta})^2}{6\ell \, I_{sp}} \frac{t_L}{D'}$$

(2) Disturbance Torque Propellant Consumption

For any coasting flight disturbance torque, T_D, the propellant weight consumption, W_D, during the life of the spacecraft, t_L, can be conservatively estimated from

$$W_D = \frac{T_D \, t_L}{\ell \, I_{sp}} \qquad \text{(kg)}$$

The environmental disturbance torques which need to be considered for an earth satellite are:

(a) Orbit rate and gravity gradient
(b) Magnetic
(c) Aerodynamic
(d) Solar.

The effects of micro-meteorite impact are generally negligible; the effects of internal motion (e.g., antenna slewing and crew movement) will be neglected, since there is no internal motion in an Agena-type spacecraft. The disturbance torque during powered flight will be considered in Section D.2.c.

(3) Disturbance Torque Descriptions

(a) Orbit Rate and Gravity Gradient

For a circular orbit with orbit rate ω_0, there is a disturbance torque due to orbit rate and the earth's gravity gradient, if the spacecraft is pointing with roll, pitch, and yaw offset angles ϕ_0, θ_0, and ψ_0, respectively. The disturbance torques, about the roll, pitch, and yaw axes T_x, T_y, and T_z, respectively, are approximately given by

$$T_x \quad -G_x \; \phi_0$$

$$T_y \quad -G_y \; \theta_0$$

$$T_z \quad -G_z \; \psi_0$$

where

$$G_x \quad 4\omega_0^2 \, (I_y - I_z)$$
$$G_y \quad 3\omega_0^2 \, (I_x - I_z)$$
$$G_z \quad \omega_0^2 \, (I_y - I_x)$$

and where I_x, I_y, I_z are the roll, pitch, and yaw principal moments of inertia. Note that even if the spacecraft geometric axes are pointing exactly at nadir, the orbit rate and gravity gradient disturbance torques still are non-zero if the principal axes of inertia are misaligned from the geometric axes by ϕ_0, θ_0, and ψ_0.

For a circular orbit, ω_0^2 is given by

$$\omega_0^2 = G_E / r_0^3$$

where G_E is the earth's gravitational constant

$$G_E \approx 4 \times 10^{14}\ m^3/sec^2\ (1.41 \times 10^{16}\ ft^3/sec^2)$$

and r_0 is the spacecraft orbital radius. If h_0 is the spacecraft orbital altitude, then

$$r_0 = R_E + h_0$$

where R_E is the radius of the earth

$$R_E \approx 6.37 \times 10^6\ m\ (2.09 \times 10^7\ ft).$$

(b) Magnetic Disturbance Torque

The peak magnetic disturbance torque is given by

$$T = mB$$

where m is the spacecraft magnetic moment and B is the earth's magnetic field at the spacecraft. The spacecraft's magnetic moment is usually estimated as that due to an equivalent current i_{eq}, circulating about an equivalent area A_{eq}:

$$m = i_{eq} A_{eq} \qquad (\text{amp-turn-m}^2)$$

The magnitude of the earth's magnetic field is approximately that of ideal dipole, whose peak value is

$$B_{peak} = m_E/r_0^3$$

where r_0 is the spacecraft orbital radius, and m_E is given by

$$m_E \approx 8.07 \times 10^{15} \frac{(\text{N-m})(\text{m}^3)}{(\text{amp-turn-m}^2)} \left(1.95 \times 10^{16} \frac{(\text{ft-lb})\ (\text{ft}^3)}{(\text{amp-turn-ft}^2)}\right).$$

(c) Aerodynamic Disturbance Torque

The peak aerodynamic disturbance torque is approximately given by

$$T = (1/2)\, \rho_0\, V_a^2\, A_a\, \ell_a$$

where ρ_0 is the air density at the spacecraft; V_a is the spacecraft's air speed [$(1/2)\, \rho\, V_a^2$ is the dynamic pressure]; A_a is the spacecraft's aerodynamic area in the direction of the air speed (a function of the aerodynamic reflectivity); and ℓ_a is the aerodynamic force lever arm (the distance between the spacecraft center of mass and the aerodynamic center of pressure). Aerodynamic forces and torques are only significant for low-altitude spacecraft [<1100 km (600 nmi) altitude]; in the region between 185 and 1100 km (100 to 600 nmi), the air density is approximately (within 25%) given by

$$\rho_0 = a_0\, h_0^{-b_0} \qquad (\text{kg/m}^3)$$

where h_0 is the spacecraft altitude in meters, and a_0 and b_0 are constants:

$$a_0 \approx 1.51 \times 10^{19}$$

$$b_0 \approx 5.365.$$

The spacecraft air speed is given by the spacecraft orbital speed minus the speed of the air. Assuming that the air is "rigidly" attached to the earth, the air speed at the spacecraft is

$$\omega_E r_0$$

where ω_E is the earth's rotation rate

$$\omega_E \approx 7.27 \times 10^{-5} \text{ rad/sec.}$$

The spacecraft orbital speed is

$$\omega_0 r_0$$

Thus, the spacecraft's air speed is

$$V_a = (\omega_0 - \omega_E) r_0$$

$$V_a \approx \omega_0 r_0 \qquad \text{for} \qquad \omega_0 \gg \omega_E$$

(d) Solar Disturbance Torque

The peak solar disturbance torque is approximately given by

$$T = P_S A_S \ell_S$$

where P_S is the solar pressure constant

$$P_S \approx 4.8 \times 10^{-6} \text{ N/m}^2 \ (10^{-7} \text{ lb/ft}^2)$$

A_S is the solar force area of the spacecraft (a function of the solar reflectivity), and ℓ_S is the solar force lever arm.

Solar forces and torques are independent of spacecraft altitude, since the distance to the sun is essentially constant for an earth satellite.

However, the solar torques are usually only significant when the other disturbance torques are small (i.e., for high altitude spacecraft).

c. POWERED FLIGHT

(1) Disturbance Torque

There are two cases to be considered: fixed ΔV engine and gimbaled ΔV engine. Large-thrust engines used for orbit-to-orbit transfer are gimbaled in pitch and yaw to provide the required pitch and yaw control torques, leaving only roll axis control propellant consumption to be considered. Smaller thrusters, used for stationkeeping and docking, for example, are usually not gimbaled, and produce disturbance torques on all three control axes. The equations for the latter case are easily derived. Taking the standard vehicle coordinate system (as shown in Figure D-1) through the vehicle center of mass, define (for the nominal thrust along the roll axis):

x_e = distance from center of mass to engine
δ_y = engine offset from roll axis in y
δ_z = engine offset from roll axis in z
θ_e = pitch angular engine misalignment
ψ_e = yaw angular engine misalignment
F = engine thrust.

The vector expression for torque is

$$\bar{T} = \bar{r} \times \bar{F}$$

where, for our definitions, the components of $\bar{r}$ and $\bar{F}$ for small θ_e and ψ_e are

$$\bar{r} = (-x_e, \delta_y, \delta_z)$$

$$\bar{F} = (F, F\psi_e, - F\theta_e).$$

Evaluating the cross product, we obtain

$$\text{Roll:} \qquad T_x = F(-\delta_y \theta_e - \delta_z \psi_e)$$

$$\text{Pitch:} \qquad T_y = F(\delta_z - x_e \theta_e)$$

$$\text{Yaw:} \qquad T_z = F(-\delta_y - x_e \psi_e)$$

The roll torque is a second-order effect and can be neglected.

For a gimbaled engine, the flight control system points the thrust nominally through the center of gravity, reducing the above torques to zero. The roll torque must go to zero along with pitch and yaw, as will now be shown. For pitch and yaw torques equal to zero, we have

$$\delta_z = x_e \theta_e$$

$$-\delta_y = x_e \psi_e$$

When these expressions are substituted into the equation for roll torque, the result is zero. The only sources of roll torque, then, are steering actions of the flight control system in pitch and yaw, which couple into roll through the engine offsets, and torques from other equipment, such as ullage rocket misalignment and turbine exhaust misalignment. The roll torque is not negligible because of the large thrust of the main engine. The exact equation is dependent on both the vehicle configuration and the powered-flight attitude profile, and thus will here be expressed as a general function of the pertinent variables:

$$T_x = \mathscr{F}\left\{F, \delta_y, \delta_z, \text{pitch profile, yaw profile, ullage engine misalignment, turbine exhaust misalignment}\right\}$$

The expressions for fuel consumption due to the disturbance torques are

$$\text{Roll:} \qquad W_{p_x} = \frac{T_x t_p}{\ell_x I_{sp}}$$

$$\text{Pitch:} \qquad W_{p_y} = \frac{T_y t_p}{\ell_y I_{sp}}$$

$$\text{Yaw:} \qquad W_{p_z} = \frac{T_z t_p}{\ell_z I_{sp}}$$

where

ℓ_x = roll control moment arm
ℓ_y = pitch control moment arm
ℓ_z = yaw control moment arm
t_p = time of powered flight
I_{sp} = specific impulse.

(2) <u>ΔV Fuel Consumption</u>

We will here determine the ΔV to deliver a payload from a low earth orbit to a synchronous earth orbit and return. The following is an analysis to determine the amount of fuel required to perform such a mission. The mass of fuel required for a powered-vehicle flight can be determined by the following expression:

$$m_F = m_V[\exp(\Delta V/I_{sp}) - 1]$$

where

ΔV = required velocity change as determined by the mission
I_{sp} = specific impulse of propellant (N-sec/kg)

m_V = mass of vehicle without fuel

m_F = mass of fuel.

The required velocity change ΔV can be computed in terms of the orbital parameters

$$\Delta V_1 = V_{H_1} - V_{LEO}$$

$$\Delta V_2 = V_{SEO} - V_{H_2}$$

$$\Delta V = 2(\Delta V_1 + \Delta V_2)$$

where

V_{H_1} = velocity for injection into Hohmann transfer ellipse

V_{H_2} = velocity for injection into synchronous orbit

V_{LEO} = velocity in low-earth orbit

V_{SEO} = velocity in synchronous earth orbit

$V_{LEO}^2 = GM/a_{LEO}$

$V_{SEO}^2 = GM/a_{SEO}$

$V_{H_1}^2 = GM\left\{\frac{2}{a_{LEO}} - \frac{1}{a_H}\right\}$

$V_{H_2}^2 = GM\left\{\frac{2}{a_{SEO}} - \frac{1}{a_H}\right\}$

and where

G = universal gravitational constant

M = mass of earth

a_{LEO} = semi-major axis of low earth orbit

a_{SEO} = semi-major axis of synchronous earth orbit

a_H = semi-major axis of Hohmann orbit.

The tankage volume, mass, and radius can be estimated by the following relationships:

$$V_F = m_F/\rho_F$$

$$m_T = \rho_T \, 4\pi \, r^2 t$$

$$r = \left(\frac{3V_F}{4\pi}\right)^{1/3}$$

where

V_F = volume of fuel
ρ_F = density of fuel
m_F = mass of fuel
r = radius of a spherical tank
t = thickness of tank
ρ_T = density of tank structural material
m_T = mass of fuel tanks.

3. SAFETY AGGREGATE EQUATIONS

a. FAILURE RATE

The failure rate for each module in the system will be determined by

$$\lambda_i = \sum_{j=1}^{n} k_j \left[d_j \lambda_{ji} + (1 - d_j) q_j \lambda_{ji}\right]$$

where

j = jth part of the n parts contained in module i
k_j = environmental stress factor associated with the jth part
d_j = duty cycle factor associated with the jth part, and $0 \le d_j \le 1$

λ_{ji} = failure rate of the jth part in module i, assumed constant for a given mode of operation

q_j = dormancy factor (the ratio of the failure rate in a dormant mode to that in an active mode) for the jth part, and $0 \leq q_j \leq 1$.

This expression assumes that all parts in module i are essential for its function, which is a conservative approach.

The environmental stress factor k will be a function of the mission profile; it will be high during high stress (boost, kick) and low during low stress periods (coast).

The probability of successful module performance (module reliability) during a time interval (t_a, t_b) is assumed to be exponential, and given by

$$R_i(t_a, t_b) = \exp[-\lambda_i(t_b - t_a)]$$

for the ith module.

The total mission time interval (0, t) consists of a collection of subintervals $(0, t_1)$, (t_1, t_2), (t_2, t_3), etc., each with a different environment, stress, or duty cycle profile. Therefore, the mission reliability for the ith module, i.e., the probability of the ith module's surviving a mission of length t, is

$$R_i(t) = \prod_{k=0}^{m} R_i(t_k, t_{k+1})$$

where

$$t \equiv t_{m+1}.$$

Using the reliability functions for individual modules, one can construct a total system reliability function R_S by considering modular redundancy within the system. This function R_S has been constructed for the three

ACS configurations being considered; these expressions are shown in subsequent paragraphs. The reliability function R_S is really $R_S(t)$ and will vary not only due to t but due to variations in mission environments and usages in the subintervals (t_k, t_{k+1}).

Using the mathematical expression for $R_S(t)$, one can calculate the probability of system survival at the end of a given subinterval, assuming that the system was operable at the beginning of that subinterval. The probability of successful system operation over the entire mission is then the product of the subinterval survival probabilities.

The reliability functions derived in the following paragraphs are for individual subintervals.

The base failure rates λ_{ji} can be derived from appropriate orbital experience with parts that are screened and burned in at specified levels. Adequate derating and thermal control must be employed. Environmental k-factors can be taken from MIL-HDBK-217A(Ref. 1)/RADC Reliability NTBK (Ref. 2) and allied sources. The dormancy factors (q's) will be based on the following philosophy:

a. q is high (~1.0) for high reliability, low stress parts.

b. q is medium for MIL parts.

c. q is low (~0.1) for high stress parts or parts without extensive history.

(1) Single-String ACS

The reliability model for a single-string ACS is sketched in Figure D-2.

The system failure rate is the sum of the individual module failure rates. The system reliability $R_S(t)$ is given by

$$R_S(t) = \exp(-\lambda_a t)$$

It is evident that successful ACS operation requires successful function of each module; i.e., there is no redundancy, and each module constitutes a single point failure hazard.

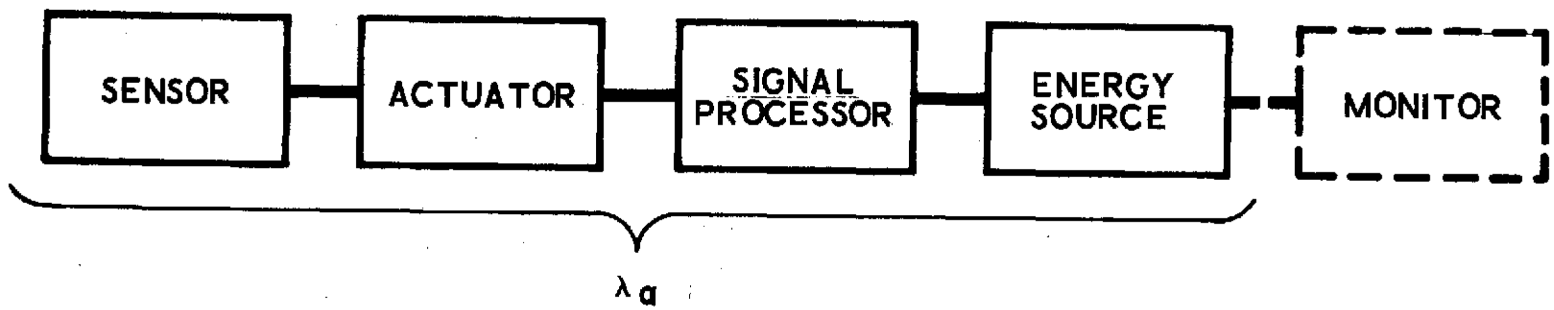

Figure D-2. Reliability Model for Single-String ACS

(2) Active ACS, with Switched Standby ACS

The reliability model for one active ACS and one standby ACS is shown in Figure D-3. This model assumes that all necessary monitoring is performed. The failure rate of the ith model in this standby string, while in the dormant mode, is given by

$$\lambda_i' = \sum_{j=1}^{n} k_j q_j \lambda_{ji}$$

The probability of the standby string not failing in the time interval (0, t), while in a dormant state, is given by

$$R_{ACS}(t) = \exp(-\lambda_a' t)$$

To assess the effect of the redundancy on overall ACS reliability, one must include the switch as shown, by failure modes. Note that this is a generalized switching mechanism; it may actually consist of many solenoids, valves, relays, electrical toggles, etc.

The probability of the ACS function being performed in the interval (0, t) by either the active string or the backup string [the reliability, $R_S(t)$] is given by

$$\begin{aligned} R_S(t) = \exp\left[-\left(\lambda_{s_1} + \lambda_{s_2}\right)t\right] \Bigg[& \exp\left[-\left(\lambda_a + \lambda_{s_3} + \lambda_{m_1}\right)t\right] \\ & + \frac{\left(\lambda_a + \lambda_{s_3} + \lambda_{m_1}\right)}{\left(q\lambda_a + \lambda_{s_3} + \lambda_{m_1} + \lambda_{s_4} + \lambda_{m_2} - \lambda_{m_3} - \lambda_{s_5}\right)} \\ & \times \exp\left[-\left(\lambda_a + \lambda_{m_3} + \lambda_{s_5}\right)t\right] \\ & \times \left\{1 - \exp\left[-\left(q\lambda_a + \lambda_{s_3} + \lambda_{m_1} + \lambda_{s_4} + \lambda_{m_2} \right.\right.\right. \\ & \left.\left.\left. - \lambda_{m_3} - \lambda_{s_5}\right)t\right]\right\}\Bigg] \end{aligned}$$

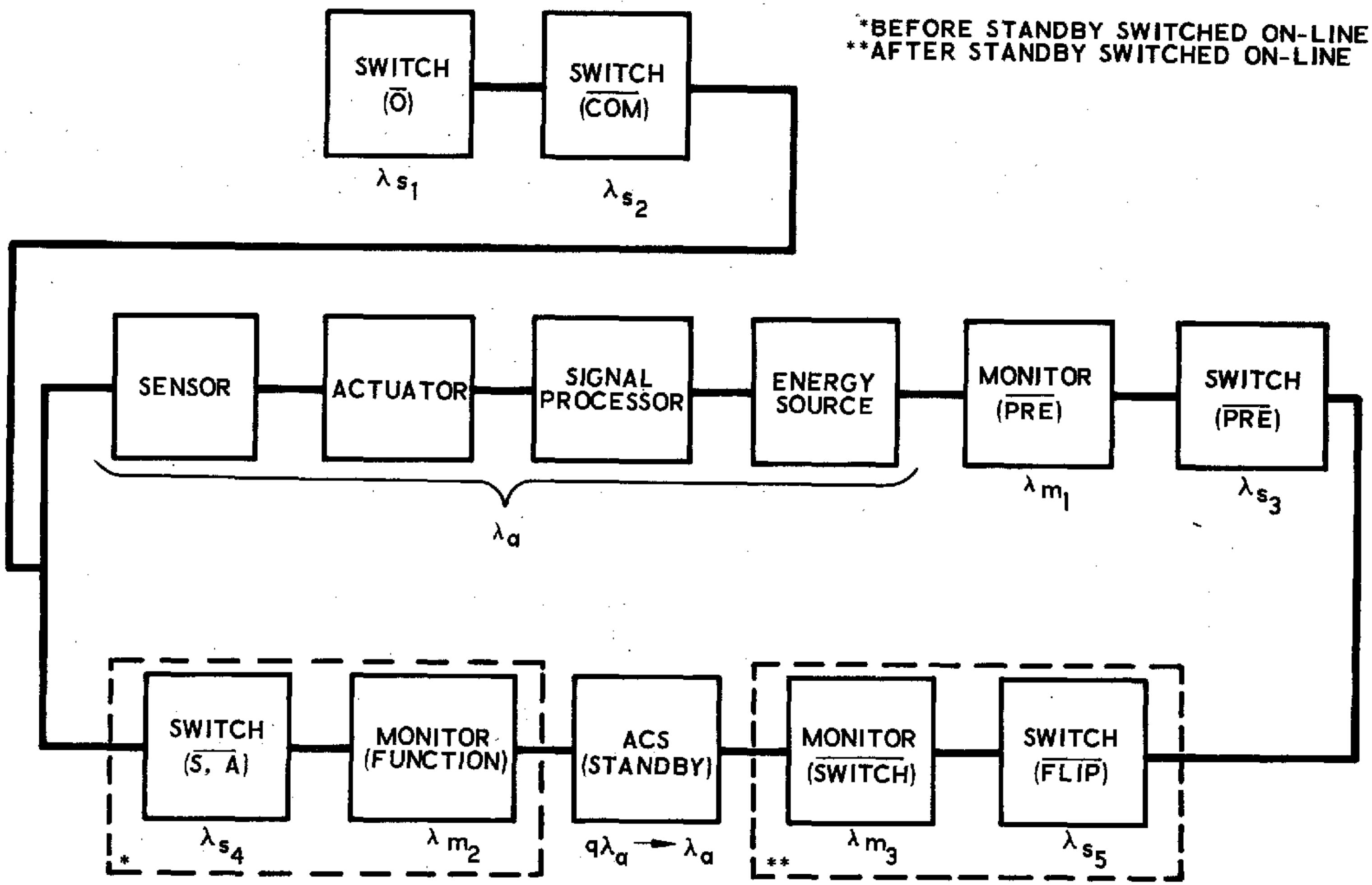

Figure D-3. Reliability Model for Active ACS with Switched Standby ACS

where

λ_{s_1} = rate of switch failures open

λ_{s_2} = rate of switch failures common, i.e., both ACSs actuated

λ_{m_1} = rate of monitor prematurely commanding switch to change state

λ_{s_3} = rate of switch changing state without command from monitor

λ_{s_4} = rate of switch failing to actuate on command

λ_{m_2} = rate of monitor failing to detect failure of active unit

λ_{m_3} = rate of monitor commanding switching from standby unit back to disabled active unit

λ_{s_5} = rate of switch changing state to put failed active unit on line, without command from monitor

$q\lambda_a = \lambda_a'$ as defined above.

(3) Triply Active ACS with Voting

A reliability model for the triple ACS with voting is shown in Figure D-4. The monitor signal processors are triply redundant (active) to reduce the impact of failure there.

The probability of successful operation R_S for this system is given by

$$R_S(t) = R_V\left[(R_A R_{SP})^3 + 3(R_A R_{SP})^2 (1 - R_A R_{SP}) + 3R_A R_{SP}(1 - R_A R_{SP})^2\right]$$

or

$$R_S(t) = R_V\left[1 - (1 - R_A R_{SP})^3\right]$$

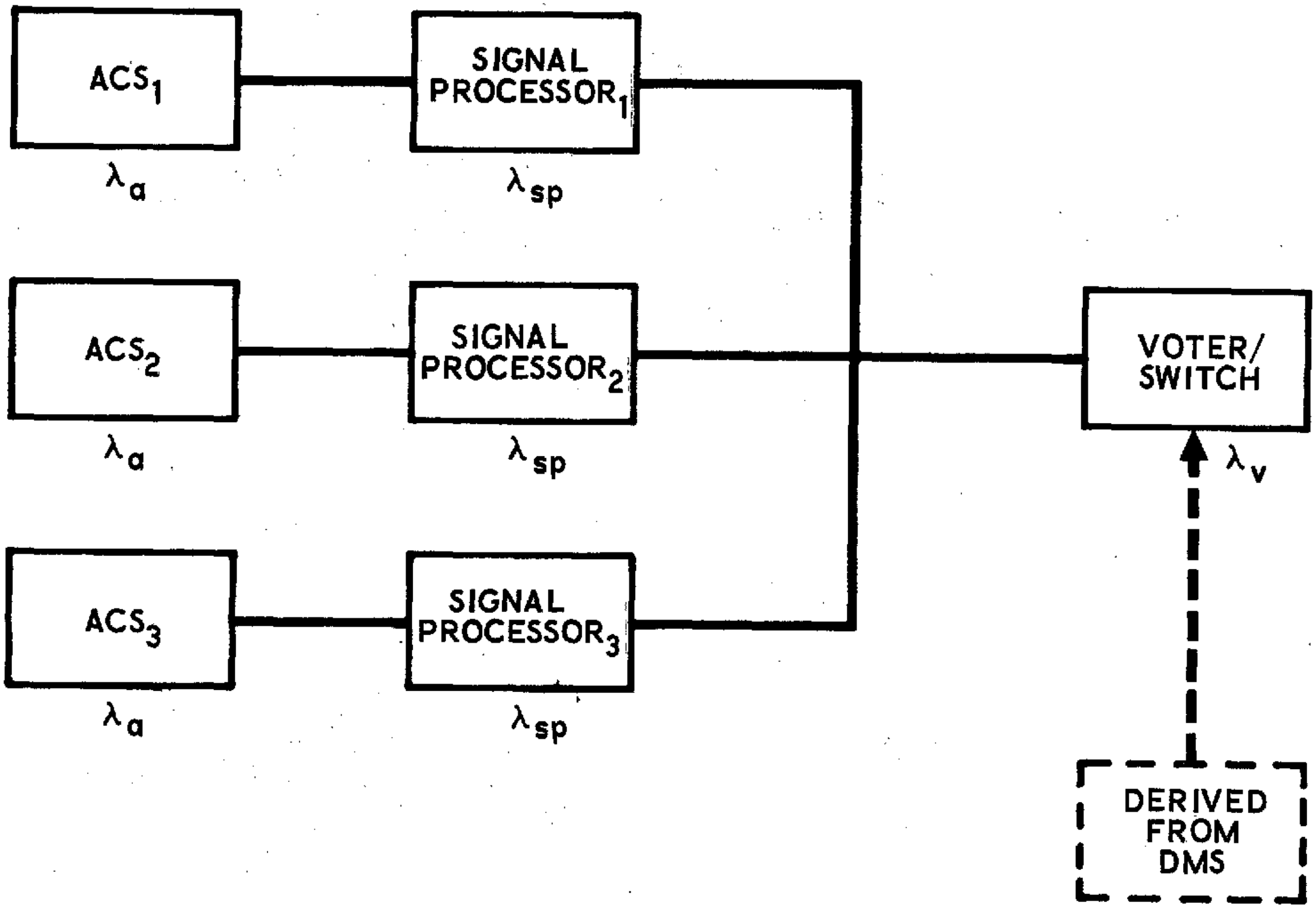

Figure D-4. Reliability Model for Triple ACS With Voting

where

R_V = probability of successful voter/switch operation

R_A = probability of successful operation of one ACS

R_{SP} = probability of successful operation of one signal processor.

From the expression for R_S, it can be seen that only one of the three ACS signal processing units is required, plus the voter, for successful system operation. However, the case of two units up and one down presents a problem in implementation; with two inputs, which does the voter choose as correct; i.e., how can it select a failure from two inputs? One solution to this problem is the submission to the voter of "derived data from the Data Management System (DMS). This data is generated by the DMS from previous ACS outputs known to be valid. Its accuracy is lacking, but its presence permits the voter to detect gross anomalies in the output of one of two ACS/SP units. The reliability of this derived data is not included in the following calculations, but its availability is assumed.

In accordance with the assumptions,

$$R_S(t) = \exp(-\lambda_v t)\left[1 - \left\{1 - \exp[-(\lambda_a + \lambda_{sp})t]\right\}^3\right]$$

The voter/switch constitutes a single point failure in the ACS; i.e., a failure in the voter/switch will result in loss of the ACS function entirely. In this regard, the reliability of this triple redundancy with voting scheme is an improvement over the reliability of the single-string ACS only if

$$R_S > R_A$$

or

$$R_V > \frac{1}{R_{SP}}\left[3 - 3R_A R_{SP} + (R_A R_{SP})^2\right]^{-1}$$

If R_{SP} and R_{ACS} are nearly one — i.e., if $R_A = R_{SP} = 1 - \epsilon$ for ϵ small, (for example, less than 0.1) — then the above implies that

$$R_V > \left[(1 - \epsilon)\ (1 + 2\epsilon + 3\epsilon^2 - 4\epsilon^3 + \epsilon^4)\right]^{-1} > (1 - \epsilon)^2 \approx R_A\ R_{SP}\ .$$

Then, $R_S > R_A$ implies $R_V > (R_A \times R_{SP})$, which, in view of the probable equipment complexities, is certainly feasible. If this condition is met, then the triply redundant system with voting is more reliable than a single-string ACS, in spite of the single point failure represented by the voter/switch.

b. FAILURE DETECTION PROBABILITY

The probability, P_D, of detection of a system or module failure, which is the probability of detection of an out-of-specification condition of any functional parameter, is determined as

$$P_D = P(X)\ P(M)$$

where

$P(X)$ = Probability that the out-of-specification parameter was monitored by the failure detection system subsequent to the failure.

$P(M)$ = probability that the monitoring system is functioning properly at the time of the failure.

The concept is shown in Figure D-5.

$P(X)$ is determined by system design. $P(X)$ may be represented as (See Figure D-6)

$$P(X) = \frac{\text{number of failures detectable by monitoring system}}{\text{total number of failures}}$$

In actuality, parameters are monitored and not failures directly. It was judged that $P(X)$ should be expressed as a function of parameters rather than failures, since this information would be available earlier in the system design process. Under the assumptions that the equipment represented by

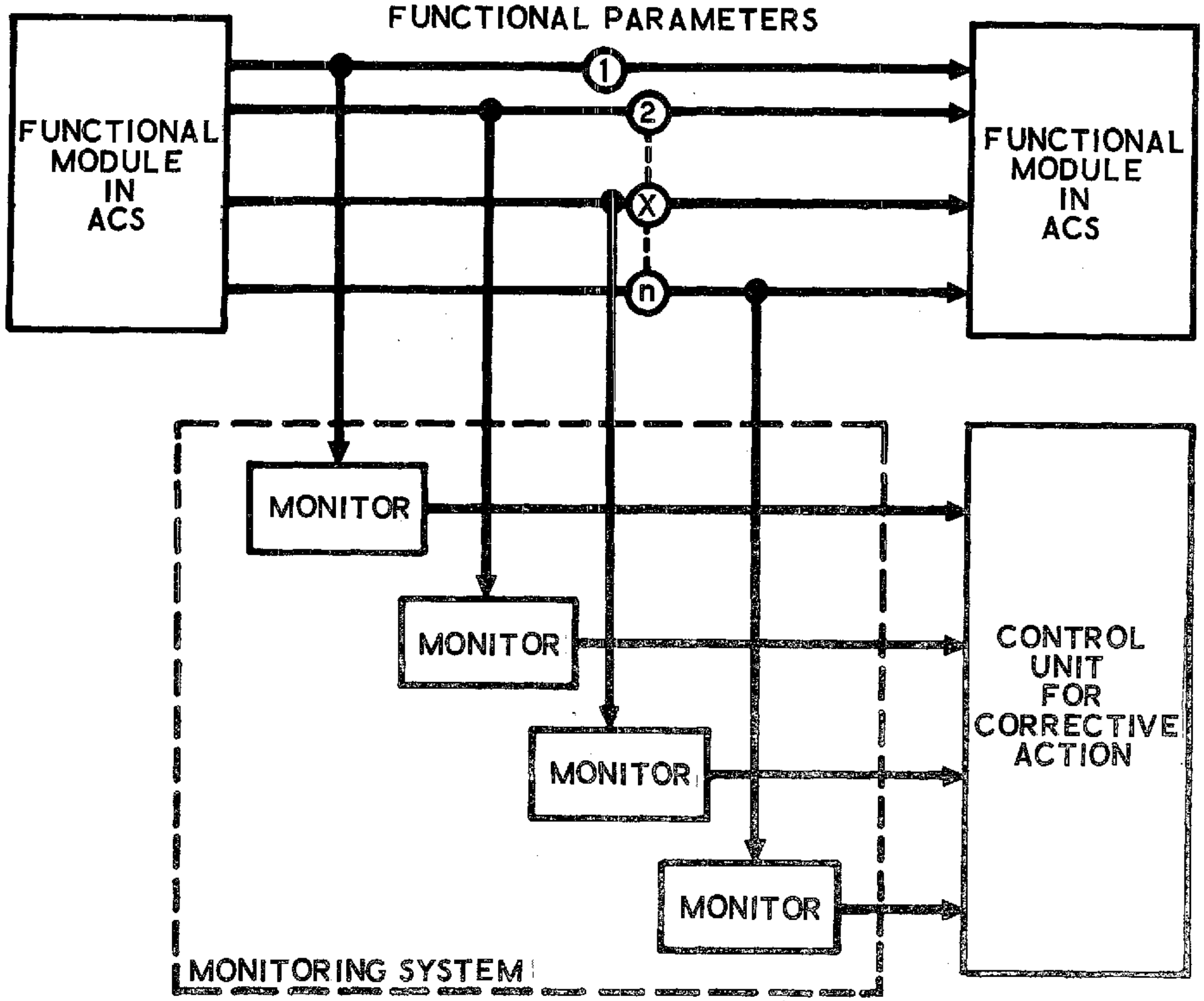

Figure D-5. Failure Detection System

FAILURE DETECTION PROBABILITY

- ON-BOARD CHECKOUT SYSTEM
  - CHECK TO SEE WHAT EQUIPMENT IS BEING USED TO MEET PERFORMANCE AND FAILURE RATE REQUIREMENTS (via Table 1-1)
  - TOTAL FAILURES $= \sum_{i=1}^{K} N_i M_i = TF$

    WHERE N_i = TOTAL NUMBER OF PARTS OF TYPE i

    i = 1, SENSOR

    = 2, ACTUATOR, etc.

    M_i = PART TOLERANCE^{-1}
  - COMPUTE DF (total failures that must be detected) $= TF \cdot p$

    WHERE p = FAILURE DETECTION PROBABILITY
  - ASSUME IT TAKES "10" COMPUTER OPERATIONS TO DETECT ONE FAILURE
  - TOTAL NUMBER OF COMPUTER OPERATIONS NEEDED = 10 DF
  - TOTAL NUMBER OF LEVELS $= \sum_{i=1}^{K} M_i$
  - $2^x = \sum_{i=1}^{K} M_i$, SOLVE FOR x

Figure D-6. Alternate Failure Detection Aggregate Equations each functional parameter has equal likelihood of failure, and that only one functional parameter is affected by any single failure, the following approximation may be made

$$P(X) \cong \frac{\text{number of parameters monitored}}{\text{total number of functional parameters}}$$

P(M) is the reliability of the monitoring system. In general, there will be more than one monitoring subsystem, each designed to monitor different parameters (e.g., voltage, pressure, temperature). $P(M_X)$ is the reliability of that portion of the monitoring system that monitors a given parameter X. All monitoring subsystems are required to function to maximize failure detection probability. Then, as in Figure D-5

$$P(M_X) \equiv R_{M_X}(t) = \exp\left(-\lambda_{m_X} t\right)$$

and

s

$$R_M(t) = \prod_{X=1}^{n} R_{M_X}(t) = \exp\left(-\sum_{X=1}^{n} \lambda_{m_X} t\right)$$

where

λ_{m_X} = failure rate of that portion of the monitoring system assigned to parameter X, one of n parameters monitored

$R_M(t)$ = reliability (probability of successful operation to time t) of the entire monitoring system.

Then, the probability of detection $P_D(t)$ of any failure in the system to time t is given by

$$P_D(t) = \frac{n}{N} \exp\left(-\sum_{X=1}^{n} \lambda_{m_X} t\right)$$

where N is the total number of functional parameters.

A reliability diagram for this system is shown in Figure D-7.

(1) Single-String ACS

The reliability model of Figure D-7 is applicable to the series case. The expression for the failure detection probability is

$$P_D(t) = \frac{n}{N} \exp\left(-\sum_{X=1}^{n} \lambda_{m_X} t\right)$$

as before.

(2) Active ACS, with Switched Standby ACS

The reliability model for this case is shown in Figure D-8. The expression for the failure detection probability is

$$P_D(t) = \left[\frac{N(n + n') - nn'}{N^2}\right] \exp\left(-\sum_{X=1}^{n+n'} \lambda_{m_X} t\right)$$

where n' is the number of monitored parameters on the backup ACS while it is in the standby mode. There may be less than $(n + n')$ terms on the right-hand side of this expression, if the monitor subsystem is time-shared between the active and standby systems.

(3) Triply Active ACS with Voting

The reliability model for this case is shown in Figure D-9. The expression for the failure detection probability is given by

$$P_D(t) = \frac{3n}{3N} \exp[-(\lambda_v - \lambda_s)t]$$

where $(\lambda_v - \lambda_s)$ is the failure rate of the voter only, excluding the switch.

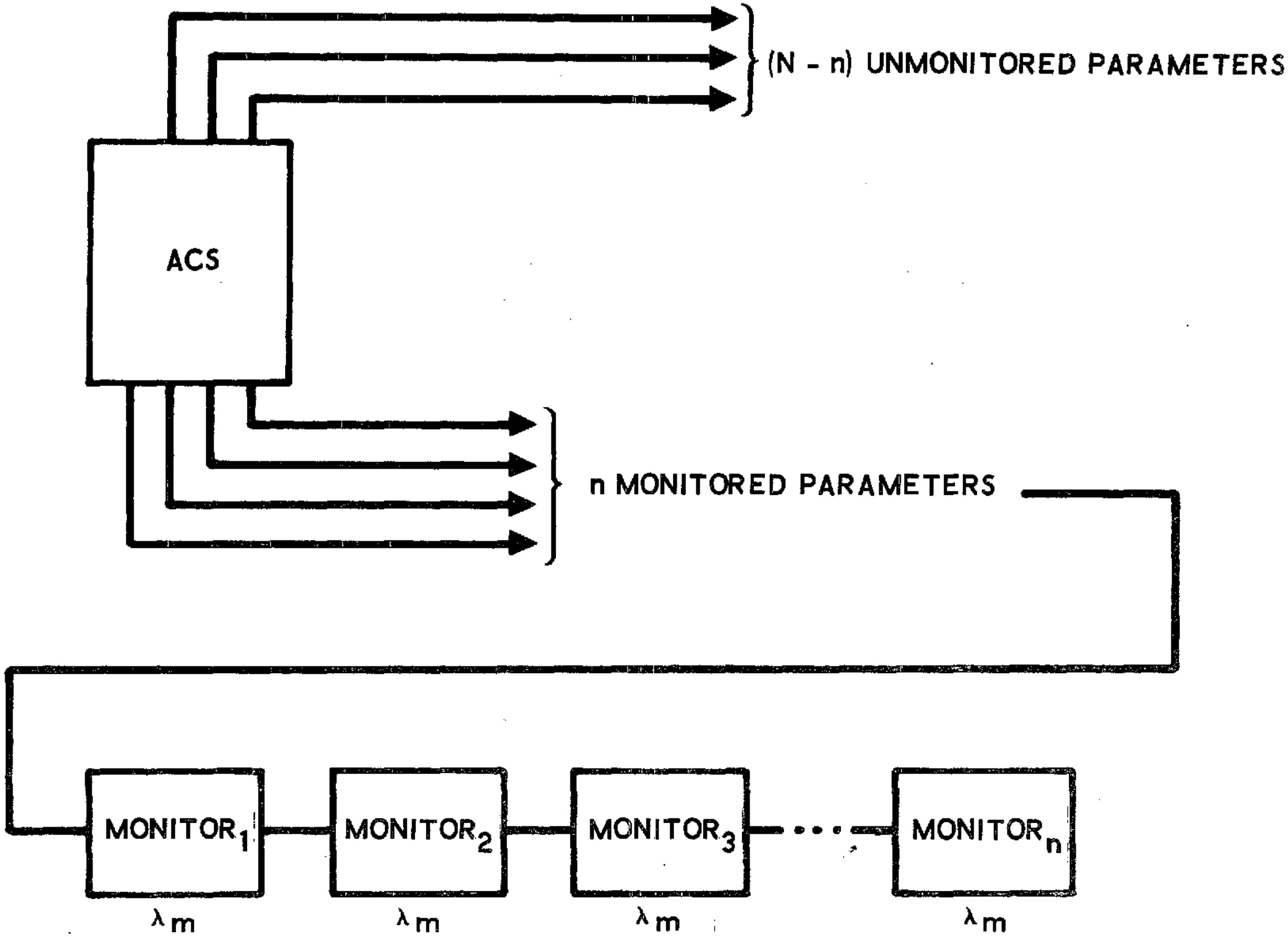

Figure D-7. Reliability Model of Failure Detection System

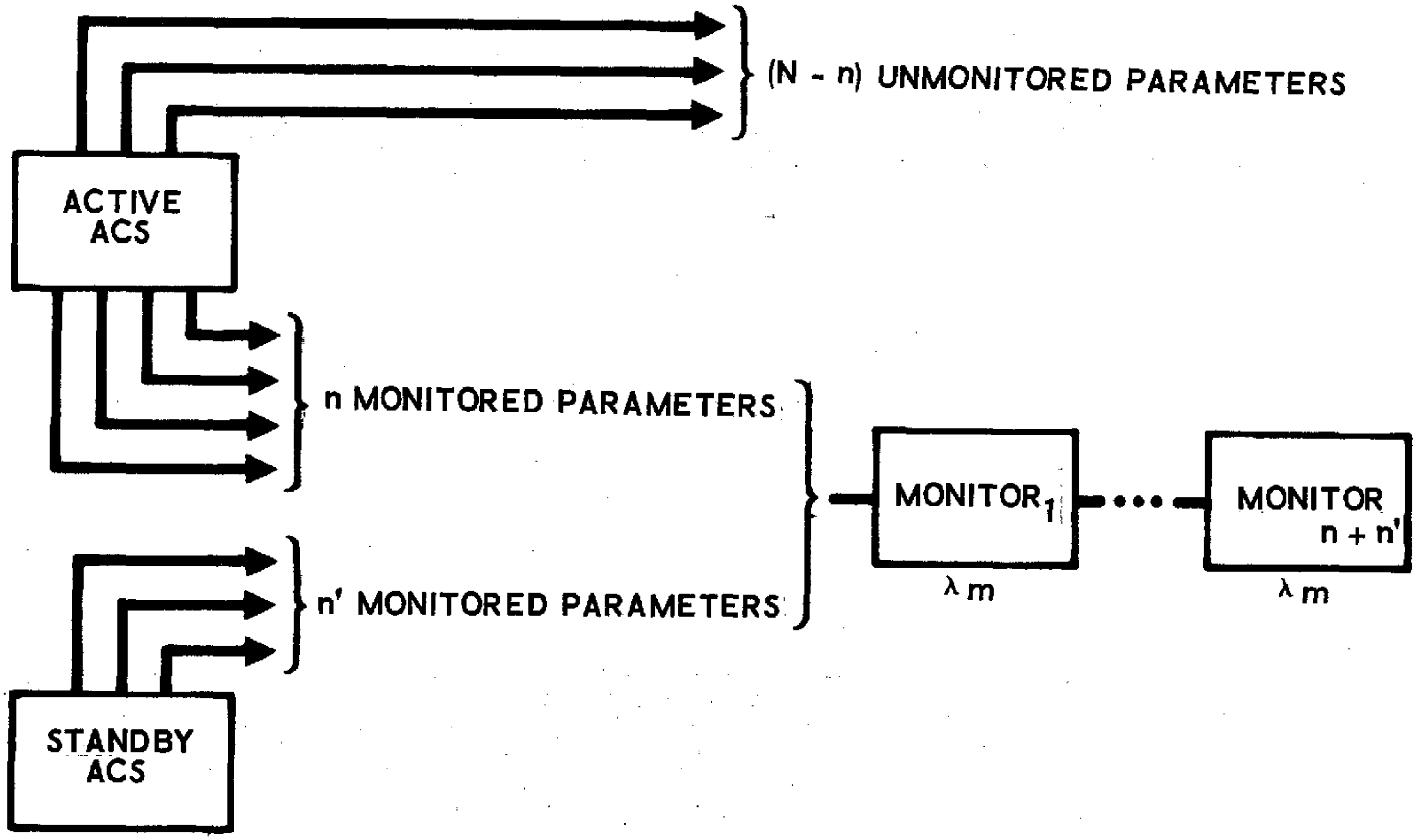

Figure D-8. Reliability Model for Active ACS with Switched Standby ACS

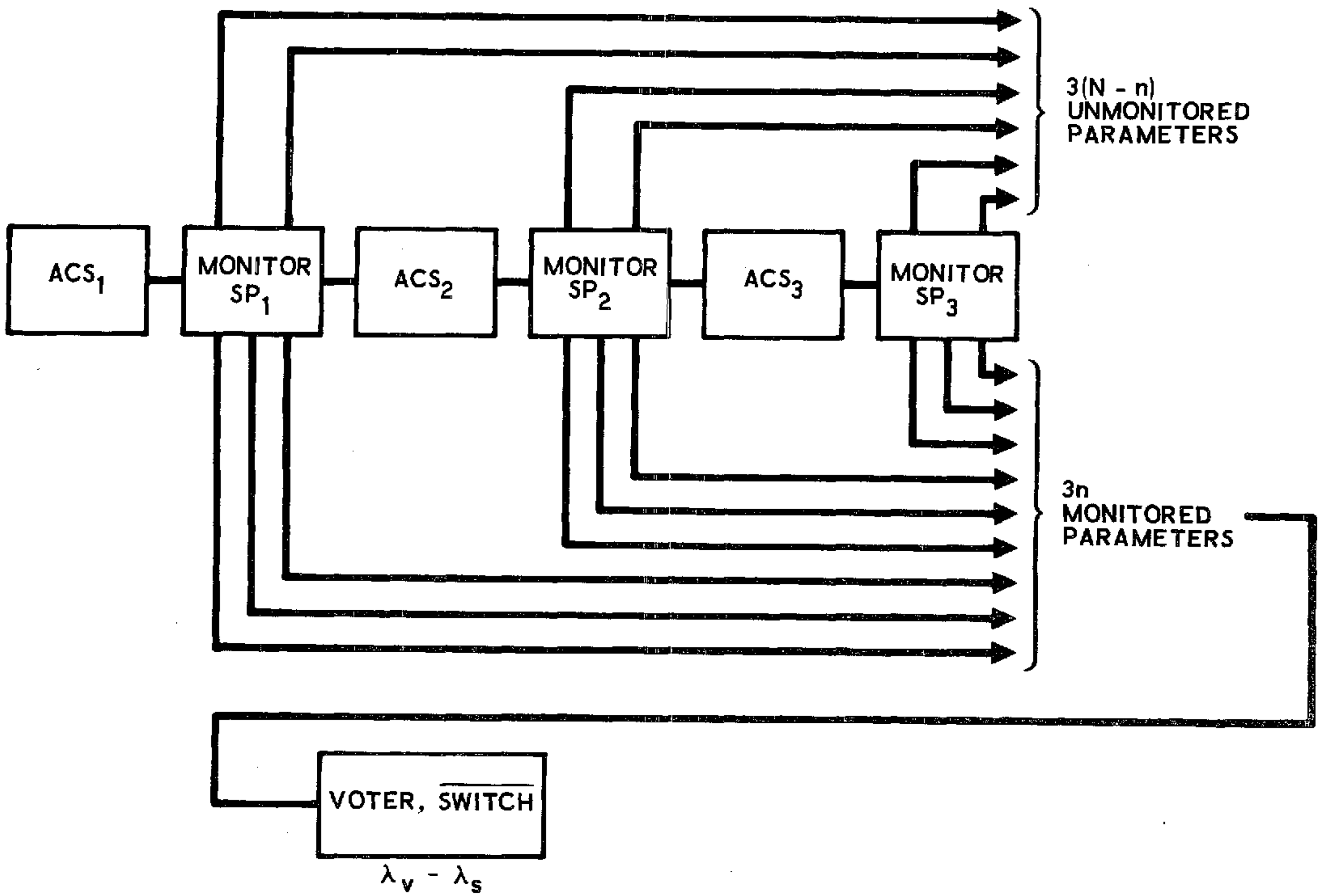

Figure D-9. Reliability Model for Triply Active ACS With Voting

c. FALSE ALARM RATE

The false alarm rate refers to the frequency of failures

(1) in the sensor/signal processor, which make up the monitoring subsystem, resulting in a command to the switch to change state

(2) in the system selection switch, which results in a state change without a command.

The result of such a failure, in either mode (1) or (2), is that an active, properly functioning ACS is switched off-line. (In the single-string case, no switching would be done, but erroneous status reports would go to the DMS and the user; sacrifice of mission objectives would result.) If ACS redundancy is still available, then this situation will not degrade performance immediately, but will likely result in a shortened mission duration. However, if ACS redundancy has been invalidated through previous failures, this inadvertant switching will degrade mission performance. In this latter case, the use of a "locked in" switch is to be recommended, i.e., a switch that cannot change state if no redundancy is present.

This approach does not consider false alarms resulting from a spurious output of the ACS into the monitoring system, such as an out-of-specification electrical spike caused by noise. Here, only hard failures of the monitor or switching subsystems are considered.

(1) Single-String ACS

The reliability model of Figure D-2 is applicable, and the probability of false alarm, P_F is given by

$$P_F(t) = 1 - \exp(-\lambda_{m_F} t)$$

where λm_F is that portion of the monitoring system failure rate that is linked to a false alarm condition, specifically, that portion associated with a false status signal of failure being issued to the DMS.

(2) Active ACS with Switched Standby ACS

The reliability model of Figure D-10 is applicable. The probability of a false alarm is given by

$$P_F(t) = 1 - \exp[-(\lambda_{m_F} + \lambda_{s_F})t]$$

where λ_{s_F} is the portion of the switch failure rate that is linked to a change of state without a command from the monitor subsystem.

(3) Triple-Active ACS With Voting

The reliability model of Figure D-11 is applicable. The probability of false alarm is given by

$$P_F(t) = 1 - \exp[-(3\lambda_{sp_F} + \lambda_{v_F})t]$$

where λ_{sp_F} is the portion of the signal processor failure rate that is associated with a false indication of failure in one of the three ACSs, and λ_{v_F} is the portion of the voter failure rate that results in the censoring of one or more ACS inputs when the inputs are, in fact, acceptable.

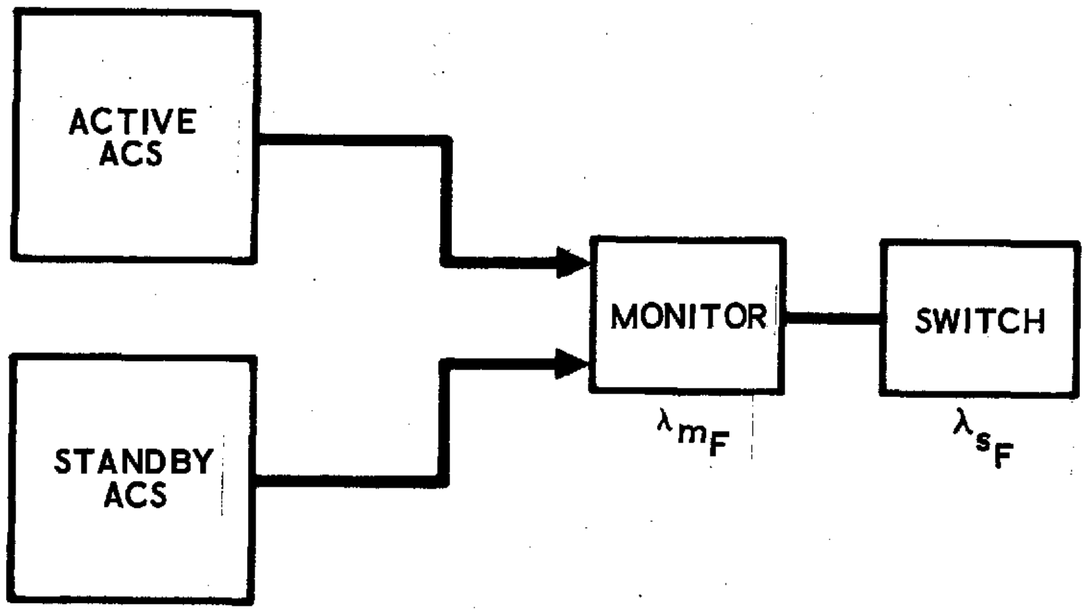

Figure D-10. Reliability Model for Active ACS with Switched Standby ACS

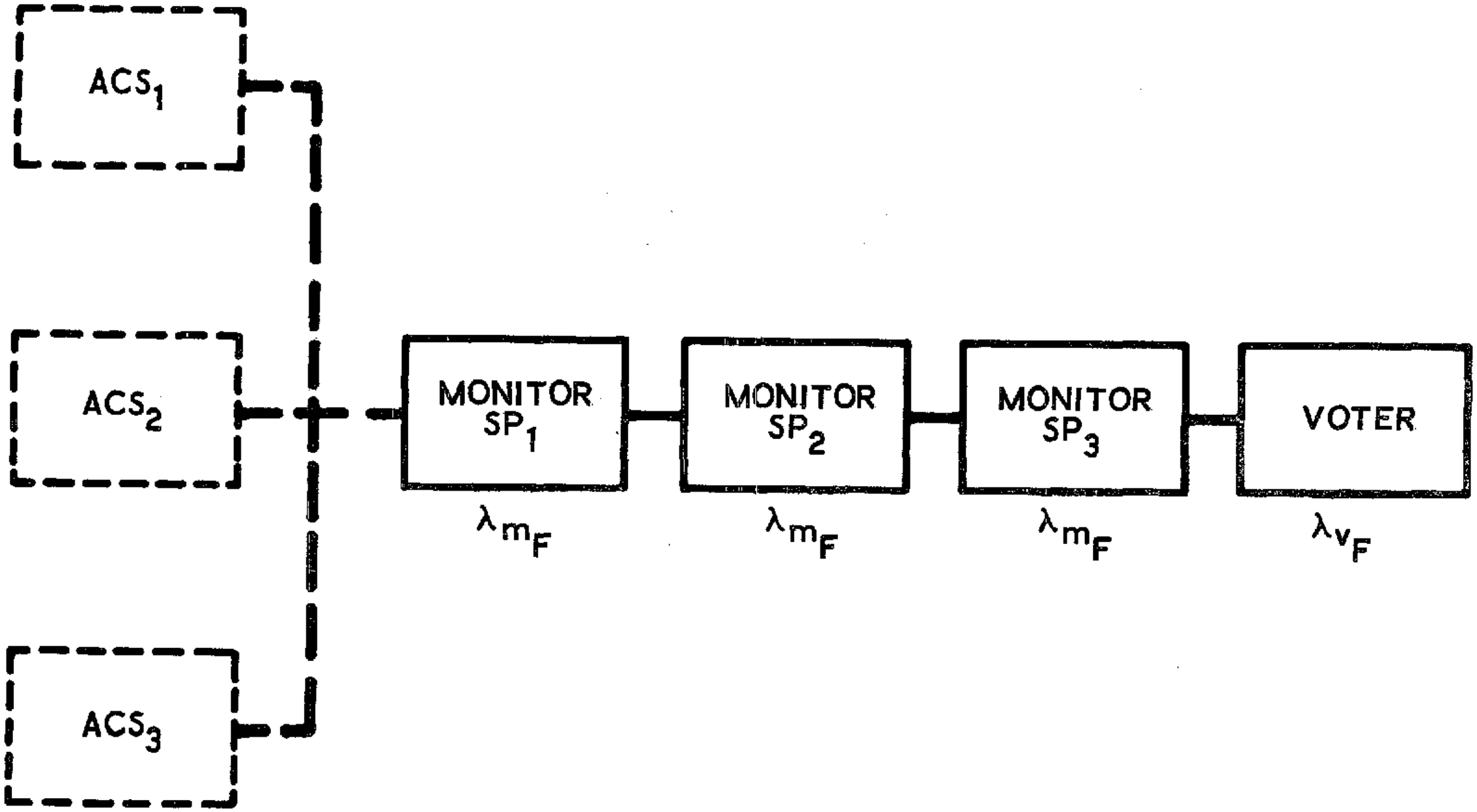

Figure D-11. Reliability Model for Triply Active ACS With Voting

REFERENCES

1. Reliability Stress and Failure Rate Data for Electronic Equipment, Bureau of Naval Weapons, Department of the Navy, MIL-HDBK-217A (1 December 1965).

2. RADC Reliability Notebook, Rome Air Development Center, Rome, New York, Technical Report No. RADC-TR-67-108 (September 1961), Vo. II.

BIBILOGRAPHY

Carley, R. R., Program Model Presentation, unpublished notes, February 1972.

A Compendium of Satellite Attitude Control System, Wolf Research and Development Corporation, Riverdale, Maryland.

Research Study on Low Cost Earth Orbital Transportation System Synthesis by Economic Analysis, Vols. 2, 3, and 4, The Boeing Company, Huntsville, Alabama, 1970.

Sabroff, A. E., "Advance Spacecraft Stabilization and Control Techniques," Journal of Spacecraft and Rockets, Vol. 5, No. 12, December 1968.

Stires, David M., and Maurice M. Murphy, Pert/CPM, Material Management Institute, Boston, 1962.

Stires, David M., and Raymond P. Wenig, Pert/Cost, Industrial Education Institute, Boston, 1964.

AFSC Regulation No. AFR 800-1, Air Force System Procurement Council (23 March 1971).

AFSC Regulation No. AFR 800-2, Program Management (16 March 1972).

AFSC Regulation No. AFR 800-4, System/Equipment Turnover and Management Transition (19 November 1972).

AFSC Regulation No. AFR 800-6, Program Control-Financial (14 July 1972).

AFSC Regulation No. AFR 800-7, Integrated Logistics Support Implementation Guide for DoD Systems and Equipment (March 1972).

AFSC Regulation No. AFR 800-8, Integrated Logistics Support (ILS) Program for Systems and Equipment (27 July 1972).

AFSC Regulation No. AFR 800-9, Production Management in the Acquistion Life Cycle (25 April 1973).

AFSC Regulation No. AFR 800-11, Life Cycle Costing (LCC) (3 August 1973).